Universitat Autònoma de Barcelona

Lipidomics studies of recombinant Pichia pastoris for improved recombinant protein secretion through cell engineering

Núria Adelantado Vallvé

Universitat Autònoma de Barcelona

Escola d'Enginyeria
Departament d'Enginyeria Química, Biològica i Ambiental

Lipidomics studies of recombinant *Pichia pastoris* for improved recombinant protein secretion through cell engineering

Memòria per a optar al grau de doctor
per la Universitat Autònoma de Barcelona,
sota la direcció de
Dr. Pau Ferrer i Dr. Francisco Valero

per

Núria Adelantado Vallvé

Bellaterra, Desembre 2015

Title	Lipidomics studies of recombinant *Pichia pastoris* for improved recombinant protein secretion through cell engineering
Author	Núria Adelantado
Supervisors	Pau Ferrer, Francisco Valero.
Keywords	*Pichia pastoris*, lipidomics, hypoxia, chemostat, cell engineering

Programa de Doctorat en Biotecnologia
Departament d'Enginyeria Química, Biològica i Ambiental
Escola d'Enginyeria
Universitat Autònoma de Barcelona. Bellaterra, Desembre 2015.

This work was supported by the project CTQ2013-42391-R of the Spanish Ministry of Economy and Competitiveness and the grant PIF of the Autonomus University of Barce-lona (UAB). The group is member of 2014-SGR-452 and the Reference Network in Biotechnology (XRB) (Generalitat de Catalunya).

Part of the manuscript analysis were performed in the Cellular Biology Laboratory of the Institute of Biochemistry at Graz University of Technology, under the supervision of Prof. Dr. Günther Daum, who we would like to thank his collaboration. We would also like to thank Ivo Feussner for the possibility to analyse the sphingolipid content, and Pablo Tarazona for kindly perform the analyses.

Pau Ferrer Alegre, Professor Agregat i Francisco Valero Barranco, Catedràtic del Departament d'Enginyeria Química, Biológica i Ambiental de la Universitat Autònoma de Barcelona i membres del Grup d'Enginyeria de Bioprocessos i Biocatàlisi Aplicada

CERTIFIQUEM:

Que la Biotecnòloga Núria Adelantado Vallvé ha dut a terme sota la nostra direcció el treball que, amb títol: **Lipidomics studies of recombinant *Pichia pastoris* for improved recombinant protein secretion through cell engineering**, es presenta en aquesta memòria i que constitueix la seva Tesi per a optar al Grau de Doctor per la Universitat Autònoma de Barcelona en el programa de doctorat en Biotecnologia.

I perque s'en prengui coneixement i consti als efectes oportuns, signem la present a Bellaterra, 9 Desembre del 2015,

Dr. Pau Ferrer Alegre (Co-Tutor)	Dr. Francisco Valero Barranco (Co-Tutor)	Núria Adelantado Vallvé (Autor)

Abstract

The increasing availability of *omics* databases provides an important knowledge base for the design of novel yeast engineering strategies, since they offer systems-level information on the physiology of the cells under diverse growth conditions and genetic backgrounds.
In a previous study, a beneficial effect of low oxygen availability on the expression of a human Fab fragment in *Pichia pastoris* has been identified. Transcriptomic analyses pointed out important regulation of the Unfolded Protein Response (UPR) and lipid metabolism, with a significant transcriptional up-regulation of ergosterol and sphingolipid biosynthetic pathways. Furthermore, cells cultured in the presence of fluconazole, an antifungal agent that inhibits sterol C14α-demethylase (Erg11p) activity in the ergosterol biosynthetic pathway, showed a reduced amount of ergosterol in the plasma membrane, resulting in increased protein secretion levels. Moreover, it is known that the transcription factor Hac1, which plays a key role by regulating the UPR, regulates lipid biosynthesis.
In the present study, a reference strain of *P. pastoris* secreting the 2F5 Fab antibody fragment as a model recombinant protein was genetically modified in order to change its lipid composition. A set of strains harbouring either deleted (*DES1, SUR2*), or overexpressed (*DES1*) genes of the sphingolipid pathway were generated. In addition, a Fab producing strain overexpressing *ERG11* was constructed and, as an alternative to the ergosterol pathway knockout, the reference strain was treated with fluconazole. Finally, the spliced form of *HAC1* was overexpressed as a strategy to deregulate the lipid metabolism network. The series of strains were cultivated in chemostat cultures under normoxic and hypoxic conditions. Strains were characterised in terms of Fab-productivity, intra/extracellular product distribution, cell morphology by transmission electron microscopy (TEM) and lipid content in terms of phospholipids, fatty acids, sterols, non-polar lipids and sphingolipids, in order to fully understand how cells adapt to genetic and environmental changes involving lipid changes. The obtained results were combined with previously published transcriptional data, allowing us to demonstrate an important remodelling of the lipid metabolism under limited oxygen availability.

Resum

L'ús cada cop més extensiu de plataformes *òmiques* per a l'estudi de llevats ha generat grans quantitats d'informació relativa a la fisiologia cel·lular sota diferents condicions de cultiu, la qual pot ser utilitzada per al desenvolupament de noves estratègies d'enginyeria genètica.

S'ha observat que els nivells d'expressió d'un fragment d'anticòs humà produït en el llevat metilotròfic *Pichia pastoris* augmenten significativament quan aquest és cultivat en nivells de baixa disponibilitat d'oxigen. Anàlisis transcriptòmics mostren que hi ha una regulació important dels gens involucrats en el metabolisme de lípids i la resposta al mal plegament de proteïnes (UPR), destacant la l'augment de transcrits provinents de gens involucrats en les rutes de biosíntesi de l'ergosterol i esfingolípids. A més, s'ha observat que la presència en el medi de cultiu de fluconazol, un agent antifúngic que inhibeix específicament l'activitat de la esterol C14α-demetilasa (Erg11p) en la ruta de biosíntesi de l'ergosterol, resulta en una disminució dels nivells d'ergosterol en les membranes cel·lulars, millorant els nivells de proteïna recombinant secretada al medi de cultiu. Finalment, el factor de transcripció Hac1, amb un paper important en la regulació de la UPR, també es troba involucrat en la regulació de la síntesi de lípids.

En el present estudi, la soca de referència, *P. pastoris* que produeix el fragment d'anticòs 2F5 de manera recombinant, s'ha modificat genèticament per tal de canviar la seva composició lipídica. S'ha generat una bateria de soques que presenten alguns gens de la ruta de biosíntesi d'esfingolípids delecionats (*DES1, SUR2*), o bé sobreexpressats (*DES1*). Al mateix temps, s'ha alterat la ruta de síntesi de l'ergosterol de la soca de referència mitjançant la sobreexpressió del gen *ERG11* o tractant les cèl·lules amb fluconazol. Finalment, també es va sobreexpressar *HAC1*. Les cèl·lules es van cultivar en cultius en continu sota condicions d'oxigen normals (normòxia), i baixos (hipòxia), i les soques van ser caracteritzades en quant a nivells de Fab produïts, la seva distribució intra/extracel·lular, morfologia a partir d'estudis de microscòpia electrònica (TEM), i el seu contingut lipídic, quantificant els nivells d'àcids grassos, fosfolípids, esterols, lípids neutres i esfingolípids. Amb tota aquesta informació es pretén comprendre com les cèl·lules s'adapten a canvis genètics i ambientals a través de canvis en el seu contingut lipídic. Els resultats obtinguts s'han combinat amb informació transcriptòmica prèviament publicada, demostrant que existeix una important remodelació del metabolisme lipídic quan les cèl·lules es troben en condicions d'hipòxia.

Contents

List of abbreviations

μ	specific growth rate (h^{-1})
μ_{max}	maximum specific growth rate (h^{-1})
AOX1	Alcohol oxidase gene
bp	base pair
CHAPS	3-[(3-Cholamidopropyl)dimethylammonio]-1-propanesulfonate
CL	cardiolipin
D	dilution rate
DAG	diacylglycerol
DCW	dry cell weight (g L^{-1})
DMSO	dimethyl sulfoxide
DO	dissolved oxygen
DPH	1-6-diphenyl-1,3,5-hexatriene
DTT	Dithiothreitol
EDTA	ethyendiaminetetraacetate
ELISA	immunoassay
ER	endoplasmic reticulum
ERAD	endoplasmatic reticulum associated degradation
Erg	ergosterol
exp	exponential
FA	fatty acid
Fab	antigen-binding fragment
Fluco	fluconazole
FS	free sterol
GAP	Glyceraldehyde-3-phosphate gene
GC	gas chromatography
GC-MS	gas chromatography mass spectrometry
Glc	glucose
Gly	glycerol
HEPES	2-[4-(2-hydroxyethyl)piperazin-1-yl]ethanesulfonic acid
HPLC	high performance liquid chromatography
Hyg	hygromycin
IMF	insoluble membrane fraction
IPC	inositol-P-ceramide
KO	knock out
LB	Luria Broth
LD	lipid droplets
MIPC	mannosyl inositol-P-ceramide
$M(IP)_2C$	dimannosyl inositol-P-ceramide
OE	overexpression
OD	optical density
PA	phosphatidic acid
PCR	polymerase chain reaction
PE	phosphatidylethanolamine
PI	phosphatidylinositol

PL	phospholipid
PMSF	phenylmethylsulfonyl fluoride
PS	phosphatidylserine
q_p	specific product production rate ($mmol_P\ g_{DCW}^{-1}\ h^{-1}$)
RQ	respiratory coefficient
RSD	relative standard deviation
RT	room temperature
SCF	soluble cytosolic fraction
SD	standard deviation
SDS	sodium dodecyl sulfate
SE	steryl ester
SN	supernatant
SL	sphingolipid
TAE	Tris-Acetate-EDTA
TEM	transmission electron microscopy
TG	triacylglycerol
TLC	Thin Layer Chromatography
Tris	Tris(hydroxymethyl)aminomethane
UPR	Unfolded Protein Response
YNB	yeast nitrogen base
YPD	yeast peptone dextrose
Zeo	Zeocin

1

General Introduction

1.1. *Pichia pastoris* as a cell factory for recombinant protein production

The methylotrophic yeast *Pichia pastoris* is one of the most effective and versatile systems for the expression of heterologous proteins [1–3]. *P. pastoris* expression system has gained importance for industrial application as stand out by the number of patents published [4] and the wide range of protein products that had entered the market for therapeutic and industrial uses in the last years [5].

P. pastoris, as a Crabtree negative yeast, has a strong preference for respiratory growth even under glucose excess. This fact limits the formation of ethanol and acetate, increases the yield in biomass from glycerol or glucose and enables obtaining highly concentrated cell broths (>100 g L^{-1} DCW) [6, 7].

This yeast has also the ability to perform some eukaryotic post-translational modifications, such as processing signal sequences, folding, disulphide bond formation, proteolytic processing, some types of lipid addition and *O*- and *N*-linked glycosilation. *P. pastoris* has been engineered in order to mimic the human *N*-glycosylation pathway and, more recently, specific types of *O*-glycosylation, becoming a potential alternative for mammalian cell culture for the production of recombinant therapeutic glycoproteins for human use [8, 9]. Techniques for genetic modifications similar to those described for *S. cerevisiae* are available, and expression vectors, methods for transformation, selectable markers and fermentation processes have been developed to exploit its productive potential [5, 10, 11].

Along with these favourable physiologic characteristics, the availability of strong and tightly regulated promoters makes this yeast an interesting host for recombinant protein production. The promoter of the alcohol oxidase I gene (*AOX1*) has been mainly employed due to its strength and tight regulation by carbon sources [10]. This promoter is repressed by glucose and glycerol, and highly induced by methanol. Interesting alternatives to the *AOX1* promoter for recombinant protein production are the glyceraldehyde-3-phosphate dehydrogenase (*GAP*) [12] and glutathione-dependent formaldehyde dehydrogenase (*FLD1*) [13] promoters. *GAP* is involved in glycolysis and gluconeogenesis and is a strong constitutive promoter [14] that

possesses its highest expression levels when using glycerol and glucose as substrates [6, 15]. The *GAP* promoter system is suitable for large-scale production, as the need to change feeding solutions and fire and safety concerns related to methanol are avoided.

Recombinant protein production in *P. pastoris* can be performed in salt-based media, with little risk of contamination [16, 17]. Nowadays *P. pastoris* has gained more and more success for recombinant protein production by means of quantity and quality, especially after the achievement in genetic engineering to make it able to produce human type *N-glycosylated* proteins [18–20]. Proteins can be produced intracellularly or secreted. Protein secretion permits simple purification strategies due to the relatively low levels of endogenous proteins in the extracellular medium [21]. A variety of proteins have been expressed, with yields up to 13 g L^{-1} of secreted protein [22] and up to 22 g L^{-1} intracellular protein [23].
In 2009, the first biopharmaceutical protein, a Kallikrein inhibitor (Kalbitor®) produced in *P. pastoris*, was approved by the FDA [24]. Since then, several biopharmaceutical products produced in *P. pastoris* have been approved for human use [25, 26]).

Recently, *P. pastoris* genome sequence has been published [27–30], increasing the genetic and physiologic understanding of this yeast and enabling new studies for strain improvement using more rational approaches.

1.1.1. Bottlenecks during recombinant protein secretion

The process of protein secretion involves protein conversion to mature form, and its traffic to the correct location. This process involves several steps catalysed by a large number of proteins, and the pass through several different organelles until the final destination (Figure 1.1) [31, 32].

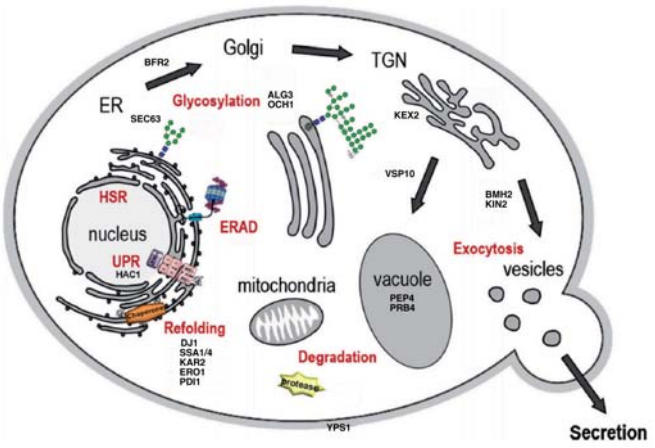

Figure 1.1: Overview of the secretory machinery in yeast [25]. Some target genes for *P. pastoris* engineering for enhancement protein secretion are represented.

Expression of heterologous proteins can lead to saturation or overloading of the secretory pathway [33, 34]. When recombinant protein fails to fold into its native state or protein expression exceeds the folding capacity of the endoplasmic reticulum (ER) [35], unfolded proteins may start to aggregate, triggering the unfolded-protein response (UPR) pathway, which is responsible for induction of genes that are involved in protein folding. In parallel, ER-associated degradation (ERAD) by the proteasome is also activated to eliminate misfolded proteins [36].

The most important bottlenecks in terms of recombinant protein production and secretion are membrane translocation, signal peptide processing and folding within the ER [36].
Commonly used strategies to overcome such secretion bottlenecks comprise engineering the protein folding and quality control systems in the ER [37–40], engineering the intracellular protein trafficking pathway [41, 42], minimisation of post-secretory degradation [43], engineering glycosylation [9], and the energy metabolism [44].

A wide range of strategies has been implemented to engineer *P. pastoris* and to optimise protein synthesis and secretion. Some of them consist of new induction methods to tightly tune expression levels using new promoters [45, 46], cell engineering methods such as the increment of copy number [47], deletion of proteases [48, 49], coexpression of helper factors [37, 41, 50–52], or glycosilation [53]. Approaches of codon optimisation of the expressed genes have also been used [54]. Additionally, operational bioreactor strategies have also been developed to increase protein production [55–60], like growth control [61, 62], medium supplementation with casaminoacids [63], surfactants [64] or trace salts [65], lower culture temperature [66, 67] or oxygen limitation [68, 69]. Each of the factors could enhance production levels of protein, and a proper combination will reach an optimal production through repeated trials.

1.2. Impact of oxygen availability on cell physiology and recombinant protein production

Environmental conditions have a significant impact on recombinant protein levels. It has been described that lower culture temperatures [67, 70], lower oxygen availability [68], as well as adequate substrate feeding strategies in high cell density cultures [62, 71–73], and type of carbon source(s) [62, 74–76] result in a positive effect on protein secretion. With the published sequence of *P. pastoris*, transcriptomic and proteomic response to some of these environmental factors have been investigated [67, 69, 77, 78].
Oxygen availability is critical for many biochemical reactions in eukaryotic cells, including yeasts. The ability to adapt to oxygen limitation is essential for cell survival but also produces important metabolic, functional and structural changes in the cell [79]. Cells can adapt to growth under severe oxygen limitation, termed hypoxia or microaerobic conditions [80]. When cells are grown aerobically, molecular oxygen serves as the final electron acceptor for respiration, while it is also used in synthesis of metabolites, e.g. sterols or unsaturated fatty acids [81]. In the presence of low amounts of oxygen, respiration is drastically reduced, and metabolism is then reprogrammed to optimise yeast cells for fermentative dissimilation of the carbon source in order to conserve energy and maintain a closed redox balance [81]. These metabolic rearrangements are easily detectable by the excretion of metabolites in the culture supernatant, such as ethanol and arabitol in the case of P. pastoris [82].
The impact of oxygen supply on the heterologous production has been studied for different hosts. Oxygen limitation in *E. coli* cultivations triggers cellular stress and formation of by-product such as acetate, which inhibits cell growth and recombinant protein production [83, 84]. In *Saccharomyces cerevisiae* it an increase on recombinant protein production under oxygen limitation was observed [85, 86]. The impact of oxygen limitation on *P. pastoris* recombinant protein production using the *GAP* promoter and glucose as carbon source, was first studied by Baumann and co-workers [68], showing a significant increase of the specific production rate. In subsequent studies, the impact of oxygen availability on the physiology of recombinant *P. pastoris* was studied integrating

transcriptomic, proteomic, metabolic flux and metabolomic analyses [69, 82, 87]. These studies pointed out to potential genes and metabolic pathways that might be potential targets for strain improvement. It was observed a strong transcriptional induction of glycolysis and the non-oxidative pentose phosphate pathways, as well as the downregulation of the TCA cycle under hypoxic conditions. These transcriptional changes were consistent with proteomic data and metabolic fluxes. Cell stress responses, specially UPR, and lipid metabolism were also strongly affected in hypoxia. The biosynthesis of membrane components like ergosterol and sphingolipids include a wide range of oxygen dependent reactions so that alterations in the lipid balance under oxygen scarcity would be expected.

1.3. Yeast lipids

Today, lipids are considered as important dynamic molecules that play vital roles that extend beyond their roles in membrane structure. For this reason, they are the focus of interest of several studies. The ultimate goal is to evolve an integrated *omics* picture (the "interactome") of the genes, transcripts, proteins, and metabolites to fully describe cellular functioning. The goal of lipidomics is to define and quantify all the lipid species in a cell. This is difficult to achieve due to the high number of combinations that exist and high variability of lipid moieties that are known [88]. The use of advanced mass spectrometry (MS) techniques [89] allowed analysing hundreds of lipid molecular species, identifying and quantifying them. Studies of cell lipidome provide a new platform to be integrated with the existing *omics* platforms (e.g. proteome, transcriptome, metabolome) to study cellular functions and regulation. Up to date, some studies integrating some of these platforms are already available in yeast, with promising results [90–93].

1.3.1. Fatty acids

Fatty acid structure and function

Fatty acids are the basic components of complex lipids. Free fatty acids (FA) are carboxylic acids with hydrocarbon chains varying in chain length. In some fatty acids, this chain is unbranched and fully saturated (i.e. contains no double bonds) while in others the chain is unsaturated (i.e. contains one or more double bonds) (Figure 1.2) [94]. These variations lead to the large variety of fatty acid molecules to synthesise many other different lipid species.

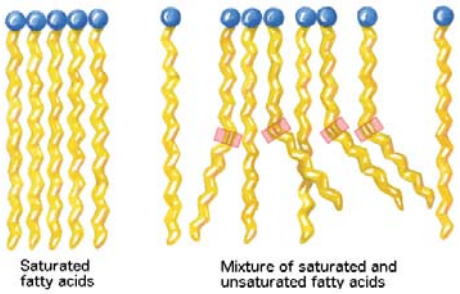

Figure 1.2: Representation of saturated and unsaturated fatty acids.

The fatty acid composition of *P. pastoris* differs from the one observed in *S. cerevisiae* as it possesses polyunsaturated fatty acids. *S. cerevisiae* major fatty acid is palmitoleic acid (C16:1) and oleic acid (C18:1), followed by palmitic acid (C16:0) and stearic acid (C18:0) [95]. Oleic acid (C18:1), linoleic acid (C18:2) and α-linolenic acid (C18:3) and palmitic acid (C16:0) are the most abundant fatty acids in *P. pastoris* [96].

Functionality of cellular membranes and activity of membrane bound proteins are dependent on the FA composition of membrane lipids. To establish and maintain the correct composition, C16 and C18 saturated FA (SFA) derived from de novo synthesis are desaturated, yielding mono- or polyunsaturated FA (UFA), and elongated to very long-chain fatty acids, up to C26 [97]. Fatty acid fluxes are important to maintain membrane lipid homeostasis.

The main function of unsaturated fatty acids is to modulate the physical properties of membranes, especially fluidity. Thus, the fatty acyl composition of membranes varies in response to environmental stress, such as temperature, ethanol concentration [98], nutrition status and other factors [99]. Several functions are associated to fatty acids, including a role as signalling molecules [95], transcriptional regulators [95] and posttranslational modifiers of proteins [95, 100]. FAs play also a role on cell secretion and providing energy trough the β-oxidation pathway [100].
Very-long chain fatty acids (VLCFA) account only for a 1 % of the cellular fatty acid content in *S. cerevisiae* [101], but play essential roles in the cell, establishing or lengthening curved membrane structures, and also defining the membrane curvature at the nuclear pore complex [100]. They also serve specific structural functions as components of sphingolipids and GPI-anchors.

Fatty acid biosynthetic pathway

Yeasts can get their fatty acids by different ways that are represented in Figure 1.3. *De novo* synthesis of fatty acids takes place in the cytosol and in mitochondria, where an acetyl-CoA derived from citrate degradation or from acetate is carboxylated to form malonyl-CoA, which serves as a two carbon building block in the following FA synthesis reactions. Further elongation steps to very long-chain FA (VLCFA) up to C26 is carried out in the endoplasmic reticulum. Desaturation and hydroxylation of FA also take place in the ER. Fatty acid synthesis is restricted to conditions of high energy load of the cells [100].

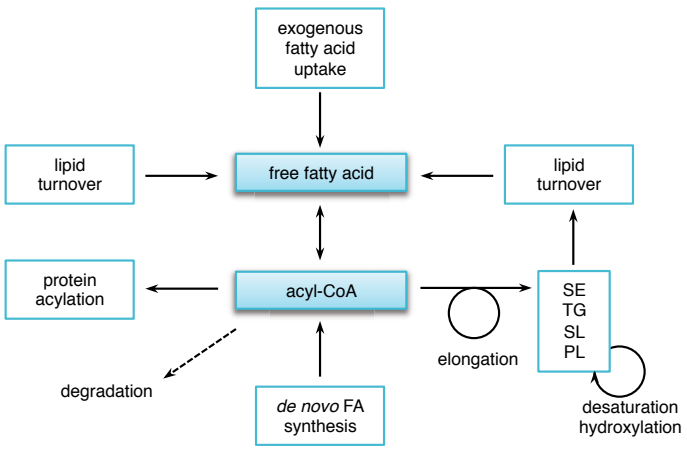

Figure 1.3: Schematic representation of fatty acid metabolism. Adapted from [100].
SE = steryl ester; TG = triacylglycerol; SL = sphingolipid; PL = phospholipid; FA = fatty acid.

Yeast cells can also take up fatty acids from the environment by diffusion or through specific transporters. The uptake step is followed by their activation, and active FA can be used for the synthesis of complex lipids, stored in form of triacylglycerols or degraded in peroxisomes by β-oxidation. Finally, lipid and protein turnover also provide a pool of free fatty acids that should be activated to acyl-CoA in order to be functional for the cell.

1

1.3.2. Phospholipids

Phospholipid structure and function

Phospholipids (PL) are the most abundant membrane lipids [89]. PL are formed by an hydrophobic moiety composed by two fatty acids attached through an ester bond to the first and second carbons of glycerol, and by an hydrophilic moiety that contains a highly polar or charged group attached through a phosphodiester linkage to the third carbon of glycerol (Figure 1.4) [94].

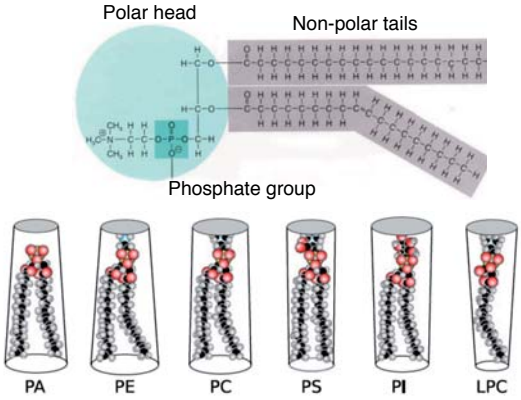

Figure 1.4: General representation of phospholipid (PL) structure and the shape of each PL class [102].

As amphipathic molecules, PL can form lipid bilayers and are the precursors of membranes. PL are subdivided according to their polar head group, which determines their physical properties and also confers a structural shape. The head group of phosphatidylcholine (PC) and phosphatidylethanolamine (PE) is zwitterionic, and anionic in phosphatidylinositol (PI), phosphatidylserine (PS) phosphatidic acid (PA) and cardiolipin (CL). The distribution of these PL varies depending on the organelle. Major phospholipids in total cell extracts from *S. cerevisiae* are phosphatidylcholine (PC), phosphatidylethanolamine (PE), phosphatidylinositol (PI), and phosphatidylserine (PS) [95], while in *P. pastoris* PC, PE, and similar levels of PS and PI are the major phospholipids [96].

Phospholipid composition can vary dramatically according to culture conditions such as temperature [103], carbon source [93, 104] or oxygen supply to the culture [105].

In addition to its structural role as components of cellular membranes, PL are involved in multitude of cellular functions. They act as reservoir of lipid messengers [106], provide precursors for the synthesis of other molecules [107, 108], are involved in activity of membrane proteins [109–111], in fission and fusion events [96], the transport to plasma membrane [112], maintaining the mitochondrial structure and function [113], and mRNA localisation [114].

Phospholipid biosynthetic pathway

Phospholipid biosynthesis is similar for all eukaryotes. Fatty acids are incorporated into phospholipids by sequential trans-esterification of two acyl-CoA molecules to glycerol-3-phosphate (G3P) to produce lyso-phosphatidic acid (lyso-PA) further transformed to phosphatidic acid (PA) (Figure 1.5) [97].

Phosphatidic acid serves as a central metabolite in the *de novo* synthesis of PL. It can either be dephosphorilated to diacylglycerol (DG) to enter the lipid storage pathway, or converted to cytydine diphosphate-diacylglycerol (CDP-DG) [115]. DG is the substrate for triacylglycerol synthesis, and contributes to PE and PC synthesis through the CDP-ethanolamine and CDP-choline branches of the so-called Kennedy pathway, which uses exogenous ethanolamine and

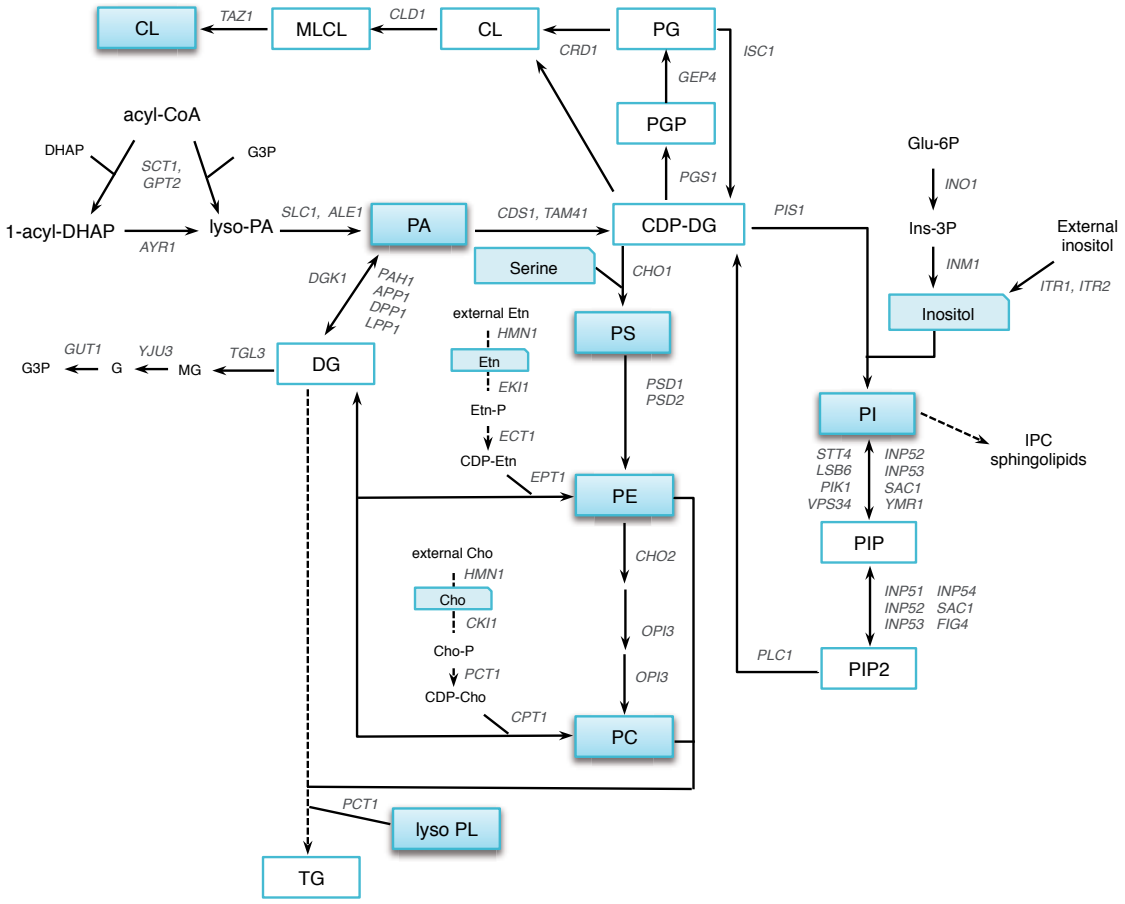

Figure 1.5: Schematic representation of the phospholipid metabolic pathway in yeast. CL = cardiolipin; MLCL = monolysocardiolipin; PG = phosphatidylglycerol; PGP = phosphatidylglycerophosphate; CDP-DG = cytidine diphosphate diacylglycerol; PI = phosphatidylinositol; PIP = phosphatidylinositol-phosphate; PIP2 = phosphatidylinositol-biphosphate; PS = phosphatidylserine; PE = phosphatidylethanolamine; PC = phosphatidylcholine; Etn = ethanolamine; Cho = choline; PA = phosphatidic acid; DG = diacylglycerol; TG = triacylglycerol; MG = monoacylglycerol; G = glycerol; G3P = glycerol-3-phosphate.

choline as substrate for PE and PC synthesis [95].
CDP-DG can be converted to PI or to PS in the ER, and to phosphatidylglycerol phosphate (PGP) in the mitochondria. PS can be decarboxylated to PE, which can subsequently be methylated to form PC [115]. PGP in the mitochondria is dephosphorylated to produce PG, which reacts with another CDP-DG molecule, obtaining CL.

PL synthesis is regulated at levels of gene expression, posttranslational modification, enzyme activity [107, 115, 116] and contact sites [117]. Genetic and biochemical mechanisms include inositol-, zinc-, CTP- (cytidine triphosphate), CDP-DG- and S-Adenosyl-L-homocysteine-mediated regulation. Enzyme activity mechanisms are mostly based on enzyme phosphorylation. Additionally, phospholipid regulation is interrelated with the synthesis and regulation of other major lipid classes that include fatty acids, triacylglycerols, sterols and sphingolipids.

1.3.3. Sterols

Sterol structure and function

Sterols are essential lipid constituents of membranes. The major sterol in yeast is ergosterol, which is the end product of the yeast sterol biosynthetic pathway. Ergosterol characteristic structure

consists of four fused rings, an acyl side chain and a hydrophilic hydroxyl group that facilitates insertion into membranes (Figure 1.6) [95]. The structure of ergosterol differs from cholesterol by two additional double bonds and an additional methyl group at C24 of the side chain [118].

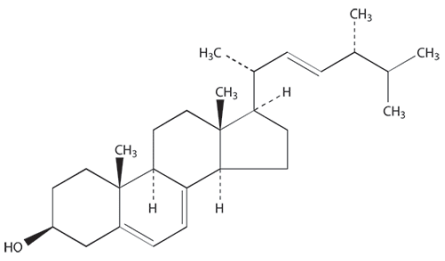

Figure 1.6: Structure of ergosterol.

Free sterols are predominantly present in the plasma membrane, where control its physical state by modulating its bilayer fluidity and permeability [119, 120]. They also constitute, together with sphingolipids, membrane microdomains.

In contrast to *S. cerevisiae*, a sterol gradient along the secretory route is not found in *Pichia pastoris* [96, 121], due to the small amounts of ergosterol present in plasma membrane (≈50 μg per mg protein in *P. pastoris* compared to the ≈400 μg per mg protein in *S. cerevisiae*) [96].

In addition to their role as membrane constituents, sterols also harbour multiple essential functions like signal transduction [122], protein lipidation (i.e. modification, usually proteins, by association with a lipid) [123] or endocytosis [124, 125].

Ergosterol biosynthetic pathway

Ergosterol is synthesised in the ER through a complicated pathway involving more than 20 enzymes. Ergosterol pathway can be divided into the pre- and post-squalene pathways (Figure 1.7). Some steps of sterol biosynthetic pathway require oxygen.

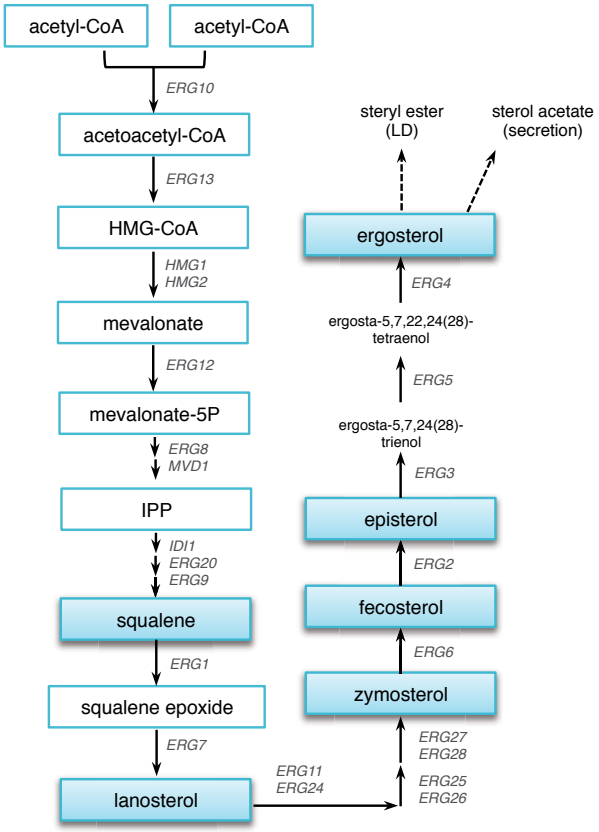

Figure 1.7: Ergosterol biosynthetic pathway in yeast. HMG-CoA = 3-hydroxy-3-methylglutaryl-CoA; IPP = isopentenyl pyrophosphate.

Yeast sterol biosynthesis starts with condensation of two acetyl-CoA molecules that yield acetoacetyl-CoA. Condensation of a third acetyl-CoA to acetoacetyl-CoA give 3-hydroxy-3-methylglutaryl-CoA (HMG-CoA) that is further reduced to mevalonate. Mevalonate is phosphorylated two times leading to mevalonate-5-phyrophosphate, which is decarboxylated to form isopentenyl pyrophosphate (IPP). IPP is then converted into dimethylallyl pyrophosphate (DPP), which is condensed with an additional IPP to geranyl pyrophosphate (GPP). If an additional IPP molecule is added, farnesyl pyrophosphate (FPP) is formed. Squalene is formed from two molecules of FPP.
Post-squalene pathway includes several oxygen-dependent reactions. Squalene is epoxidised to squalene expoxide and further transformed to lanosterol. Several demethylation, reduction and desaturation steps lead to zymosterol, which is further converted to fecosterol, episterol, and reduced to ergosterol.
Once synthesised, free ergosterol is transported to the plasma membrane trough both vesicular and non-vesicular transport to prevent its accumulation, which may become toxic for the cell [126].

Yeast cells synthesise sterols in excess, so that mechanisms to maintain sterol homeostasis should be present. They include the esterification of free sterols together with fatty acids and its storage in lipid droplets, downregulation of sterol biosynthesis at transcriptional level [127] and sterol acetylation to be secreted into the medium as sterol acetate [123].

1.3.4. Non-polar lipids

Yeast cells are able to overcome a possible toxic effect of sterols and free fatty acids by converting them into molecules that lack charged groups. Free fatty acids are converted to triacylglycerols (TG) and sterols to steryl esters (SE), and they cluster and form an hydrophobic core called lipid droplet (LD). These non-polar lipids are not suitable as membrane constituents, but serve as energy source and precursors for membrane lipid synthesis.

TGs consist of a glycerol backbone esterified with three long-chain fatty acids. Their biogenesis takes place in the ER with the esterification of their precursor diacylglycerol (DG) (Figure 1.8) [128].

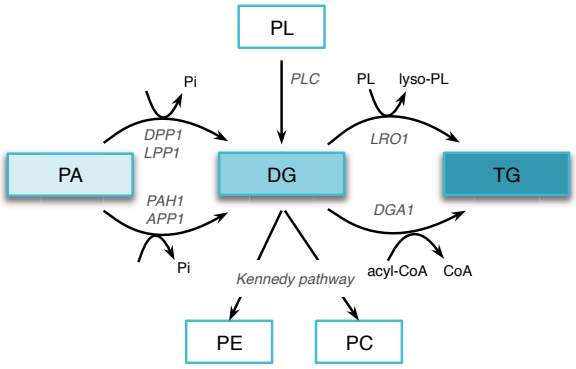

Figure 1.8: Synthesis of triacylglycerols (TG) and diacylglycerols (DG) in yeast. Adapted from [129].

DG can result from dephosphorilation of *de novo*-synthesised phosphatic acid (PA), degradation of PL, TG deacylation [129] or during sphingolipid synthesis, where one molecule of DG is produced each time a PL head group is transferred onto a ceramide backbone by sphingolipid synthases [116]. DG can be further converted to TG by acyl-CoA-dependent or acyl-CoA-

independent acylation, which requires a PL as an acyl donor, usually PE or PC [129]. In contrast to *S. cerevisiae*, where the acyl-CoA-dependent pathway is the major contributor to TG synthesis, the acyl-CoA-independent pathway seems to be the preferred in*P. pastoris* [129].
Steryl esters are synthesised by the addition of an activated fatty acid to the hydroxyl group at C3 of a sterol molecule (Figure 1.9) [128].

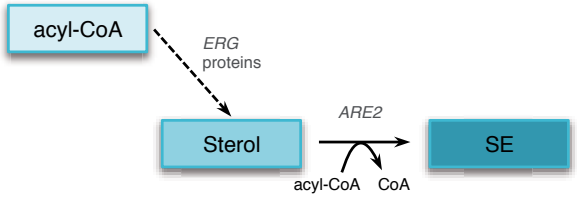

Figure 1.9: Synthesis of steryl esters (SE) in yeast. Adapted from [129].

SEs provide a way to maintain sterol homeostasis (i. e. the balance between the inactive storage SE and the biologically active free sterols) [130, 131]. Steryl esters are present in *P. pastoris* at a much lower amount than in *S. cerevisiae*. They only account for 10 % of total non-polar lipids in *P. pastoris*, whereas *S. cerevisiae* are almost 50 % [132]. This can be a consequence of the small amounts of sterols present in this organism. SEs in lipid droplets from *P. pastoris* are present as esters of ergosterol and ergosterol precursors in comparable amounts [133].
Lipid droplets are composed by a core of randomly packed TG surrounded by SE. This core is highly hydrophobic, and is covered by a phospholipid monolayer with a specific set of proteins embedded. Most of these proteins are involved in lipid metabolism and homeostasis [129]. The amount of proteins found in LD from *P. pastoris* was lower compared to the proteome of LD in *S. cerevisiae* [133].

If required, yeast cells can mobilise TG and SE to provide sterols, FA and DG for the synthesis of membrane lipids or for the production of energy. Degradation of TG is mainly achieved by the TG lipases yielding fatty acids than can be used to provide precursors for membrane lipid synthesis [134]. DG released by degradation of TG can be used as a substrate for the synthesis of PE and PC via the Kennedy pathway [116, 134], but also as a second messenger in signal transduction [135].
Sterols released from SE by hydrolisation, and can be incorporated into membranes to regulate membrane stability, fluidity and permeability [120].
Apart from its function as storage molecules, they have other functions, especially TG, which is involved in iron, PL and SL metabolism, lipotoxicity and cell cycle progression [136].

1.3.5. Sphingolipids

Sphingolipid structure and function

Sphingolipids share the common structural feature that all are comprised of backbones called long chain bases (LCB). They are amide-linked with a long or very-long-chain fatty acid to form ceramides. Ceramides are the simplest sphingolipids and the precursor onto which different head groups can be added to form more complex sphingolipids [137].
Unlike *S. cerevisiae*, where only inositol containing phosphorylceramides exist, in *Pichia pastoris* two ceramide synthases coexist, showing different affinities for specific LCB and/or acyl-CoA substrates [138]. Their specificity allows them to catalyse two classes of ceramide precursors that will be specifically destined to the production of either inositol containing phosphorylceramides

(IPCs) or the neutral sphingolipids, ceramides (Cer) and hexosylceramides (HexCer) (Figure 1.10). These sphingolipids have different polar head groups and ceramide backbones. IPCs are ceramides linked to glycosyl moieties via inositol phosphate, which occur as free membrane lipids and as membrane anchors of covalently bound proteins (GPI-anchors), while hexosylceramides contain mainly β-D-glucose or β-D-galactose as substituents of the C-1 hydroxy group of the ceramide and serve as precursors for a large variety of higher glycosilated sphingolipid species (GlcCer) [139].

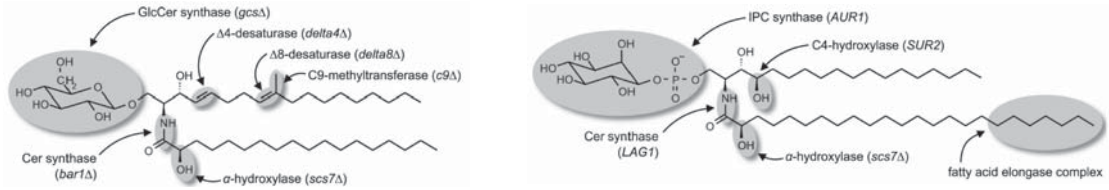

Figure 1.10: Sphingolipids present in *P. pastoris*. **(a)** Neutral sphingolipids (GlcCer); **(b)** Inositol containing phosphorylceramide (IPC) [138].

Additional differences between these two organisms comprise the length of the fatty acids of their IPC sphingolipids. While *S. cerevisiae* consist basically on C26 fatty acid and a small percentage of C22 and C24, *P. pastoris* contains mostly C24 fatty acids.
Studies of lipid composition of *P. pastoris* organelles performed by Grillitsch *et al.* [96, 121] showed an organelle dependent distribution of sphingolipids. Ceramides and hexosylceramides were predominant in Golgi fractions, whereas inositol containing phosphorylceramides with C42 - C46 backbones were almost exclusively enriched in plasma membrane fractions.

Sphingolipids (SL), together with phospholipids, are essential structural components of membranes. Sphingolipids have saturated (or trans-unsaturated) tails so they are able to form taller, narrower cylinders than PC lipids of the same chain length and they pack more tightly, adopting the solid gel phase, which is fluidised by sterols [140].
Apart from the well known structural function, sphingolipids also play additional roles as second messengers for regulating signal transduction pathways [141].
Sphingolipids playing roles in heat stress [142, 143], endocytosis [108, 141], intracellular protein trafficking [108, 144], lifespan [145, 146]. Furthermore, it has been also described the role of LCB as signalling molecules [147, 148].

Sphingolipid biosynthetic pathway

De novo sphingolipid synthesis (Figure 1.11) begins in the endoplasmic reticulum (ER) with the condensation of serine and palmitoyl-CoA into 3-ketodihydrosphingosine by serine palmitoyltransferase (SPT). Reduction of 3-ketodihydrosphingosine by an NADPH-requiring reaction results in the long-chain base (LCB) dihydrosphyngosine (DHS) [149]. DHS can be hyroxylated at C4 to give phytosphingosine (PHS).
DHS and PHS can enter two possible routes. They can be phosphorylated to form phyto- or dihydrosphingosine phosphate (PHS-1P and DHS-1P), which can be cleaved and generate fatty aldehydes and ethanolamine phosphate. This degradation pathway may serve to regulate overall sphingolpid levels. Ethanolamine phosphate can be recycled for phosphatidylethanolamnie (PE) biosynthesis through the Kennedy pathway [150]. This phosphorylation step is reversible. The second route produces complex sphingolipids. DHS and PHS are amide-linked to a very long

chain fatty acid (usually C26) to yield dihydrocermaide (DHC) and phytoceramide (PHC), and further hydroxylated. Fatty acids are elongated from C14 - C18 to C26 to very-long-chain-fatty acids (VLCFA) by elongases in the ER.

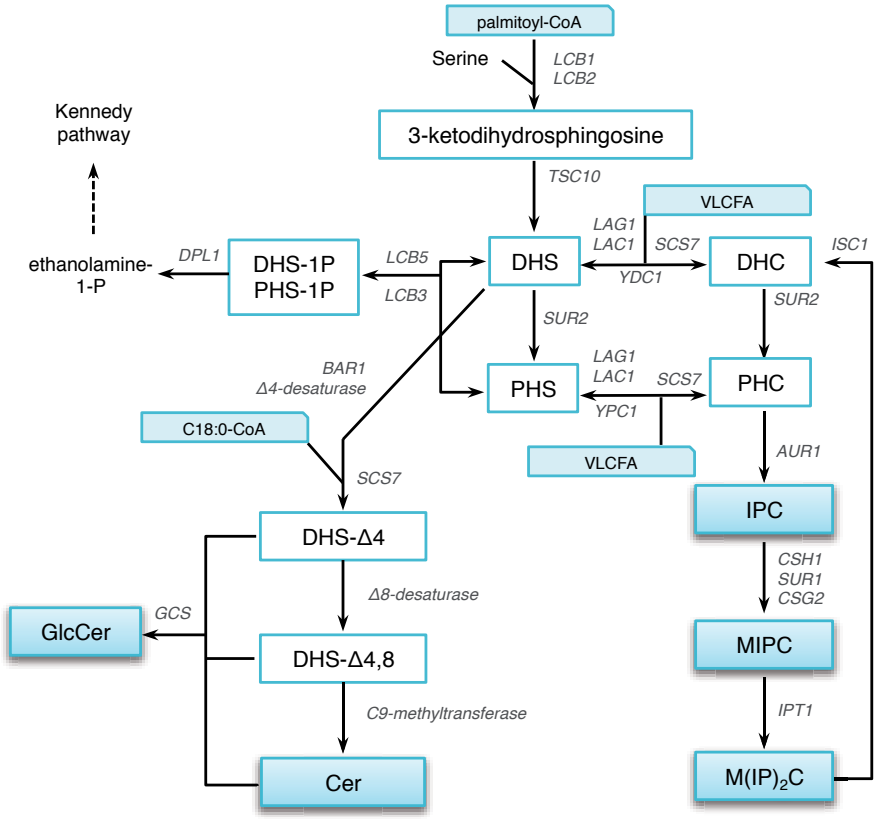

Figure 1.11: Sphingolipid metabolic pathway of *P. pastoris*.

Ceramides are simple SL molecules without head groups that serve as substrates for the synthesis of complex lipids.

Further steps into complex sphingolipids include the addition of a phosphoinositol headgroup to the ceramide, forming inositolphosphorylceramides (IPCs), which can undergo mannosylation to generate mannosyl-inositolphosphorylceramide (MIPC). After mannosylation, another inositol phosphate group can be added, forming mannosyl(inositol)$_2$phosphorylceramide (M(IP)$_2$C).

Additionally, *P. pastoris*, unlike *S. cerevisiae*, can synthesise ceramides and hexosylceramides. In this pathway, a molecule of DHS is used by an alternative ceramidase, desaturated, hydorxylated and desaturated again. Further methylation can yield additional species. These ceramides can be transformed in glucoceramides by the addition of a glucose moiety [138].

About three-fourths of the mass of the sphingolipids in *S. cerevisiae* cells is M(IP)$_2$C, with the rest being equal parts of IPC and MIPC [151]. The shear mass of these sphingolipids and their negative charge are likely to affect processes dependent upon the plasma membrane [152]. Plasma membrane of *P. pastoris* is enriched in hexosylceramides and inositol containing sphingolipids with C42-C46 backbones [96].

The initial steps of sphingolipid biosynthesis, including sphingoid base and ceramide formation, take place in the endoplasmic reticulum (Figure 1.12). Complex sphingolipids are produced by the addition of the polar head groups in the Golgi apparatus, where they are transported by both vesicular and non-vesicular transport [152]. Enzymes involved in *de novo* sphingolipid

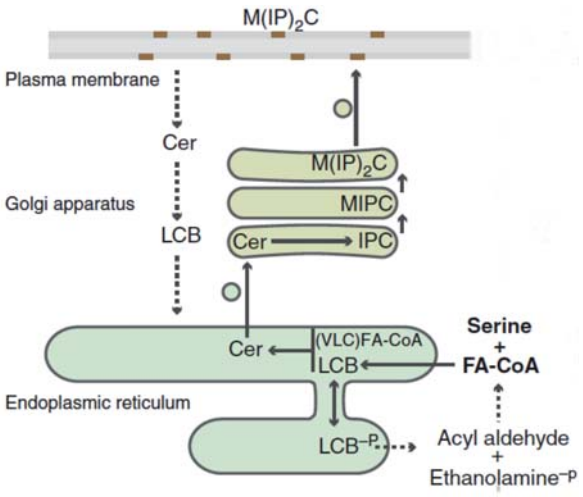

Figure 1.12: Overview of the *S. cerevisiae* sphingolipid metabolism. Adapted from [153].
Filled arrows indicate biosynthetic steps; dashed arrows indicate degradative and recycling steps.

synthesis are tightly regulated through the action of mechanisms that modulate their activity in response to environment, substrate availability and the presence of cofactors, connecting sphingolipids to other metabolites such as lipids, amino acids or sugars [154]. Sphingolipids can be catabolised by hydrolysing their polar head group to yield the ceramides DHC or PHC, which can be further cleaved to free fatty acids and LCB (DHS and PHS) [95]. LCBs, as mentioned before, can be phosphorylated and cleaved to generate ethanolamine phosphate to generate phosphatidylethanolamine (PE). Extended reviews about sphingolipid regulation have been published [137, 150, 152, 153].

Crosstalk between sphingolipid biosynthesis and other lipid pathways

The crosstalk between sphingolipids and fatty acid metabolism starts in the first step of sphingolipid biosynthesis, where the enzyme palmitoyltransferase (SPT) condenses a serine and the long fatty acid palmitoyl-CoA. Furthermore, the very-long-chain fatty acid content of sphingolipids is of great importance for cell growth and development.

Yeast cells adjust their sphingolipid profile in response to changes in sterol structures, and genetic experiments show that sterols and sphingolipids functionally interact in biological membranes [149, 155].
Sphingolipids along with sterols are critical for formation of microdomains within membranes that have been referred to as lipid rafts. In *S. cerevisiae* rafts have been referred to be involved in several cellular functions, which are summarised in Figure 1.13.
Sphingolipids are closely related to phospholipids because they share some parts of their metabolic pathways, such as the synthesis of polar head groups or fatty acyl-CoAs. Both lipid classes can feed each other and impact their concentration.

Moreover, triacylglycerols (TG) synthesis and breakdown directly impacts the acyl composition of sphingolipids [116]. Diacylglycerols also play a pivotal role in the convergence of sphingolipids, phospholipids and non-polar lipid metabolic pathways.

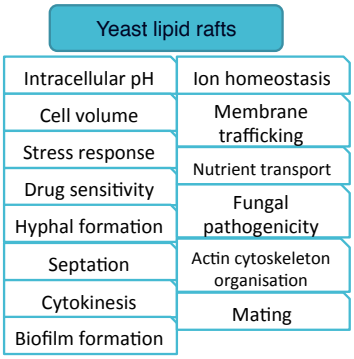

Figure 1.13: Putative involvement of lipid rafts in different yeast functions. Adapted from [156].

1.3.6. Antibody fragment as model protein

In the current work, *P. pastoris* strains producing the antigen-binding fragment (Fab) 2F5, a neutralising antibody against HIV-1, have been used as a model protein to characterise the heterologous protein production impact over changes on cell physiology. Fab fragments are the antigen binding regions of an antibody molecule, with a molecular weight around 50 kDa [157]. They can be used as model for complex protein production, as contain five disulphide bonds, one thereof required to connect the heavy chain - light chain dimer. Because of their properties, antibody fragments have important industrial applications as therapeutic and diagnostic molecules, but also in purification and bioseparation applications [158].

The absence of glycosylation on Fab regions allows their production to be less complex and enables easier engineering and cultivation of microbial host organisms such as bacteria and yeasts [159]. Described product yields of Fab in *P. pastoris* are up to 30 mg L^{-1} in fed-batch GAP cultivations [160] and 40.5 mg L^{-1} in methanol induced fed-batches [161–163], while 5 mg L^{-1} were described in chemostat cultures under *GAP* promoter (Garcia-Ortega 2015, submitted).

Aims of the study

The aim of the present work was the characterisation of a recombinant *Pichia pastoris* strain producing a human antibody Fab fragment in terms of lipid composition. Based on previous results showing a strong regulation of lipid metabolism when cells are cultured under low oxygen conditions, one of the objectives was to study the impact of oxygen availability on the lipidome of the recombinant strain.

Transcriptomic data under these oxygen conditions allowed for selecting target genes involved in the ergosterol and sphingolipid pathway, in order to study the effect of genetic modifications on two of the most regulated pathways whose products are essential elements of the plasma membrane. Punctual modifications would give information about membrane modifications related to increased protein secretion.

Summary

The aim of this thesis was to characterise the lipid composition of *Pichia pastoris* cells producing a recombinant protein under low oxygen conditions (hypoxia), under which a beneficial effect on protein production has been previously observed. A *P. pastoris* strain expressing the antibody fragment 2F5 under the constitutive *GAP* promoter was chosen as a case study. The investigation focused on the analysis of influence of lipid composition on protein secretion.

In Chapter 3, transcriptomic data of genes related to lipid metabolism of *P. pastoris* growing under normoxic and hypoxic conditions was used to perform a cluster analysis in order to select the most regulated genes. It was observed that ergosterol and sphingolipid pathways were manly upregulated under hypoxia. Notably, most of the corresponding enzymes catalyse oxygen dependent reactions. Following this analysis, some of the genes involved in these biosynthetic pathways were selected as engineering targets.

In Chapter 4, a battery of strains with the selected genes deleted or overexpressed was obtained. The aim of these modifications was to evaluate their impact on the overall lipid class composition of the cell as well as on protein secretion. In Chapter 5, small-scale cultures were performed in order to characterise the obtained strains and select clones for further characterisation in chemostat cultures (Chapter 6), under both normoxic and hypoxic conditions. Cell behaviour in terms of protein production, cell morphology and lipid composition were determined for all the strains in both oxygen conditions.

Finally, in Chapter 7, lipidomic results were integrated with previously published transcriptomics data in order to gain further insights on the physiological response of *P. pastoris* to hypoxic conditions and its interconnections with protein secretion. The ultimate goal of these studies is to enlarge the knowledge base for the selection of new potential targets to improve recombinant protein secretion through cell engineering.

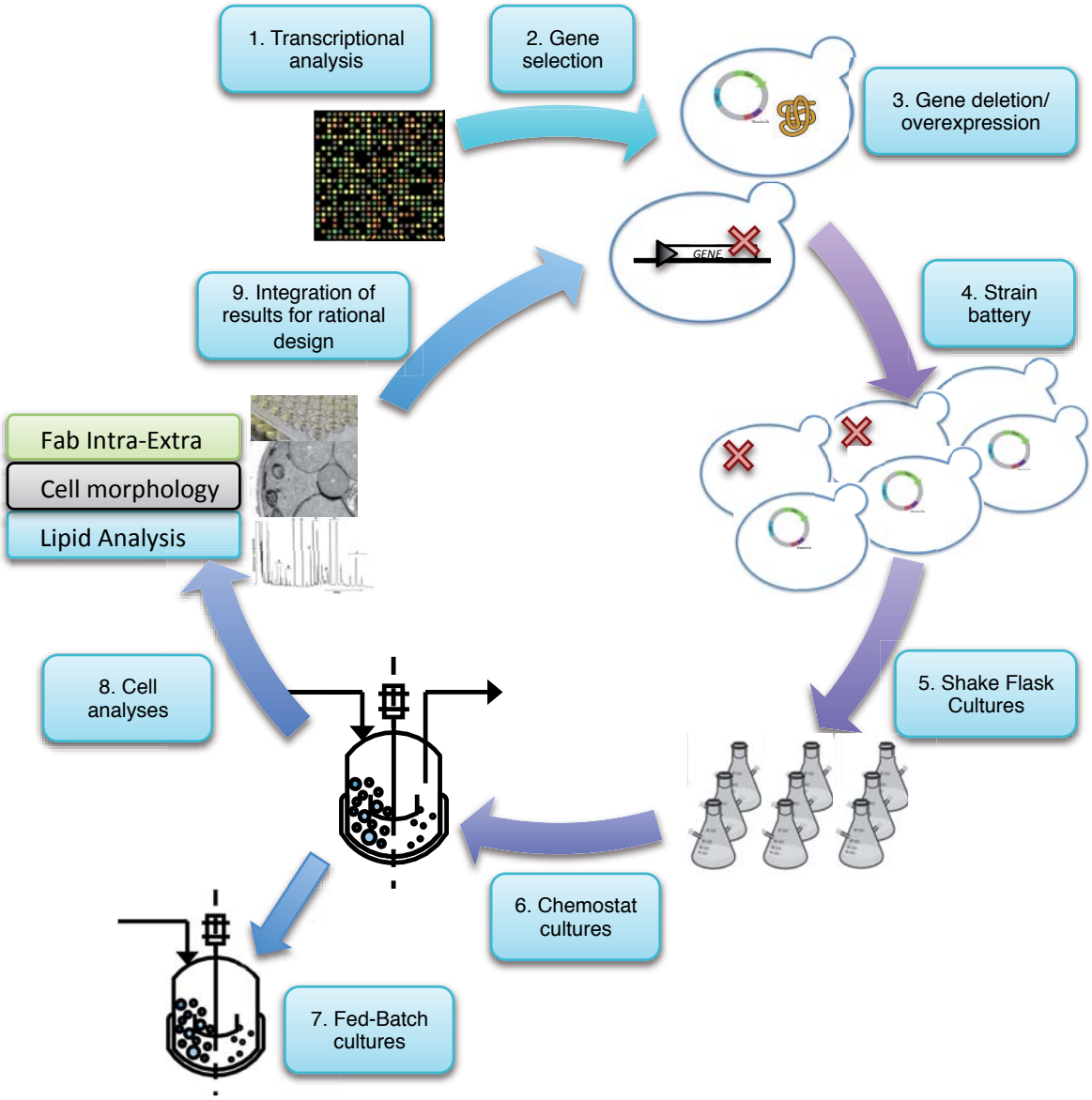

Figure 1.14: Graphic summary including the principal steps of the present work.

2

Materials and Methods

2.1. Strains

Escherichia coli

E. coli was used to amplify plasmid DNA for transformation into *P. pastoris* and subcloning tasks. *E. coli* DH5α (Invitrogen) with genotype F^{-1} *sup*E44 *thi*-1 *gln*V44 *rec*A1 *rel*A1 *gyr*A96 *deo*R *nup*G Φ80d *lacZ* Δ M15 Δ (*lacZYA-argF*)U169 *hsd* R17(r_k^{-1} m_k^{-1}) λ^{-1} was employed.

Pichia pastoris

The *P. pastoris* starting strain was a X33 pGAPαA-Fab2F5 strain. The expression cassettes for the light and heavy chain of the human 2F5 antigen-binding fragment (Fab) were separately placed under the control of the *P. pastoris* GAP (glyceraldehyde-3-phosphate dehydrogenase) constitutive promoter and the *S. cerevisiae* α-mating factor leader and combined on one plasmid. This vector, conferring resistance to Zeocin™, was integrated into the genome of *P. pastoris* host strain X33 (*his*$^+$ derivative of the GS115, wild type phenotype) from Invitrogen.

Strain maintenance

For long term stocks, cells were grown in YPD media until exponential phase was reached, harvested, resuspended in 50 % YP medium with 50 % Glycerol (50 % (v/v)) and frozen stored at -80 °C. For short-term cell maintenance, cells were grown on YPD plates containing 100 μg mL^{-1} Zeo at 30°C.

2.2. Molecular Biology

2.2.1. Media Composition

LB (Luria Bertani) Medium

1 % Tryptone, 0.5 % Yeast Extract, 1 % sodium chloride (NaCl). Store at RT.
To prepare LB-Agar plates add 1.5 % Agar. Store at 4 °C.

SOC Medium

SOC medium is used in the final step of bacterial cell transformation to obtain maximal

transformation efficiency of *E. coli*. Medium composition: 2 % tryptone, 0.5 % yeast extract, 8.56 mM sodium chloride (NaCl), 2.5 mM potassium chloride (KCl), 10 mM magnesium chloride ($MgCl_2$), 10 mM magnesium sulphate ($MgSO_4$), 20 mM glucose. Autoclave at 121 °C for 30 min. Store aliquoted at 4 °C.

YPD Medium

1 % (w/v) yeast extract, 2% (w/v) peptone. Autoclave at 121 °C for 20 min. Add 2 % (w/v) glucose autoclaved separately. Store at RT.
Add 2 % Agar to prepare YPD-Agar plates. Store at 4 °C.

2.2.2. Buffers

TAE Solution

A stock solution of 50x TAE was prepared. 1x Buffer composition: 40 mM Tris pH 7.6, 20 mM Acetic acid, 1 mM EDTA.

BEDS solution

10 mM Bicine-NaOH, pH 8.3, 3 % (v/v) ethylene glycol, 5 % (v/v) dimethyl sulfoxide (DMSO), and 1 M Sorbitol. Store at 4 °C.

2.2.3. Vectors

pBR326 (Figure 2.1)

pBR326 was a kindly provided by Dr. Mansur, and consists on a pPICZαA vector with the hygromycin resistance cassette that replaces the original Zeocin present in the commercial vector.

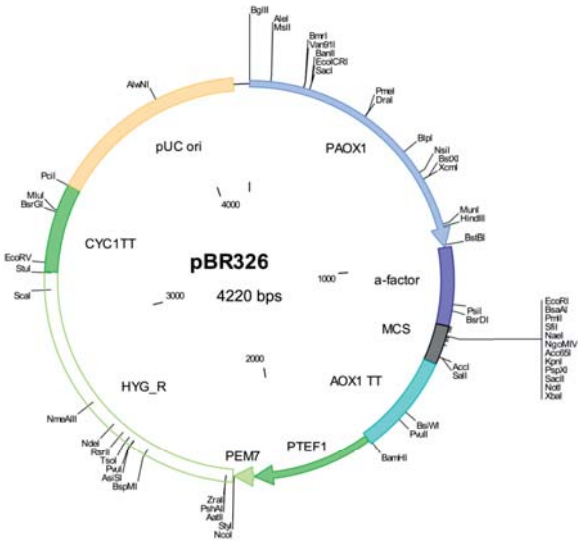

Figure 2.1: Schematic view of the expression vector pPB326, composed by the AOX1 inducible promoter, the *S. cerevisiae* α-factor secretion sequence, a multi-cloning site (MCS), and some tags for purification. An origin of replication for *E. coli* is also present, as well as the Zeocin resistance cassette for selection.

pGAPHis (Figure 2.2)

pGAPHis has been used for intracellular constitutive gene expression, as it carries the GAP promoter and no secretion signal is present. Apart from the conventional replication origin, it carries two selection systems, the histidine gene (*his*) for auxotrophy selection when his$^-$ strains

are employed, as well as the Ampicillin antibiotic resistance cassette. pGAPHis was used together with pBR326 to generate the working vector pGAPHA.

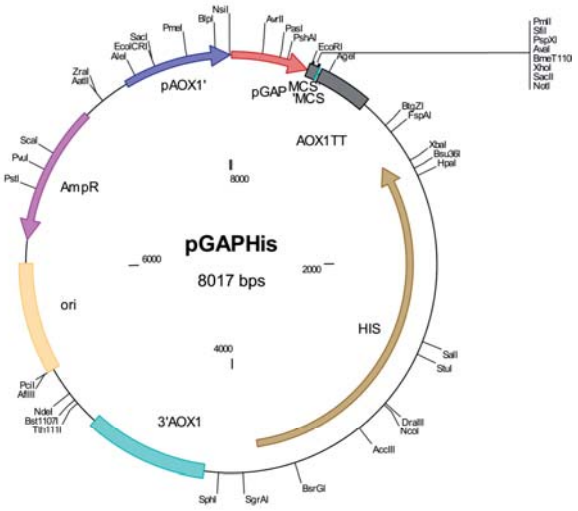

Figure 2.2: Schematic view of the expression vector pGAPHis, composed by the GAP constitutive promoter, a multi-cloning site (MCS) and the *his* and Ampicillin resistance ORFs. An origin of replication for *E. coli* is also present.

pPUZZLE (Figure 2.3)
pPUZZLE was used for intracellular expression. It is a versatile vector backbone based on a modular design [164]. It contains the GAP promoter, the Kanamycin resistance, which confers kanamycin resistance in *E. coli* and Geneticin (G418) resistance when used in *P. pastoris*.

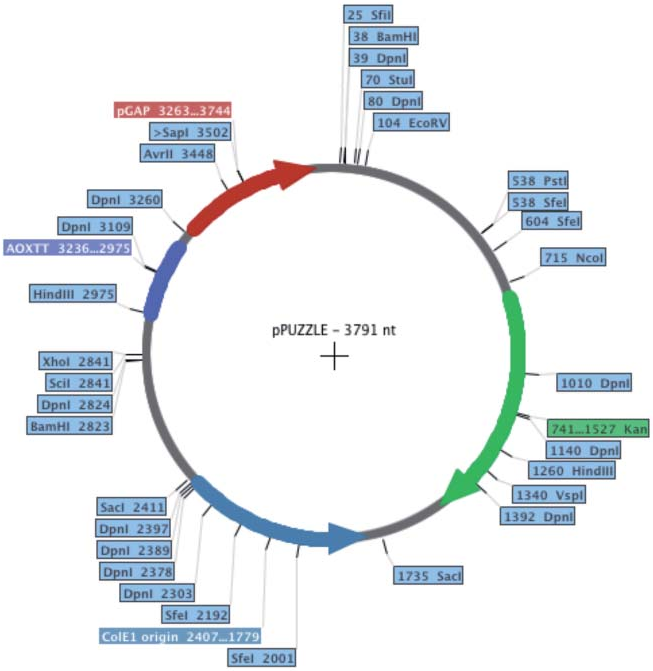

Figure 2.3: Schematic view of the expression vector pPUZZLE, composed by the GAP constitutive promoter (red), a multi-cloning site (MCS) and the Kanamycin resistance ORFs (green). An origin of replication for *E. coli* is also present (blue).

2.2.4. Antibiotics

Zeocin™

The *Sh ble* gene confers resistance to this antibiotic. It was purchased from InvivoGen. Working concentrations were 50 μg mL^{-1} for *E. coli* and 100 μg mL^{-1} for *P. pastoris*. When used, it was wrapped in foil due to light sensitivity. Stored at -20 °C.

Hygromycin B

HygroGold™ (InvivoGen) was used as antibiotic for dual selection experiments, including gene knockout and overexpression, as an alternative mode of action than Zeocin™ is used. The *hph* gene from *Streptomyces hygroscopicus* confers hygromycin resistance. Working concentrations for *E. coli* were 100 μg mL^{-1} as indicated by the manufacturer.

P. pastoris optimal working concentration of antibiotic was tested by culturing cells in different antibiotic concentrations. An initial cultivation test was performed in 5 mL of YPD media with a hygromycin range between 0 and 1000 μg mL^{-1} (Figure 2.4 A). Cells were cultured for 120 h and samples were taken to determine the OD_{600} of the cultures. A second round with a narrower range of antibiotic concentrations [0 - 100 μg mL^{-1}] was carried out in shake flask cultures for 174 h (Figure 2.4 B). Finally, 100 μg mL^{-1} was selected as working concentration in *P. pastoris* cultures. When used, it was wrapped in foil due to light sensitivity. Stored at -20°C.

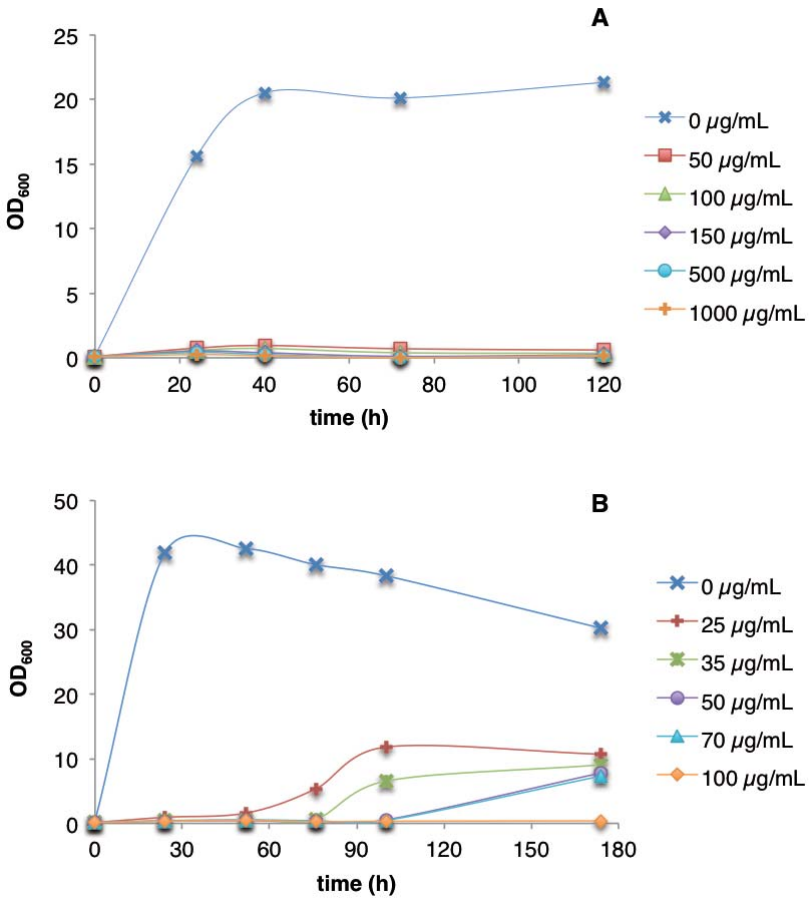

Figure 2.4: *P. pastoris* X33-Fab2F5 growing in YPD with different Hygromycin concentrations. A. Initial screening in 5 mL cultures. B. Second screening performed in 25 mL Shake Flasks.

2.2.5. Enzymes

Restriction enzymes

Several restriction enzymes were used for DNA digestion and all were purchased from Fermentas, in the FastDigest version when available, and enzyme details and reaction conditions were performed according the provider's guidelines.

Phosphatase

Dephosphorilation of 5' ends of DNA to prevent self-ligation of fragments by removing the 5'-phosphoryl termini required by ligases, was carried out using rAPid Alkaline Phosphatase (Roche) according to the standard dephosphorilation procedure. Briefly, up to 1 μg of vector DNA was mixed with 2 μL of rAPid Alkaline Phosphatase Buffer (10x) , 1 μL of the enzyme and filled with distilled water up to 20 μL. The mixture was incubated 30 min at 37 °C, then incubated for 2 min at 75 °C to inactivate the enzyme and directly used in the ligation reaction.

Ligase

Ligations were performed using T4 DNA Ligase (Roche) according to manufacturer's standard assay. A vector to insert ratio of 1:3 was used for optimal ligation results and the amount of needed DNA was calculated using Equation 2.1.

$$\frac{ng \text{ vector} \cdot kb \text{ instert}}{kb \text{ vector}} \cdot \text{molar ratio } \frac{\text{insert}}{\text{vector}} = ng \text{ insert} \tag{2.1}$$

Up to 1 μg of total DNA (vector and insert) was mixed with 3 μL of 10x Ligation Buffer, 2 μL of T4 DNA ligase and filled up to 30 μL with distilled water, and incubated overnight at 16 °C. Ligation mixture was used directly to transform *E. coli* competent cells [2.2.11].

DNA polymerases

Different DNA polymerases were used depending on the PCR use. For knock-out cassette generation and gene amplification for co-expression, High-Fidelity SAHARA™ and RANGER DNA polymerases (Bioline) were used. When PCR was used for detection purposes, GoTaq® Green Master Mix (Promega) was chosen.

2.2.6. DNA extractions

Gel Bands

DNA fragments from agarose gels and enzymatic reactions (i.e. PCR, DNA digestion, DNA ligation) were recovered using the Wizard® SV Gel and PCR Clean-Up System (Promega). All methods used for DNA recovery are based on the capacity of DNA to bind silica in the presence of high concentrations of chaotrophic salts that will be removed later with an alcohol-based wash and DNA will be finally eluted in a low-ionic-strength solution such as water.

Plasmidic DNA

Plasmidic DNA extractions were performed using both PureYield™ Plasmid Miniprep System and PureYield™ Plasmid Midi-prep System (Promega). For plasmid DNA purification, an initial step to generate a cleared lysate that removes protein, lipids and chromosomal DNA from plasmid DNA is required. The SDS-alkaline denaturation method is the one used in the kits. DNA is denatured in alkaline conditions and the rapid neutralisation causes that chromosomal DNA forms an insoluble aggregate that precipitates out of solution, while plasmid DNA rehybridises and remains in

solution. Moreover, potassium salt of SDS leads to protein precipitation and aggregation, assisting in the entrapment of the chromosomal DNA. Midiprep System also incorporates an endotoxin removal wash to remove substantial amounts of protein, RNA and endotoxin contaminants.

2

Genomic DNA

Genomid DNA from *P. pastoris* was extracted using the Wizard® Genomic DNA Purification Kit (Promega) following the Yeast Isolation Protocol. The isolation system is based on sample enzymatic lysis and purification by silica.

2.2.7. Primer design

Primers (Table 2.1) were all designed using Clone Manager 9 (Sci-Ed Software) and purchased from Biomers.net. Primers were designed to have a GC-content of 40-60 %, reduced intra- or intermolecular complementary sequences to minimise the production of primer-dimer, and reduced intramolecular regions of secondary structure to favour primer annealing. Pairs of primers were designed with similar melting temperature ($T_m \pm 5$ °C).

Table 2.1: Primers used for gene amplification from genomic DNA for co-expression in *P. pastoris* Fab 2F5, knock out generation, sequencing and clone selection

Primer name	Primer sequence	Use
F-pGAP	5′-GATTATTGGAAACCACCAGAATCG	sequencing and clone selection
R-AOX1TT	5′-GCAAATGGCATTCTGACATCC	
R-pPUZZLE	5′-GGCGTGAATGTAAGCGTGACT	
F-DES1_*Sfi*I	5′-CGTATCGGCCCAGCCGGCCATGATAACTCACAGATCCAATAACG	overexpression
R-DES1_*Not*I	5′-CTGACGCGGCCGCTTAAAAGTCATGTGCTATGGTTCTC	
F-SUR2_*Sfi*I	5′-CTACAGGCCCAGCCGGCCATGGACAAGTTCAGTCAGTATATCC	
R-SUR2_*Not*I	5′-GCCTAGCGGCCGCTTACTGTTCTTTCTTTTGGTGATCC	
F-ERG11_*Sfi*I	5′-CTACAGGCCCAGCCGGCCATGAGTCTGGTCCAGGAGTTG	
R-ERG11_*Not*I	5′-CTTAGCGGCCGCCTAATTATCGCGTCTTTCCCAT	
F-Hac1s_*Sbf*I	5′-GCTAGCCCTGCAGGACCATGCCCGTAGATTCTTC	
R-Hac1s_*Sfi*I	5′-CCTAGACGGCCCAGGGGGCCGCCTATTCCTGGAAGAATAC	
F-Hyg-pTEF1	5′-GGATCCCCCACACACCATAG	Knock-out
R-Hyg-CYC1TT	5′-TCTCCAGCTTGCAAATTAAAGCCTTC	
Hyg-Int-R	5′-CCGCCCTTAGATTAGATTGC	
F-Down2.1	5′-TCTCTTTCAGTGACCTCCATTG	
Hyg-Int-F	5′-CGAGGGCAAAGAAATAGAGG	
DES1-Up-F	5′-ATGATAACTCACAGATCCAATAACGTTC	*DES1* knock-out
DES1-Down-R	5′-CTAACTTTGGGTTTTGGTGGTTTTTG	
DES1-UP-Nested-F	5′-TAGGCCCACAGTTTGAGTTC	
DES1-Up-R-Hyg-F	5′-CTATGGTGTGTGGGGGATCC-TGAATGCCAGGTTATGGCTCAG	
DES1-Down-Nested-R	5′-GATTTGTCCTTTGCGGTCTC	
DES1-Down-F-Hyg-R	5′-GAAGGCTTTAATTTGCAAGCTGGAGA-GTTCCTTCTTTGCGGGTTCG	
DES1-Int-F	5′-AGCCTTCTTCGCCACTTTC	
DES1-Int-R	5′-GTGGCGAAGAAGGCTTTACC	
R-Down2.0cm	5′-GATTTGTCCTTTGCGGTCTCTCTC	
SUR2-Up-F	5′-ATGGACAAGTTCAGTCAGTATATCC	*SUR2* knock-out
SUR2-Down-R	5′-TTACTGTTCTTTCTTTTGGTGATCCG	
SUR2-Up-Nest-F	5′-CTTGATTCAAGGCGTTCCTG	
SUR2-Up-R-Hyg-F	5′-CTATGGTGTGTGGGGGATCC-GGTTTGCTATCGTGTCATTCCATTTG	
SUR2-Down-F-Hyg-R	5′-GAAGGCTTTAATTTGCAAGCTGGAGA-GCCTAGCTGCCATATTCAC	
SUR2-Down-Nest-R	5′-TCTGTCTAGAGGCCAAGAAC	
SUR2-Int-F	5′-GACCCATTTGAAGGATTTCTCTTG	
SUR2-Int-R	5′-TACGGGACATACAGCTTGTG	

2.2.8. PCR

GoTaq® Green Master Mix It was used for detection purposes. It is a premixed ready-to-use solution containing a modified form of *Taq* DNA polymerase, dNTPs, $MgCl_2$, reaction buffer and two dyes (blue and yellow) that allow monitoring of progress during electrophoresis. The standard amplification program for this polymerase is described in Table 2.2.

Table 2.2: Standard PCR amplification program for GoTaq Green Master Mix (Promega)

Step	Temperature	Time	Cycles
Initial denaturation	94°C	5 min	1
Denaturation	94°C	1 min	30
Annealing	5°C below T_m	1 min	
Extension	72°C	1 min/kb	
Final extension	72°C	5 min	1
Hold	4°C	Indefinite	

RANGER DNA Polymerase

Was used to amplify the knock out cassette, as it is designed to amplify long templates with extreme sensitivity. It is supplied with a Reaction Buffer containing dNTPs, $MgCl_2$ and enhancers at optimal concentrations. Standard amplification protocol is described at Table 2.3.

Table 2.3: Standard PCR amplification program for RANGER DNA polymerase (Bioline)

Step	Temperature	Time	Cycles
Initial denaturation	95°C	1 min	1
Denaturation	98°C	20 sec	30
Annealing/Extension	2-5°C below T_m	1 min/kb	
Hold	4°C	Indefinite	

SAHARA DNA Polymerase

Was used to amplify genes from genomic DNA for plasmid insertion and further gene co-expression (Table 2.4).

Table 2.4: Standard PCR amplification program for SAHARA DNA polymerase (Bioline)

Step	Temperature	Time	Cycles
Initial denaturation	95°C	10 min	1
Denaturation	95°C	1 min	30
Annealing	5°C below T_m	1 min	
Extension	68°C	1 min/kb	
Final extension	68°C	5 min	1
Hold	4°C	Indefinite	

2.2.9. DNA quantification

The concentration of DNA was determined by using a NanoDrop 1000 Spectophotometer (Thermo Scientific). 2μL of water were loaded to blank it. 2μL of sample were loaded and the software calculated the absorbance corresponding to the concentration of DNA present in the sample. 260/280 and 260/230 values were also monitored in order to determine DNA purity.

2.2.10. Agarose Gel Electrophoresis

1-1.5 % (w/v) agarose gels were run to verify the required DNA after amplification or restriction, as well as to purify the bands for further work with the selected DNA. Agarose gels were performed by heating the desired amount of agarose in TAE buffer until dissolved. Once cooled, SYBR® Safe DNA Gel Stain (Invitrogen) was added. Samples were set up by adding 2 μL of 6x loading buffer before dispensing into the wells of the gel. Gels were loaded with the GeneRuler™ 1 kb DNA Ladder, ready-to-use (Fermentas) to determine DNA fragments size. Gel images were obtained with Gel Doc™ EZ System from Bio-Rad.

2.2.11. *E. coli* Transformation

Chemical competent *E. coli* cells were prepared according to Nishimura's protocol [165]. For the transformation, 5-10 ng of ligation mixture were added to 80 μL of competent cells and incubated on ice for 20 min. The mixture was heat shocked at 42 °C for 60 sec, chilled on ice for 1-2 min, and resuspended into pre-warmed SOC medium. Resuspended cells were incubated at 37 °C for 1-2 h to allow expression of the antibody resistance. Finally, volumes of 50 μL, 100 μL and 200 μL were plated onto LB agar plates containing the required antibiotic and incubated overnight at 37 °C.

2.2.12. Screening of transformants

After transformation into *E. coli* DH5α cells, clones were screened to determine if the insert was successfully cloned by colony PCR [166] or plasmid purification followed by restriction enzyme digestion. Selected plasmids were sequenced with the primers F-pGAP and R-AOX1TT for pGAPHA, and F-pGAP and R-pPUZZLE for pPUZZLE. Sequencing was performed at UAB's Genomics and Bioinformatics Service. The sequences were aligned using Clone Manager software.

Verified plasmid constructs were then linearised with *Avr*II for integration into the transcription termination locus of AOX1 (AOX1TT) and transformed into X33 pGAPZαA Fab2F5 competent cells.

2.2.13. *P. pastoris* transformation

Electrocompetent *P. pastoris* cells were prepared according to Lin-Cereghino's protocol [167] as follows: cells were grown overnight in 5 mL YPD medium in a 30°C shaking incubator, diluted to Abs_{600} of 0.2 in 25 mL YPD and grown until an Abs_{600} of 0.8 - 1 was reached. Cells were harvested at 500 *g* for 5 min at RT and the supernatant discarded. Pellet was resuspended in 9 mL of ice-cold BEDS solution supplemented with 1 mL 1.0 M Dithiothreitol (DTT) and incubated for 5 min at 100 rpm at 30 °C. Cell suspension was centrifuged at 500 *g* for 5 min at RT and resuspended in 1 mL of BEDS.

Fresh competent cells (40 μL) were mixed with 100-200 ng of DNA in an electroporation cuvette (Bio-Rad, Gene Pulser cuvette gap 2 mm) and incubated on ice for 2 min. Samples were electroporated using a GenePulser® II electroporator (Bio-Rad) using a charging voltage of 1500 V, a resistance of 400 Ω and a capacitance of 25 μF.

After electroporation, samples were resuspended in a cold mixture of 0.5 mL 1.0 M Sorbitol and 0.5 mL YPD, incubated at 30 °C in a 15 mL Falcon tube for 2-4 h and 50-200 μL of the cell suspension were plated on YPD agar plates containing 100 μg mL^{-1} Zeocin and Hygromycin and incubated at 30 °C until colonies appear (2-4 days).

2.2.14. *P. pastoris* clone selection

Colonies were picked, extracted the genomic DNA and checked for correct integration or deletion by PCR screening. Primers for integration: pGAP and AOX1TT.

P. pastoris colony PCR

*DES*1 knock-out transformant colonies were checked for gene deletion by colony PCR according to The Murray Lab protocol, as follows: PCR tubes filled with 5 μL of distilled water were mixed with cells from a colony. Tubes were frozen for 10-15 min, microwaved for 1 min on high power and frozen again for 15 min. The PCR mix was added to the tube to final 25 μL volume, mixed, spinned down and PCR was performed as usual for GoTaq polymerase.

2.3. Cell Cultivation

2.3.1. Stock solutions

10x YNB

13.4 % (w/v) Yeast Nitrogen Base with ammonium sulphate and without amino acids. Filter sterilised. Stored at 4 °C.

500x Biotin

0.02 % (w/v) Biotin. Filter sterilised. Stored at 4 °C

10x Glucose

20 % (w/v) Glucose. Autoclaved at 121 °C for 30 min and cooled down to RT. Stored at RT.

10x Glycerol

10 % (w/v) Glycerol. Autoclaved at 121 °C for 30 min and cooled down to RT. Stored at RT.

2.3.2. Media

YPG medium

2 % (w/v) peptone, 1 % (w/v) yeast extract, 2 % (w/v) glycerol, pH 7.0

BMG (Buffered Minimal Glycerol) and BMD (Buffered Minimal Dextrose) Medium

100 mM Potassium Phosphate pH 6.0, 1.34 % (w/v) YNB, $4{\cdot}10^{-5}$ % (w/v) Biotin, 1 % (w/v) Glycerol or 2 % (w/v) Dextrose. Components are prepared as stock solutions separately, sterilised and mixed together. Stored at RT.

Batch Medium

40 % (w/v) glycerol, 1.8 % (w/v) citric acid, 12.6 % (w/v) ammonium phosphate dibasic ($(NH_4)_2HPO_4$), 0.022 % (w/v) calcium chloride dihydrate ($CaCl_2 \cdot 2H_2O$), 0.9 % (w/v) potassium chloride (KCl) , 0.5 % (w/v) magnesium sulphate heptahydrate ($MgSO_4 \cdot 7H_2O$), 2 mL Biotin, 4.6 mL PTM1 trace salts stock solution. The pH was set to 5.0 with 37 % hydrogen chloride (HCl).

Chemostat Medium

50 % (w/v) glucose, 0.9 % (w/v) citric acid, 4.35 % (w/v) ammonium phosphate dibasic ($(NH_4)_2HPO_4$), 0.01 % (w/v) calcium chloride dihydrate ($CaCl_2 \cdot 2H_2O$), 1.7 % (w/v) potassium chloride (KCl), 0.65 % (w/v) magnesium sulphate heptahydrate ($MgSO_4 \cdot 7H_2O$), 1 mL Biotin, and 1.6 mL PTM1 trace salts stock solution. The pH was set to 5.0 with 37 % hydrogen chloride (HCl).

Fed Batch Feeding Medium

400 % (w/v) glucose, 10 % (w/v) potassium chloride (KCl), 6.45 % magnesium sulphate heptahydrate ($MgSO_4 \cdot 7H_2O$), 0.35 % (w/v) calcium chloride dihydrate ($CaCl_2 \cdot 2H_2O$), 6 mL Biotin, 15 mL PTM1 trace salts solution and 0.2 mL of antifoam Struktol J650.

Trace Salt Stock Solution (PTM1)

6.0 % (w/v) cupric sulphate pentahydrate ($CuSO_4 \cdot 5H_2O$), 0.08 % (w/v) sodium iodide (NaI), 3.36 % (w/v) manganese sulphate monohydrate ($MnSO_4 \cdot H_2O$), 0.2 % sodium molybdate dihydrate ($Na_2MoO_4 \cdot 2H_2O$), 0.02 % boric acid (H_3BO_3), 0.82 % cobalt chloride ($CoCl_2 \cdot 6H_2O$), 20.0 % zinc chloride ($ZnCl_2$), 65.0 % ferrous sulphate heptahydrate ($FeSO_4 \cdot 7H_2O$), and 5.0 mL sulphuric acid (H_2SO_4).

2.3.3. Buffers

PBS

137 mM sodium chloride (NaCl), 2.7 mM potassium chloride (KCl), 10 mM disodium phosphate (Na_2HPO_4), 1.8 mM monopotassium phosphate (KH_2PO_4). Adjust the pH to 7.4 with hydrogen chloride (HCl).

Potassium Phosphate Buffer

First, 1 M stock solutions of dipotassium phosphate (K_2HPO_4) and monopotassium phosphate (KH_2PO_4) were prepared. To obtain a 10 mM buffer at pH 6.0, 1.32 mL of 1M K_2HPO_4 and 8.68 mL of 1M KH_2PO_4 were combined and diluted to 1 L with distilled water. pH is calculated according the Henderson-Hasselbalch equation 2.2:

$$\mathrm{pH} = \mathrm{pK'} + \log\left\{\frac{\text{proton acceptor}}{\text{proton donor}}\right\} \tag{2.2}$$

where pK′ = 6.86 at 25 °C.

2.3.4. Fluconazole treatment

Lyophilised Fluconazole was diluted to 5 mg mL^{-1} in DMSO. The stock solution was diluted to 100 μg mL^{-1} in sterile distilled water, and added to the culture medium BMD at final concentration of 0.6 μg mL^{-1}.

2.3.5. Shake Flask Cultivation

For small-scale cultivations, first a fresh colony was grown overnight in 5 mL YPD-Zeo-Hyg at 30 °C and 150 rpm and used to inoculate a 25 mL BMG culture at an initial OD_{600} of 0.1. Cells were incubated at 25 °C, 150 rpm until they reach exponential phase (Minimal medium adaptation). The screening cultures were performed in 1 L baffled shake flasks with 100 mL of BMD medium inoculated to an initial OD_{600} of 0.1 and incubated as previously until cells reached the end of exponential phase.

Dry cell weight (DCW), Fab yield, cell wall porosity and membrane fluidity were determined from shake flask cultures.

2.3.6. Inoculum

Inoculum cultures were grown in 1 L baffled shake flasks with 100 mL YPG + 100 μg mL^{-1} Zeocin (+ 100 μg mL^{-1} Hygromycin for mutant strains cultures). Cells were grown for 24 h at 25 °C and

130 rpm in a Khuner LS-X incubator. Shake flasks were inoculated from cryostocks of the strains, grown, harvested by centrifugation and resuspended in batch medium to be inoculated into the bioreactor.

2.3.7. Chemostat cultivations

Chemostat cultivations were performed at a working volume of 1 L in a 2 L bench-top bioreactor (Biostat B or Biostat B+, Braun Biotech) connected to a DCU digital control unit and the MFCS/win process supervisory system (Braun Biotech International). Cells were grown under glucose-limited conditions at a constant dilution rate of 0.1 ± 0.01 h^{-1} using a peristaltic pump (Ismatec) to control the feeding. Cultivations were carried out using the batch medium and chemostat medium, with the antifoam Glanapon 2000 (0.2 mL per litre of chemostat medium). The pH value was maintained at 5.0 by addition of 15 % (v/v) ammonium hydroxide, the temperature was set to 25 °C and an overpressure of 1.2 bars. The aeration rate was 1 vvm controlled by means of thermal mass-flow controllers (TMFC; Bronkhorst Hi-Tech). The oxygen supply was varied by varying the percentage of oxygen in a gas mixture of air and N_2 while stirring the culture at a constant speed of 700 rpm. Dissolved oxygen (DO) saturation was monitored online with an oxygen probe (Mettler Toledo). Samples were taken for each physiological steady state condition after at least five residence times.

2.3.8. Fed-batch cultivations

Fed-batch cultivations were carried out in a 5 L Biostat B Bioreactor (Braun Biotech) working at initial volume of 2 L and finishing the process at approximately 4 L. All fed-batch cultivations were carried out at a specific growth rate of 0.15 h^{-1}. The culture conditions were monitored and controlled at the following values: temperature, 25 °C; pH, 5.0 with addition of 30 % (v/v) ammonium hydroxide (NH_4OH); pO_2, above 20 % saturation by controlling the stirring speed between 600 and 1200 rpm and using mixtures of air and O_2 at aeration within 1.0 and 1.25 vvm. Water evaporation losses were minimised during the processes using an exhaust gas condenser with cooling water at 8 °C.

The standard fermentation strategy consisted of two phases. First, the batch phase starts with a standard carbon source concentration of 40 g L^{-1} and it is performed using the batch medium. During this step, yeast grows at maximum specific growth rate until the depletion of the C-substrate achieving a moderate concentration of biomass (≈ 20 g L^{-1}). Thereafter, the fed-batch phase starts, where the culture reaches high concentrations of biomass and product. The fed-batch phase was carried out by adding feeding medium. The fermentation strategy during the fed-batch phase aimed to achieve pseudo steady-state conditions for specific rates during carbon-limiting growth. A pre-programmed exponential feeding rate profile for substrate addition derived from mass balance equations to maintain a constant specific growth rate (μ) was implemented [168]. This open-loop control structure allows maintaining a constant μ, which enhances process reproducibility and facilitates the systematic study of growth rate-related effects on heterologous protein production. The equations derived from the fed-batch substrate balance used to apply this strategy were described elsewhere [168, 169]. A constant biomass to substrate yield ($Y_{X/S}$ = 0.5 g_{DCW} g_S^{-1}) was considered to determine the initial feed rate. The feeding medium was added by automatic micro-burettes (MicoBU-2031, Crison).

2.4. Analytical methods

2.4.1. Cell culture analytical methods

Biomass determination

Cell density analyses were always performed by triplicate and the relative standard deviation (RSD) was no higher than 4 %.

Dry Cell Weight (DCW)

DCW was determined by filtering a known volume of cultivation broth using pre-weighted dried glass microfibre filters (0.47 μm pore size, Millipore). Then the filters were washed with two volumes of distilled water, and dried to constant weight at 105 °C for 24 h. Cell weight was defined as the weight filter difference before and after cell filtration.

Optical density

Alternatively, biomass was measured by optical density at 600 nm. Samples were diluted with distilled water to be on the range of absorbance 0.1-0.9.

Total protein concentration

Total protein was determined with the bicinchoninic acid protein assay kit (Pierce BCA Protein Assay) according to the manufacturer's instructions.
Bovine serum albumin (BSA) was used as the protein standard for the calibration curve.

Quantification of extracellular metabolites

Samples were clarified at 6000 rpm for 3 min in a micro centrifuge (Minispin, Eppendorf) and subsequently filtered through 0.45 μm-filters (Millipore). Glucose, glycerol, ethanol, arabitol and organic acids concentrations were determined by HPLC with a HP 1050 liquid chromatography (Dionex Corporation) using a ionic exchange column (ICSep ICE COREGEL 87H3 column, Transgenomic Inc.). As mobile phase, 8 mM sulphuric acid was used. Metabolites were quantified with the Chromeleon 6.80 Software (Dionex Corporation).

Off-gas analysis

Accurate estimation of oxygen uptake rate (OUR), carbon dioxide production rate (CPR), and respiratory quotient (RQ) was carried out through O_2 and CO_2 balances [170].

BlueSens sensors

When chemostat cultivations were performed in a Biostat B, online concentrations of the O_2 and CO_2 in the exhaust gas of the bioreactor cultivations were determined after being cooled in a condenser (4 °C), dried with two silica gel columns and subsequently analysed using specific O_2 and CO_2 sensors (BCP-CO2 and BCP-O2. BlueSens).

Mass spectrometry

Biostat B+ chemostat cultivations used a quadrupole mass spectrometer (Balzers Quadstar 422, Pfeiffer-Vacuum) for on-line exhaust gas analysis. Exhaust gas humidity was reduced by using a condenser (water at 4 °C) and two silica gel columns. The Faraday cup detector was used for its simplicity, stability, and reliability, determining responses of m/z corresponding to the major gas peaks (N_2: 28, O_2: 32, CO_2: 44, Ar: 40). Normalised mass spectrometer signals were used to reduce errors caused by variations on operating conditions such pressure and temperature as well

as others that can generate some drift and noise of signals. Multivariate calibration was performed by ordinary least squares (OLS) minimisation with suitable standard calibration mixtures according to the components to be analysed and its concentration range. The total humid off-gas flow rate was not measured directly and it was calculated by inert balance around the reactor. To properly estimate this flow rate, determination of water composition is necessary and it can be calculated from the quotient between the off-gas O_2 composition without bioreaction, due to water stripping, and the corresponding inlet O_2 molar fraction. Inlet air composition was obtained from a 12 h measurement average before inoculating.

Process parameters determination, consistency check and data reconciliation

Specific rates (q_i) and yields are parameters of capital importance for comparing different culture conditions and allow the identification of changes in the physiological cell state that can impact into product quality [33]. Their calculation is based on the conversion rates (r_i) determined in the general mass balance of the cultivation. Specific rates are typically conversions rates related to the biomass concentration. Yields are defined as ratios between rates, and positive.

The consistency of the measurements was checked by standard statistical tests considering elemental balances as constraints [171]. With the current experimental set-up it was possible the measurement of the five key specific rates in the black-box process model: biomass generation (μ), glucose uptake (q_S), product formation (q_P), oxygen uptake (q_{O2}), and carbon dioxide production (q_{CO2}). The carbon balance and the redox balance were used as constraints and protein production considered negligible in these balances. So, the system is overdetermined and the degree of redundancy is the same as the number of constraints. This fact can be used to check the measurements for gross errors or unidentified metabolites, respecting the covariance for each measurement [172], and to improve the accuracy of the measured conversion rates by data reconciliation methods [173]. The h value given by the sum of the weighted squares of the residuals (ε) is the output of the statistical test for the presence of gross errors or neglected components.

$$h = \varepsilon P^{-1} \varepsilon \tag{2.3}$$

If h exceeds the threshold value that depends on the significance level α (0.95 in this work) and degree of redundancy according to the χ^2 distribution, it is concluded that there are significant errors in the measurements or any compound has not been taken into account in the black box process model. The variances of all specific rate measurements were considered uncorrelated and estimated by replicates and/or error propagation. The χ^2-test performed for all the experimental data obtained from chemostat cultivations showed the measurements satisfied mostly the stoichiometric model and hence, both C-balance and e-balance.

Data reconciliation procedures are also based on the use of elemental balances according to a black box reaction scheme to improve the accuracy of the measured specific rates or yields and also to determinate the unknown specific rates [171]. A measurement error vector δ is found by using a least squares approach to calculate the reconciled vector which includes the best estimates of reaction rates to fit all constraints imposed.

Cell disruption and protein extraction

High-pressure homogenization

Cells from the cultures were harvested by centrifugation (4500 *g*, 3 min, 4 °C) and pellets were washed twice in cold PBS (pH 7.0) in order to remove all media components and other contaminants. Cells were then resuspended in 8 mL of cold breaking buffer (PBS, pH 7.0, 1mM

PMSF) and disrupted by high-pressure homogenisation using a One-Shot Cell Disrupter (Constant Systems). Once disrupted, homogenates were clarified by centrifugation (15000 *g*, 30 min, 4 °C). Supernatants were collected and stored as soluble cytosolic fraction (SCF) while pellets were kept as the insoluble membrane fraction (IMF). The protease inhibitor (1 mM PMSF) and chilling conditions were always used during the whole process to minimise the risk of protein degradation by endogenous proteases, as well as to preserve protein properties in the case of low temperature.

Evaluation of cell disruption efficiency

Cell number was determined after each disruption pass by means of flow cytometry assays (Guava EasyCute™ Mini cytometer, Millipore). The degree of disruption was expressed as Equation 2.4:

$$X = 100 \cdot \frac{n\text{-}n_i}{n} \ (\%) \tag{2.4}$$

where *X* (%) is the degree of disruption; *n*, the initial number of cells before disruption; n_i, the number of non-disrupted cells after each pass.

Protein extraction from insoluble membrane fraction (IMF)

Protein extraction was carried out in chilly conditions. Fraction pellets were resuspended by pipetting in 1 mL extraction buffer supplemented with detergent and then vortexed. Extracts were incubated in gently shaking at 4°C, clarified by centrifugation (2300 *g*, 5 min, 4 °C) and supernatants were stored as insoluble membrane fraction (IMF) extracts.

Extraction detergent and buffers

For the initial study focused on a screening for the detergent and buffer optimisation, three different buffers were compared for the target protein extraction.

- Buffer A: 50 mM Tris-HCl pH 7.4, 300 mM NaCl, 5 mM EDTA, 1 mM PMSF
- Buffer B: 10 % glycerol, 20 mM HEPES pH 7.0, 100 mM NaCl, 1 mM PMSF
- Buffer C: 8 % glycerol, 10 mM sodium phosphate pH 8.0, 5 mM EDTA, 500 mM NaCl, 1 mM PMSF.

In addition, all the extraction buffers were also supplemented with 1 % of three different detergents, Tween 20, Triton X100 and CHAPS for the detergent and buffer screening.
Once the optimal combination of buffer and detergent was selected, different concentrations of CHAPS were tested for an improved Fab extraction. They were also screened different incubation times. In this sense, extractions combining 1 - 2.5 % CHAPS and 0 h, 2 h and 16 h (overnight) incubation times were performed and compared.

ELISA

Fab 2F5 was quantified by sandwich ELISA in the secreted fractions, as well as in the SCF and the IMF. 96-well microtiter plates (MaxiSorb) were coated with anti-*h*IgG (Fab specific, 1:1.000 in PBS, pH 7.4) overnight at RT. Samples were serially diluted in dilution buffer (PBS pH 7.4, 1 % (v/v) Tween20, 2 % (w/v) bovine serum albumin (BSA)) and incubated in gently agitation for 2 h at RT. A papain digested purified normal human Fab/kappa from IgG was used as a standard protein at a starting concentration of 200 ng mL^{-1}. After each incubation step plates were washed three times with washing buffer (PBS pH 7.4, 1 % Tween20). Anti-kappa light chain - alkaline phosphatase conjugate was added as secondary antibody (1:1.000 in dilution buffer) and incubated for 1 h at

RT. Finally, plates were stained with *p*-nitrophenyl phosphate (pNPP) (1 mg mL^{-1} in coating buffer, 0.1 N Na_2CO_3/$NaHCO_3$ pH 9.6) and read at 405 nm (reference wavelength 620 nm).
Data analysis was performed by using the standard curve (*h*Fab standard) and a polynomial function.

2.4.2. Plasma membrane fluidity determination by anisotropy measurements

Dynamic and structural characteristics of membranes can be changed, either by changing the environmental conditions, the molecular composition of the membrane, or by adding foreign molecules that interact with membrane constituents. Cells can control their fluidity by modulation of their membrane composition in order to maintain an optimal level of fluidity [224]. Fluidity is a vital parameter of membrane function, affecting permeability and functions of membrane-associated proteins, such as receptors, enzymes and transporters [225].
Usually, the fluidity of a membrane is measured as anisotropy by fluorescence polarisation of a probe [224]. A lipophilic fluorescent molecule, 1-6-diphenyl-1,3,5-hexatriene (DPH), is commonly used in such experiments and the measurement of the steady-state anisotropy of DPH is the most common technique to estimate ordering of the membrane lipid constituents, which is inversely proportional to membrane fluidity [226].
The origin of anisotropy is the existence of transition moments for absorption and emission that lie along specific directions within the fluorophore structure. In homogeneous solution the ground-state fluorophores are all randomly oriented. When exposed to polarised light, those fluorophores that have their absorption transition moments oriented along the vector of the incident light are preferentially excited. Hence the excited-state population is partially oriented.

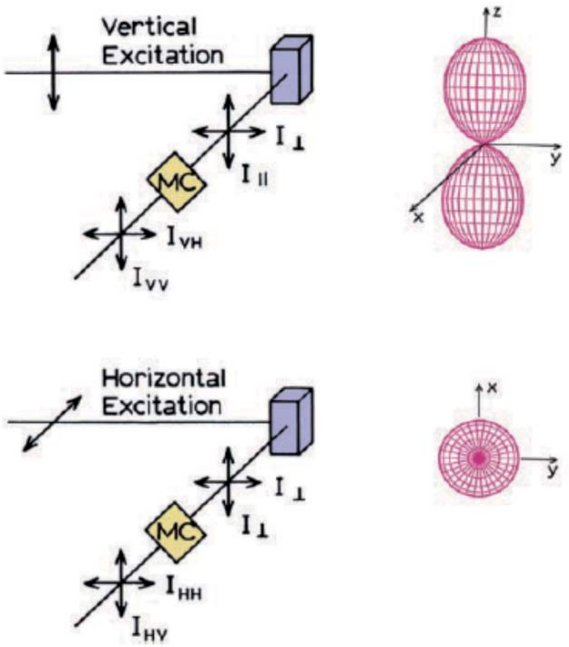

Figure 2.5: General scheme of Anisotropy determination. From [227]

The measurement of fluorescence anisotropy is illustrated in Figure 2.5. The sample is excited with vertically polarised light and the emission is observed. Different transmission efficiencies for vertically and horizontally polarised light are described, thus the rotation of the emission polariser changes the measured intensities. The measured intensity ratio is different from the true value by a factor of *G*. To calculate the actual intensity ratio, the *G* factor is described as the ratio

of sensitivities of the detection system for vertically and horizontally polarised light. The *G* factor is easily measured using horizontally polarised excitation, where the excited-state distribution is rotated to lie along the observation axis and the horizontally and vertically polarised components are equal [227]. The anisotropy is calculated as Equation 2.5.

Membrane fluidity was assessed by measuring fluorescence anisotropy of 1,6-diphenyl-1,3,5-hexatriene (DHP), following incorporation into the plasma membrane. A LS 55 Luminescence Spectrometer (Perkin Elmer) with fixed excitation and emission polarisation filters was used to measure fluorescence intensity parallel and perpendicular to the polarisation phase of the exciting light. DHP was excited at 360 ± 10 nm and emission was measured at 450 ± 10 nm. The measured fluorescence intensities were corrected for background fluorescence and light scattering from the unlabelled sample. The degree of fluorescence anisotropy (*r*) was calculated according to Equation 2.5:

$$r = \frac{I_{VV} - G \times I_{VH}}{I_{VV} + 2G \times I_{VH}}; \; G = \frac{I_{HV}}{I_{HH}} \tag{2.5}$$

I_{VV} and I_{VH} are the fluorescence intensities determined at vertical and horizontal orientations of the emission polariser, when the excitation polariser is set in the vertical position. I_{HV} and I_{HH} are the fluorescence intensities determined at vertical and horizontal positions of the emission polariser when the excitation polariser is set horizontally. *G* is a correction factor for background fluorescence and light scattering.

Cells were suspended in 10 mM potassium phosphate buffer (pH 6.0) to a final OD_{600} of 2.5 (500 μg DCW mL^{-1}). DHP stock solution (100 μM in tetrahydrofuran) was added at a final concentration of 0.5 μM, the suspension was incubated in the dark at 25 °C and 150 rpm for 30 min, clarified (4000 rpm, 3 min, 20 °C) and resuspended again in 10 mL of potassium phosphate buffer. Following labelling, 3 mL of cells were placed in 1-cm path length quartz cuvettes. Fluorescence anisotropy was determined in triplicates.

2.4.3. Electron microscopy

An electron microscope is similar to a light microscope, but instead of using electrons at a wide range of wavelengths, a high-energy beam of electrons at the same wavelength is used. In TEM, electrons emitted are focused by a set of condenser lenses into a coherent parallel beam that pass through the sample to create the image. Electron-dense areas in the sample deflect the electrons from their straight paths, producing darkened areas that form the image.

Analysis of subcellular structures in living or fixed yeast cells using light microscopic techniques is a particular experimental challenge due to the small size of the cells. Resolution is rather limited and microscopic results are often not very satisfying. Furthermore, the thick yeast cell wall is highly diffractive and causes interference patterns [252]. Many of these limitations can be partially overcome by using specialised equipment and careful sample preparation.

A major advantage of a small cell is the excellent statistics of localisation patterns: the homogeneity of a staining pattern and the significance of structural features can be assessed by visual inspection of a large population of cells, which is easy to achieve with yeast like *P. pastoris*.

When preparing cells for TEM studies, different steps of sample preparation are involved [253]:

- Fixation. The most common fixation method used for TEM of yeast is based on chemical cross-linking. For ultrastructural analysis, fixation is accomplished in two steps: treatment with an aldehyde cross-linker followed by osmium or potassium permanganate.

- Post-Fixation. Initial fixation with aldehyde cross-linkers preserves overall cell structure, but does not fix lipids. Osmium reacts strongly with unsaturated fats, providing good fixation of membranes and lipids.
- Dehydration. Cells are dehydrated by incubation in increasingly concentrated ethanol (or acetone) solutions (25, 50, 75, 95, 100 %) in order to remove water before the resin is infiltrated.
- Infiltration, embedding, thin-sectioning. Preparation of cells for TEM derives from the need to produce ultra-thin sections that will allow passage of some electrons. Cutting thin sections requires support of cell structure by resins that infiltrate the molecular matrix of the cell and solidify, allowing sections as thin as 50 to 100 nm to be cut. Unless cells are well infiltrated with resin, the thin sections will have large holes that prevent or limit obtaining ultrastructural data. Yeast is notoriously difficult to infiltrate and the use of low viscosity resins, such as Spurr's resin [254] or ultra-low viscosity formulas, may help to produce well-infiltrated samples.
- Post-staining. Cut samples in the grids are stained with acetate before viewing [175].

Cell morphology studies were carried out at the Microscopy Service of the UAB, using a similar protocol as described by Lunsdorf *et al.* [174].
Samples from bioreactor cultivations were immediately fixed at RT in 2.5 % (v/v) glutardialdehyde in 20 mmol L^{-1} HEPES buffer (pH 7.1) for 30 min. Cells were stored until embedment for several days at 4 °C. Then, cells were fixed in 1 % (w/v) osmiumtetroxide in 75 mM cacodylate buffer (pH 7.2). Cells were dehydrated on ice in ethanol series, stained with 1 % (w/v) uranylacetate in 70 % (v/v) ethanol, infiltrated with Spurr resin and finally polymerized at 70 °C for 8 hours. Ultrathin sections (70 nm) were cut with a diamond knife using an ultramicrotome (EM UC7, Leica), picked with Formvar-coated 300 mesh copper grids and post-stained with uranyl acetate and lead citrate as described previously [175].
Ultrathin sections were analysed with an energy-filtered transmission electron microscope (JEM-1400, Jeol) and images were captured with a CCD ES1000W Erlangshen camera (Gatan) using as software the Digital Micrograph (Gatan).

2.4.4. Lipid analysis

Cell homogenisation, protein quantification and lipid extraction

Cell homogenates were obtained by shaking cell pellets in presence of glass beads using a Disruptor Genie (Scientific Industries Inc.) at 4 °C for 10 min. Proteins were precipitated with trichloroacetic acid (TCA) at a final concentration of 10 % to circumvent disturbing components and quantified by the method of Lowry *et al.* [176]. Briefly, proteins were diluted to a final concentration of 10 % in a chilled mix of 50 % (v/v) TCA in water, incubated on ice for 1 h, centrifuged at max. speed and 4 °C for 10 min. Supernatant was discarded by aspiration and the pellet resuspended in 100 μL 0.1 M sodium hydoxide (NaOH), 0.1 % SDS solution. Samples were heated at 56 °C for 30 min and mixed with 300 μL of water and 2 mL of fresh prepared buffer A (2.2 % potassium sodium tartrate, 1% copper sulphate pentahydrate ($CuSO_4 \cdot 5H_2O$), 20% SDS, 2% sodium carbonate (Na_2CO_3) in 0.1 M sodium hydroxide (NaOH)) and incubated at RT for 10 min. 200 μL of folin-ciocalteu's reagent (1:2) were added, vortexed and incubated at RT for at least 30 min before its Absorbance at 546 nm was determined.
Lipids from homogenates were extracted according to Folch *et al.* [177]. Cell fraction

corresponding to 1 mg total cell protein was mixed with 4 mL chloroform: methanol ($CHCl_3$: MeOH, 2:1) in clean Pyrex tubes. Samples were extracted by vigorous shaking in a Vibrax® orbital (IKA) for 30 min. 1 mL of 0.034 % (w/v) magnesium chloride ($MgCl_2$) was added and extraction was continued for 30 min. Then samples were centrifuged (1500 rpm, 3 min, RT), the aqueous phase was removed and the organic phase washed with 1 mL 2N potassium chloride / methanol (KCl / MeOH, 4:1). Phase was shaken for 1 min, centrifuged, aqueous phase discarded and the remaining organic phase was washed with 1 mL methanol / water / chloroform (MeOH / H_2O / $CHCl_3$, 48/47/3 (v/v/v)) and shaken again for 10 min. The final organic phase was transferred to a new pyrex tube and taken to dryness under a stream of nitrogen.
The obtained amounts for all lipids were related to 1 mg total cell protein.

Glycerolipid analysis

Fatty acids were converted to methyl esters by methanolysis adding 2.5 % sulphuric acid in methanol and heating at 85 °C for 90 min. Fatty acid methyl esters were extracted two times in a mixture of light petroleum and water (3:1 v/v), centrifuged (1500 rpm, 3 min, RT) and the organic phase transferred to a new Pyrex tube. The solvent was removed under a stream of nitrogen. Samples were analysed by gas chromatography (HP 6890 Gas-chromatograph, Agilent Technologies) using an HP-INNOWax capillary column (15 m x 0.25 mm i.d. x 0.50 µm film thickness) with helium as carrier gas. Fatty acids were identified by comparison to the fatty acid methyl ester standard mix GLC-68B (NuCheck, Inc.).

Phospholipid analysis

Lipid extracts were loaded manually onto ALUGRAM® SIL G plates (Macherey-Nagel). Individual phospholipids were separated by two-dimensional thin layer chromatography. Chloroform / methanol / 25 % ammonia (65:35:5; v/v/v) was used as first, and chloroform / acetone / methanol / acetic acid / water (50:20:10:10:5; v/v/v/v/v) as second dimension solvent. Phospholipids were visualised by staining with iodine vapour, scraped off and quantified by the method of Broekhuyse [178]. Briefly, samples were incubated at 100 °C for 15 min. 0.2 mL of an acid-mixture (90 % (v/v) sulphuric acid (H_2SO_4), 10 % (v/v) perchloric acid ($HClO_4$)) were added and hydrolysed at 180 °C into heating plates under the hood. In this step dangerous acidic fumes are formed. Samples were cooled down at RT under the hood, then 4.8 mL of freshly prepared molybdate / Aminonaphthol sulphonic acid (ANSA) mixture (500:22 (v/v)) was added, vortexed and incubated at 105 °C for 30 min. Samples were clarified (1500 rpm, 3 min, RT) and the samples were measured spectrophotometrically at λ 830 nm. The amount of phosphate for each sample was calculated as a relative amount of the total phosphate (%).
Total phospholipids were estimated by the same procedure, using a standard curve with inorganic phosphate at known amounts.

Sterol analysis

Individual sterols were analysed by gas-liquid chromatography-mass spectrometry (GC-MS) after alkaline hydrolysis and subsequent lipid extraction [179]. Lipid extracts were resuspended in 0.6 mL methanol, 0.4 mL 0.5 % (w/v) pyrogallol dissolved in methanol and 0.4 mL 60 % (w/v) aqueous potassium hydroxide solution. 5 μL of a cholesterol solution (2 mg mL^{-1} in ethanol) were added as an internal standard. Tubes were heated in a sand bath for 2 h at 90 °C, extracted three times by adding 1 mL *n*-heptane, vortexing, and centrifuging (1500 rpm, 3 min, RT), and the upper phase transferred into a new tube. Samples were derivatised by adding 10 μL of *N'O'*-bis(trimethylsilyl)-trifluoracetilamide.

GLC-MS was performed on a Hewlett-Packard 5690 Gas-Chromatograph equip-ped with a mass selective detector (HP 5972) using an HP 5-MS capillary column (30 m x 0.25 mm i.d. x 0.25 μm film thickness). Sample aliquots of 1 μL were injected in the splitless mode at 270 °C injection temperature with helium as carrier gas and a flow rate set to 0.9 mL min in constant flow mode. The temperature program was 100 °C for 1 min, 10 °C min^{-1} to 250 °C, and 3 °C min^{-1} to 310 °C. Sterols were identified by their mass fragmentation pattern.

Neutral lipid analysis

For neutral lipid analysis, lipid extracts were applied to ALUGRAM® SIL G plates (Macherey-Nagel), and chromatograms were developed in an ascending manner to half of the plate using the solvent system light petroleum / diethyl ether / acetic acid (35:15:1; v/v/v). Then plates were briefly dried and further developed to the top using the solvent system light petroleum / diethyl ether (39.2:0.8; v/v). To visualise the bands, plates were dipped into a developing solution consisting of 0.63 g manganese chloride tetrahydrate ($MnCl_2 \cdot 4H_2O$), 60 mL water, 60 mL of methanol and 4 mL of concentrated sulphuric acid, briefly dried and heated at 105 °C for 30 min. Bands were scanned at 400 nm with a TLC Scanner 3 (winCATS Software, CAMAG) and quantified using triolein, cholesteryl oleate and ergosterol as standards.

Sphingolipid analysis

For lipid extraction, 100 mg frozen aliquots were processed. Samples containing 300 μg protein were spiked with 30 μL of a sphingolipid internal standard mix (0.15 nmol *N*-(dodecanoyl)-sphing-4-enine, 0.15 nmol *N*-(dodecanoyl)-1-β-glucosyl-sphing-4-enine, 4.5 nmol C17 sphinganine; Avanti Polar Lipids Inc.), suspended in 6 mL propan-2-ol / hexane / water (60:26:14; v/v) and incubated at 60 °C for 30 min slightly modifying a protocol of Markham *et al.* [180]. During the incubation, samples were briefly vortexed and sonicated after 0, 10, 20 and 30 min. Then, extracts were cleared from cell debris by centrifugation, dried under a stream of nitrogen, dissolved in 800 μL tetrahydrofuran/methanol/water (4:4:1; v/v) and stored under argon at -20 °C. For analysis, samples were solubilised by gentle heating and sonication.

Molecular species separation was achieved by Ultra-Performance Liquid Chromatography (UPLC) using an ACQUITY UPLC® system (Waters Corp.) equipped with an ACQUITY UPLC® HSS T3 Column (100 mm x 1 mm, 1.8 μm; Waters Corp.). Aliquots of 2 μL were injected in partial loop with needle overfill mode. The flow rate was 0.10 mL min^{-1}, and the separation temperature was 35 °C. Solvent A was methanol/20 mM ammonium acetate (3:7 v/v) containing 0.1 % (v/v) acetic acid and solvent B was tetrahydrofuran/methanol/20 mM ammonium acetate (6:3:1 v/v/v) containing 0.1 % (v/v) acetic acid. All lipids were separated with linear binary gradients following the same scheme: start conditions (50, 65, 80 or 100 % solvent B) held for 2 min, linear increase to 100 % solvent B for 8 min, 100 % solvent B held for 2 min and re-equilibration to start conditions in 4 min. The start conditions were 80 % solvent B for ceramides (Cer) and hexosylceramides (HexCer) and 65 % solvent B for inositol containing sphingolipids.

Chip-based nanoelectrospray ionisation was achieved with a TriVersa Nanomate® (Advion Inc.) in both positive and negative ion modes with 5 μ internal diameter nozzles, a flow rate of 250 nL min^{-1} and a voltage of 1.3 V. The ion source was controlled with the Advion ChipSoftManager software.

Fungal sphingolipid molecular species were detected with 4000 QTRAP® tandem mass spectrometer (AB Sciex) by monitoring

- the transition from $[M+H]^+$ molecular ions to dehydrated long chain base (LCB) fragments for Cer, HexCer and LCB
- the loss of phosphoinositol containing head groups for inositol containing sphingolipids [181, 182].

Dwell time was 30 ms and MS parameters were optimised to maximise detector response.

3

Transcriptomic analysis

3.1. Introduction

The availability of completely sequenced and well-annotated genomes of organisms has created opportunities for studying numerous aspects of gene function at the genomic level. Gene expression, defined by steady-state levels of cellular mRNA, was one of the first aspects of gene function amenable to genome-scale measurement [183]. Genome-wide analytical tools like DNA microarrays are regarded as data mining sources for physiological effects, stress regulation and host engineering.

3.1.1. DNA Microarrays

Microarrays involve the production of a series of PCR products (or synthetic oligonucleotides), which correspond to all the predicted genes from a specific organism. They assess the amount of a specific transcript in a specific sample at a specific time [184]. Fluorescent cDNA microarray assays use direct incorporation of tagged nucleotides in the cDNA prepared by reverse transcription of mRNA from the source of interest (Figure 3.1). Database analysis make it possible to define patterns of genes expressed consistently across experiments [183].
Initial processing of data requires the application of significance filters to the raw data set so that only meaningful measurements enter into downstream analysis. It has to be considered that the amount of mRNA present does not necessarily correlate with the amount of protein made [184].

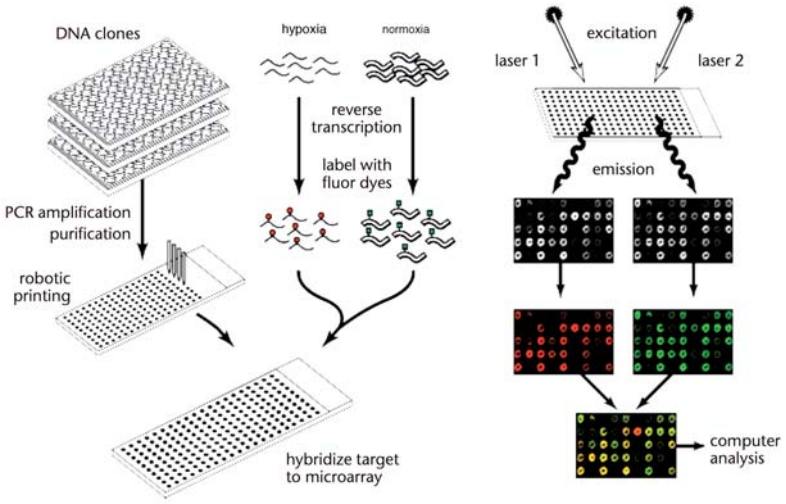

Figure 3.1: Scheme of microarray proceeding. Adapted from [185]. Microarrays are artificially constructed grids of DNA, such that each element of the grid probes for a specific RNA sequence. The basic technique involves extraction of RNA from biological samples, copied while incorporating either fluorescent nucleotides or a tag later stained with fluorescence. The labelled RNA is then hybridised to a microarray for a period of time, after which the excess is washed off and the microarray is scanned under laser light.

3.1.2. Cluster analysis

The goal of cluster analysis is to identify patterns of similarities and differences among samples. If two genes are similarly expressed, it can be hypothesised that the respective genes are co-regulated and possibly functionally related [186]. Clustering can be defined as the process of separating a set of objects into several subsets (clusters) on the basis of their similarity. The aim is to find clusters which members are similar to each other, but distant to members of other clusters in terms of gene expression.

A number of tools for clustering have been developed, which are freely available. In general, these are based on conventional statistical techniques [183]. K-means algorithm [187] is a commonly used clustering method because it is based on a very simple principle and provides good results. This algorithm partitions *N* genes into *K* clusters, where *K* is pre-determined by the user [186].

3.1.3. The impact of oxygen on the transcriptome of recombinant *P. pastoris*

The impact of oxygen limitation on recombinant protein production in *P. pastoris* was first studied by Baumann and co-workers [68], showing a significant increase of the specific production rate of an antibody fragment. In a subsequent study, the impact of oxygen availability on the physiology of recombinant *P. pastoris* was studied integrating transcriptomic, proteomic, metabolic flux and metabolomic analyses [69, 82, 188]. In response to oxygen limitation, a wide range of transcriptional modifications occur, resulting in extensive changes in cellular protein levels and activities, highlighting the ones related to cell respiration, lipid metabolism, cell membrane and cell wall structure [85]. Increased transcript levels were observed for a number of enzymes that catalyse oxygen-consuming reactions of the ergosterol pathway (*ERG1, ERG3, ERG5, ERG11* and *ERG25*). Similarly, sphingolipid synthesis genes (*SUR2, SCS7, DES1* and *SLD1*) were also upregulated under hypoxic conditions, as all these enzymes need molecular oxygen as substrate [69].

3.2. Results and discussion

A study of the transcriptomic changes under hypoxic conditions focused on the genes related to lipid metabolic pathways was carried out using transcriptomic data from Baumann *et. al.* [69] in order to select the genes to further investigate its role on membrane composition and it effect on recombinant protein secretion.

3.2.1. *k*-means clustering

Transcriptional data corresponding to genes related to lipid metabolism were extracted from the transcriptional dataset from Baumann *et. al.* [69], and data from control strain (*P. pastoris* X33, wild-type) and the Fab producing strain was analysed in terms of transcriptional differences between hypoxic and normoxic conditions.

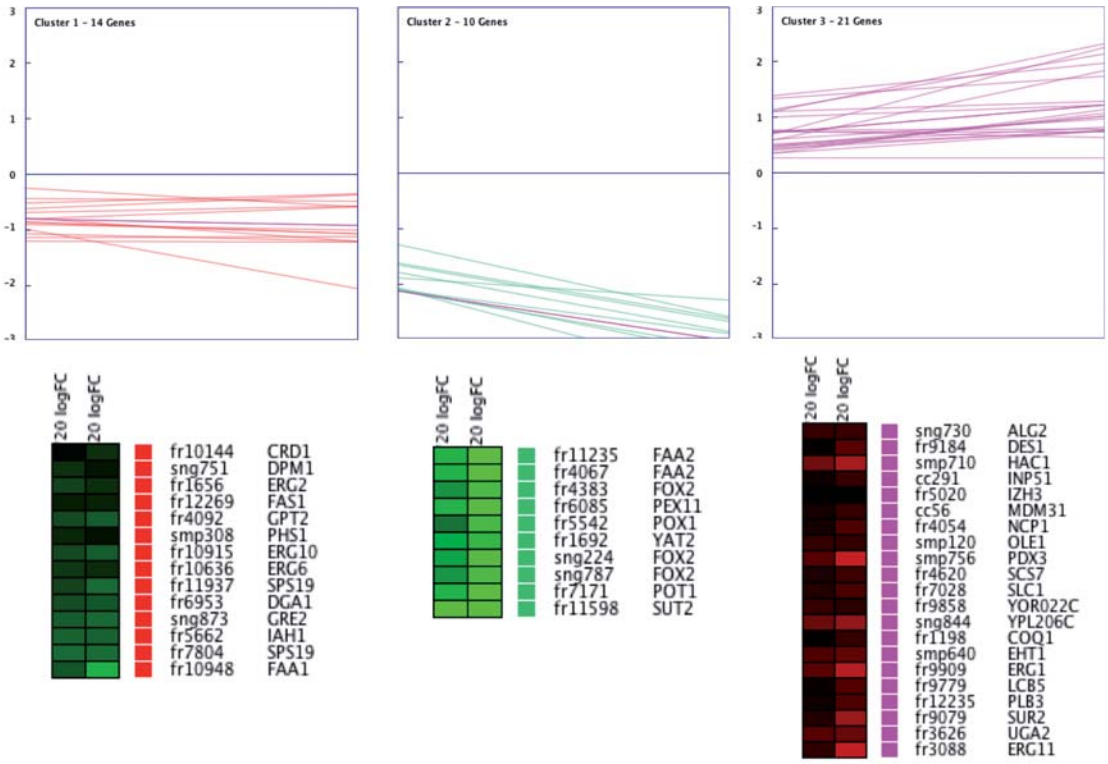

Figure 3.2: Cluster analysis of the genes related to lipid metabolism from [69], using Euclidean distance and k = 3. Log2 FC of the control strain (X33, left) and the reference strain (X33-Fab, right) were used. Red labels denote higher levels of hypoxia versus normoxia, and green labels lower levels of transcript in hypoxia compared to normoxia.

First, a threshold of *p*-values ≤ 0.05 and fold change FC $\geq \pm 1.5$ were chosen to identify significantly regulated genes. Then, selected genes were subjected to k-means cluster analysis using the Genesis tool (`http://genome.tugraz.at`). A k-means clustering using the log2 of the fold change as input file was performed, and the Euclidean distance and a k = 3 were selected as running settings. Obtained results are shown in Figure 3.2.

Cluster 1 contained genes from fatty acid, phospholipid, sterol and non-polar lipid pathways, with repressed transcripts in hypoxic compared to normoxic conditions and with similar levels of repression for the two strains.

Cluster 2 was mainly composed of genes from the fatty acid metabolism, which were downregulated in hypoxic conditions, but with a notable effect on the recombinant strain.

Genes from cluster 3, with induced transcripts in hypoxic compared to normoxic conditions, were potentially candidates to be used for gene modification. This cluster was mainly enriched with genes from the ergosterol and sphingolipid pathways, as some of their enzymes are oxygen-dependent.

3.2.2. Gene mapping

Transcriptional changes of the lipid biosynthesis pathways were mapped in Figure 3.3, were significant (p-value ≤ 0.05) regulated genes under hypoxic conditions are illustrated.

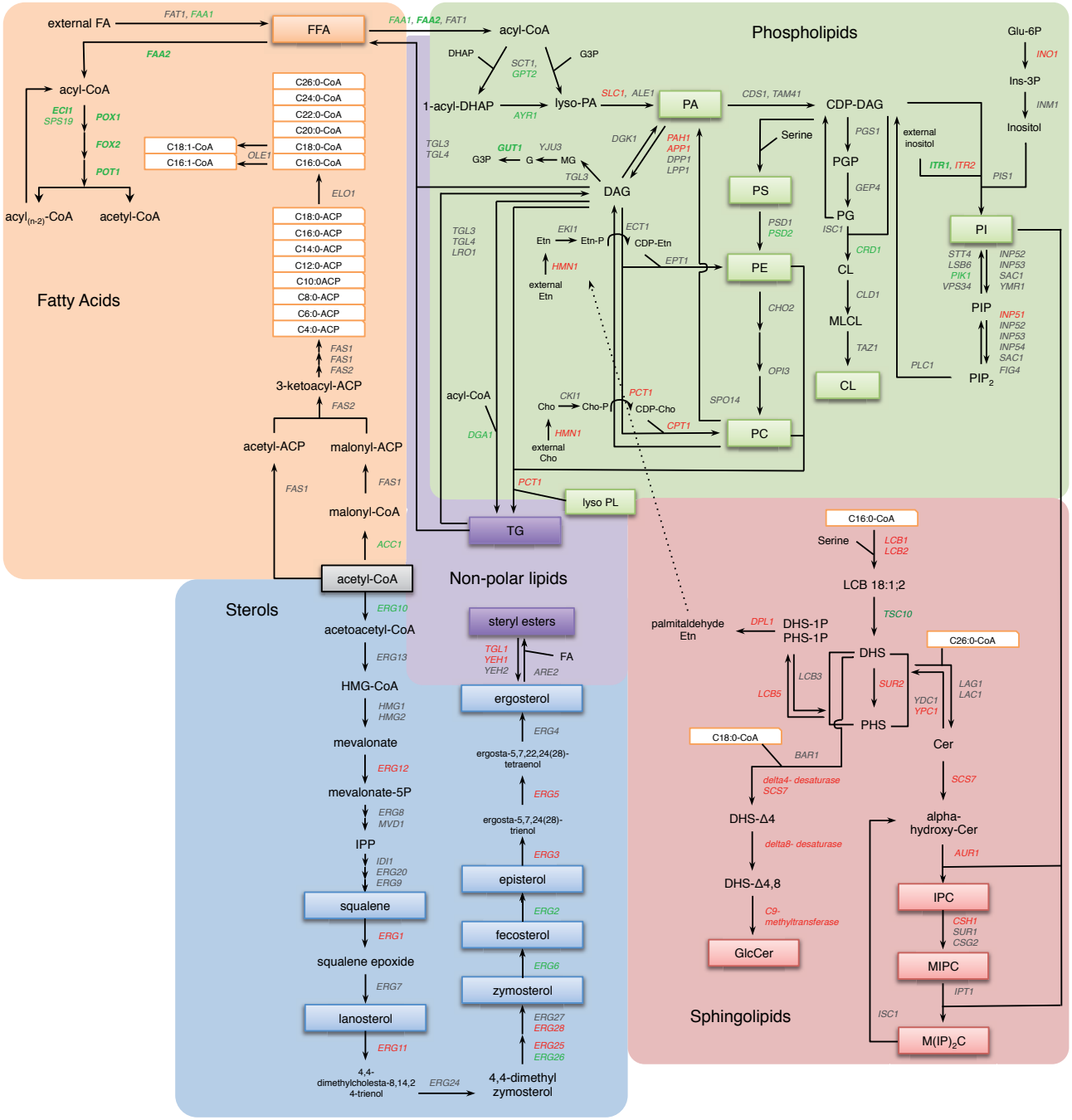

Figure 3.3: Transcriptome map of main lipid biosynthetic pathways. Genes upregulated are in red, and the downregulated ones in green. Data was from previous studies of the group [69].

Ergosterol biosynthetic pathway is an oxygen-requiring process. Therefore, most of the genes whose products catalyse oxygen-depending reactions were strongly upregulated in hypoxia. A similar behaviour was observed for the sphingolipid pathway, where most of the biosynthetic steps require molecular oxygen and were highly upregulated under hypoxic conditions.
Genes involved in the *de novo* synthesis of fatty acids (*ACC1, FAS1-2*) and fatty acid activation (*FAA1, FAA4*) were downregulated. The metabolic pathway involved in the breakdown of triacylglycerides (TGs) from the lipid droplets to obtain free fatty acids (*TGL3* and *TGL4*) did not change at transcriptomic level. However, SE breakdown pathway (*TGL1, YEH1, YEH2*) to obtain free sterol and fatty acids was upregulated. The oxygen-dependent β-oxidation process to obtain energy from fatty acids was strongly downregulated.
The phospholipid pathway did not show any significant changes at level of transcriptomic profile. Only some genes involved in the synthesis of phosphatidylcholine (PC) through the so-called Kennedy pathway (*PCT1, CPT1*) were upregulated in hypoxia. *SLC1*, involved in the generation of phosphatidic acid (PA) from lyso-PA, was upregulated along with the genes transforming PA to diacylglycerol (DAG). A significant downregulation of *ITR1* was observed meaning that a lower uptake of external inositol could be occurring. Effect of hypoxic conditions on transcriptional factors involved in the lipid metabolism were also analysed, and Hac1 resulted to be the most regulated transcriptional factor (Figure 3.4).

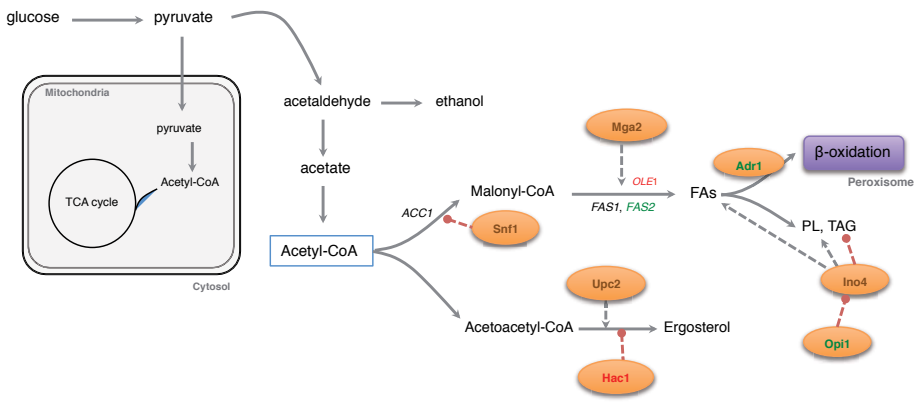

Figure 3.4: Transcriptional factors related to lipid metabolism and its transcriptional regulation under hypoxic conditions. Adapted from [90, 189].

HAC1 regulation could also reasonably be linked to changes in the lipid balance, since UPR has been suggested to be activated upon lipid deprivation in order to coordinate membrane synthesis, with Hac1 as important regulator [190]. Additionally, alterations in membrane fluidity could trigger the upregulation of *P. pastoris HAC1*. Hac1 triggers downregulation of ergosterol synthesis, and it also has an effect on membrane proliferation and morphology [78, 191]. *ADR1*, together with all the genes involved in β-oxidation, was tightly downregulated under hypoxic conditions.

3.2.3. Gene selection

It has been previously observed a beneficial effect of hypoxic conditions in recombinant protein production. The current work is focused on determining whether changes triggered by hypoxic conditions have an impact on protein secretion and to determine which are those changes.
For this reason, after a transcriptomic analysis focused on lipid metabolism, a set of genes were

selected in order to further investigate its role on defining membrane properties and their effect on recombinant protein secretion.

It is known that sterols and sphingolipids are important components of membranes and that changes on their levels can directly affect membrane morphology and its properties. Furthermore, since hese biosynthetic pathways are oxygen-dependent, a tight regulation of the involved genes have been observed.

Focused on sphingolipid metabolism, genes involved in the early steps of sphingolipid biosynthesis were preferred, as their alteration can lead to deeper changes on lipid composition. Two major sphingolipids are present in *P. pastoris*, ceramides and inositol containing phospholipids. Two different genes related to these two different pathways were selected: *DES1*, which codifies for a Δ4-desaturate involved in ceramide biosynthesis, and *SUR2*, a C4-hydoxylase that plays a role in inositol containing sphingolipids.

Ergosterol is an essential compound of the cell. Consequently, no gene deletion can be performed in its biosynthetic pathway. As it will be described later in more detail, fluconazole is an antifungal that inhibits Erg11p and it has been described to alter ergosterol levels [192]. For this reason, fluconazole-treated cells, and *ERG11* were also selected as target gene.

Finally, Hac1, the only transcription factor involved in lipid metabolism that was regulated in hypoxic conditions was also selected. In this case, only gene overexpression was considered, considering that a gene deletion could lead to not viable cells, as Hac1 is involved in several cellular processes.

A strain battery (Table 3.1) was finally defined with the selected genes, with both deletion and overexpression, in order to determine its implication on recombinant protein secretion.

Table 3.1: Battery of genes that will be used in this study, with the gene selected and the expected phenotype

strain	gene	expected phenotype
X33-Fab2F5	-	reference strain
X33-ΔDES1-Fab2F5	*DES1*	no ceramides
X33-Fab2F5-DES1	*DES1*	overexpressed ceramides
X33-ΔSUR2-Fab2F5	*SUR2*	altered inositol sphingolipids
X33-Fab2F5-SUR2	*SUR2*	altered inositol sphingolipids
X33-Fab2F5 + Fluconazole	*ERG11*	low levels of ergosterol
X33-Fab2F5-ERG11	*ERG11*	higher levels of ergosterol/intermediates
X33-Fab2F5-Hac1	*HAC1*	altered lipid composition

3.3. Conclusions

- A deep analysis of the transcriptomic data from hypoxic culture conditions focused on lipid metabolism was carried out.
- Cluster analysis provided candidate genes with significant regulation in hypoxia
- Genes *DES1*, *SUR2*, *ERG11*, *HAC1* were selected for further investigations of the role of lipids on recombinant protein secretion

4

Strain generation

4.1. Introduction

4.1.1. Genes selected for cell engineering

Sphingolipid Δ4-desaturase (*DES1*)

P. pastoris, like many fungi, synthesises glucosylceramides (GlcCers) predominantly in the form of 9-methyl-sphinga-4,8-dienine, that contain (*E*)-double bounds at the Δ4 and Δ8 positions of LCBs (long chain bases) and a methyl branch at the C9-position [139]. First examples of sphingolipid Δ4-desaturase were isolated by Ternes *et al.* [193], who functionally identified candidate desaturases by heterologous expression in *S. cerevisiae* Δ*SUR2* mutants.

Previous studies indicate that *P. pastoris* strains with the endogenous sphingolipid Δ4-desaturase disrupted do not contain Δ4-unsaturated LCB and are completely devoid of GlcCers [194, 195]. The requirement for Δ4-unsaturated LCBs to initiate the synthesis of GlcCers in *P. pastoris* implies that this modification is the first committed step for the biosynthesis of this class of sphingolipids in this organism [138]. The absence of GlcCers in *P. pastoris* is not essential for its normal growth [194].

Sphingolipid C4-hydroxylase (*SUR2*)

The C-4-hydroxylase, encoded by the *SUR2* gene, hydroxylates sphingolipids at the C-4 position of the sphingoid base, resulting in the formation of 4-hydroxy-sphinganine (phytosphingosine). It is involved in the IPC biosynthetic pathway, regulating relative levels of dihydrosphingosine (DHS) and phytosphingosine (PHS) [196].

Δ*SUR2* strains of *S. cerevisiae* are viable and C4-hydoxylation of the LCB is not required for IPC biosynthesis [197, 198]. However, Ternes *et al.* [138] could not delete this gene. The authors suggest that the requirements for C4- hydroxylation of the LCB differ between fungal species, and that in *P. pastoris* the C4-hydroxylation is required for IPC biosynthesis, which are essential for viability in this organism.

Lanosterol 14-α-demethylase (*ERG11*)

Lanosterol 14-α-demethylase is the major cytochrome P450 in *S. cerevisiae*. It is encoded by the gene *ERG11* and catalyses the oxidative removal of the C-32 methyl group of lanosterol,

an essential reaction in the biosynthesis of ergosterol. *ERG11* knockouts and strains with non-functional Erg11p enzyme are non viable unless exogenous ergosterol is supplied in the medium [118]. Gene over-expression studies suggest that Erg11p and Erg1p are the major regulatory steps for the ergosterol pathway [199]. It has also been reported Erg11 as the juncture for functional sterol molecules, as disruptions at this point or before result in non viable cells, while gene knockout after this point of the route are viable even even significant changes are observed in the membranes of these strains [200]. Overexpression of *ERG11* results in a decrease of lanosterol and an increase of downstream sterols [199].

Protein levels of this protein are known to be affected by carbon source, oxygen, heme and growth state of the culture [201]. *ERG11* transcript levels have been determined to increase during growth on glucose, presence of heme and during oxygen limiting growth conditions [202]. These results are in concordance with the ones of *P. pastoris* cultured in low hypoxia, where *ERG11* was also upregulated [69].

Hac1 Transcription Factor (*HAC1*)

Hac1p is a transcription factor that is required for the unfolded protein response (UPR), a stress response pathway triggered when unfolded or misfolded proteins accumulate in the ER [203]. It induces the expression of UPR-responsive genes like chaperones and other enzymes involved in the secretion process (e.g. foldases, proteins involved in glycosylation [204]. The principal components regulating UPR are the Ire1p (a kinase/RNase) and Hac1p (Figure 4.1). Under non-stress conditions, Ire1p is a protein associated with BiP/Kar2p. As unfolded proteins

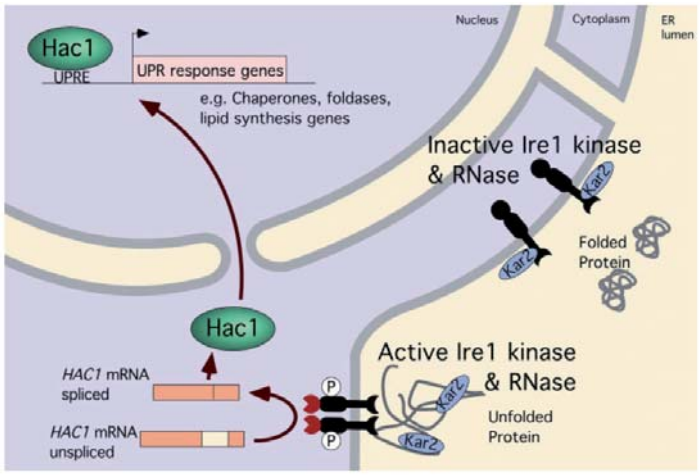

Figure 4.1: The unfolded protein response (UPR). From [205] (Reproduced with permission of John Wiley and Sons).

accumulate in the ER lumen, BiP is released from Ire1p to interact with unfolded proteins, which induces autophosphorilation of Ire1p and activates its RNase function. Active Ire1p splices the constitutively expressed *HAC1* mRNA, the spliced form of which produces Hac1p. Hac1p is translocated to the nucleus, where it binds to UPR responsive elements (UPRE) in the promoter of UPR responsive genes [191]. Other studies reported that, apart from splicing, the last five amino acid residues of PpHac1p are essential for activation of the UPR [206].

The effect of *HAC1* overexpression is protein and/or host specific. In *P. pastoris* it also depends on the inducible/constitutive expression of the *HAC1* [39, 191, 204, 207]. However, Gasser *et al.* [41] proved the beneficial effect of constitutive overexpressed ScHac1p from in *P. pastoris* for the production of a Fab fragment. *HAC1* knockout strains of *S. cerevisiae* and *P. pastoris* are viable and they have been characterised as being inositol auxotrophs, due to the involvement of the UPR

in lipid biogenesis [203, 206].

4.1.2. Knockout generation in *Pichia pastoris*

Gene targeting is one of the main molecular tools used in yeast science, which helps in understanding gene functions and interactions as well as molecular processes [208]. Targeted chromosomal integration of foreign DNA is mainly dependent on DNA double stranded breaks (DSB) and their repair mechanisms [209]. In yeast, two major pathways coexist to repair these DSB: homologous recombination (HR) and the non-homologous end-joining (NHEJ). The HR pathway requires interaction between homologous sequences and is responsible for the targeted integration of DNA. [210], whereas NHEJ integrates DNA randomly, with little or no sequence integration. When foreign DNAs are transformed into cells, they are competed by these two recombinant pathways. Therefore, efficient gene targeting is determined by the relative strength of the HR pathway compared with that of the NHEJ pathway [208].

Unlike most of the yeast, *S. cerevisiae* has a very efficient gene targeting system. Disruption cassettes with short flanking regions that range from 30 bp to 50 bp can integrate with high efficiencies via homologous integration at the correct genomic locus (>70 %) [211]. In contrast, the gene targeting efficiencies of some "non-conventional" yeast (i.e. *Pichia pastoris, Hansenula polymorpha, Yarrowia lipolytica, Pichia stipitis*) can be extremely low (<1 %) with the same length of flanking regions. In these cases, homologous arms varying from 200 bp to 2000 bp are required to ensure efficient gene replacement [208]. For *P. pastoris*, it has been estimated a targeted gene replacement efficiency of 0.1 % when the total length of the target fragments is <500 bp [212], and 10-20 % [213, 214] or up to 30 % [212] when extensive ~1 kb regions of homology are used. However, NHEJ pathway is not the only factor that contributes to the low targeting efficiency of non-conventional yeasts. The efficiency of homologous integration can be very locus specific [214–216]. This locus specific phenomenon can be due to the presence of "hotspot" regions for yeast genome or maybe the loss of function effect. For some genes, the probability of obtaining the desired gene replacement event is so low that transformation and screening procedures have to be iteratively performed, being laborious and time-consuming [210]. The knockout of genes with important physiological functions often means great loss of cellular fitness, which would lead to a delayed or failed appearance of correct disruptants [210]. Moreover, studies with *Hansenula polymorpha* showed different gene deletion efficiency depending on the antibiotic markers used, being Hygromycin B the one with the best efficiency (40 %) [217].

The frequency of targeted gene disruption can be improved by a split marker disruption strategy [10]. It consists on fusing the target DNA fragments with truncated but overlapping within the selectable marker gene. Only after a successful HR of the two fragment the selection marker become active and cells can grow on a medium containing the selection agent [218]. Split marker-based transformation decreases multiple and tandem integration events, decreasing the total number of transformants being screened. At the same time, it has been shown to increase the frequency of targeted gene disruption and homologous integration at 100 % in some fungi [219, 220]. This methodology has been already used to delete genes in *P. pastoris* [46, 50, 221].

4.2. Results and discussion

4.2.1. Construction of the knockout cassette

The method used for knock-out the target genes was based on the method used by Ternes *et al.* [194] but applying the concept of the split-marker approach [218]. Because the dominant marker gene is split in separate fragments, the gene is not functional unless homologous recombination occurs between two overlapping fragments. Transformants will not grow on a medium containing the selection agent unless homologous recombination occurs between the overlapping regions of the dominant marker gene. The marker gene cassette fused with homologous flanking sequences is integrated into the target locus via double cross over recombination. The split-marker gene fragments, flanked with the gene of interest were constructed using a fusing PCR approach, which eliminates tedious cloning procedures and allows quick generation of split-marker fragments for targeted gene disruption.

As illustrated in Figure 4.2, the target gene was amplified from the *P. pastoris* X33 chromosome using the primer pair Up-F and Down-R. At the same time, hygromycin resistance was amplified

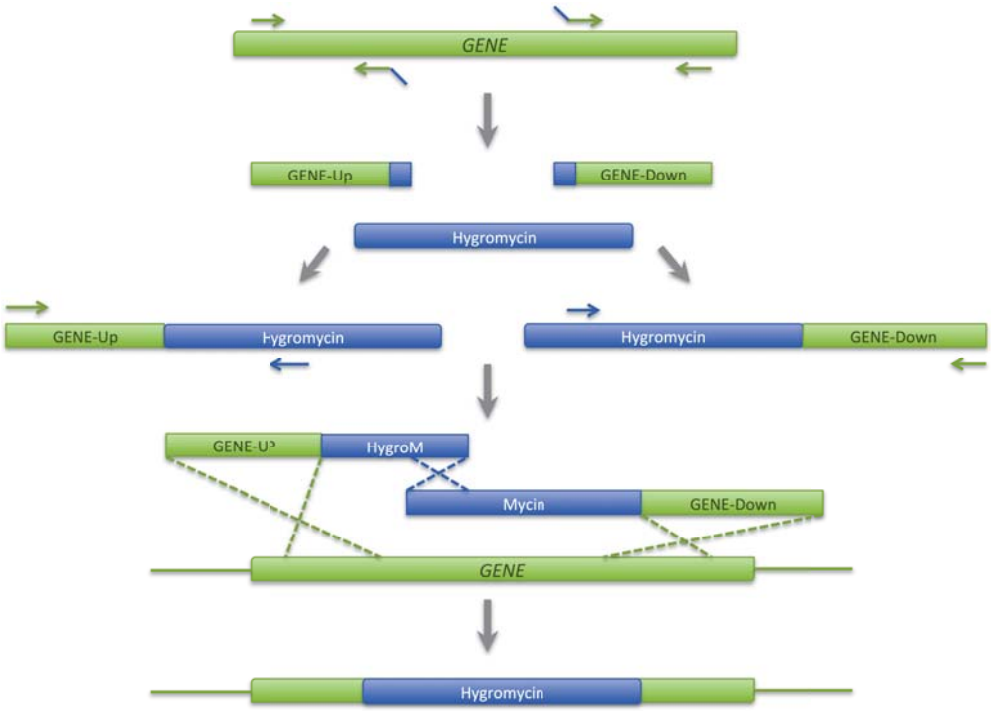

Figure 4.2: Split-marker approach. The selection marker (Hygromycin) is split into two fragments. Homologous recombination is needed to activate the resistance gene. It also favours the homologous recombination at the adjacent sites in the flanking regions of the targeted gene.

from pBR326 vector with primers F-Hyg-TEF1 and R-Hyg-CYC1TT (1811 bp fragment) in order to be used a selection marker of the disruption cassette. Nested plasmids (Up-Nested-F/Up-R-Hyg-F and Down-F-Hyg-R/Down-Nested-R) were used to amplify the 5′ and the 3′ flanking regions of around 300 bp of the target gene. Then primers Up-Nested-F and Hyg-Int-R, and Down2.1-F and Down-Nested-R were used in a second reaction with one of the first-round templates and the hygromycin cassette to generate an overlap product that contained the 5′ and a truncated part of the selection marker (400 bp), and the 3′ with the rest of the selection marker with an overlapping fragment of 142 bp. Those PCR products were then directly employed for transformation with selection on medium containing 100 μg mL^{-1} hygromycin.

Primers Up-F and Hyg-Int-R, and Hyg-Int-F and Down-R were used to confirm proper integration of the cassette at the 5′ and 3′ junctions, respectively, and primers Up-F and Int-R, and Int-F and Down-R were used to confirm the absence of the wild-type allele.

4.2.2. Deletion of *DES1*

The whole gene *DES1* was amplified from a genomic DNA extraction of *P. pastoris* X33, using the primers Des1-Up-F and Des1-Down-R, and the sahara. A product of 1083 bp was obtained. In a separate PCR reaction, hygromycin resistance cassette was amplified using the primers F-Hyg-pTEF1 and R-Hyg-CYC1TT (Figure 4.3).

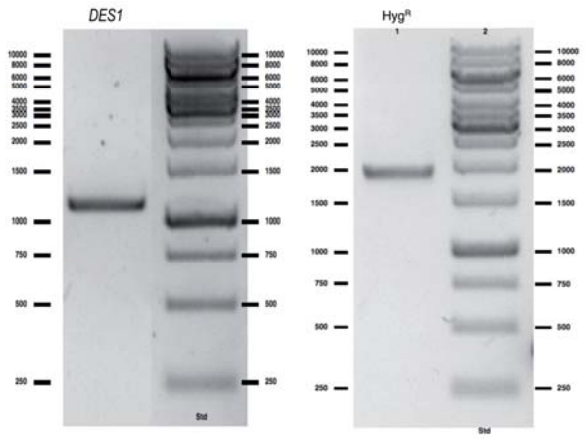

Figure 4.3: Amplification of *DES1* and hygromycin resistance.

The purified gene was used to amplify nested upstream (308 bp) and downstream (378 bp) regions of the target gene in two different PCR reactions (Figure 4.4a). For these reactions, primers Des1-Up-Nested-F paired with Des1-Up-R-Hyg-F and Des1-Down-F-Hyg-R with Des1-Down-Nested-R were used.

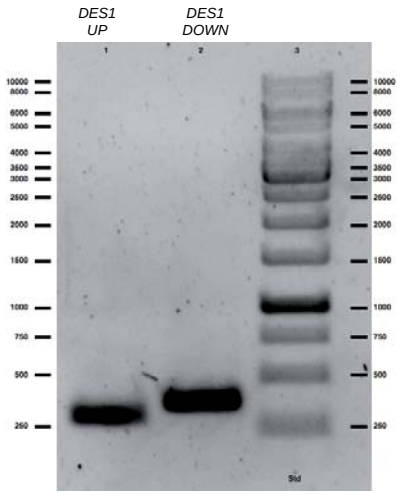

(a) *DES1* upstream and downstream fragment amplification

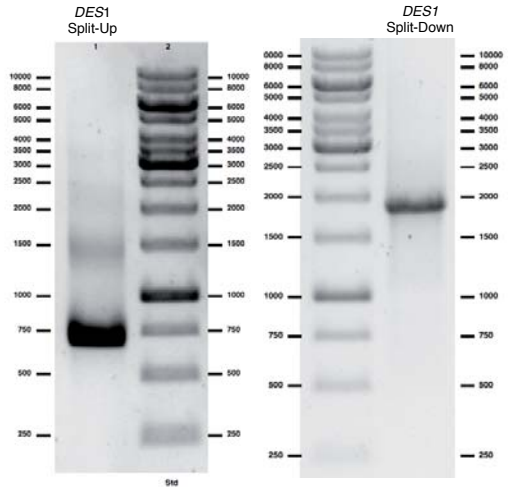

(b) *DES1* split marker up and down fragments

Figure 4.4: Amplification of *DES1* fragments to generate the knockout cassette

In order to generate the split marker, the 5' upstream fragment of *DES1* and 400 bp of the hygromycin cassette were fused in a two-step PCR reaction. In the first one, Des1-Up and Hyg fragments were combined in a ratio of 5:1 and amplified for 12 cycles without primers in order to fuse both fragments. The second PCR step added the primers (Des1-Up-Nested-F and Hyg-Int-R) and a conventional PCR was performed for 30 cycles. A fragment of ≈700 bp was obtained, named Des1-Split-Up (Figure 4.4b). The same strategy was used to obtain the Des1-Split-Down fragment (1910 bp, and use of F-Down2.1 and R-Down2.0cm). Fragments Des1-Split-Up and Des1-Split-Down shared an overlapping fragment of the marker gene of 142 bp. About 200 ng of each fragment were transformed by electroporation (Materials and methods 2.2.13), and a triple recombination event should take place in order to integrate the correct deletion cassette in the target gene. Clones were selected in hygromycin plates, and checked for gene disruption by colony PCR using primers Des1-Up-F and Des1-Down-R, where no amplification was related to gene deletion.

Only two clones out of more than 175 screened were selected as potential positive knockouts. Further characterisation of these clones included genomic DNA extraction and different PCR amplifications for correct integration of the deletion cassette and lack of presence of the target *DES1* gene (Figure 4.5). Clones C#15 and C#28 showed to be positive knockout, as amplified fragments were observed for the OK PCR amplifications.

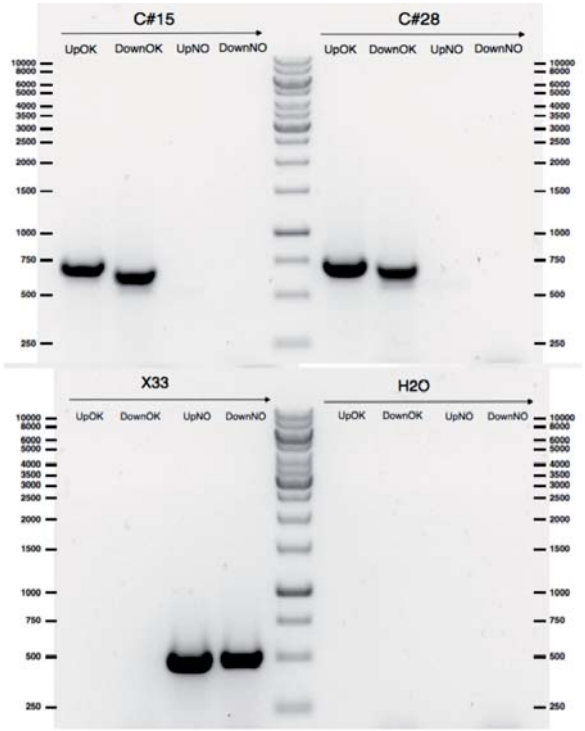

Figure 4.5: Des1 knockout characterisation. UpOk reactions used Des1-Up-F/Hyg-Int-R to confirm the upstream part of the gene, while DownOK reactions used Hyg-Int-F/Des1-Down-R to confirm the downstream part of the gene. Reactions UpNO and DownNO used Des1-Up-F/Des1-Int-R and Des1-Int-F/Des1-Down-R respectively to confirm no wild-type gene was present in the chromosome. X33 wild type strain was used as a control and H_2O as a negative amplification control.

4.2.3. Deletion of *SUR2*

The strategy to generate *SUR2* knockout clones was similar to the one for *DES1* with some modifications. First, hygromycin resistance cassette was amplified as previously described. *SUR2*

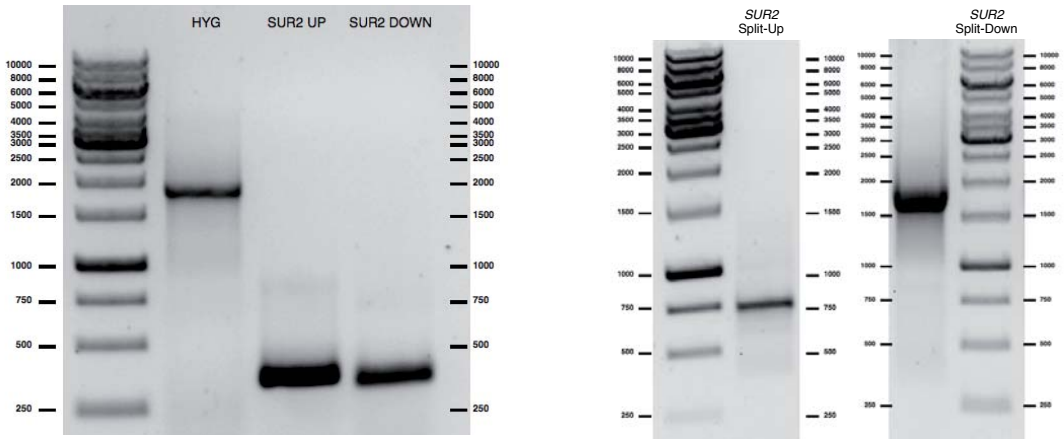

(a) *SUR2* up and down fragments

(b) *SUR2* split marker up and down fragments

Figure 4.6: Amplification of *SUR2* fragments to construct the knockout cassette

gene was amplified by PCR using primers Sur2-Up-F and Sur2-Down-R. This fragment was used to amplify the nested fragments of ≈300 bp at 5′ and 3′ of the gene (Figure 4.6a). These fragments were combined in separate PCR reactions together with hygromycin resistance, and a 2 step PCR reaction was performed as for *DES1* knockouts. In this case, *SUR2*-Split-Down fragments were combined in equimolar amounts with a total DNA quantity of 100 ng in order to obtain pure amplification bands (Figure 4.6b). Once both Up and Down fragments of the Split-marker were obtained, cells were transformed and selected for gene deletion with hygromycin agar plates. Unlike with *DES1*, colony PCR lead to very faint bands, which made this method not viable for the selection for *SUR2* knockouts. Thus, conventional genomic DNA extraction of the clones followed by PCR amplification was performed. Out of 110 screened clones, one clone was selected as a knockout candidate (H#25). Further confirmation was performed by different PCR reactions (Figure 4.7).

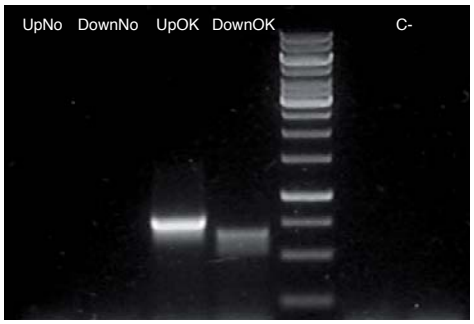

Figure 4.7: PCR amplification of the fragments to confirm the clone H25 as a positive knockout for *SUR2*.

4.2.4. Construction of the vector pGAPHA

A new vector carrying the GAP promoter for constitutive intracellular expression was generated by mixing two vectors available: pGAPHis and pBR326. pGAPHis was digested with *Bgl*II and *Eco*RI and fragments 494, 684, 2403 and 4436 bp were obtained. The band of 494 bp corresponding to pGAP promoter was extracted and purified.

At the same time, the pBR326 vector was also digested with *Bgl*II and *Eco*RI, obtaining a band of 1207 bp that contains the AOX1 promoter inducible by methanol followed by a secretion signal (α-factor form *S. cerevisiae* and a second band of 3013 bp corresponding to the hygromycin

resistance cassette and the *E. coli* replication origin. The last fragment was purified and ligated with the pGAP promoter from pGAPHis as represented in Figure 4.8. The new pGAPHA vector was obtained and correct vector construction was confirmed by different restriction assays.

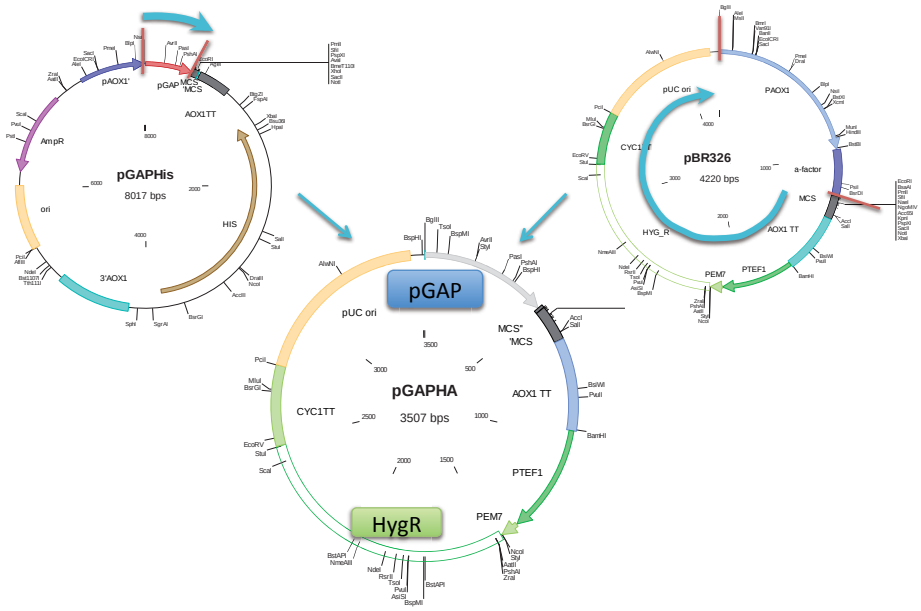

Figure 4.8: Schematic representation of the strategy used to construct the vector pGAPHA, where the promoter of pGAPHis and the backbone of pBR326 were combined.

4.2.5. Gene overexpression

DES1, SUR2, ERG11 overexpression

pGAPHA was used as a vector for constitutive intracellular overexpression of *DES1, SUR2* and *ERG11*. All genes were amplified by PCR using forward primers harbouring the *Not*I restriction sequence, and reverse primers that include the *Sfi*I restriction sequence (Primers 2.1). Gene amplifications together with pGAPHA were digested with *Not*I and *Sfi*I and purified. The digested vector was dehosphoryated before the ligation with the gene inserts to avoid religation events. Ligations were then transformed to *E. coli* DH5α cells and transformants were selected by their ability for growing into agar plates containing hygromycin. Plasmid extractions (MiniPreps) from resulting colonies were examined for correct integration by colony PCR, ER digestion using *EcoR*V for pGAPHA-Des1 and pGAPHA-Sur2, and *Nco*I for pGAPHA-Erg11, and finally by sequencing. Correct vectors were linearised with *Avr*II and used to electroporate *P. pastoris*-Fab2F5 competent cells (2.2.13). Transformants were selected in YPD agar plates containing Zeocin and Hygromycin and correct vector integration was determined by genomic DNA extraction and gene amplification by PCR. Around 10 positive clones carrying each of the genes were selected for further clone screening.

HAC1 overexpression

The DNA sequence corresponding to the functional Hac1p was cloned into the pPUZZLE vector, allowing the constitutive expression of the transcriptional factor. The vector was used to transform *P. pastoris*-Fab2F5 competent cells. In this case, clone selection was performed using YPD agar plates containing Zeocin and Geneticin.

4.3. Conclusions

In this chapter, a battery of strains altering the genes related to lipid meta-bolism that were selected from the transcriptomic analysis has been generated. In order to understand the effect of these genes on altering the membrane and, thus affecting the recombinant protein secretion, strains with both deletion and overexpressing the target genes were generated. The main conclusions of this chapter are:

- Knockout strains of two genes involved in the sphingolipid biosynthesis pathway *DES1* and *SUR2* were obtained for the *P. pastoris* strain producing recombinant Fab 2F5. As previously described in the bibliography, an efficiency of 1 % (± 0.1) was obtained.
- A knockout of *SUR2* in *P. pastoris* has been described for the first time.
- Vectors for the expression of *DES1*, *SUR2* and *ERG11* were constructed and used to obtain a battery of clones overexpressing these genes in a *P. pastoris* strain producing recombinant Fab 2F5.

5

Small-scale cultivations for strain characterisation

5.1. Introduction

5.1.1. Blocking the ergosterol biosynthetic pathway. Fluconazole treatment

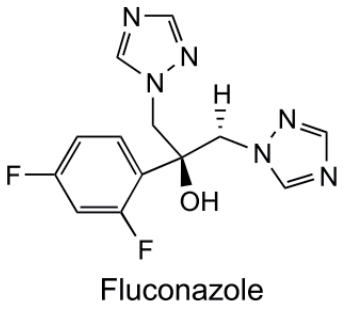

Fluconazole

Figure 5.1: Fluconazole structure [222].

Fluconazole (Figure 5.1) is one of the azole antinfungals that inhibit the synthesis of ergosterol in yeast by direct binding to lanosterol 14-α-demethylase (Erg11p). This inhibition results in a depletion of ergosterol from cellular membranes that are replaced with 14α-methylated sterols. Presence of an additional 6-OH group disturbs membrane packing, increases membrane fluidity and drug permeability, which finally interferes on cell viability [223].

Previous studies of the group used fluconazole as a modulator of Erg11p levels in the cell, and therefore, cellular amounts of ergosterol [192]. Cells were cultured in presence of different concentrations of fluconazole (0 - 2 μg mL^{-1}) in order to determine the concentration of antifungal not affecting cellular growth (Figure 5.2), and a range between 0.2 and 1 μg mL^{-1} turned out to be the optimal.

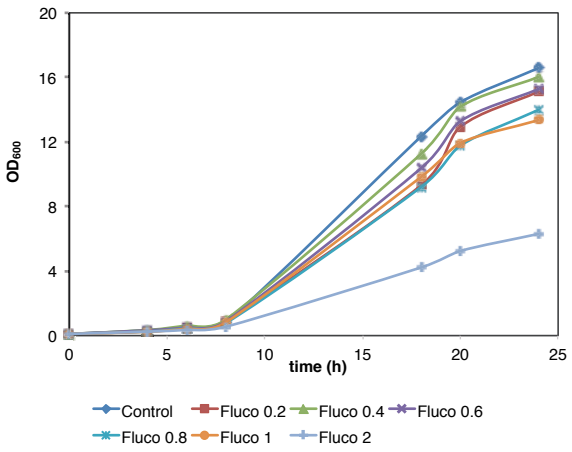

Figure 5.2: Extracted from [192]. Growth curves of *P. pastoris* expressing the Fab 2F5 grown on BMD medium and treated with fluconazole in a range of concentrations between 0 and 2 μg mL^{-1}. Cell growth was not significantly affected in concentrations up to 1 μg mL^{-1}

Further cultivations with the reference Fab 2F5 strain showed a beneficial effect on Fab secretion when cells were treated with fluconazole concentrations up to 0.6 μg mL^{-1}, while higher concentrations lead to a negative effect (Figure 5.3).

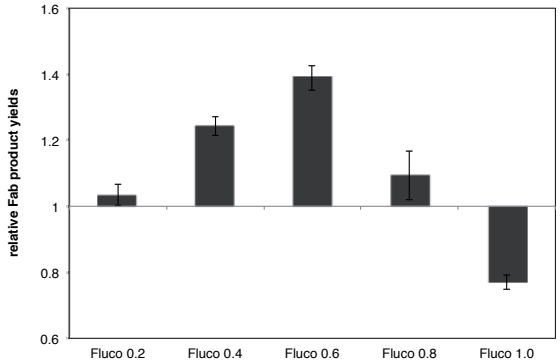

Figure 5.3: Extracted from [192]. Fab 2F5 productivities of cultures treated with fluconazole in a range of concentrations between 0.2 and 1.0 μg mL^{-1} were normalised to the values obtained from the non-treated reference cells. Fluconazole concentrations up to 0.6 μg mL^{-1} had a beneficial impact on Fab secretion. Error bars indicate the standard error of the means.

5.1.2. Cell disruption and intra-extracellular protein distribution

A key advantage of *P. pastoris* as a host organism in front of other alternatives, especially the prokaryotic systems, is its ability to secrete the product to the cultivation broth, which facilitates importantly the downstream processes [5]. The passage of proteins through the secretory pathways permits post-translational events that usually are essential for the biological activity of the proteins [36]. Nevertheless, high levels of heterologous protein expression can lead to saturation or overloading of the secretory pathways, where the product is accumulated intracellularly and often also degraded, resulting into an important decrease of the production yield. This fact turns out to be a major bottleneck for biotechnological process development [37, 204].

To study the effect of the secretory pathway saturation on the bioprocess efficiency, it is of capital interest the reliable quantification and recovery of the total amount of product accumulated

intracellularly along a cultivation. In yeast cells, presence of the cell wall requires the selection of disruption methods that destructs the wall in order to release all the product of interest [228]. In particular, *P. pastoris* cells present important difficulties to obtain reproducible and reliable results for cell disruption procedures due to the important thickness of its cell wall. Several methods for cell disruption have been used with *P. pastoris*, like sonication [229], bead milling [96, 230], enzymatic and chemical lysis [231, 232], cell permeabilisation [233, 234], and high-pressure homogenisation [235–237]. In all cases, a fast and efficient cellular disruption is desirable, that does not alter the protein chemically or physically.

A high pressure homogeniser consists on a positive-displacement pump that forces a cell suspension through the centre of a valve seat and radially across the seat face. Pressure is controlled by adjusting the force of the valve, which is spring-loaded or hydraulically controlled. Fluid flows radially across the valve and strikes an impact ring until suspension exits the valve assembly [238]. Previous studies in the group were focused on the efficacy of high-pressure homogenisation disruption procedures on methanol-based cultivations, as it is known that cells growing on this substrate present a significant widening of the cell wall thickness [239, 240]. A specific disruption method for cells growing on glucose or glycerol was required. Since an important amount of the protein of interest is expected to be retained through the secretory pathway, besides the soluble part of the cell lysates, the insoluble fraction must be taken into account in order to avoid a misestimation of the target product, as it contains the cell membranes, endoplasmic reticulum (ER), Golgi and other organelles where the protein of interest may be retained [241]. In addition, a reliable quantification of the product present in the insoluble fraction requires an extraction procedure that involves the use of detergents, which must be optimised for each protein, in this case for the Fab 2F5.

5.2. Results and discussion

5.2.1. Determination the optimal fluconazole treatment for Fab 2F5 secretion

Optimal fluconazole concentration required to increase protein secretion without altering cell growth was previously determined in shake flask cultures [192]. In this work, further studies on fluconazole treatement were carried out in shake flasks in order to establish the optimal amount of fluconazole in relation to cell mass allowing for the maximal protein secretion (Figure 5.4). Cells were cultured for 24 hours in presence of different fluconazole concentrations. Fab secreted was related to the ratio of fluconazole to final biomass value for each cultivation, and a value of 80 µg fluconazole per g_{DCW} turned out to be the optimal, leading to a 1.5-fold increase in yield of secreted Fab.

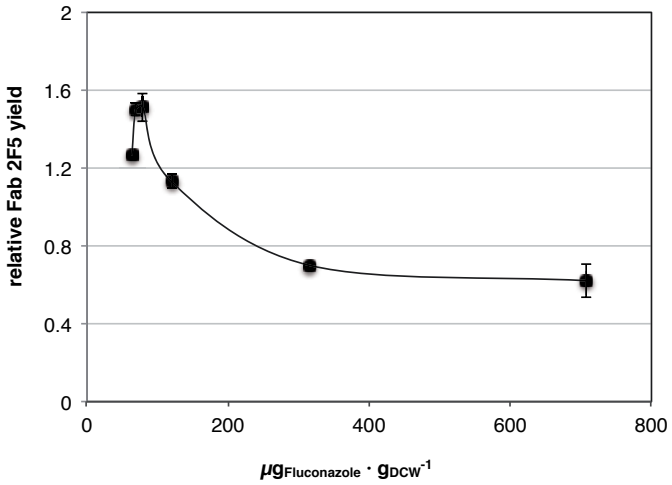

Figure 5.4: Relative Fab 2F5 yield as function of specific amount of fluconazole per gram of biomass.

Higher ratios of fluconazole per biomass lead to decreased Fab secretion levels compared to the reference strain not treated with fluconazole.

Fluconazole effect on protein secretion over the time was also determined. In this case, cells cultured with different amounts of fluconazole were analysed in terms of cell density and Fab secreted after 20, 43 and 48 h of cultivation (Figure 5.5).

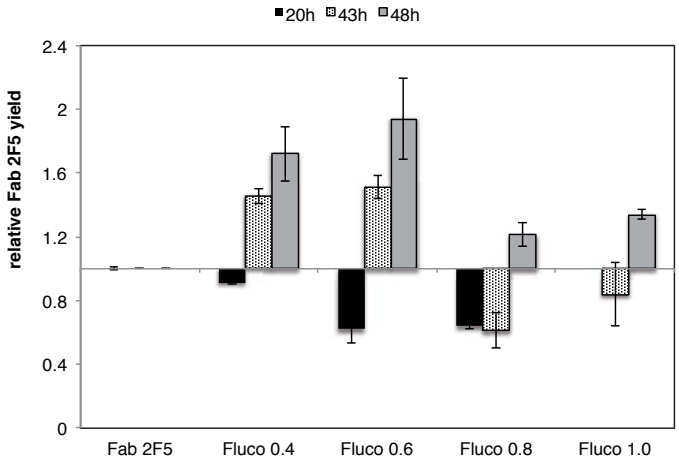

Figure 5.5: Time effect on Fab production when cultures are treated with different amounts of fluconazole. The studied range was from 0 to 1 μg mL^{-1}.

Initially, a negative effect of fluconazole treatement on Fab secretion was observed for the cultures with higher initial fluconazole concentration, probably caused by the low biomass concentration present in the cultures that result in a high fluconazole to biomass ratio and lead to low levels of secreted Fab. Longer incubation times (40-48 h), prompted increased Fab secretion up to a positive effect of fluconazole as previously described. The most significant change for all the concentrations was at the longest incubation time (48 h), being 0.6 μg mL^{-1} the optimal fluconazole amount for Fab secretion. Higher levels of Fab obtained for longer cultivation times can be the result of an improved cell secretion capacity due to lower cell growth rates during stationary phase. After 48 hours, up to 2-fold increment in fluconazole treated cells was observed compared to the 1.3-fold obtained after 24 hours of cultivation. It can be due to the fact that cells have been reach stationary phase were no longer grow and they had longer times to secrete the produced protein.

5.2.2. Cell disruption and protein extraction

Disruption of *P. pastoris* by using One-Shot Cell Disrupter has been previously reported for cells growing on mixed feeds of glucose and methanol [240]. For this study, the disruption process was optimised in terms of recovery of the working antibody fragment (Fab 2F5) produced constitutively by cells growing on glycerol and glucose.

Determination of the optimal disruption pressure and number of passes

The first step to optimise cell disruption was to determine the working pressure and number of disruption passes that lead to the best Fab 2F5 recovery. Since *P. pastoris* cell wall is thick and resistant, high pressures (2, 2.5 kbar) were considered as initial testing conditions to obtain high amounts of cell disintegration. Chemostat samples were used directly whereas fed-batch samples were diluted to cell densities similar to chemostat ones, which were used to optimise the process before starting the disruption analyses.

Cell cytometry was used as direct indicator of cell disruption. Cell number has been described as the most accurate and reproducible measure of cell rupture, but it requires significant analysis time [242]. In this sense, flow cytometry allows for counting cell number while gathering specifically whole cells from cell debris (Figure 5.6), being a fast and reliable system for cell disruption determination.

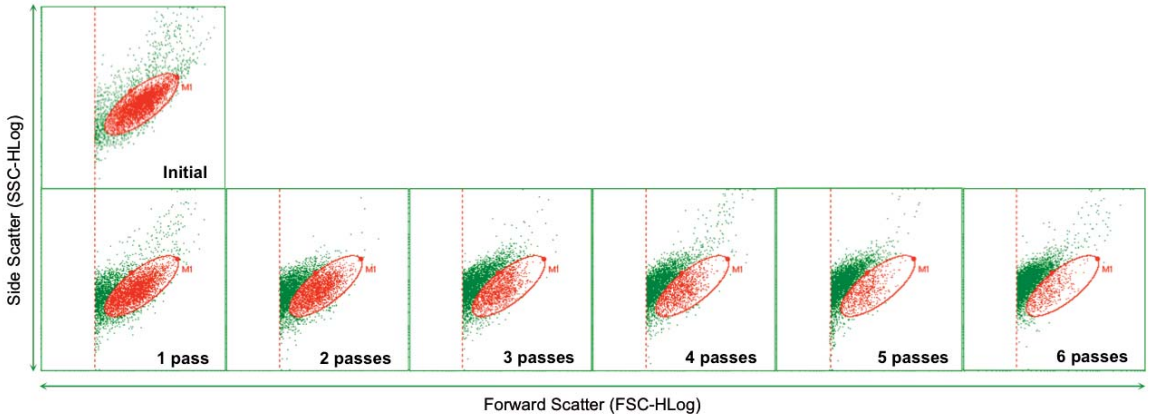

Figure 5.6: Cell counting by flow cytometry used to determine the extent of cell disruption after different passes; ellipse gate differentiates the whole undamaged cells from damaged and broken cells.

The use of optical density as cell disruption indicator has been systematically used but it can bring to misestimated results, as cell debris can be quantified together with whole cells.
Initial cell number was counted by flow cytometry and 8 mL of cell aliquots were used and disrupted at 2 kbar or 2.5 kbar for 1 to 6 passes (Figure 5.7). Cell number was then determined and percentage of disruption was calculated using Eq. 2.4. Cell membranes and debris, as well as not disrupted cells, were separated from the soluble cytosolic fraction by centrifuging.
The decreased percentage of cell number was used as an indicator of cell disruption. Like other indicators described in the literature, it can be used to relate the degree of cell disruption with the release of the component of interest when determining the desired component is not possible or it requires difficult and time consuming methods [242]. Thus, determination of cell disruption by calculating changes on the percentage of cell number was directly related to higher levels of released Fab. Figure 5.7 compares the levels of cell disruption and Fab 2F5 recovered for each pressure and number of passes.

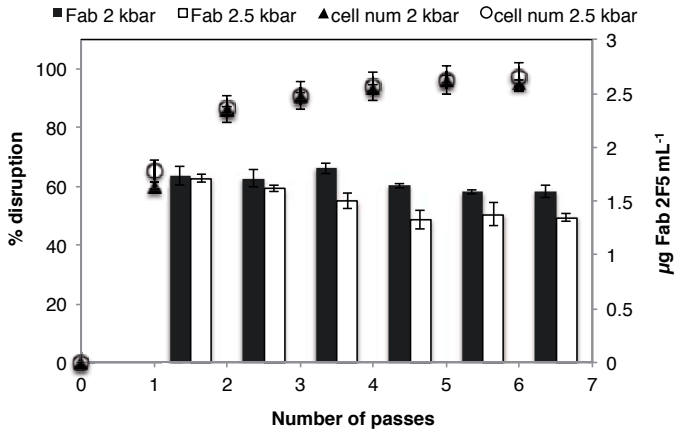

Figure 5.7: Comparison between extent of cell disruption and amount of 2F5 Fab released after different passes. Error bars indicate standard deviation.

It was observed a huge increase of cell disruption from one disruption pass to two disruption passes, while further passes increased only slightly the cell disruption amounts. It was also noticed that no major differences were observed in terms of cell disruption between 2 kbar and 2.5 kbar. In relation to Fab 2F5 amounts, recovered levels were similar when using 2 kbar regardless disruption passes, while a decrease on Fab recovered amounts was present when 2.5 kbar were used.
Optimal disruption conditions were defined as those including a high percentage of cell disruption combined with high amounts of detected Fab, considering that in these conditions no high amounts of unbroken cells would be present in the insoluble membrane fraction (IMF) and thus, the highest amount of protein of interest would be quantified. It was also important to consider working with as few passes as possible to overcome protease degradation problems and to avoid time consuming steps. Therefore, two passes at 2 kbars were chosen as working conditions for Fab 2F5 quantification. These settings fit with the ones previously determined using the same high-pressure homogeniser [240].

Optimisation for the protein extraction of the insoluble fraction

In order to achieve a reliable quantification of intracellular proteins and their recovery, a protein extraction step is necessary to determine the amounts of protein associated to membrane fraction and cell organelles (IMF), which allows comparing changes among different cultivation conditions,

as well as along bioprocesses.

Based on other studies, different extraction buffers, detergents and incubation times were tested in order obtain the maximum Fab extracted from IMFs. Once the best combination of buffer and detergent was selected, additional studies for optimal detergent concentration and incubation time were performed. With these results, when the secreted, SCF and IMF fractions are counted together, it can be assumed as the total Fab produced that is not degraded. Pfeffer *et al.* [243] observed high degradation levels (58 %) of a recombinant secreted Fab in *P. pastoris*, which should be taken into account as cell modifications in the degradation or secretion processes can lead to higher detected protein.

Selection of lysis buffer and detergent for protein extraction

Buffers A, B and C (2.4.1) where selected from the bibliography [237, 243, 244] and their extraction efficiency was compared when combined with 1 % of three candidate detergents (Tween 20, Triton X-100 and CHAPS). Detergents are amphipathic molecules having a hydrophilic portion, usually ionic, and a hydrophobic region, usually a hydrocarbon, which make them bind to the lipid membrane until saturation is reached. Increased amounts of surfactant lead to the formation of mixed micelles with membrane lipids [238]. Initial extractions of Fab from IMF used SDS as extracting detergent, but this anionic surfactant was discarded because of its effect on the Fab quantification system, altering its detected levels.

As it can be observed in Figure 5.8, CHAPS turned out to be the detergent showing the best results in terms of solubilisation of membranes and membranous structures, and therefore, extracted Fab. CHAPS is a zwitterionic detergent, as compared to the other non-ionic candidate detergents

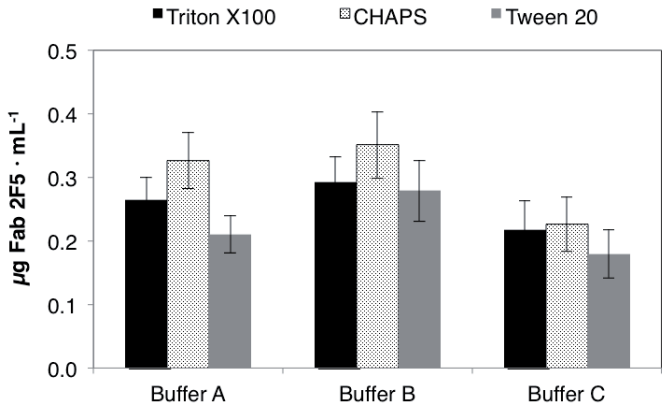

Figure 5.8: Release of 2F5 Fab obtained by using the buffers and detergents compared. Error bars indicate standard deviation.

(Tween20 and Triton X-100). Zwitterionic detergents combine properties of ionic and nonionic detergents, as they are composed of head-groups bearing anionic and cationic net charges [245]. Higher levels of solubilisation were observed for CHAPS in all tested buffers, being Buffer B the one with higher levels of extracted Fab.

Solubilisation step it is defined as a protein dependent step, where the optimal extracting detergent changes depending on protein characteristics. For example, the best solubilisation agent for the human μ-opioid receptor (HuMOR) was the anionic detergent *N*-Laurosyl sarcosine [246], and the optimal extraction detergent for hepatitis B surface antigen was reported to be 1.5-2 % Tween 20 [237], while G-protein-coupled receptors prefer decylglucopyranoside [244], both non-ionic detergents.

Determination of detergent concentration and extraction time

Extraction time is a key parameter when optimising protein extraction, since short incubation times result into an incomplete protein extraction from the membrane fraction and prolonged extractions may result in proteolytic action from residual proteases in crude extract. Although higher temperature (e.g. room temperature) accelerates the extraction step, a temperature of 4-10 °C was used in the process in order to maintain product integrity.

Once CHAPS was selected as the working detergent for Fab 2F5 solubilisation, different detergent concentrations were tested in order to maximise the quantity of Fab extracted. Furthermore, different incubation times at 4 °C and gently agitation were also tested. The amounts of solubilised Fab (Figure 5.9a) and total protein extracted (Figure 5.9b) were determined.

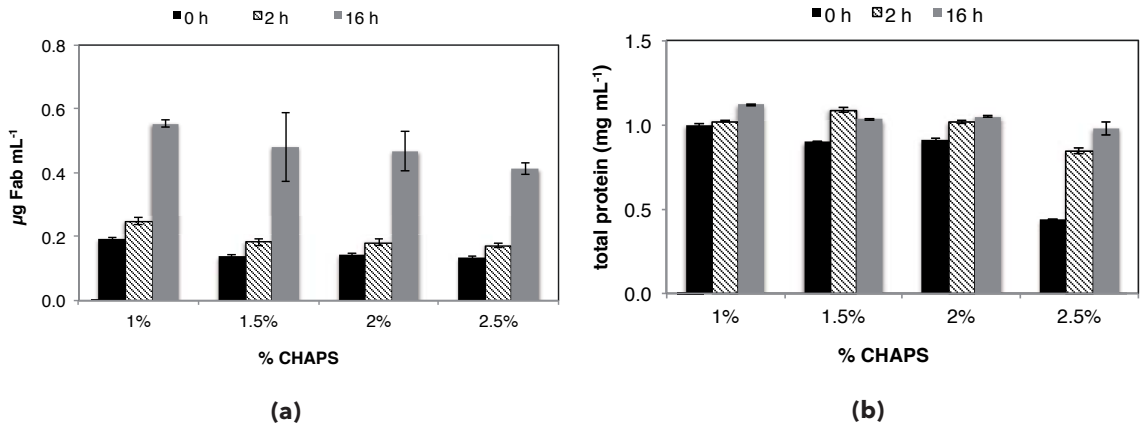

Figure 5.9: 2F5 Fab **(a)** and total protein **(b)** obtained by using different concentrations of CHAPS and incubation times. Error bars indicate standard deviation.

Incubation time had an important impact on Fab extraction, where long incubation times (overnight incubation) resulted in a 2.5-fold higher recovered Fab. However, the range of CHAPS concentrations tested did not alter significantly the extracted Fab amounts; being 1 % CHAPS the best concentration.

When the effect of incubation time and CHAPS concentration were related to total protein released from cells, none of these parameters seem to change the total protein detected. This could indicate that an important percentage of total cellular protein is released from the cell faster than the Fab in a similar was as previously described for hepatitis B surface antigen (HBsAg) [247]. When 2.5 % CHAPS were selected, total protein extracted of the IMF was controversially low. Selected conditions for Fab extraction were 1 % CHAPS with Buffer B incubated during 16 h (overnight) at 4 °C.

5.2.3. Screening for Fab 2F5 expression

DES1 Knock-out screening

The two positive clones of *P. pastoris* with the gene *DES1* deleted (#C15 and #C28) were grown in shake flasks cultures with minimal media BMD in order to characterise both cellular growth and Fab production. Cell growth was followed by means of OD_{600} and after 24 hours of cultivation all clones reached similar optical density (Figure 5.12). These results are consistent with the ones obtained by Ternes *et al.*, that deleted *DES1* of a *P. pastoris* wild-type strain [194] and growth rate was maintained. Levels of secreted Fab were quantified by ELISA and relative Fab yield of the clones were calculated using the strain without deletion (X33-Fab2F5) as reference. As it shows

Figure 5.10, the two knockout clones secreted less Fab into the culture medium, with almost no Fab secreted by the clone *DES1#C28*.

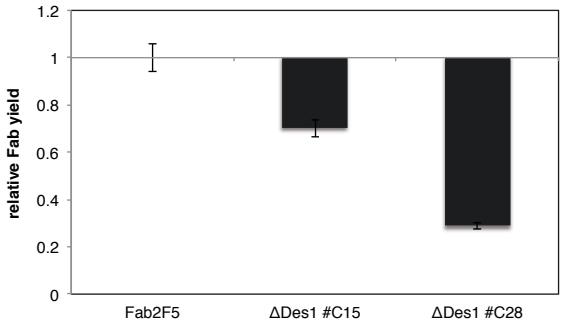

Figure 5.10: Relative Fab 2F5 yield obtained for the two knockouts when compared to the reference strain without the deletion

Clone #C15 was selected as the working ΔDES1 strain, so that Fab levels were not so close to the detection limit.

Further studies with the ΔDES1 strain included cultures where control and mutant strain were cultured in presence and absence of fluconazole. The aim of these cultures was to determine whether the combination of ceramide depletion (as it should be expected when *DES1* is deleted [194]) and ergosterol reduction caused by ergosterol lead to a beneficial effect on protein secretion. Fab levels of secreted fraction, cytosolic fraction (SCF) and membrane fraction (IMF) were determined for all the cultures in order to observe the distribution of the Fab within the cellular fractions (Figure 5.11).

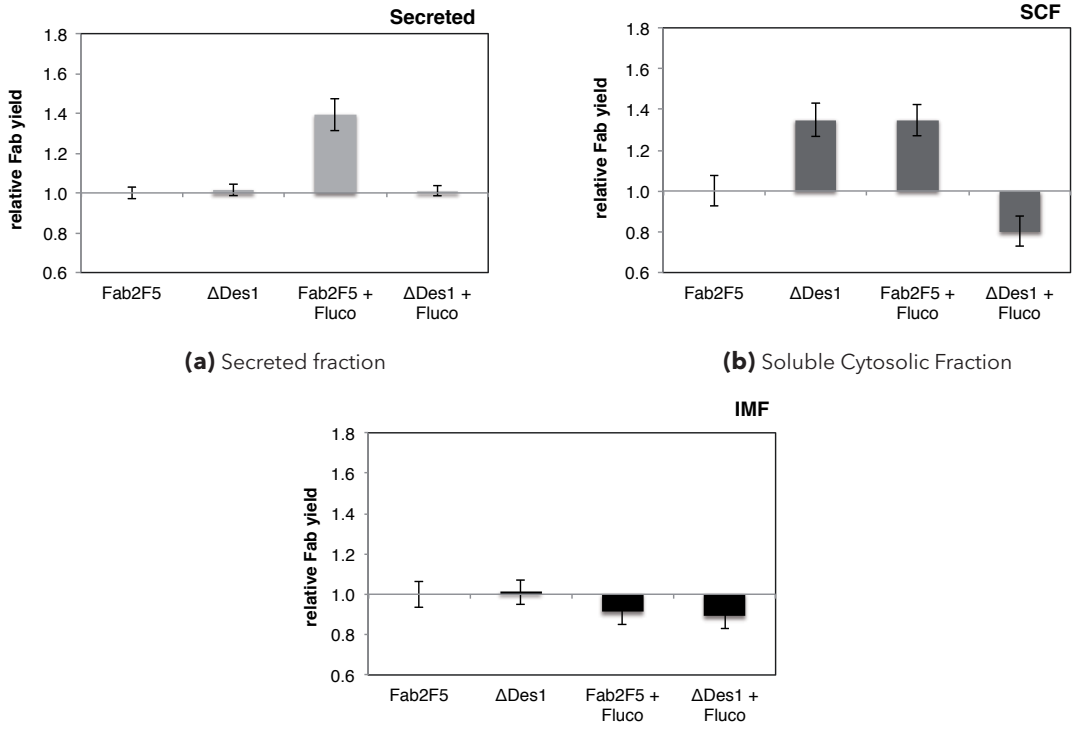

(a) Secreted fraction

(b) Soluble Cytosolic Fraction

(c) Insoluble Membrane fraction

Figure 5.11: Fab fraction distribution of shake flask cultivations of the reference strain and the knockout, with or without fluconazole treatment.

The already described fluconazole effect on protein secretion was observed in the cultures, with around 1.4-fold increase on Fab yield. These cultures presented also 1.3-fold Fab in the soluble cytosolic fraction, and a reduction of Fab levels in the insoluble fraction compared to the reference strain. Knock-out strain did not present production changes in terms of secreted Fab, but the levels in the cytosolic fraction were 1.3-fold higher. Finally, the combination of fluconazole treatement and *DES1* deletion resulted on lower Fab yields in all fractions.

Table 5.1 shows the percentage of Fab distributed in the three working fractions (Secreted, Cytosolic Soluble and Membrane Insoluble). In all cases, secreted Fab represented more than 90 % of the detected Fab. ΔDES1 strain presented slightly higher intracellular Fab levels (SCF + IMF) compared to the reference strain, and fluconazole treatement lead to a reduced intracellular amounts of Fab.

Table 5.1: Fab distribution on cellular fractions

	Fab2F5	**ΔDES1**	**Fab2F5+Fluco**	**ΔDES1+Fluco**
Secreted	99.7% ± 0.11%	93% ± 7%	99.7% ± 0.02%	99.7% ± 0.04%
SCF	0.14% ± 0.05%	0.18% ± 0.03%	0.13% ± 0.02%	0.11% ± 0.02%
IMF	0.2% ± 0.07%	0.2% ± 0.06%	0.13% ± 0.0%	0.17% ± 0.02%

In order to determine plasma membrane fluidity, anisotropy analysis were carried out. As anisotropy values are cell growth dependent, cell density was determined before, and anisotropy was analysed for cells with similar cell density (Figure 5.12). No significant differences were observed between cultures, which indicates that using this methodology, similar fluidity results are obtained. As membrane fluidity can be calculated as the inverse of anisotropy, slightly higher fluidity could define ΔDES1 membrane.

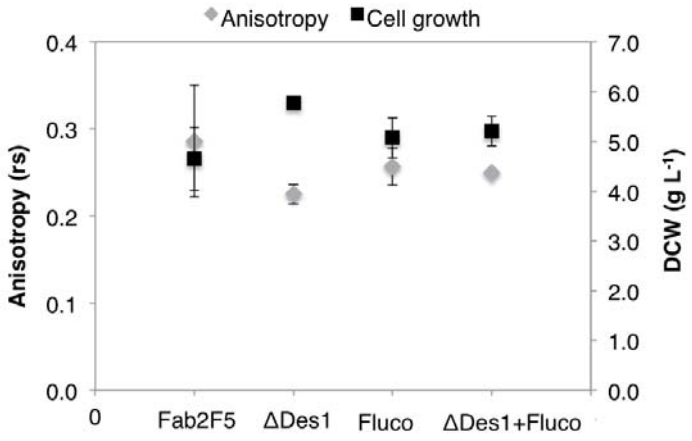

Figure 5.12: Values of snisotropy and OD_{600} of the cultures.

SUR2 Knock-out screening

Once a clone with the *SUR2* deletion (ΔSUR2) was obtained, it was characterised in terms of cell growth, Fab production and compared to the reference strain (Fab 2F5) and the ΔDES1 strain, all of them treated and untreated with fluconazole. The mutant strain grew similarly to the reference strain, and a beneficial effect on Fab secretion was observed (Figure 5.13). Relative levels of secreted Fab were 1.4-fold higher than the reference strain, which coincides with the previous results obtained when cultures where treated with fluconazole.

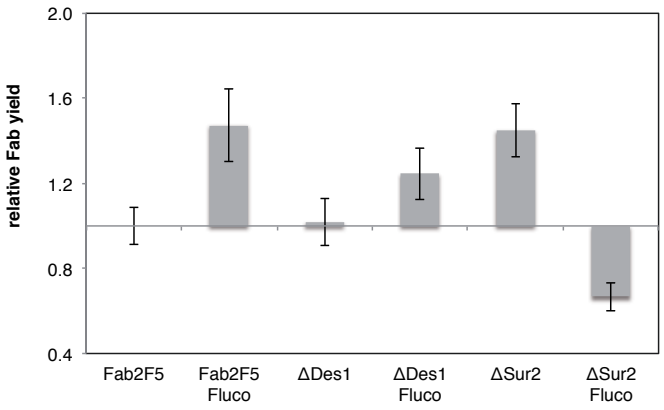

Figure 5.13: Fab normalized productivities for all the KO strains combined with fluconazole treatement

Fluconazole treatment was also studied, so that the two strains with a deletion in the sphingolipid pathway could be compared with the reference strain with and without fluconazole. The aim of this cultures was to characterise the strains when components of the so-called "lipid rafts" were altered and possibly affect on protein secretion.

In Figure 5.13, relative secretion levels were plotted, and the presence of fluconazole in the culture medium reduced the secreted Fab of ΔSUR2 cells. ΔDES1 cells improved its secretion levels as it was observed with the reference strain. It can be concluded that presence of inositol containing species with an altered hydroxylation pattern due to the *SUR2* deletion lead to increased protein secretion, while the lack of ceramides did not have significant changes on protein secretion.

Ternes et al. [138] characterised *P. pastoris* sphingolipid composition, showing that only 10 mol % of the total sphingolipid content of the cell correspond to ceramides. Lack of cellular ceramides, and specifically in the plasma membrane would not affect membrane morphology and fluidity, whereas changes on IPC-species that are the major part of membrane sphingolipids could alter membrane properties and lead to increased protein secretion, even when the performed anisotropy studies did not show any fluidity differences.

As no fluidity changes were observed with the anisotropy analysis, they were not further used to characterise cell membrane properties in new cultivations.

DES1 overexpression screening

Gene *DES1* was cloned into pGAPHA as previously described 4.2.5, and clones were obtained. Ten clones were selected and screened for cell growth and protein production in shake flask cultures. Figure 5.14 shows how, except for clone #33, all clones grew slower than the reference strain. Changes on the intracellular-extracellular distribution of the Fab produced were also observed. Most of the overexpressing clones presented more Fab in the insoluble membrane fraction than the reference strain, with clone #10 with more than the 20 % of the Fab in this fraction. Regarding the soluble cytosolic fraction, most clones presented almost all of its Fab in this fraction, which represents up to 90 % of the total Fab.

These results could indicate changes in cell membrane composition by being increasing ceramide content, which can affect membrane properties in such a way that cells cannot grow properly and the protein secretion pathway is damaged and low amounts of Fab in the supernatant are detected.

For further studies, clone #11 was selected as the overexpressing *DES1* (OE DES1) strain.

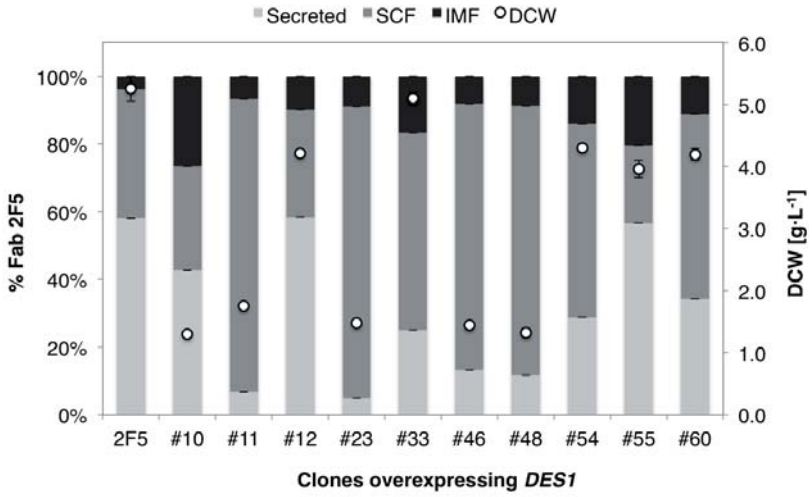

Figure 5.14: Screening *DES1* overexpression clones

ERG11 overexpression screening

Same proceeding as with the overexpressed *DES1* was used to screen clones overexpressing the *ERG11* gene. Figure 5.15 shows how in this case cell growth for almost all selected clones was slightly lower to the reference strain, except for the clones #25 and #46 that reached significant lower cell densities at the end of the culture.

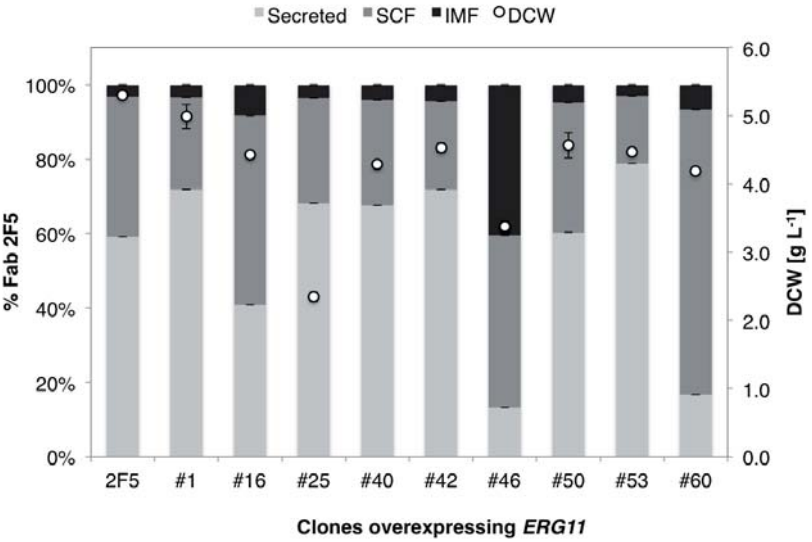

Figure 5.15: Screening *ERG11* overexpression clones

Fab distribution among cellular fractions was also studied, 60 % of the cultured clones appear to have similar Fab distribution, with 60-70 % of the Fab secreted and less than 10 % in the IMF fraction. Totally different Fab distribution was observed for clones #16, #46 and #60, with Fab secreted fractions corresponding to less than 40 %. Clone #46 presented high amounts of Fab in the membrane fraction and almost no Fab secreted. Overall results demonstrate that increased levels of Erg11p in the cell does not have a beneficial impact on protein secretion, but Fab secretion levels and distribution among the cellular fractions was rather similar for most of the clones. Clone #40 was used as overexpressing *ERG11* (OE Erg11) strain for further analysis.

SUR2 overexpression screening

SUR2 gene was overexpressed using the same approach as with *ERG11* and *DES1* genes. In this case cell growth was significantly affected, so that only four positive clones were obtained for cell characterisation (Figure 5.16).

Cells were cultured until similar levels of cell density to the reference strain were achieved, meaning cell cultures of around 7 days and indicating a reduced specific growth rate (μ) for this clones. The amounts of Fab present on the supernatant were quantified, and for 3 out of 4 clones, relative Fab yield in the secreted fraction was lower.

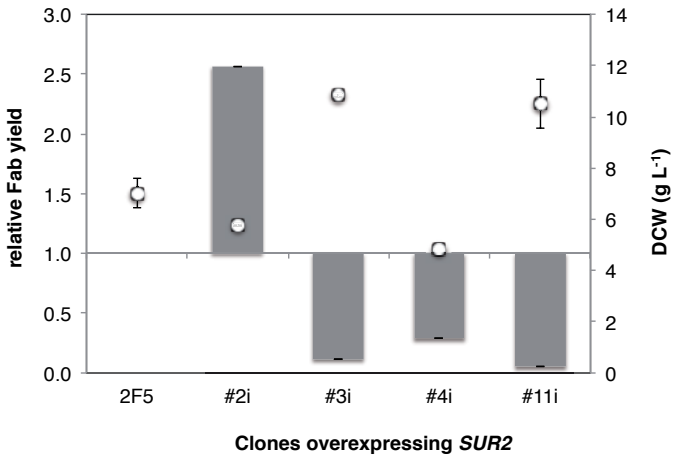

Figure 5.16: Screening of the clones overexpressing *SUR2*. Grey bars represent the relative Fab 2F5 yield compared to the reference strain. Empty dots represent the biomass concentration at the end of the culture.

Further studies of clones overexpressing *SUR2* were not feasible because cells could not be maintained in agar plates and no growth was achieved using glycerol stocks.

The possible presence of more sphingolipid content in the strains with overexpressed key genes of the sphingolipid biosynthetic pathway can indicate a negative effect on membrane composition that could lead to a loss of cell growth, which is not viable for cells in the case of increased Sur2p in the cell. In this case, sphingolipid moieties can be over hydroxylated and these changes can affect drastically membrane morphology.

Kim *et. al* [248] overexpressed *SUR2* gene in *S. cerevisiae* and obtained ≈ 50 % higher ceramide production than the control strain, meaning that an increase of ceramides in this organism is viable. These results are in contrast with our results, where *P. pastoris* cells overexpressing *SUR2* resulted in non-viable clones. The reason of this non-viability can be the result of an organism dependence (e.g. *P. pastoris* needs a tighter balance of ceramide to survive than *S. cerevisiae*), or due to an effect of the recombinant protein production, which results in cell stress and requires a more balanced membrane composition to sustain cell viability.

Hac1 overexpression screening

For Hac1, the sequence of the transcription factor was cloned into the pPUZZLE vector and selected for Geneticin resistance. Cell growth was not affected because of overexpression, with all the clones presenting similar growth rate or even higher than the reference strain. In terms of secreted Fab, a negative effect on protein secretion was observed for most of the clones (Figure 5.17). These results are not consonant with previous results from Guerfal *et al.* [191]. They observed that when Hac1 was coexpressed under the control of the GAP promoter, no effect

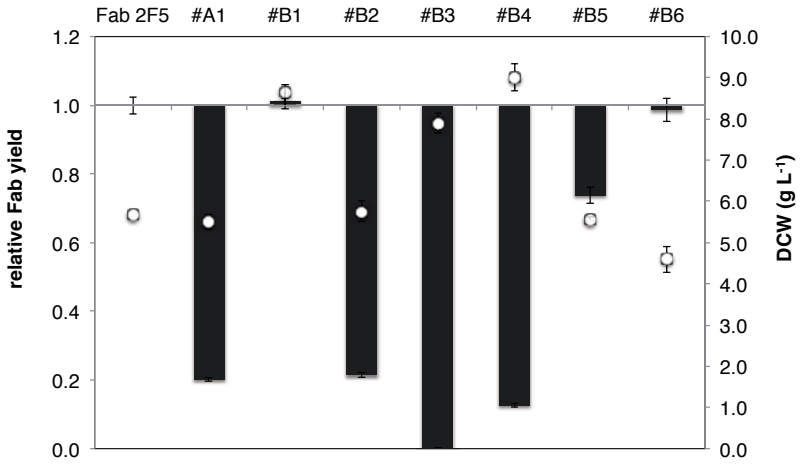

Figure 5.17: Screening *HAC1* overexpression clones. Black bars represent the relative Fab 2F5 yield compared to the reference strain. Empty dots represent the biomass concentration at the end of the culture.

on recombinant protein production was observed, while when it was coexpressed under the methanol inducible AOX1 promoter it affected the recombinant protein production. The effect could be positive or negative in a protein dependent way.

A negative effect rather than no effect was observed for most of the obtained clones in this study. Clone B#5 was selected for further analysis as overexpressing Hac1 strain (OE Hac1) This clones was selected as its growth rate is similar to the reference strain and their production levels were low, representing the major part of the clones, but still not close to the detection limit of the quantification method.

5.2.4. Lipid composition

In order to have an initial overview of the lipid pattern of the mutant strains generated, shake flask cultures in YPD were performed, followed by pellet homogenisation and lipid analysis. Although a constant cell density was obtained for all de cultured strains, lipid composition depends on cell growth and environment composition, so that small changes in the culture environment could lead to changes on the lipid pattern. Sterols, fatty acids, phospholipids and non-polar lipids were quantified.

Sterols

The total sterol content (Figure 5.18) of the analysed strains fluctuated up to 0.3-fold higher (OE Hac1) or lower (ΔSUR2) than the reference strain.

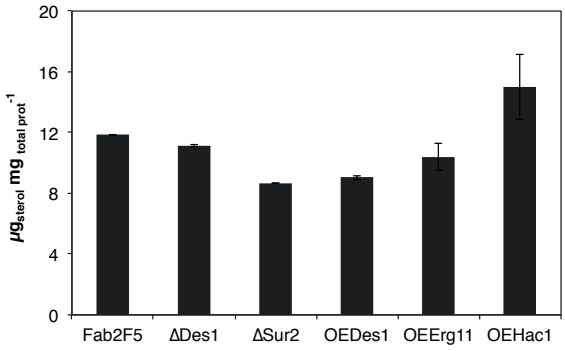

Figure 5.18: Total sterol content of shake flask cultures.

In terms of single sterol content (Figure 5.19), ergosterol was the major sterol in all cell homogenates, while sterol intermediates were present in small amounts. A 30 % reduction of ergosterol was observed for ΔSUR2 strain, while other mutant strains present just a small reduction of ergosterol content compared with the reference one. Other sterol intermediates presenting levels above the detection limit were zymosterol, episterol, 4-Methylzymosterol, were some differences were observed. Zymosterol was 2.2-fold increased in the overexpressing Hac1 strain, while ΔSUR2 and OE Des1 strains decreased zymosterol levels by 55 % and 72 % respectively. Reduced levels of 4-methylzymosterol were also observed for ΔSUR2 and OE Des1 strains.

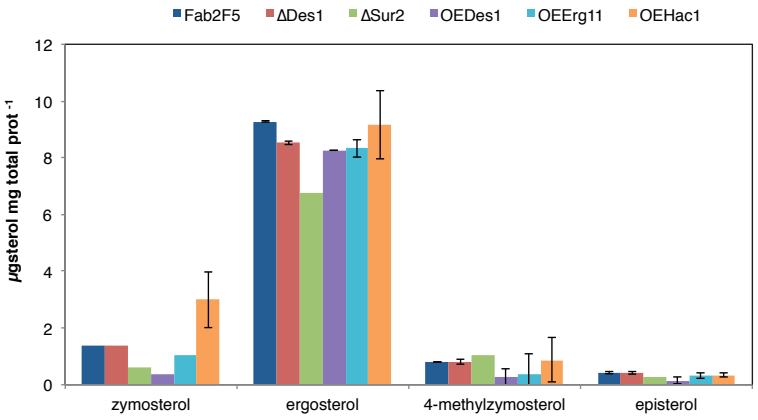

Figure 5.19: Sterol content of shake flask cultures.

Fatty acids

Figure 5.20 shows how oleic acid (18:1) and linolenic acid (18:2) were the two major components of the cell homogenates for all the strains. These results are consistent with the ones previously described by Grillitsch *et al.* [96], where they analysed lipid composition of the plasma membrane and the whole cell homogenate of the strain CBS7435.

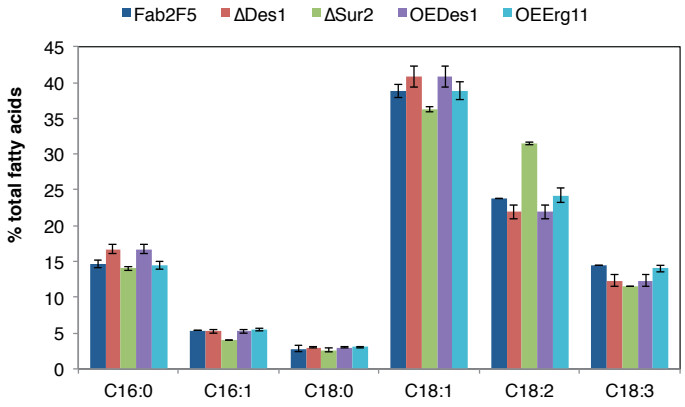

Figure 5.20: Fatty acid content of shake flask cultivations

Levels of palmitic acid (C16:0), palmitoleic acid (C16:1), stearic acid (C18:0) and α-linolenic acid (C18:3) were quite similar among the strains, while some changes were present for oleic acid (C18:1) and linoleic acid (C18:2), where ΔSUR2 strain presented 32 % increased linoleic acid and a reduction of 19 % of oleic acid. It seems that ΔSUR2 strain compensates the reduction of oleic acid by increasing the level of linolenic acid.

Phospholipids

Total phospholipid (PL) levels were slightly decreased for the *DES1* overexpressing strain (11 %) and Hac1 overexpressing one (17.8 %). Similar levels were obtained for the rest of the clones. (Figure 5.21).

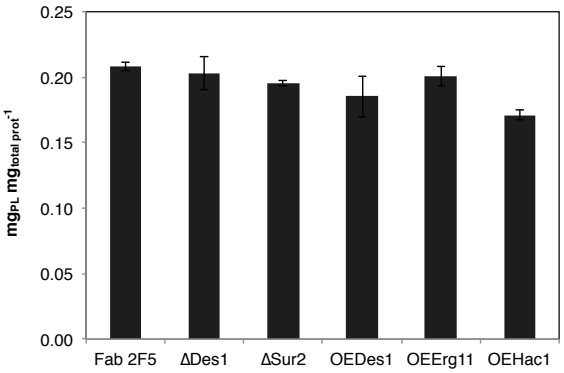

Figure 5.21: Total phospholipid content of shake flask cultivations

Figure 5.22 shows individual phospholipid composition of the homogenates. It can be observed that phosphatidylcholine (PC) was the major phospholipid for all the strains, corresponding to 50 % of the total PL content. The presence of phosphatidylethanolamine (PE), was around 25 %, being the second major PL in all cell homogenates.

PL amounts were similar to those previously described for yeast by Klug *et al.* [95]. PC levels were lower in the ΔSUR2 strain (-15 %), and the overexpressed *ERG11* (-10 %) . Decreased amounts of PC in these strains were compensated by the cell by increased amounts of PI for ΔSUR2 strain (60 % higher) and PS (61.7 % higher) and lyso-PA (3-fold higher) for the strain coexpressing *ERG11*.

It was also relevant the absence of PA in the strain overexpressing *DES1*, since PA plays an important role in lipid metabolism by being a central metabolite in the *de novo* synthesis of phospholipids. The absence of this phospholipid can be due to the fact that it's used for the synthesis of other phospholipids, not being accumulated into the cell.

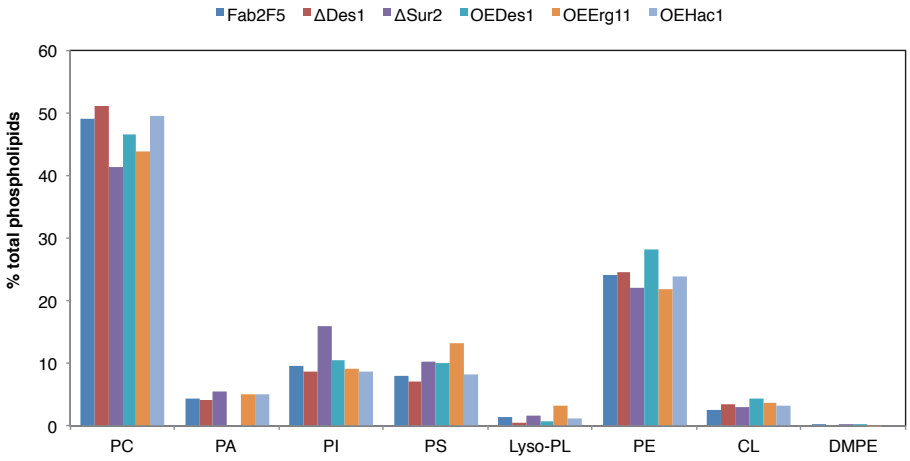

Figure 5.22: Phospholipid content of shake flask cultivations

Non-polar Lipids

Non-polar lipids are composed by sterol esters (SE), triacylglycerols (TAG) and free sterols (FS) (mainly ergosterol). TAGs and SEs serve as intracellular storage molecules for sterols, free fatty

acids and diacylglycerols (DAGs).

The amounts of SEs were lower for all mutant strains compared to the reference strain (Figure 5.23b). A 3-fold reduction was present on the strain coexpressing *DES1*. Levels of free ergosterol were also reduced for all the mutant strains (Figure 5.23c), with levels ranging from 10-25 %). Triacylglycerol (Figure 5.23a) amounts were also lower in all the strains. 1.4-fold reduction was present in the ΔDES1 strain, 2-fold lower for ΔSUR2, and 1.6-fold lower in the overexpressiong *DES1* strain.

Globally, total levels of non-polar lipids in cell homogenates had a reduction in all mutant strains when compared to the reference strain.

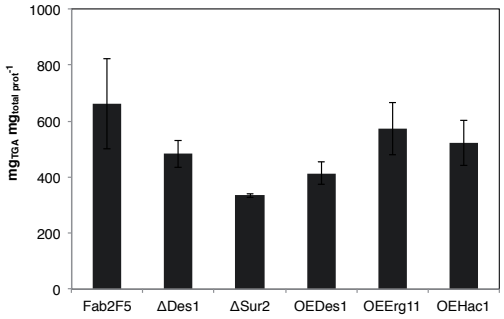

(a) TAG content of shake flask cultivations

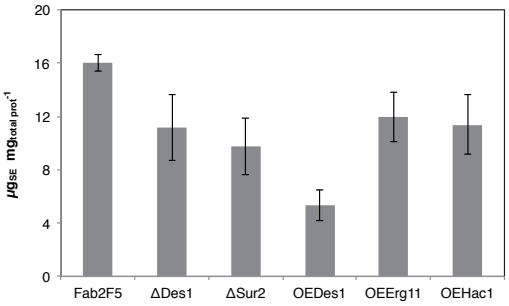

(b) SE content of shake flask cultivations

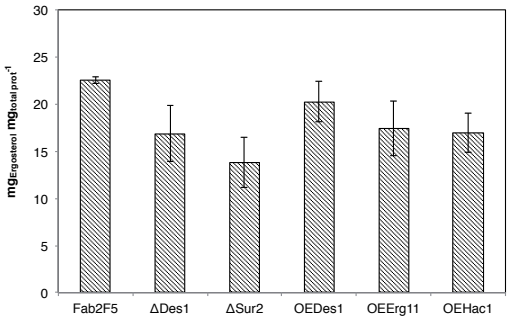

(c) Free Sterol content of shake flask cultivations

Figure 5.23: Non-polar lipid content of shake flask cultivations

5.3. Conclusions

- A ratio of fluconazole per biomass of 80 $\mu g_{Fluco}\ g_{DCW}^{-1}$ was defined as the optimal for Fab secretion. A fluconazole ratio per biomass was defined as the optimal to obtain maximal secretion of Fab into the culture medium. This ratio was 80 $\mu g_{Fluco}\ g_{DCW}^{-1}$.
- Optimised disruption parameters were defined in order to detect high quantities of Fab corresponding to the intracellular fraction. Two passes at 2 kbar were the best disruption settings, and the use of a buffer containing 10 % glycerol, 20 mM HEPES(pH 7.0), 100 mM NaCl and 1 mM PMSF combined with 1 % CHAPS during 16 h (overnight) was selected as the best combination to extract the Fab from the insoluble fraction. A new Buffer, detergent and incubation times were stablished as the optimal for Fab recovery from the intracellular membrane fraction.
- Knockout clones of deleted *DES1* and *SUR2* were cultured, and and the effect on cellular growth and Fab production were determined.
- Clones with overexpressed *DES1, ERG11 and HAC1* were cultured and the effect on Fab production and cellular growth was determined. A clone representing the major part of the clones obtained was selected as a strain representative to be further used.
- *SUR2* overexpression resulted into non-viable clones.
- Major differences compared to reference strain in terms of lipid composition were observed for the clone ΔSUR2 in shake flask cultures. Lipid composition of all clones was determined and some differences were observed, mainly for the ΔSUR2 strain.

6

Bioreactor cultivations and strain characterisation

6.1. Introduction

6.1.1. Bioreactor cultivations

Unlike small-scale shake flasks, bioreactors provide a system to perform cell cultures in a well-monitored and controlled environment. This system allows maintaining controlled most of the culture conditions, such as temperature, pH, dissolved oxygen or volume. One of the main differences from small-scale cultivation systems is that the oxygen transfer rate can be controlled in a bioreactor, allowing achieving higher cell densities and production rates. Depending on the mode of operation, bioreactors can be classified as batch, fed-batch or continuous.

The preference of *P. pastoris* for respiratory growth allows reaching very high cell densities when cultured in a controlled environment of a bioreactor, which can improve overall protein yields. Some general guidelines to perform bioreactor cultures with this organism are available from Invitrogen (https://tools.thermofisher.com/content/sfs/manuals/pichiaferm_prot.pdf). Bioreactor cultivations are normally performed in a fed-batch mode with two phases for constitutive expression (e.g., when using the GAP promoter) or three phases for inducible expression [10]. Glycerol is the preferred carbon source for the batch phase [62], as it is a non-fermentable carbon source that allows high specific growth rates. The optimum growth temperature for *P. pastoris* has been defined as 28-30 °C, however, it has been established that lower cultivation temperatures (e.g. 25 °C) can improve the yields of recombinant protein by decreasing folding stress and enabling more efficient protein secretion without hampering cell growth [11, 249]. *P. pastoris* is capable of growing across a relatively broad pH range (3.0 - 7.0). Optimum pH is critical for protein formation and stability. Generally, the working pH ranges between 5.0 and 5.5 [213].

Chemostat cultivations

Chemostat cultures provide a method to grow microorganisms in constant, carefully controlled conditions, as it enables strict control of culture pH, dissolved oxygen concentration, and temperature, all of which are known to affect cell physiology. The nutrient medium contains saturating concentrations of all of the growth components with the exception of one, the concentration of which determines both cell density and the growth rate.

In chemostat cultures, the dilution rate (D) is defined as the ratio of the flow rate of the ingoing medium (f, L h^{-1}) and the culture volume (V, L). When the culture volume is kept constant by continuous removal of culture broth, a steady-state is reached in which the specific growth rate (μ, h^{-1}) is equal to the dilution rate (when D is smaller than the maximum specific growth rate).
Because concentrations of all metabolites and substrates in steady-state chemostat cultures are constant in time, these cultures provide a flexible and reproducible platform for studies on microbial physiology and gene expression, allowing a good methodology to perform comparisons between different environmental conditions or between different strains at an identical growth rate [250, 251].

Fed-Batch cultivations

Fed-batch cultivations allow high biomass and product concentrations. Processes are shorter, and strain stability and contamination are much less of an issue than in continuous cultures. These features make them suitable to produce recombinant proteins for industrial uses.
In a fed-batch fermentation system an initial batch phase is used for fast initial growth of biomass and a starting point for a controlled feed to the culture. The feed will often consist of concentrated medium that will be applied in such a way that the carbon source is limited to maintain an optimal growth rate in a pseudo steady state condition, which is suited for heterologous protein production. By continuing the feed, the total volume, biomass and product concentrations increase to high levels. Oxygen uptake and heat production also increase, until a point where these parameters can no longer be controlled to the optimum level.

6.1.2. Yeast lipid composition

Lipid metabolism has become an increasing focus of attention, not only because of their structural and functional role as membrane components, but also for their interplay with many important metabolic processes [255]. The goal of lipidomics is to define and quantitate all the lipid molecular species in a cell, but that is complicated by the high number of combinations possible with the large number of known fatty acids that can be occupying a position [88]. The full lipid content of cells comprises several molecular lipid species produced by a metabolic network that interconnects the lipid metabolism of fatty acids, glycerophospholipids, glycerolipids, sphingolipids and sterol lipids [89, 256]. Changes on lipid metabolism can affect lipid composition of the membrane, changing its fluidity [120, 257–259] and other physiological traits [140, 260–263], some of which could ultimately favour recombinant protein secretion.
Up to date, lipid composition of *P. pastoris* have been little investigated. The composition of *P. pastoris* organelles such as plasma membrane [96], peroxisomes [264], mitochondria [265], lipid droplets [133] and endoplasmic reticulum [266] have been characterised. Furthermore, lipid changes with regard to carbon source effect [93] have been recently described. However, such fundamental studies were performed exclusively using wild type strains.
In this work, the lipid composition of a recombinant *P. pastoris* strain is used as a reference strain and lipid changes are described from environmental alterations, as well as genetic modifications on lipid biosynthetic pathways in order to determine lipid changes leading to a secretion improvement.

Yeast lipid analysis

Independently of the subsequent analysis, the first step of lipid analysis is normally the extraction of lipids. Because lipids are water-insoluble, their extraction requires a combination of polar and non-polar organic solvents. The goal of the extraction procedure generally is a quantitative recovery of all the different lipid classes. The commonly used methods for total lipid recovery are Folch *et al.* [177] and its modified version by Bligh and Dyer [267]. The method of Folch involves two successive steps: homogenisation of tissues and extraction with chloroform/methanol, followed by filtration and removal of non-lipid contaminants by washing with potassium chloride (KCl) solution, obtaining a layer containing the lipids [268].

In order to extract lipids from whole yeast cells a first step to break open the yeast cell wall is included, which usually consists on the disintegration in the presence of glass beads. A typical lipid extract contains polar and non-polar lipids. The main components of the polar lipids are glycerophospholipids and sphingolipids. The main components of the non-polar lipids are free fatty acids (FA), diacylglycerols (DAG), triacylglycerols (TG), sterols, and steryl esters (SE) [269]. Different methods are employed for the separation and analysis of different classes of lipids. Moreover, several techniques of lipid analysis exist, all of them presenting their advantages and drawbacks, as it is reported in Table 6.1. The complexity of natural lipid extracts is such that it is

Table 6.1: Advantages and drawbacks of the most important techniques of lipid analysis. Adapted from [270]

	Principle	**Advantages**	**Drawbacks**	**Additional commentaries**
Thin-layer chromatography (TLC)	Separation by polarity differences on a "stationary phase" (silica gel)	Inexpensive, fast, separation of complex mixtures, different staining	oxidation of unsaturated lipids when TLC stored for a while, limited preparative applications	initial method for complex mixtures
High-performance liquid chromatography (HPLC)	Separation under high pressure by elution with different solvents on a "stationary phase"	High quality separations, applicable on preparative scale, possibility of coupling with MS	more time-consuming and expensive than TLC, difficult detection of saturated lipids	Routine method in many laboratories. Composition mobile phase challenging
Gas chromatography (GC) / GC-MS	Separation of volatile compounds on a carrier gas. Detection by MS	Fatty acid analysis. Automated devices commercially available	Only volatile compounds can be analysed. Derivatisation is required	Widely applied for fatty acyl lipids
Soft ionisation mass spectrometry	MALDI and ESI MS enable lipid characterisation without major analyte fragmentation	highly sensitive, direct analyte detection, simple handling	ion suppression, impurities affect significantly	ESI most frequently used. Screening of lipid tissues possible
$^{1}H/^{13}C$ NMR	Differences in electron densities lead to different chemical shifts of the observed nucleus within a given compound	All lipids detectable, interaction studies can be easily performed	Complex spectra obtained, limited sensitivity, need deuterated solvent, expensive equipment	NMR can be used under *in vivo* conditions
^{31}P NMR	Differences in electron densities lead to different chemical shifts of the observed compound	direct absolute quantitation possible, differentiation of isomeric lipids	only lipids with phosphorus detectable, limited sensitivity, expensive equipment	detergents required to suppress PL aggregation

rarely possible to claim that all the lipid classes of a sample can be separated in one operation. It is, therefore, often worthwhile to be able to isolate distinct simple lipid fractions for further analysis [271].

By "shotgun lipidomics", where lipid extracts are directly subjected to MS, Ejsing *et. al.* [89] provided a system to analyse ≈95 % of the *S. cerevisiae* lipidome by monitoring lipid species constituting 21 major lipid classes and several biosynthetic intermediates. Furthermore, the analysis required little sample compared to previous methods.

Thin Layer Chromatography

Thin Layer chromatography (TLC) has been used to quantify levels of non-polar lipids using a 1D TLC, as well as phospholipid content by a 2D TLC. It is a common technique as it is a simple, versatile and highly sensitive and it can be used as a detective or quantitative technique. It is based on the separation of lipids using aluminium foil sheets coated with silica gel adsorbent. Silica gel is a polar adsorbent so that polar lipids are more tightly adsorbed then the non-polar ones. Different solvent systems are used to separate the lipid class of interest. Once separated, plates must be stained in order to visualise the position of the lipids, where the most common used is iodine vapour.

For the separation and detection of neutral lipids, TLC is a suitable technique because the equipment used is very simple, although is generally time-consuming and does not determine molecular species like DAG. On the other hand, 2D TLC has been used to analyse phospholipids, as it is a powerful tool to separate complex lipid mixtures. However, several disadvantages limit their applications, as only a single sample can be investigated, being much more time-consuming than 1D TLC, and simultaneous application of standards is impossible. Normally, a solvent mixture with high elution power is used first, followed by eluents with lower elution power, concentrating the analyte in each step [270].

TLC separation is of low resolution and does not provide molecular information of the diversity of fatty acyl compositions.

Gas Chromatography

Gas chromatography (GC) and gas chromatography - mass spectrometry (GC-MS) has been used to quantify fatty acids and sterols respectively. GC is a form of partition chromatography in which the mobile phase is a gas and the stationary phase is a liquid. A sample is injected into the gas phase where it is volatilised and passed onto the liquid phase, which is held in some form in a column; components spend different times in the mobile phase and the stationary phase, depending on their relative affinities for the latter, and emerge from the end of the column exhibiting peaks of concentration, ideally with a Gaussian distribution [271]. Before the fatty acid components of lipids can be analysed by GC, it is necessary to convert them to low molecular weight non-polar derivatives.

GC-MS is most frequently used to quantify sterols in extracts. The separation of sterols in GC systems depends on the polarity and molecular weight of the molecule. Derivatisation to trimethylsilyl (TMS) ethers is required in order to properly analyse the sterols, as it enables more efficient volatilisation and more sensitive analysis [179]. Mass spectrometers can be coupled to GC to monitor molecular weight of the components, as well as the purity of the samples [272].

6.2. Results and discussion

6.2.1. Establishing hypoxic conditions in chemostat cultures

First hypoxic chemostat studies of *P. pastoris* revealed that stringent hypoxia leads to bioreactor wash out [68]. In order to establish less severe working hypoxic conditions (i.e. allowing for a respirofermentative metabolism) that would prevent this phenomenon, *P. pastoris* producing Fab 2F5 was grown in glucose-limited chemostat cultures at a dilution rate of 0.1 h^{-1} using different percentages of oxygen in the inlet gas, ranging from 0.4 L min^{-1} to 0.20 L min^{-1} (Figure 6.1). Biomass concentration and glucose, ethanol and arabitol quantities were measured 2.4.1 in each steady state.

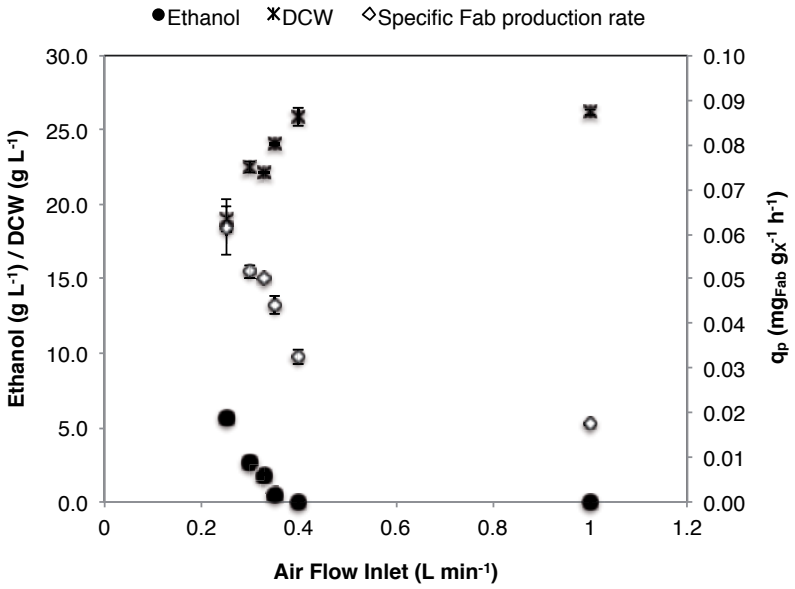

Figure 6.1: Specific Fab 2F5 production rates were determined at different oxygen molar fractions bu changing the air flow in the inlet gas. Ethanol production was monitored as the by-product of hypoxic conditions.

The desired working hypoxic condition was defined as the lower air flow that permitted a stable cell concentration (i.e. no washout in the bioreactor) while significant amounts of ethanol and arabitol, were present in the media, thereby indicating respirofermentative metabolic condition. Based on this preliminary series of chemostats, a mixture of 0.25 L min^{-1} air and 0.75 L min^{-1} of N_2 in the inlet gas was selected, corresponding to a q_p of ethanol and arabitol of 0.434 $mmol_{EtOH}$ $g_{DCW}{}^{-1}$ h^{-1} and 0.048 $mmol_{Arab}$ $g_{DCW}{}^{-1}$ h^{-1}, respectively (Table 6.2). Data was consistent with the previous results presented by Baumann and co-workers [68]. Decreased biomass yield coefficient due to the partially fermentative metabolism was also observed in both studies.

Table 6.2: Comparison of hypoxic parameters in a Biostat B and a Biostat B+ system

Culture	Oxygen conditions	DCW (g L^{-1})	$Y_{X/S}$ (g_{DCW} $g_{glc}{}^{-1}$)	Fab secreted (mg_{Fab} L^{-1})	q_{Fab} (mg_{Fab} $g_{DCW}{}^{-1}$ h^{-1})	q_{EtOH} ($mmol_{EtOH}$ $g_{DCW}{}^{-1}$ h^{-1})	q_{Arab} ($mmol_{Arab}$ $g_{DCW}{}^{-1}$ h^{-1})	C-balance
Biostat B	1 L min^{-1}	28.5 ± 0.0	0.58 ± 0.00	5.0 ± 0.2	0.017 ± 0.008	0.001 ± 0.000	n.d.	1.02
	0.25 L min^{-1}	20.5 ± 0.4	0.42 ± 0.01	11.0 ± 0.1	0.049 ± 0.012	0.434 ± 0.058	0.048 ± 0.017	0.97
Biostat B+	1 L min^{-1}	30.3 ± 0.1	0.64 ± 0.00	4.4 ± 0.1	0.016 ± 0.003	0.006 ± 0.001	n.d.	1.2
	0.25 L min^{-1}	25.9 ± 0.1	0.54 ± 0.00	7.5 ± 0.2	0.031 ± 0.007	0.244 ± 0.022	0.033 ± 0.005	1.03

DCW = dry cell weight; $Y_{X/S}$ = yield of biomass on glucose; q = specific production rate; C-balance = carbon balance.

Once established the hypoxic conditions for the Biostat B, same parameters were used in a Biostat B+ with an identical vessel and where the impeller for steering was adjusted at the same position. Thus, similar oxygen transfer and hypoxic conditions would be expected. Resulting parameters for the two reactor systems using the same settings are shown in Table 6.2, where it can be observed a 1.9-fold increase of q_{Fab} when Biostat B+ is used under hypoxic conditions, while equivalent conditions in Biostat B lead to an increase of q_{Fab} up to 2.9-fold. In hypoxic conditions, q_{EtOH} and q_{Arab} increased compared to normoxia in both bioreactors, but lower levels were present in Biostat B+, consistent with the less stringent hypoxia achieved.
Less air flow in the inlet gas led to the wash out of the reactor, indicating that 0.25 L min^{-1} was the most restrictive air flow to work with Biostat B+ without washing out, even when they provide less restrictive hypoxic conditions than in Biostat B.
Once the hypoxic conditions were established, chemostat cultivations with the battery of strains generated were performed in both normoxic and hypoxic conditions.

6.2.2. Chemostat cultivations

Chemostat cultivations were performed as indicated in the Materials and Methods section 2.3.7. Except for OE DES1, all strains were cultured at a growth rate of 0.1 h^{-1}, corresponding to the half of their μ_{max}. OE DES1 exhibit a lower maximum growth rate and it was cultured at 0.05 h^{-1}, corresponding to its half μ_{max}, which ensures equal cell metabolic state than the rest of strains.
Samples were taken after a minimum of five residence times to ensure cell metabolic steady state. Cultivations were analysed in terms of growth and Fab productivities (Table 6.3). For all the cultures in hypoxic conditions, lower biomass concentrations were obtained due to the lower biomass to substrate yield of the partially fermentative metabolism of cells cultured under low oxygen conditions. Furthermore, all strains achieved higher Fab productivities in hypoxia, where the highest increase observed in the strain overexpressing *ERG11* (OE ERG11, 3.9-fold), ΔDES1 (3.6-fold), and OE Hac1 (3.3-fold). All of them exhibited higher Fab productivities due to the cultivation in hypoxic conditions than the reference strain (2.9-fold). Under normoxic conditions, most of the strains presented similar Fab production rates than the reference strain, except for ΔSUR2 and the fluconazole-treated cells, with 2.12-fold and 1.24-fold increase respectively.
Glucose and glycerol were measured by HPLC and values where always under the detection level. Ethanol and arabitol were detected in the culture medium of hypoxic cultivations, although their specific production rates were lower than in previous hypoxic studies [82], indicating less stringent hypoxic stress and providing true steady state conditions in the bioreactor (i.e. no washing out). OE DES1 levels of ethanol and arabitol were similar in hypoxic and normoxic conditions, indicating that no change to respirofermentative metabolism was achieved. In order to establish hypoxic conditions for this strain, air flow was reduced proportionally to the dilution rate. Thus, an air flow 0.12 L min^{-1} was used instead of 0.25 L min^{-1}. Ethanol and arabitol production rates denoted the selected air flow was not restrictive enough to shift to respirofermentative metabolism.
As expected, RQ was also increased in hypoxia, except for the strain overexpressing Hac1, which presented reduced RQ levels in hypoxia, even cells were growing under respirofermentative conditions.
The carbon recovery data of the chemostat cultivations was above 87 %, and the obtained data is consistent with previous results [68], which proves a well defined system and the reproducibility of the cultivation system.

Table 6.3: Physiological parameters of the chemostat cultures of the working strains grown under normoxic and hypoxic conditions

Culture	Oxygen conditions	DCW ($g\ L^{-1}$)	$Y_{X/S}$ ($g_{DCW}\ g_{glc}^{-1}$)	Fab secreted ($mg_{Fab}\ L^{-1}$)	q_{Fab} ($mg_{Fab}\ g_{DCW}^{-1}\ h^{-1}$)	q_{EtOH} ($mmol_{EtOH}\ g_{DCW}^{-1}\ h^{-1}$)	q_{Arab} ($mmol_{Arab}\ g_{DCW}^{-1}\ h^{-1}$)	q_{O2} ($mmol_{O2}\ g_{DCW}^{-1}\ h^{-1}$)	q_{CO2} ($mmol_{CO2}\ g_{DCW}^{-1}\ h^{-1}$)	RQ	C-balance
Fab2F5	Normoxia	28.5 ± 0.0	0.58 ± 0.00	5.0 ± 0.2	0.017 ± 0.008	0.001 ± 0.000	n.d.	2.04 ± 0.01	2.00 ± 0.01	1.0 ± 0.0	1.02
	Hypoxia	20.5 ± 0.4	0.42 ± 0.01	11.0 ± 0.1	0.049 ± 0.012	0.434 ± 0.058	0.048 ± 0.017	1.89 ± 0.05	2.60 ± 0.05	1.4 ± 0.0	0.97
ΔDES1	Normoxia	25.8 ± 0.1	0.53 ± 0.01	4.14 ± 0.2	0.015 ± 0.008	0.002 ± 0.000	n.d.	2.14 ± 0.02	2.06 ± 0.01	1.0 ± 0.0	0.94
	Hypoxia	18.0 ± 0.3	0.37 ± 0.01	10.6 ± 0.0	0.054 ± 0.010	0.406 ± 0.039	0.053 ± 0.013	2.06 ± 0.10	2.99 ± 0.09	1.5 ± 0.1	0.88
OE DES1	Normoxia	24.6 ± 0.1	0.52 ± 0.01	4.7 ± 0.2	0.010 ± 0.006	0.004 ± 0.001	n.d.	1.29 ± 0.04	1.14 ± 0.02	0.9 ± 0.0	0.93
	Hypoxia	25.1 ± 0.4	0.53 ± 0.01	8.3 ± 0.4	0.016 ± 0.010	0.004 ± 0.001	n.d.	0.87 ± 0.02	0.98 ± 0.01	1.1 ± 0.0	0.90
ΔSUR2	Normoxia	25.2 ± 0.1	0.50 ± 0.01	10.5 ± 0.3	0.036 ± 0.012	0.010 ± 0.001	n.d.	2.38 ± 0.01	2.44 ± 0.02	1.0 ± 0.0	0.98
	Hypoxia	20.6 ± 0.0	0.41 ± 0.00	10.0 ± 0.4	0.045 ± 0.018	0.442 ± 0.035	0.048 ± 0.004	2.09 ± 0.02	2.77 ± 0.01	1.3 ± 0.0	0.98
Fluco	Normoxia	25.0 ± 0.0	0.50 ± 0.01	5.6 ± 0.1	0.021 ± 0.004	n.d.	0.001 ± 0.000	2.25 ± 0.05	2.57 ± 0.05	1.1 ± 0.0	0.98
	Hypoxia	8.94 ± 0.0	0.28 ± 0.00	3.0 ± 0.1	0.033 ± 0.014	1.18 ± 0.02	0.456 ± 0.009	3.74 ± 0.07	5.60 ± 0.10	1.5 ± 0.0	1.18
OE ERG11	Normoxia	29.5 ± 0.3	0.58 ± 0.02	4.8 ± 0.2	0.016 ± 0.008	0.001 ± 0.002	n.d.	1.50 ± 0.04	1.83 ± 0.02	1.2 ± 0.0	1.00
	Hypoxia	19.5 ± 0.1	0.42 ± 0.02	13.0 ± 1.9	0.063 ± 0.102	0.434 ± 0.005	0.048 ± 0.008	1.06 ± 0.08	2.15 ± 0.02	2.0 ± 0.2	0.98
OE Hac1	Normoxia	32.0 ± 0.4	0.63 ± 0.01	6.3 ± 0.2	0.019 ± 0.007	0.005 ± 0.001	n.d.	1.00 ± 0.02	2.15 ± 0.05	2.1 ± 0.1	1.13
	Hypoxia	16.3 ± 0.5	0.32 ± 0.01	10.3 ± 0.3	0.063 ± 0.027	1.608 ± 0.179	0.086 ± 0.027	4.08 ± 0.08	5.89 ± 0.12	1.4 ± 0.0	1.03

DCW = dry cell weight; glc = glucose; $Y_{X/S}$ = biomass to substrate yield; q = specific product formation rate; n.d. = not detected. Values represent the mean ± standard error.

6.2.3. Intra-extracellular distribution of the Fab

Cells were disrupted using the methodology described in the Materials and Methods (Section 5.2.2). Fab 2F5 amounts present in the supernatant (SN), soluble cytosolic fraction (SCF) and insoluble membrane fraction (IMF) were quantified by ELISA. Thus, intracellular and extracellular distribution of the Fab 2F5 within the cells was determined (Table 6.4).

The percentage of secreted Fab 2F5 was calculated as the amount of Fab present in the supernatant in relation to the total Fab (SN + SCF + IMF). Under all conditions tested, relative secretion levels of Fab were above 80 %, suggesting that no important secretion limitations were present in producing cells under steady state conditions.

Whereas Fab specific productivities were higher under reduced oxygen availability, Fab yield in the intracellular fraction was very low and similar in both conditions. That is, increased Fab synthesis levels caused by the upregulation of the *GAP* promoter under hypoxic conditions [69] did not result in an overload of the secretion capacity.

Although secretion of heterologous proteins is liable to several bottlenecks that limit yield [38, 41, 204], our results suggest that no secretion limitations are present when cells are producing higher amounts of protein under the selected hypoxic conditions. This may indicate that membrane alterations due to hypoxic culture conditions favour protein secretion, avoiding intracellular accumulation even when Fab production is increased.

It has also been observed that the insoluble fraction (IMF), where the membrane related fractions are present (i.e. endoplasmic reticulum, plasma membrane), presented almost no recombinant protein, indicating no protein accumulation in the ER due to misfolding events. Moreover, no accumulation of Fab in the cytosolic fraction was detected, which can be due to a high degradation of misfolded protein within the cell, which Pfeffer *et al.* reported to be around 60 % of the total protein produced in their studies performed with an antibody fragment [243].

6.2.4. Cell lipid composition

Lipid composition of cell homogenates was determined for all the cultures and oxygen conditions to investigate the correlation between changes on protein production and altered lipid profiles. Lipid changes were expected in all strains, as genetic modifications in the mutated strains were pointed to lipid biosynthetic pathways. Additionally, changes under hypoxic conditions were also presumed, as biosynthesis of certain lipids (e. g. ergosterol, unsaturated fatty acids) require oxygen, and previous transcriptomic studies revealed that ergosterol and sphingolipid biosynthetic pathways were regulated under hypoxia [69].

Fatty acid composition

Relative amounts of fatty acids of the cell lipid extracts were analysed for each strain and culture condition and are shown in Table 6.5. In all cases, oleic acid (C18:1) was the major fatty acid in the cell homogenates, followed by linoleic acid (C18:2) and palmitic acid (C16:0). All strains presented similar levels of fatty acid species with the major differences observed for the strain OE Hac1, which showed 35 % decrease of linoleic acid and an increase of palmitic acid by 53 % compared to the reference strain. Fluconazole-treated cells presented 12 % reduction of oleic acid amounts, ΔSUR2 showed 45 % higher amounts of α-linolenic acid (C18:3) and 45 % reduction of cerotic acid (C26:0).

Regarding total amounts of saturated fatty acids, an increase of 61.8 % was observed for OE Hac1 strain compared to the reference strain. Total monounsaturated fatty acids remained similar for all the strains in normoxic conditions, except for fluconazole-treated cells, showing a reduction of

Table 6.4: Fab product distribution within the cell under normoxic and hypoxic conditions.

Culture	Oxygen conditions	D (h^{-1})	q_{Fab} (mg_{Fab} g_{DCW}^{-1} h^{-1})	Total Fab (mg)				Expression (mg_{Fab} g_{DCW}^{-1})			% Secretion
				SN	SCF	IMF	Total	SN	SCF	IMF	
Fab2F5	Normoxia	0.094	0.017 ± 0.008	6.4 ± 0.4	0.57 ± 0.02	0.13 ± 0.01	7.1 ± 0.4	0.25 ± 0.02	0.02 ± 0.0	0.005 ± 0.000	90 ± 5
	Hypoxia	0.092	0.049 ± 0.012	11.8 ± 0.1	0.73 ± 0.04	0.11 ± 0.02	12.7 ± 0.2	0.53 ± 0.01	0.03 ± 0.0	0.005 ± 0.001	93 ± 1
ΔDES1	Normoxia	0.092	0.015 ± 0.008	4.1 ± 0.2	0.71 ± 0.03	0.17 ± 0.01	4.9 ± 0.2	0.16 ± 0.01	0.03 ± 0.0	0.010 ± 0.000	82 ± 3
	Hypoxia	0.092	0.054 ± 0.010	10.5 ± 0.5	0.90 ± 0.04	0.12 ± 0.01	11.5 ± 0.5	0.60 ± 0.03	0.05 ± 0.0	0.010 ± 0.001	91 ± 3
OE DES1	Normoxia	0.050	0.010 ± 0.006	4.4 ± 0.2	0.46 ± 0.01	0.09 ± 0.0	5.0 ± 0.2	0.19 ± 0.01	0.02 ± 0.0	0.004 ± 0.000	89 ± 4
	Hypoxia	0.050	0.016 ± 0.010	8.0 ± 0.4	0.91 ± 0.03	0.14 ± 0.02	9.0 ± 0.4	0.33 ± 0.02	0.04 ± 0.0	0.010 ± 0.001	88 ± 4
ΔSUR2	Normoxia	0.088	0.036 ± 0.012	11.0 ± 0.3	1.07 ± 0.05	0.13 ± 0.01	12.2 ± 0.3.	0.41 ± 0.01	0.04 ± 0.0	0.005 ± 0.000	90 ± 2
	Hypoxia	0.092	0.045 ± 0.018	10.5 ± 0.4	1.14 ± 0.03	0.15 ± 0.01	11.8 ± 0.4	0.49 ± 0.02	0.05 ± 0.0	0.010 ± 0.001	89 ± 2
Fluco	Normoxia	0.094	0.021 ± 0.004	5.3 ± 0.1	0.57 ± 0.04	0.17 ± 0.03	6.1 ± 0.1	0.22 ± 0.01	0.02 ± 0.0	0.010 ± 0.000	88 ± 1
	Hypoxia	0.099	0.033 ± 0.014	2.8 ± 0.1	0.33 ± 0.02	0.10 ± 0.01	3.25 ± 0.1	0.33 ± 0.02	0.04 ± 0.0	0.010 ± 0.000	87 ± 3
OE ERG11	Normoxia	0.099	0.016 ± 0.008	4.8 ± 0.2	1.01 ± 0.01	0.17 ± 0.01	6.0 ± 0.2	0.16 ± 0.01	0.03 ± 0.0	0.010 ± 0.000	80 ± 3
	Hypoxia	0.095	0.063 ± 0.102	13.2 ± 2.0	1.03 ± 0.03	0.12 ± 0.01	14.3 ± 2.0	0.67 ± 0.10	0.05 ± 0.0	0.010 ± 0.000	92 ± 11
OE Hac1	Normoxia	0.096	0.019 ± 0.007	6.2 ± 0.2	0.77 ± 0.03	0.17 ± 0.03	7.1 ± 0.2	0.20 ± 0.00	0.02 ± 0.0	0.010 ± 0.000	87 ± 2
	Hypoxia	0.099	0.063 ± 0.027	10.2 ± 0.3	0.91 ± 0.05	0.10 ± 0.01	11.21 ± 0.3	0.63 ± 0.02	0.06 ± 0.0	0.010 ± 0.001	91 ± 2

Values represent the mean ± standard deviation.

Table 6.5: Fatty acid composition of reference strain and mutant strains cultured in normoxic and hypoxic conditions

Culture	Oxygen conditions	% of total fatty acids									C16/C18	UFA/SFA
		C14:0	C16:0	C16:1	C18:0	C18:1	C18:2	C18:3	C26:0	Others		
Fab2F5	Normoxia	0.61 ± 0.19	13.5 ± 0.8	6.7 ± 0.1	3.4 ± 0.5	37.5 ± 1.0	25.8 ± 1.5	8.0 ± 0.4	2.2 ± 0.7	1.2 ± 0.4	0.27	3.9 ± 0.2
	Hypoxia	0.72 ± 0.04	13.2 ± 0.2	5.4 ± 0.2	3.7 ± 0.3	46.4 ± 1.7	26.6 ± 1.1	1.5 ± 0.1	1.9 ± 0.5	0.47 ± 0.11	0.24	4.1 ± 0.2
ΔDES1	Normoxia	0.69 ± 0.18	15 ± 1.7	7.2 ± 0.7	3.6 ± 0.7	36.6 ± 1.3	25.9 ± 1.6	7.4 ± 0.6	2.9 ± 0.7	0.56 ± 0.28	0.30	3.5 ± 0.2
	Hypoxia	0.58 ± 0.08	13.3 ± 1.9	4.2 ± 0.5	4.0 ± 0.8	42.3 ± 6.5	20.8 ± 1.3	1.6 ± 0.3	2.5 ± 0.3	0.48 ± 0.36	0.25	3.4 ± 0.4
OE DES1	Normoxia	0.68 ± 0.15	13.6 ± 0.5	7.1 ± 0.3	2.8 ± 0.2	38.0 ± 0.4	28.9 ± 0.0	6.8 ± 0.9	1.8 ± 0.1	0.35 ± 0.09	0.27	4.3 ± 0.1
	Hypoxia	0.91 ± 0.25	14.1 ± 2.1	5.4 ± 0.5	4.1 ± 0.5	46.9 ± 3.4	21.4 ± 5.6	1.6 ± 0.4	5.5 ± 3.9	0.64 ± 0.24	0.26	3.1 ± 0.6
ΔSUR2	Normoxia	0.44 ± 0.00	11.9 ± 0.3	5.8 ± 0.1	2.6 ± 0.0	36.7 ± 0.3	29.5 ± 0.1	11.6 ± 0.1	1.2 ± 0.1	0.56 ± 0.05	0.22	5.2 ± 0.0
	Hypoxia	0.77 ± 0.15	14.5 ± 1.7	4.3 ± 0.4	3.6 ± 0.4	48.3 ± 1.0	23.5 ± 3.6	1.8 ± 0.1	2.2 ± 1.2	0.99 ± 0.62	0.24	3.7 ± 0.3
Fluco	Normoxia	0.66 ± 0.19	12.5 ± 2.0	4.1 ± 0.4	4.0 ± 0.7	33.1 ± 2.9	27.5 ± 2.5	6.5 ± 0.9	4.1 ± 2.1	0.34 ± 0.17	0.23	3.4 ± 0.4
	Hypoxia	0.56 ± 0.05	14.9 ± 1.9	6.9 ± 0.2	3.7 ± 0.5	42.0 ± 1.1	25.7 ± 3.5	4.7 ± 0.4	1.2 ± 0.3	0.30 ± 0.15	0.29	3.9 ± 0.2
OE ERG11	Normoxia	0.76 ± 0.03	16.0 ± 1.4	7.7 ± 0.9	4.3 ± 0.7	39.1 ± 1.0	21.1 ± 3.5	5.1 ± 1.6	5.2 ± 2.6	0.68 ± 0.24	0.34	2.7 ± 0.3
	Hypoxia	0.83 ± 0.10	13.6 ± 1.1	5.1 ± 0.4	3.9 ± 0.3	50.0 ± 0.8	22.4 ± 2.5	1.1 ± 0.3	2.7 ± 1.3	0.36 ± 0.09	0.24	3.7 ± 0.3
OE Hac1	Normoxia	0.93 ± 0.39	20.7 ± 7.0	5.3 ± 0.7	5.9 ± 1.7	40.4 ± 3.3	16.5 ± 5.9	4.4 ± 1.1	4.5 ± 1.5	1.6 ± 1.1	0.39	2.1 ± 0.3
	Hypoxia	0.73 ± 0.05	13.7 ± 1.1	5.0 ± 0.3	4.0 ± 0.3	56.5 ± 0.9	17.2 ± 1.5	0.5 ± 0.1	1.9 ± 0.6	0.51 ± 0.20	0.24	3.9 ± 0.2

C14:0 = myristic acid; C16:0 = palmitic acid; C16:1 = palmitoleic acid; C18:0 = stearic acid; C18:1 = oleic acid; C18:2 = linoleic acid; C18:3 = α-linolenic acid; C26:0 = cerotic acid. Values represent the mean ± SD from triplicates.

16 %. Finally, total levels of polyunsaturated fatty acids were 21.7 % higher in the ΔSUR2 strain, and 22.4 % and 38.2 % lower for OE ERG11 and OE Hac1 respectively. Therefore, a change of polyunsaturation to saturation of the fatty acid species in the strain OE Hac1 was observed that could lead to changes in the membrane properties.

In hypoxia, a change in the degree of unsaturation was given by the increment of oleic acid and the decrease of α-linolenic acid species present in the homogenates. High saturation of fatty acids acts as a protective mechanism by creating a more rigid membrane and reducing the oxidative stress that results from the oxidation of unsaturated fatty acids [273]. In this sense, OE Hac1 strain exhibit the most severe change, with levels of oleic acid higher than 50 % of the total fatty acid content and levels of linoleic acid accounting for the 65 % of the reference strain. Levels of oleic acid and α-linolenic acid exhibit milder changes compared to the rest of strains.
In *P. pastoris*, it has been shown than the relative amount of polyunsaturated fatty acids is much higher than in *S. cerevisiae* [264, 265].

Phospholipid composition

Total phospholipid (PL) content lipid extracts were determined and are shown in Figure 6.2. Slightly reduced total amounts were present in strains OE DES1, OE ERG11 and OE Hac1 strains, while the rest of strains maintained similar levels to the reference strain. Hypoxic conditions were translated to different effects on total PL content depending on the strain. Fab 2F5 and fluconazole-treated cells presented reduced levels of total PL in hypoxia, while the opposite effect was observed for ΔDES1, ΔSUR2, OE ERG11 and OE Hac1. Finally, OE DES1 strain did not change its PL levels due to hypoxic conditions.

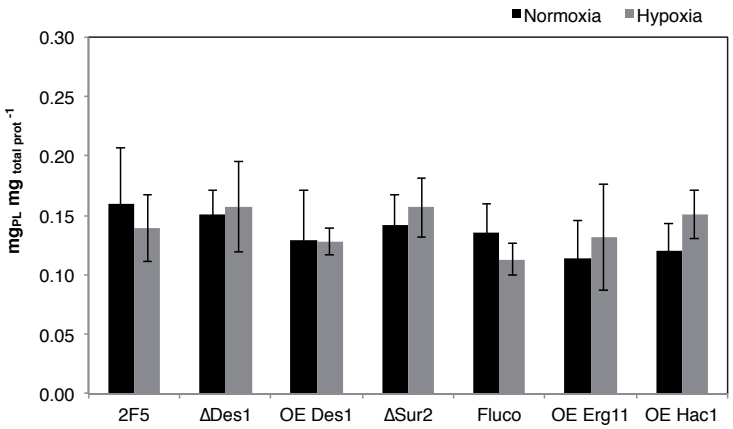

Figure 6.2: Total PL content of the strains in both normoxic and hypoxic conditions

In terms of specific phospholipids (Table 6.6), phosphatidylcholine (PC) and phosphatidylethanolamine (PE), phosphatidylinositol (PI) and phosphatodylserine (PS) were the major phospholipids in the homogenates. This results are in concordance with previous phospholipid characterisation of *P. pastoris* [96, 274].
Hypoxic conditions resulted in higher amounts of phosphatidylethanolamine (≈22 %) except for ΔDES1 and OE ERG11, and a notable increase of phosphatidylserine (PS), while levels of phosphatidylinositol (PI) were substantially reduced in all the strains.
Phospholipids are the major lipids of cellular membranes, thus changes on the relative amounts of phospholipids can alter significantly its properties. Moreover, cellular amounts of PI can

Table 6.6: Phospholipid composition of reference strain and mutant strains cultured in normoxic and hypoxic conditions

Culture	Oxygen conditions	% of total phospholipids							
		PC	PE	PI	PS	PA	CL	lyso-PL	DMPE
Fab2F5	Normoxia	43.4 ± 1.3	19.2 ± 2.2	12.8 ± 1.2	7.7 ± 0.1	4.2 ± 1.5	13.3 ± 1.8	n.d.	n.d.
	Hypoxia	48.5 ± 3.0	24.6 ± 1.3	3.7 ± 0.1	15.0 ± 1.6	3.6 ± 1.2	3.3 ± 0.3	n.d.	1.43 ± 1.12
ΔDES1	Normoxia	48.5 ± 1.5	24.9 ± 1.7	12.6 ± 0.7	7.8 ± 0.5	4.6 ± 1.3	2.2 ± 0.5	n.d.	n.d.
	Hypoxia	45.4 ± 0.2	24.6 ± 1.6	6.6 ± 4.7	14.0 ± 4.3	5.1 ± 2.5	3.9 ± 1.2	n.d.	0.49 ± 0.69
OE DES1	Normoxia	53.4 ± 6.8	21.3 ± 2.3	12.7 ± 1.0	8.4 ± 1.9	2.9 ± 0.8	3.2 ± 1.0	n.d.	n.d.
	Hypoxia	47.0 ± 0.5	26.0 ± 0.2	5.3 ± 1.9	12.5 ± 3.0	3.9 ± 0.6	4.1 ± 0.9	n.d.	1.29 ± 0.27
ΔSUR2	Normoxia	40.3 ± 1.9	23.8 ± 4.7	10.5 ± 2.2	10.7 ± 1.6	4.3 ± 0.5	3.1 ± 0.1	2.4 ± 1.6	0.24 ± 0.63
	Hypoxia	40.7 ± 3.9	28.7 ± 0.2	7.0 ± 1.4	14.7 ± 0.3	4.4 ± 0.5	3.3 ± 1.0	0.76 ± 0.36	0.39 ± 0.83
Fluco	Normoxia	49.0 ± 3.1	17.5 ± 5.1	10.5 ± 2.2	11.3 ± 5.0	6.9 ± 1.6	4.2 ± 1.0	0.37 ± 2.3	0.35 ± 1.09
	Hypoxia	47.8 ± 4.0	23.1 ± 0.7	3.7 ± 0.8	15.2 ± 1.8	5.1 ± 0.9	3.2 ± 0.8	0.62 ± 1.6	1.07 ± 0.74
OE ERG11	Normoxia	54.2 ± 0.2	22.8 ± 1.0	8.7 ± 0.1	7.5 ± 1.7	4.4 ± 0.5	3.3 ± 0.4	n.d.	n.d.
	Hypoxia	47.7 ± 1.0	24.1 ± 1.4	2.2 ± 0.6	16.7 ± 0.6	5.3 ± 0.3	3.8 ± 0.5	n.d.	1.3 ± 1.27
OE Hac1	Normoxia	49.8 ± 2.7	21.7 ± 3.4	11.2 ± 2.5	8.4 ± 0.1	5.6 ± 0.1	3.9 ± 1.0	n.d.	n.d.
	Hypoxia	43.6 ± 2.8	25.6 ± 1.5	2.0 ± 0.0	18.3 ± 1.3	4.9 ± 0.8	4.0 ± 0.7	0.54 ± 0.46	1.1 ± 0.36

PC = phosphatidylcholine; PA = phosphatidic acid; PI = phosphatidylinositol; PS = phosphatidylserine; Lyso-PL = lysophospholipids; PE = phosphatidylethanolamine; CL = cardiolipin; DMPE = dimethyl phosphatidylethanolamine. Values represent the mean ± SD from duplicates.

have an important impact on cell membrane composition, as it is involved in inositol containing sphingolipid biosynthesis. It has been reported that both PI and PS are anionic (charge -1), and PI can substitute PS in order to preserve PL balance, but not the inverse [275], which make the observed results be the consequence of major important changes on cell during hypoxic conditions.

Non-polar lipid composition

Non-polar lipids were analysed in order to explain the whole lipidomic pattern of the strains. Triacylglycerols (TG), steryl esters (SE) and free sterols (FS) were quantified using TLC and the results are shown in Table 6.7.

Almost all strains presented both TG and SE increased when cells were cultured in hypoxia, up to 3.2-fold for TG in fluconazole treated cells and 5-fold for SE in ΔDES1. Increased levels of TG under hypoxia are consistent with preliminary lipid analyses previously performed by our group [82]. In the case of free sterols, levels decrease for most of the strains when changing from normoxic to hypoxic conditions probably due to low levels of sterol biosynthesis, except for ΔSUR2, fluconazole treated cells and OE Hac1, were FS levels remained equal or raised in hypoxia.

Table 6.7: Non-polar lipid composition of reference strain and mutant strains cultured in normoxic and hypoxic conditions

Culture	**Oxygen conditions**	**TG** (μg lipid $mg_{tot.\ prot.}^{-1}$)	**SE** (μg lipid $mg_{tot.\ prot.}^{-1}$)	**Free Sterols** (μg lipid $mg_{tot.\ prot.}^{-1}$)
Fab 2F5	Normoxia	93 ± 26	6.9 ± 1.4	19 ± 2
	Hypoxia	156 ± 33	9.4 ± 0.5	16 ± 2
Δ DES1	Normoxia	66 ± 23	4.8 ± 0.3	21 ± 1
	Hypoxia	133 ± 30	24 ± 6	20 ± 0
OE DES1	Normoxia	55 ± 10	5.2 ± 2.2	22 ± 4
	Hypoxia	96 ± 24	5.3 ± 2.5	17 ± 5
Δ SUR2	Normoxia	153 ± 16	23 ± 6	16 ± 1
	Hypoxia	178 ± 12	23 ± 3	17 ± 2
Fluco	Normoxia	150 ± 29	4.6 ± 2.3	22 ± 9
	Hypoxia	480 ± 55	6.4 ± 2.5	25 ± 4
OE ERG11	Normoxia	57 ± 13	6.1 ± 2.9	24 ± 8
	Hypoxia	126 ± 20	4.5 ± 0.8	21 ± 5
OE Hac1	Normoxia	49 ± 22	4.1 ± 1.1	21 ± 5
	Hypoxia	137 ± 26	4.5 ± 0.8	21 ± 5

TG = Triacylglycerols; SE = Sterol Esters, FS = Free Sterols. Values represent the mean ± SD from triplicates.

Non-polar lipid synthesis in yeast is involved in the maintenance of the equilibrium of saturated and unsaturated fatty acids, and also in membrane composition regarding fatty acids and phospholipids in order to preserve membrane fluidity [97]. Changes on TG levels related to growth phase (stationary vs. exponential) have been reported [97], suggesting a possible non-polar lipid storage that depends on cell growth and that could explain increased levels of both TG and SE under hypoxic conditions since it is known that 0.1 h^{-1} corresponds to 50 % of μ_{max} in normoxic conditions, but no data for hypoxic conditions are available.. A lower μ_{max} under hypoxia

would mean a higher relative growth rate of cells cultured under these conditions, and thus, altered levels of storage lipids due to a different cell metabolism. Moreover, it has been described that changes in glucose metabolism caused by the shift from respiratory to respirofermentative metabolism can impact non-polar lipid homeostasis by changing activity of TG lipases [97].

Sterol composition

As shown in Table 6.8, the major sterol found under all analysed conditions was ergosterol. Compared to the reference strain, lower levels of ergosterol were present in ΔSUR2, fluconazole-treated cells, OE ERG11 and OE Hac1. Intermediates of the ergosterol pathway, like 4-methyl zymosterol, zymosterol or episterol were also detected, but only in small amounts.

Strains reacted to hypoxic conditions in different ways. While Fab 2F5, OE DES1 and OE ERG11 reduced their ergosterol content up to 29% in the case of the reference strain, ΔDES1, ΔSUR2, fluconazole-treated cells and OE Hac1 presented higher levels of ergosterol in their cell homogenates. Regarding to ergosterol intermediates, higher levels of episterol were present in most of the strains, except for ΔSUR2 (7.7 % decrease) and OE ERG11, which presented no changes. Significant changes wer also observed for zymosterol, with lower levels on the reference strain, OE DES1, ΔSUR2 and OE Hac1 and 2.2-, 5.8- and 2.1-fold increase for ΔDES1, fluconazole-treated cells and OE ERG11 strains respectively.

Furthermore, fluconazole-treated cells exhibited additional intermediates (e.g. lanosterol, 4,14-dimethylcholesta-8,24-dienol) as a result of its effect on inhibit Erg11p. Cultivation under hypoxic conditions resulted in 3.6-fold increased levels of these intermediates.

Ergosterol is an essential component of membranes and regulates fluidity and permeability of the plasma membrane [199]. It has a broad function in cellular processes like plasma membrane fusion, pheromone signalling or protein sorting [276, 277]. Presence of sterols in the membranes decrease membrane fluidity, thus the reduction of ergosterol amounts induced by hypoxic conditions can result on higher membrane fluidity. Sharma [120] suggested an adaptive response to altered sterol structures through changes in lipid composition and fluidity that can be also present when sterol is deprived. Despite reduced amounts of sterols in hypoxia, genes of the ergosterol biosynthetic pathway were highly upregulated in hypoxia due to its dependence on oxygen availability. As ergosterol is an essential component of the cells, high transcript levels of intermediate reactions aim for sufficient amounts of ergosterol for cell survival. Ergosterol levels in the cell would be influencing the entire lipid metabolism, since it has been described that *ERG* mutants in *S. cerevisiae* led to changes of more than 30 % of PL and more than 45 % of sphingolipid species [257].

Sphingolipid composition

Shpingolipid analyses were kindly performed by Pablo Tarazona at Georg-August-University (Göttingen, Germany) following the protocol described in Materials and Methods 2.4.4. Sphingolipid species were quantified as the percentage of relative peak area for each specie and are shown in Figure 6.3.

In addition to the typical inositol containing sphingolipids, *P. pastoris*, as most yeasts, contains ceramides and hexosylceramides, which are missing in *S. cerevisiae*.

Long chain bases (LCB) of ceramides were mostly sphing-4-enine (18:1;2), sphingadienine (18:2;2) and phytosphingosine (18:0;3). The major ceramide was phytosphingosine (18:0;3) combined with monohydroxylated lignoceric acid (24:0;1), followed by sphing-4-enine (18:1;2) combined with stearic acid (18:0) in both mono- and unhydroxylated forms.

Table 6.8: Sterol composition of reference strain and mutant strains cultured in normoxic and hypoxic conditions

Culture	Oxygen conditions	$\mu g_{Sterol}\ mg_{total\ prot.}^{-1}$							
		Squalene	Lanosterol	4,14-dimethylcholesta-8,24-dienol	4-methyl zymosterol	Zymosterol	14-methyl fecosterol	Episterol	Ergosterol
Fab2F5	Normoxia	n.d.	n.d.	n.d.	0.89 ± 0.36	0.75 ± 0.44	n.d.	0.17 ± 0.05	8.8 ± 2.0
	Hypoxia	n.d.	0.14 ± 0.00	n.d.	0.80 ± 0.18	0.52 ± 0.23	n.d.	0.38 ± 0.00	6.2 ± 1.2
ΔDES1	Normoxia	n.d.	n.d.	n.d.	0.75 ± 0.21	0.63 ± 0.33	n.d.	0.16 ± 0.05	8.8 ± 1.4
	Hypoxia	n.d.	n.d.	0.18 ± 0.00	1.5 ± 1.2	1.4 ± 1.2	n.d.	0.34 ± 0.00	9.5 ± 2.0
OE DES1	Normoxia	n.d.	n.d.	n.d.	1.4 ± 0.0	0.9 ± 0.5	n.d.	0.19 ± 0.03	8.7 ± 2.2
	Hypoxia	n.d.	n.d.	n.d.	1.7 ± 0.0	0.7 ± 0.5	n.d.	0.26 ± 0.12	7.0 ± 0.9
ΔSUR2	Normoxia	n.d.	n.d.	n.d.	1.1 ± 0.6	1.2 ± 0.6	n.d.	0.26 ± 0.12	7.1 ± 1.4
	Hypoxia	n.d.	n.d.	n.d.	2.0 ± 1.0	0.95 ± 0.44	n.d.	0.24 ± 0.14	8.2 ± 1.9
Fluco	Normoxia	n.d.	1.4 ± 0.4	0.21 ± 0.06	n.d.	0.10 ± 0.00	0.78 ± 0.00	0.18 ± 0.00	6.4 ± 1.2
	Hypoxia	0.18 ± 0.00	5.1 ± 0.3	0.77 ± 0.20	n.d.	0.58 ± 0.00	0.90 ± 0.25	0.94 ± 0.00	7.7 ± 1.5
OE ERG11	Normoxia	n.d.	n.d.	n.d.	0.53 ± 0.21	0.39 ± 0.18	n.d.	0.15 ± 0.05	7.2 ± 0.5
	Hypoxia	n.d.	n.d.	n.d.	2.0 ± 0.6	0.83 ± 0.46	n.d.	0.15 ± 0.00	7.0 ± 1.2
OE Hac1	Normoxia	n.d.	n.d.	n.d.	0.39 ± 0.18	0.50 ± 0.28	n.d.	0.19 ± 0.06	7.3 ± 1.4
	Hypoxia	n.d.	0.88 ± 0.00	0.16 ± 0.00	n.d.	0.26 ± 0.00	n.d.	0.52 ± 0.00	9.6 ± 2.9

n.d. = not detectable. Values represent the mean ± SD from triplicates.

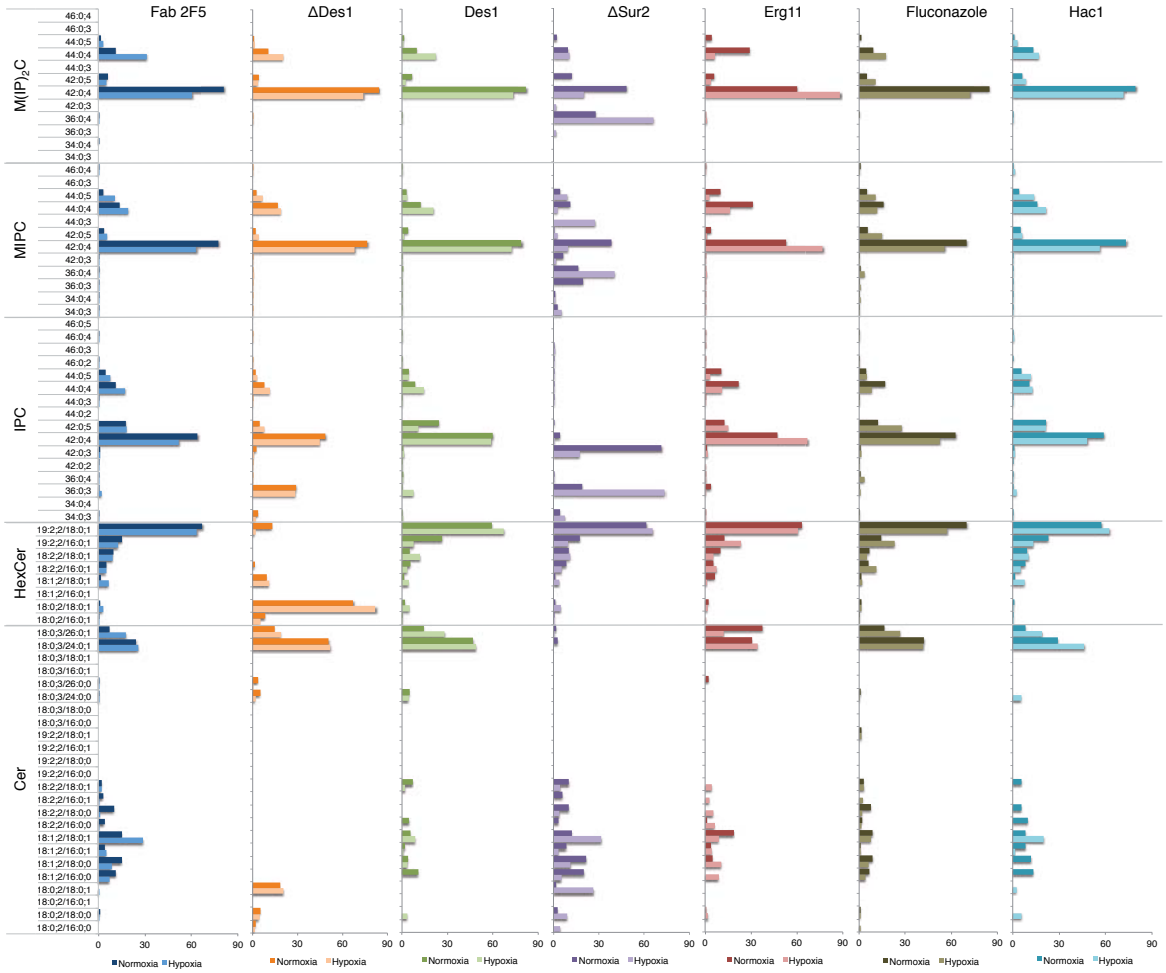

Figure 6.3: Sterol composition of reference strain and mutant strains cultured in normoxic and hypoxic conditions. Values are given as the relative peak area (%) for each SL specie.

For hexosylceramides, methylated sphingadienine (19:2;2) was the major LCB, and monohydroxylated stearic acid (18:0;1) the preferred fatty acyl. Inositol containing sphingolipids were enriched in phytosphingosine (18:0;3) as the LCB containing monohydoxylated lignoceric acid (C24:0) as the fatty acyl moiety.

ΔDES1 strain exhibited a lack of most of the ceramide species, as it would be expected based on previous studies of Ternes *et. al.*, where a wild-type strain of *P. pastoris* with a deletion of *DES1* gene was described [194]. In this strain, hexosylceramides changed its distribution compared to the reference strain, with higher content of species containing shorter LCB and fatty acyl moieties. However, inositol containing SL remained similar to the reference strain. It was also observed that overexpression of *DES1* did not trigger significant differences on sphingolipid relative amounts.

ΔSUR2 strain, carrying a deletion of the C4-hydoxylase, presented an altered distribution of relative amounts of inositol containing sphingolipids, with the presence of species missing in the reference strain, such as 36:0;3 species for all IPC, MIPC and $M(IP)_2C$ sphingolipid types. Furthermore, a lack of ceramides with very long fatty acids was also observed.

Overexpression of *ERG11* resulted in a preference for ceramides with very long fatty acids, and higher relative amounts of C44 species of inositol containing sphingolipids, while no significant changes in fluconazole-treated cells were observed compared to the reference strain.

Finally, overexpression of Hac1 presented similar relative amounts of sphingolipids as the

reference strain.

P. pastoris ceramide synthase Bar1p was reported to have specificity for dihydroxy LCB and C_{16}/C_{18} fatty acids [138]. Our results showed elevated relative amounts of trihydroxy LCB and very long chain fatty acids in the reference strain, which differs from the previous results of the *P. pastoris* wildtype strain, but are similar to the ones reported for strains with Δ4-desaturase deleted and the glucoceramide overexpressed [138]. (A possible reason could be the effect of recombinant protein production, which could activate UPR in the cell and therefore, change lipid composition of the cells.).

6.2.5. Fed-Batch cultures

In order to characterise knockout strains for Fab production, ΔDES1 strain was selected and cultured following a fed-batch strategy (Materials and Methods 2.3.8). Cells were monitored in terms of cell growth, Fab secretion and membrane fluidity (Figures 6.4 and 6.5).

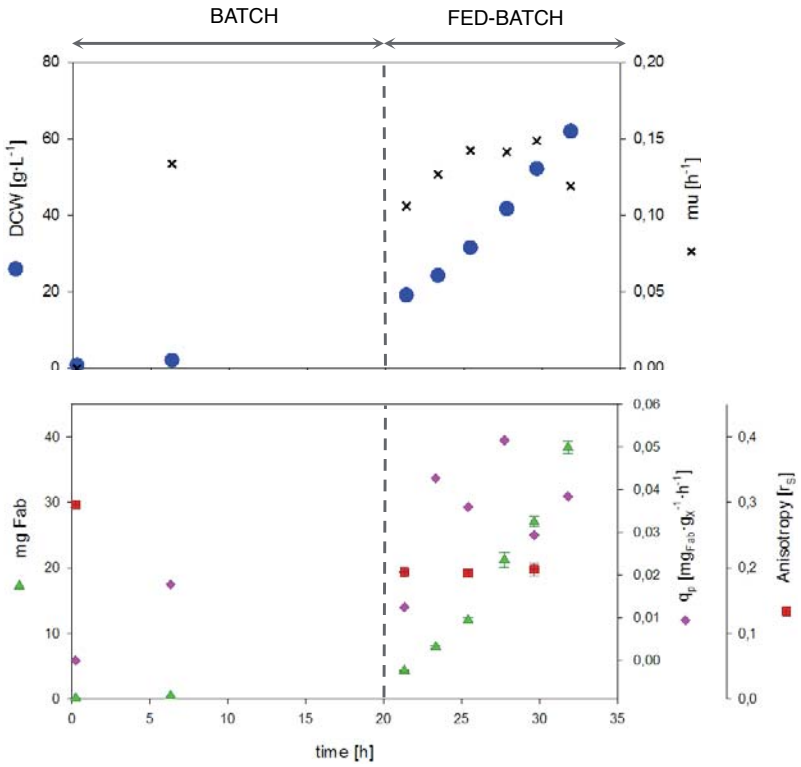

Figure 6.4: Fed-batch profile of the reference strain Fab 2F5. DCW, μ, Fab specific production rates and anisotropy were monitored.

These results were compared to the ones obtained for the reference. The main parameters for each strain are resumed in Table 6.9.

No significant growth differences were detected between both strains. ΔDES1 exhibited slightly lower Fab extracellular titres. Results derived from fed-batch cultivations were consistent with shake flask cultures.

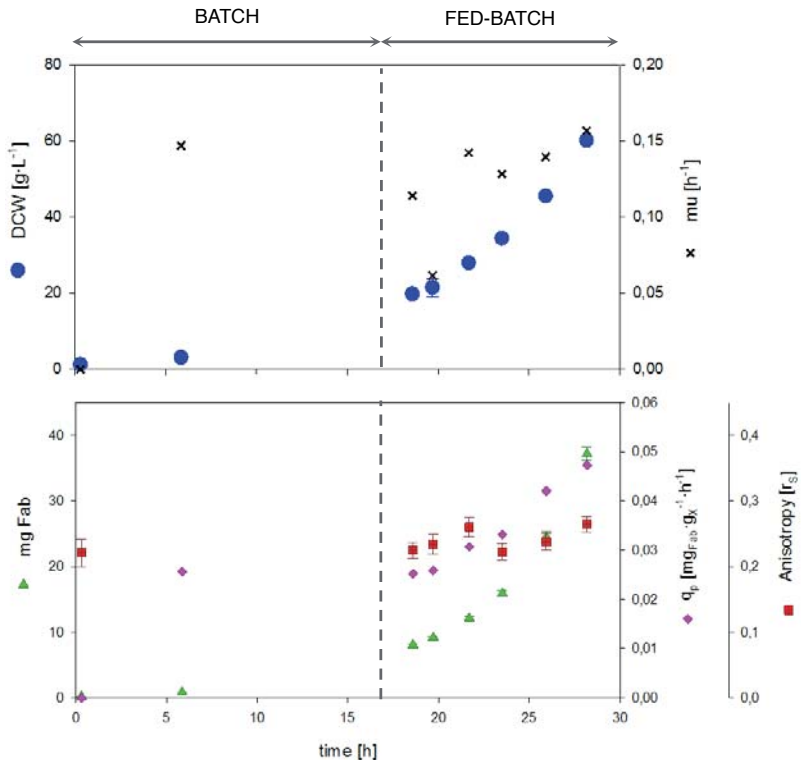

Figure 6.5: Fed-batch profile of the reference strain ΔDES1. DCW, μ, Fab specific production rates and anisotropy were monitored.

Table 6.9: Culture parameters of two fed-batch cultures using glycerol as a carbon source in the batch phase and glucose in the fed-batch phase.

	$Y_{Y/S}$ Batch Phase	**μ mean** (h^{-1})	**q_{Fab} mean** (mg_{Fab} g_{DCW}^{-1} h^{-1})	**Total Fab production** (mg_{Fab})	**Max. biomass** (g L^{-1})	**$Y_{X/S}$** (g_{DCW} g_{gly}^{-1})	**$Y_{P/X}$** (mg_{Fab} g_{DCW}^{-1})	**Total prod.** (mg_{Fab} h^{-1})	**Q_P** (mg_{Fab} L^{-1} h^{-1}
Fab 2F5	0.53 ± 0.01	0.136 ± 0.012	0.040 ± 0.008	38.4 ± 0.94	61.9 ± 1.1	0.39 ± 0.02	0.21 ± 0.04	1.2	0.48 ± 0.01
ΔDES1	0.48 ± 0.01	0.127 ± 0.031	0.036 ± 0.008	37.2 ± 1.0	60.2 ± 0.6	0.39 ± 0.03	0.24 ± 0.04	1.3	0.56 ± 0.01

$Y_{X/S}$ = Biomass to substrate yield; μ = specific growth rate; q_{Fab} = specific Fab production rate; $Y_{P/X}$ = Fab to biomass yield; Q_P = volumetric productivity

6.3. Conclusions

- Hypoxic conditions without washing out reactor have been defined as the ones corresponding to an air flow in the inlet of 0.25 L min^{-1}, mixed with nitrogen up to 1 vvm. These conditions provide hypoxic environment in a Biostat B and a Biostat B+ with the same vessel and impeller.
- Cells cultured under hypoxic conditions secrete higher amounts of Fab
- No significant morphological differences can be observed between strains and oxygen conditions.
- Changes in the lipid content of the strains have been observed.
- Hypoxia has an effect on altering lipid composition of the cells, as it has been observed by all the strains
- Fab-batch cultures showed that shake-flask results are consistent.

7

Integrated analysis of hypoxic conditions and engineered lipid metabolism effect on recombinant *P. pastoris*

7.1. Introduction

Lipids, as essential components of cell membranes in living organisms, require complex regulatory mechanisms to generate and maintain lipid composition [104, 108, 278]. Cells employ coordinated pathways of synthesis and degradation of phospholipids, sphingolipids and sterols [107, 155, 256, 279–281]. These interconnected networks constitute a highly dynamic biological core that allows cells not only to adapt their lipid profile to environmental changes, such heat stress, osmotic stress or nutrient and oxygen availability [89, 104, 257, 281–284], but also to sense the levels of different lipids and adjust their lipid composition to preserve cellular functions [257, 284–287]. Punctual perturbations could be compensated by the interlinked pathways, preserving cell viability with no obvious physiological consequences [91]. In the present chapter, previous transcriptional dataset of recombinant *P. pastoris* strains is integrated with lipidomic profiling analyses, aiming at the identification of potential changes correlating positively with improved protein secretion.

7.2. Integrated analysis of the hypoxia effect on the reference strain (Fab2F5)

Cultivation of recombinant *P. pastoris* under hypoxic conditions has been previously reported to have a strong positive effect on specific productivity [68, 69]. Baumann *et at.* [69] found lipid metabolism as a highly transcriptionally regulated pathway when cells were cultured in hypoxia. In the present study we integrate previous transcriptional dataset of recombinant *P. pastoris* strain with lipidomic profiling analyses, aiming at the identification of potential changes correlating positively with improved protein secretion.

Fatty acid desaturases are subject to tight control at transcriptional level, on the level of mRNA stability [288], and also with respect to protein stability through the ubiquitin-proteasome-dependent ER-associated degradation pathway [289, 290]. Transcript levels of our reference

strain in hypoxic conditions resulted in upregulation of the O_2-dependent Δ9 fatty acid desaturase encoded by the gene *OLE1* and involved in the biosynthesis of unsaturated fatty acids. High saturation of fatty acids acts as a protective mechanism by creating a more rigid membrane and reducing the oxidative stress that results from the oxidation of unsaturated fatty acids [273]. Yeasts can regulate the production of polyunsaturated fatty acids (PUFA) to control the membrane fluidity in stress conditions. Adding a double bond in a fatty-acyl substrate is a very demanding process that involves two electrons and the cleavage of two C-H bonds (98 kCal/mol) and consumes molecular oxygen [274]. This oxygen-dependent activity could explain the increased relative amounts of monounsaturated FA and an opposite trend for polyunsaturated FA in hypoxia, even if levels of *OLE1* transcript were upregulated (Figure 7.1). The presence of the monounsaturated FA oleic acid as the major FA, and not saturated fatty acids, could indicate that it is responsible of maintaining membrane fluidity, enabling protein secretion.

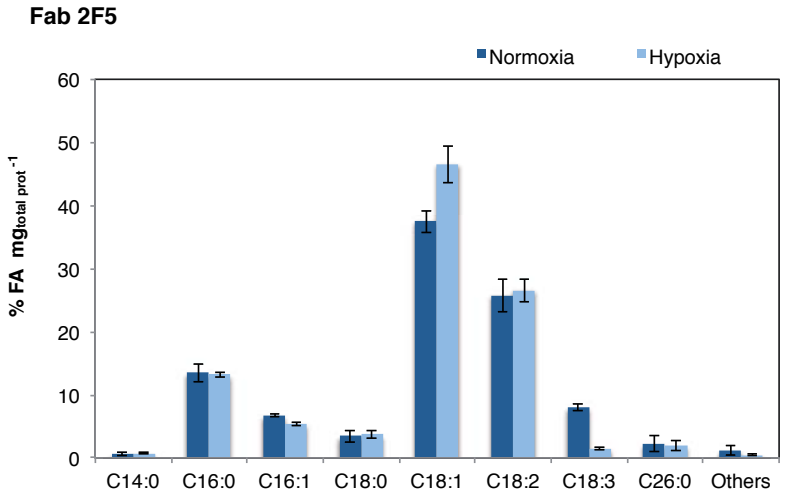

Figure 7.1: Relative amounts of fatty acids (%) of the reference strain (Fab 2F5) in normoxic and hypoxic conditions.

Transcriptomic data (Figure 3.3) revealed a repression of genes involved in the *β*-oxidation of fatty acids. These results were also reported for *S. cerevisiae* grown in hypoxic conditions, and it is known that a repression of this pathway exists when glucose is present as carbon source [97, 273].

Phosphatidylinositol (PI) and phosphatidylserine (PS) are synthesised by Pis1p and Cho1p respectively, which compete for CDP-DAG, making this branch an important point of regulation [116]. No significant changes at transcriptomic level were observed for these two genes in hypoxia, however, as it can be observed in Figure 7.2, levels of PS increased significantly, while PI levels drop in this culture condition.

PS and PI are key determinants of membrane surface charge. Both types of phospholipids are anionic (charge -1), but they differ on their shape. PS is cylindrical-shaped, which preferentially forms flat bilayer structures, while PI has an inverted conical shape and form structures with positive curvatures [110]. Additionally, distribution of PS and PI causes the electrostatic properties of the membrane to vary, making a highly charged cytosolic leaflet on plasma membrane due to its abundance [291]. Membrane deforming domains are crucial for protein-membrane interactions, and both mediate functional interactions with positively charged regions of peripheral and integral membrane proteins [292, 293]. However, some domains and proteins tend to prefer PI

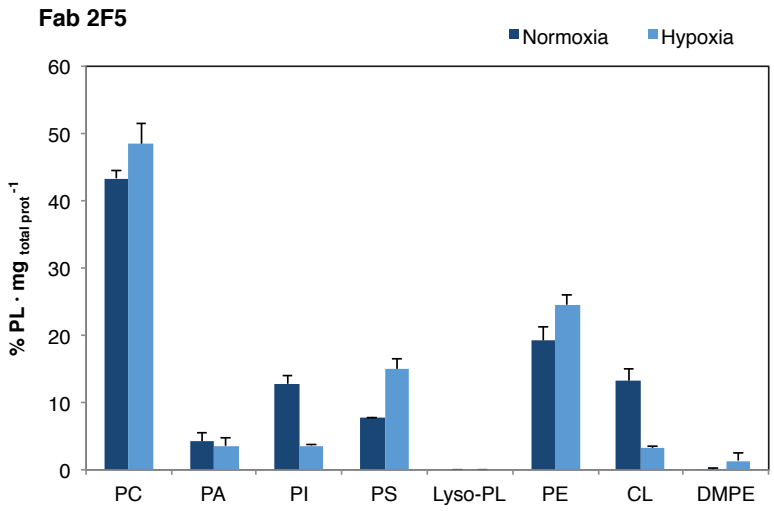

Figure 7.2: Relative amounts of phospholipids (%) of the reference strain (Fab 2F5) in normoxic and hypoxic conditions.

rather than PS, making PI a major player on controlling a variety of cellular functions [294]. It has also been reported for *S. cerevisiae* that PI can substitute PS in order to preserve phospholipid balance, but not the inverse [275].

Inositol is a potent regulator of phospholipid metabolism in yeast. Both transcription of genes encoding enzymes required for synthesis of PL and activities of these enzymes are regulated primarily by the intracellular concentration of free inositol, a precursor in the synthesis of PI [295]. Most of the genes that are regulated in response to presence of inositol contain the UAS_{INO} element, whereas the majority of the genes that respond to both inositol and choline fall into other categories (e.g. unfolded protein response (UPR) pathway, low oxygen response element (LORE)) [296, 297].
Inositol used in PI synthesis is either synthesised *de novo* or obtained from the growth medium via the *ITR1*- and *ITR2*-encoded inositol transporters [116].
Our transcriptional dataset indicated that *ITR1* transcript levels were highly downregulated under hypoxic conditions, while *ITR2* was upregulated. It has been described for *S. cerevisiae* that *ITR1* is repressed by inositol and choline via Opi1p, while *ITR2* is expressed constitutively [298]. In addition, when intracellular inositol levels fall, the transcription of a wide variety of genes that are required for *de novo* phospholipid synthesis including *INO1*, *CHO1* and *OPI3* are induced, favouring PS and PE and PC pathways [275]. Our transcriptomic data only indicate upregulation of *INO1*, while no significant changes on *CHO1* and *OPI3* were observed. However, PS and PE relative amounts increased in hypoxia. This change on the relative amounts of these phospholipids could be the result of decreased inositol availability for cells growing under hypoxic conditions. This theory would be supported by the increment of TG levels in hypoxia, which has been already related to the absence of inositol [116]. On the other hand, Gaspar2006 *et al.* [286] studied alterations of membrane lipids of *S. cerevisiae* in response to presence of inositol and choline in the culture medium and they pointed out that a lack of inositol lead to a drop of PI levels while PS levels remained constant, which would only partially explain our results.

The negative regulator Opi1p, which represses many of the genes containing UAS_{INO} elements regulated by inositol, including *INO1* [286], was transcriptomically downregulated in hypoxic conditions. *INO1*, at the same time, is one of the most highly induced genes by the unfolded protein response (UPR) [299], which occurs via repression of Opi1p by Hac1 [190].
Studies with phospholipids indicate that changes on their levels do not only occur by changes on transcription levels of the genes involved in the phospholipid pathway, but also by changes on contact sites and transporters [300]. It could explain the increment of PS and PE in hypoxia even when transcriptional levels of the genes involved in their synthesis were not regulated.

Briefly, hypoxic conditions could trigger low levels of inositol in the cell. This fact would explain the downregulation of *OPI1*, which would prompt the upregulation of *INO1* and *ITR2* genes. Hypoxia also changed the levels of phospholipids, presenting lower levels of PI, and higher levels of PS and PE. Furthermore, triacylglycerols were also higher in hypoxia, probably caused by a lack of inositol. UPR could also be induced as result of hypoxic conditions, as it has been recently reported cellular stress as a consequence of hypoxia [301], which would explain the transcriptional changes occurring in the cell in this condition.

Surma *et al.* [302] reported the existence of a crosstalk between unfolded protein response (UPR) (*IRE1, HAC1*), the endoplasmic-reticulum-associated protein degradation (ERAD) machinery (*UBX2*), fatty acid metabolism (*OLE1*) and consequently membrane lipid saturation, and how *UBX2* modulates Ole1p levels. The accumulation of misfolded proteins in the ER activates the UPR [303], and this is especially common when recombinant proteins are expressed, but perturbations with lipid metabolism can also induce UPR signalling [304, 305].

Despite reduced amounts of ergosterol in hypoxic conditions, genes of the ergosterol biosynthetic pathway were highly upregulated due to its dependence on oxygen availability. Molecular oxygen is essential for ergosterol synthesis from squalene, requiring 12 oxygen molecules in the whole reaction. Bien *et al.* [306] suggested an interplay between hypoxic stress and sterol homeostasis for *S. pombe*, showing how Sre1p controls sterol homeostasis and also functions as an hypoxic transcription factor. When sterol synthesis decreases under low oxygen, Sre1p is proteolytically activated to increase transcription of genes required for ergosterol synthesis and cell growth [307]. A similar effect could be occurring in *P. pastoris* in order to maintain lipid homeostasis. Additionally, Sharma [120] suggested an adaptive response to altered sterol structures through changes in lipid composition and fluidity that can be also present when sterol is deprived. Ergosterol levels in the cell could be influencing changes into the entire lipid composition, since changes of more than 30 % of PL and more than 45 % of sphingolipid species have been reported in *ERG* mutants of *S. cerevisiae* [257], pointing out a crosstalk between lipid biosynthetic pathways.

Excess of fatty acids that are derived from endogenous *de novo* synthesis, lipid turnover or nutritional supply are stored as triacylglycerols in cytosolic lipid droplets, keeping the total amount of cellular phospholipids within a narrow range [97]. The regulatory interplay and metabolic interconversion between storage lipids (i.e. triacylglycerols) and membrane lipids (i.e. phospholipids) have been recognised as an important determinant of cellular growth and proliferation in yeast [308, 309].
Hypoxic conditions resulted in higher levels of triacylglycerols and steryl esters, as it can be observed in Figure 7.3. As stated before, TG increment can be the result of low levels of inositol

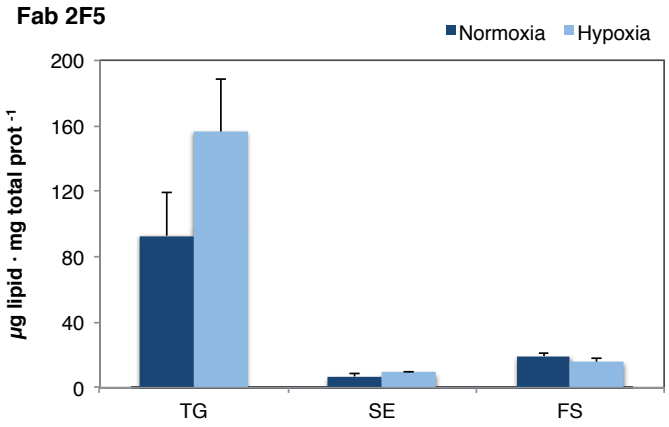

Figure 7.3: Amounts of non-polar (μg_{lipid} $mg_{total\ prot}{}^{-1}$) of the reference strain (Fab 2F5) in normoxic and hypoxic conditions. Triacylglycerols (TG), steryl esters (SE) and free sterols (FS) are represented.

present in the cell. Moreover, changes in glucose metabolism caused by the shift from respiratory to respirofermentative metabolism can also impact non-polar lipid homeostasis by changing activity of TG lipases [97].

Both enzymes Nte1p and Lro1p, which turned out to be upregulated in hypoxia, catalyse reactions that, either directly or indirectly, promote synthesis of TG and contribute to the adjustment of the molecular species composition of membrane phospholipids [97].

Sphingolipids, apart from its function defining membrane structure, associate to ergosterol to form microdomains ("lipid-rafts") and also have an important role as second messengers. That is, changes in sphingolipid levels can impact on cell metabolism as it exist an interconnection between sphingolipid biosynthesis and other metabolic pathways [137].

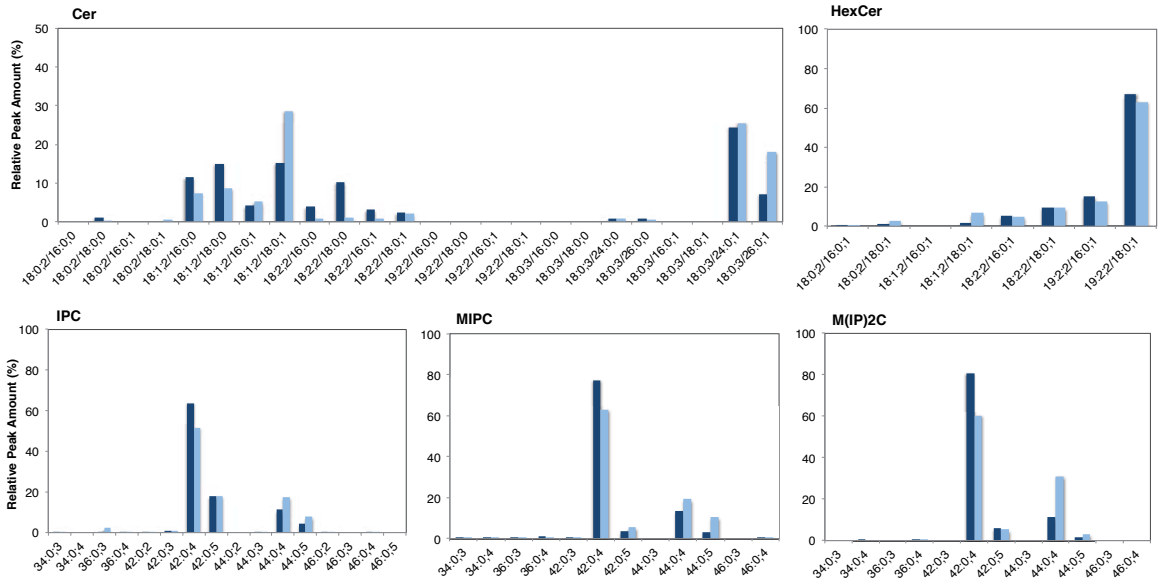

Figure 7.4: Relative amounts of sphingolipids (relative peak amount, %) of the reference strain (Fab 2F5) in normoxic and hypoxic conditions. Triacylglycerols (TG), steryl esters (SE) and free sterols (FS) are represented.

Sphingolipid pathway was tightly upregulated under hypoxic conditions, since most of the reactions involved in the pathway require oxygen.

Figure 7.4 show how in hypoxic conditions some classes of sphingolipids changed their relative amount in cell homogenates. Ceramides with polyunsaturated fatty acid decreased, which is consistent with the fact that less polyunsaturated fatty acids were present in hypoxia. An increase of ceramides carrying methylated moieties was also observed. Notably, ceramide 18:0;3/26:9;1 doubled its content, although *SUR4*, responsible to transform C24 into C26 fatty acyls of ceramides, was not upregulated in hypoxia. Hypoxia had also an effect on inositol containing sphingolipids, reducing relative amounts of C42 (i.e. containing C24 fatty acids) species and favouring the amounts of C44 species (i.e. containing C26 fatty acids), which is in agreement with the previous results with ceramides. These results could indicate that sphingolipid species with longer chain fatty acids and more methylations that form membranes in hypoxic conditions could have an impact on membrane properties that results in a beneficial effect on Fab secretion.

Decreased levels of ergosterol under hypoxic conditions could be involved in changes of sphingolipid species observed in cell homogenates. A plausible explanation to these changes would be that cells adapt to sterol changes by altering the rest of membrane lipids in order to maintain membrane homeostasis. Such adaptation would be mainly achieved through modulation of their sphingolipid composition, and would be reflected in the observation that these compositional changes were not related to an altered membrane fluidity measured by fluorescence anisotropy. Similar results have been previously reported in *S. cerevisiae* by Guan *et al.* [257].

Hypoxic conditions yield to strong transcriptional regulation of key parameters of protein production, as already reported by Baumann*et.al.* [69]. In the current study, it has been confirmed that changes in cellular processes such as lipid metabolism led to altered changes on relative amounts of lipids in cell homogenates, which in turn, would lead to changes in the composition of cellular membranes. These changes might also contribute to the observed enhanced levels of protein secretion, through changes on membrane fluidity that permit higher secretion rates and no recombinant protein accumulation within the cell.
At the same time, it has also been observed that activation of UPR as a consequence of both recombinant protein production and hypoxia imply alteration of cellular lipid composition, i. e. altered lipid composition could be the result of low oxygen environmental conditions and protein production stresses.

7.3. Effect of hypoxic culture conditions on cell lipid composition of engineered strains

In order to determine significant changes on cell lipid composition as a result of cell engineering of lipid pathways and hypoxic culture conditions, log2 of the fold change for each lipid specie comparing normoxia versus hypoxia was performed. Data was plotted as a heat map, where reduction of lipid levels is shown in green, no changes in white and increased levels in red. This method allowed easily observing significant changes on lipid composition between oxygen conditions for each strain.

The effect of hypoxic conditions compared to normoxic conditions for each strain of the present study are shown in Figure 7.5. General trends common among all strains were reduced amounts of polyunsaturated fatty acids, phosphatidylinositol (PI), and some ceramides builded up with

polyunsaturated fatty acids. Some other lipid species, like oleic acid (C18:1), triacylglycerols (TG), steryl esters (SE) and episterol increased their levels when strains were cultured in hypoxia. In addition, inositol-containing sphingolipids presented a diverse alteration of their species that was strain-dependent. Reduced amounts of ergosterol due to hypoxic conditions resulted in higher amounts of sterol intermediates.

The effect of hypoxia in the ΔDes1 strain, when compared to the effect on the reference strain (Fab 2F5), exhibited a higher increment on SEs and reduced levels of ceramides 18:9;3/26:0;0 and hexosylceramides 19:2;2/18:0;1. Furthermore, changes in the levels of the MIPC 34:0;3 were not as severe as the ones observed in the reference strain.

The strain overexpressing *DES1* (OE Des1), hypoxic conditions led to changes on lipid composition that appeared to be the opposite of the reference strain. It was the case of cerotic acid (C26:0), most of the ceramides, hexosylceramides, and some inositol containing sphingolipids like IPCs 36:0;3, 46:0;2, 46:0;4, and all MIPC and $M(IP)_2C$ sphingolipid species.

Major changes on ΔSur2 strain due to hypoxia were the reduction of phospholipid levels, IPC 44:0;4 and 42:0;4, accompanied with a high increase of ceramide C18:0;2/18:0;1, hexosylceramide C18:0;2/16:0;1 and MIPC 42:0;5.

Fluconazole-treated cells exhibited major differences on sterols, as a high increment of sterol intermediates were observed due to hypoxic conditions compared to the hypoxic effect on the reference strain.

Effect of hypoxia on overexpressing Erg11 cells resulted in lower levels of cerotic acid, free sterols, ceramide 18:1;2/16:0;1, 18:2;2/18:0;1, hexosylceramide 19:2;2/16:0;1, and IPC; MIPC and $M(IP)_2C$ 42:0;5 species. In addition, levels of 4-metylzymosterol, zymosterol and IPC 36:0;3 showed a higher increment than in the reference strain.

Finally, effect of hypoxia on the strain overexpressing Hac1 had an increment on lysophospholipids, 4-methylzymosterol and hexosylceramide 18:0;2/16:0;1, and decreased levels of cerotic acid, zymosterol, ceramide 18:1;2/16:0;1, hexosylceramide 18:0;2/18:0;1, and IPC and $M(IP)_2C$ 36:0;4.

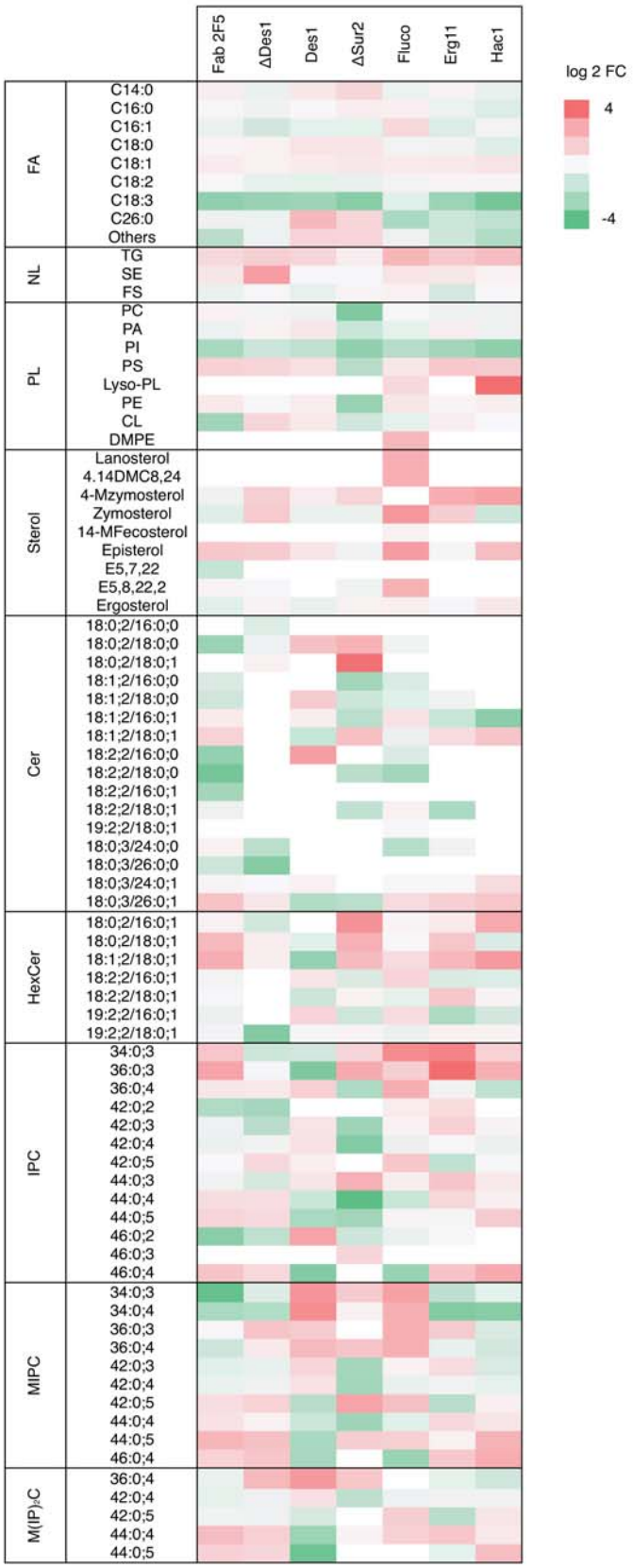

Figure 7.5: Heat map of the effect of hypoxia on the lipid species for each strain. The log2 of the FC of hypoxia versus normoxia is plotted in order to see major differences.

7.4. Effect of strain engineering through sphingolipid pathway

Principal changes in terms of lipid composition of all the strains generated in this study when compared to the reference strain are shown in Figure 7.6. These changes were obtained from normoxic conditions in order to study the effect of genetic modifications in terms of cell physiology.
In general terms, the most significant changes were observed for sphingolipid composition, with the most important changes observed for the strains whose sphingolipid pathway was engineered. In contrast, strains with engineered sterol pathway did not present significant changes on the levels of the species involved in the sterol pathway.

One of the most significant changes was that all strains contained lower levels of cardiolipin (CL) compared to the reference strain. Levels of cardiolipin in the reference strain were higher than the usual, with levels more similar to the ones observed in mitochondrial membranes, which are enriched in this phospholipid. CL plays an important role not only in mitochondrial biogenesis, but also in essential cellular fractions not generally associated with respiratory functions (e.g. mitochondrial protein import, cell wall biogenesis, translational regulation of electron transport chain component, ageing, apoptosis) [113]. It has been reported that CL is enriched in contact sites [310]. High levels of CL have not been reported before.

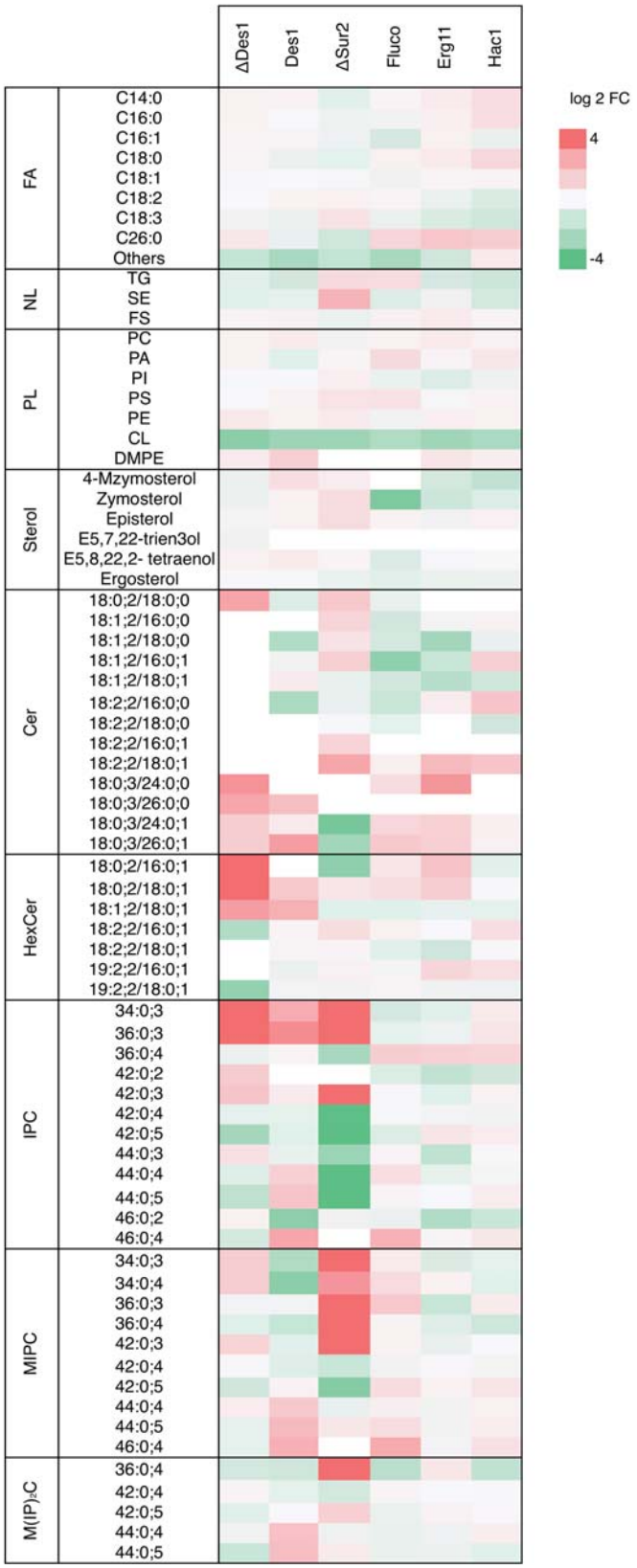

Figure 7.6: Heat map of the strains versus reference strain in normoxic conditions. Log2 of the FC was plotted in order to see major differences.

7.4.1. Engineering neutral sphingolipid pathway through *DES1*

Two major classes of complex sphingolipids have been identified in *P. pastoris*, namely the inositol containing sphingolipids (IPC, MIPC and $M(IP)_2C$) and the neutral sphingolipids (Cer and HexCer) [138]. These sphingolipid classes vary in their polar head groups as well as their ceramide backbones [142]. The pathway leading to glucosylceramide biosynthesis is mainly composed by four enzymes: Bar1p, which occupies the key branch point, preferring dihydroxyl sphingoid bases and C16/C18 acyl-CoA as substrates, and producing ceramide species; sphingolipid Δ4- and Δ8-desaturases, fatty acid α-hydroxylase and a glucosylceramide synthase that adds the glucose head group.

Ternes *et al.* [138] reported that deletion of Δ4-desaturase in *P. pastoris* wild type results in absence of glucoceramides (HexCer) in the cell. The gene encoding for this enzyme was selected as target for cell engineering of our recombinant protein strain in order to determine levels of protein secretion due to changes on ceramide amounts in cell membranes.
Figure 7.7 shows the lipid profile of the reference strain producing the recombinant Fab and the strains generated in this study, carrying a deletion of the gene encoding for the Δ4-desaturase (ΔDES1) or overexpressing it. It can be observed that only ceramides and hexosylceramides composed by saturated LCB were present in cell homogenates of the ΔDES1 strain, as it would be expected by the absence of the Δ4-desaturase, involved in the unsaturation of the LCB and required for the activity of the Δ8-desaturase. Ceramide species detected in ΔDES1 homogenates are in concordance to the ones present in Ternes studies [138], where neither mono- nor diunsaturated Cer could be detected in ΔDES1 strain, but levels of saturated Cer were enhanced in comparison to the wild type.
According to Ternes *et al.* results, a lack of hexosylceramides would be expected for the strain ΔDES1. Instead, we detected the presence of some HexCer species in ΔDES1 cell homogenates, although the species that were present were totally different from the ones present in the reference strain. The 18:0;2/18:0;1 was the most predominant specie in ΔDES1 cells and almost not detected in the reference strain, where the major specie was 19:0;2/18:0;1. These results are in contrast with the ones of Ternes *et al.* previously mentioned.

It should be mentioned that relative amounts of sphingolipids were determined, however total amounts of sphingolipids were not quantified. Therefore, only differences between species of the same sphingolipid class can be noted. Hence, it could be possible that relatively small amounts of ceramides would be present in cell homogenates compared to the reference strain. The same situation could be occurring to the strain overexpressing *DES1*, which could be containing higher levels of ceramides and hexosylceramides compared to the reference strain.

It was also observed the presence of relative amounts of IPC species of 34 and 36 carbons in the knockout strain, which were not present in the reference strain. Ternes *et al.* investigated a possible interconnection between biosynthesis of HexCer and IPC, MIPC and $M(IP)_2C$, and they determined that some ceramides were incorporated into IPC to a limited extent but that these IPC species were not processed further into MIPC and $M(IP)_2C$. This fact can be the reason of the presence of IPC species with fewer carbons, which would be generated from the ceramide species with this carbon composition.

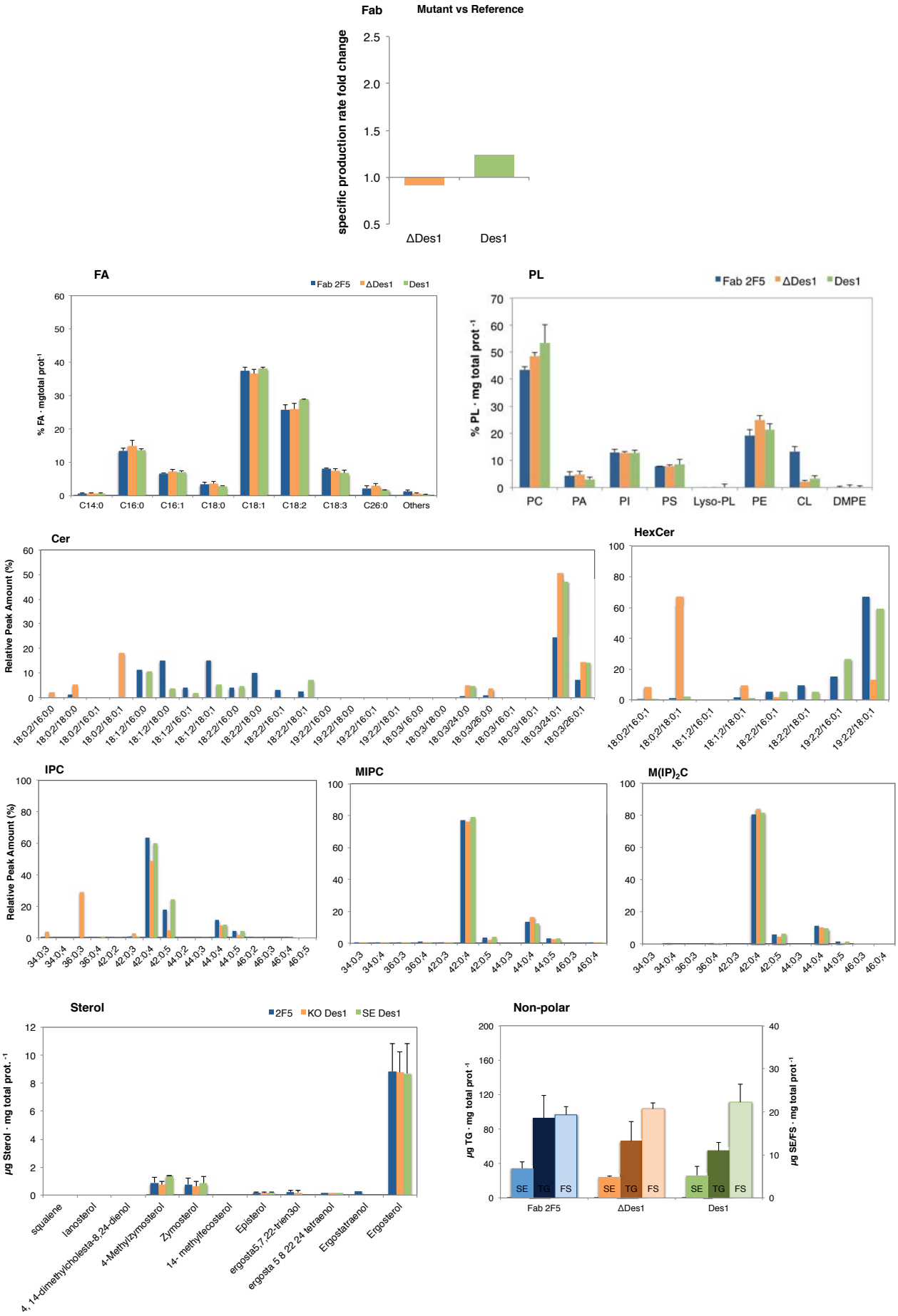

Figure 7.7: General overview of the recombinant protein production and lipid composition of the cells carrying a deletion of the gene *DES1* (orange) or with the gene overexpressed (green) and the values of the reference strain (blue) without the genetic modifications.

Distribution of ceramides and hexosylceramides in the strain overexpressing Des1 was more similar to the reference strain, composed by the same sphingolipid species although enriched with species formed with saturated very long chain fatty acyls.
Apart from sphingolipid, only non-polar lipids had differences with the reference strain. In this sense, levels of triacylglycerols (TG) for both ΔDes1 and OE Des1 were lower than the reference strain while levels of steryl esters and free sterols were slightly lower and higher, respectively.

According to the observed results, ceramides are important for cell secretion, as absence of this sphingolipid class lead to lower levels of Fab secretion. Moreover, we can not determine whether overexpression of Δ4-desaturase results in higher amounts of neutral sphingolipids, but changes on the relative amounts of sphingolipids species were observed and they result in slight increase on the levels of secreted Fab, as observed in Figure 7.7 (Fab panel).

7.4.2. Altering inositol containing sphingolipids pathway (*SUR2*)

Sur2p is required for hydroxylation of dihydrosphingosine at C4 position to yield phytosphingosine, in one of the first steps of the inositol containing sphingolipid (IPC) biosynthesis.
Deletion of *SUR2* in *S. cerevisiae* results in viable strains lacking completely C4-hydroxylated sphingolipids (i.e. phytosphingosine, 18:0;3) and accumulation of dihydrosphingosine (18:0;2) and dihydrosphingosine-1-phosphate [311]. These observations indicate that C4-hydroxylation of the LCB is not required for IPC biosynthesis in this organism [197, 198]. Additionally, *SUR2* mutants were reported to display altered phospholipid composition and abnormal morphology in stationary phase [312]. Klose *et al.* [313] observed lower membrane order of *SUR2* mutants, which have been shown to trigger defective plasma membrane transport of integral membrane proteins [277, 314].

Ternes *et al.* could not obtain *P. pastoris* strains with deleted *SUR2*, and proposed C4-hydroxylation of the LCB to be required for the Lag1p synthase to use it for IPC biosynthesis. In the current study, a strain with *SUR2* was obtained, suggesting that requirements of both *P. pastoris* and *S. cerevisiae* are similar regarding inositol containing sphingolipids.

Figure 7.8 Cer panel, shows how ceramide species with trihydoxylated LCB were almost absent in ΔSUR2 strain, as a consequence of the lack of C4-hydoxylase in the knockout strain. Relative amounts of hexosylceramides and the species that constituted them were similar between the knockout strain and the reference strain.

Notably, the main differences were observed with IPC, MIPC and $M(IP)_2C$, where species present in the ΔSUR2 strain were derived from dihydrosphingosine, in contrast with the reference strain, which contained species derived from phytosphingosine. These observations are in agreement with the results reported for *S. cerevisiae* strains with the same deletion.
An increment on the relative amounts of sphingolipids with shorter chains was also observed in the ΔSUR2 strain. Shortening of very long fatty acids, as it was observed for the *P. pastoris* ΔSUR2 strain, could have an effect on sorting and plasma membrane composition.

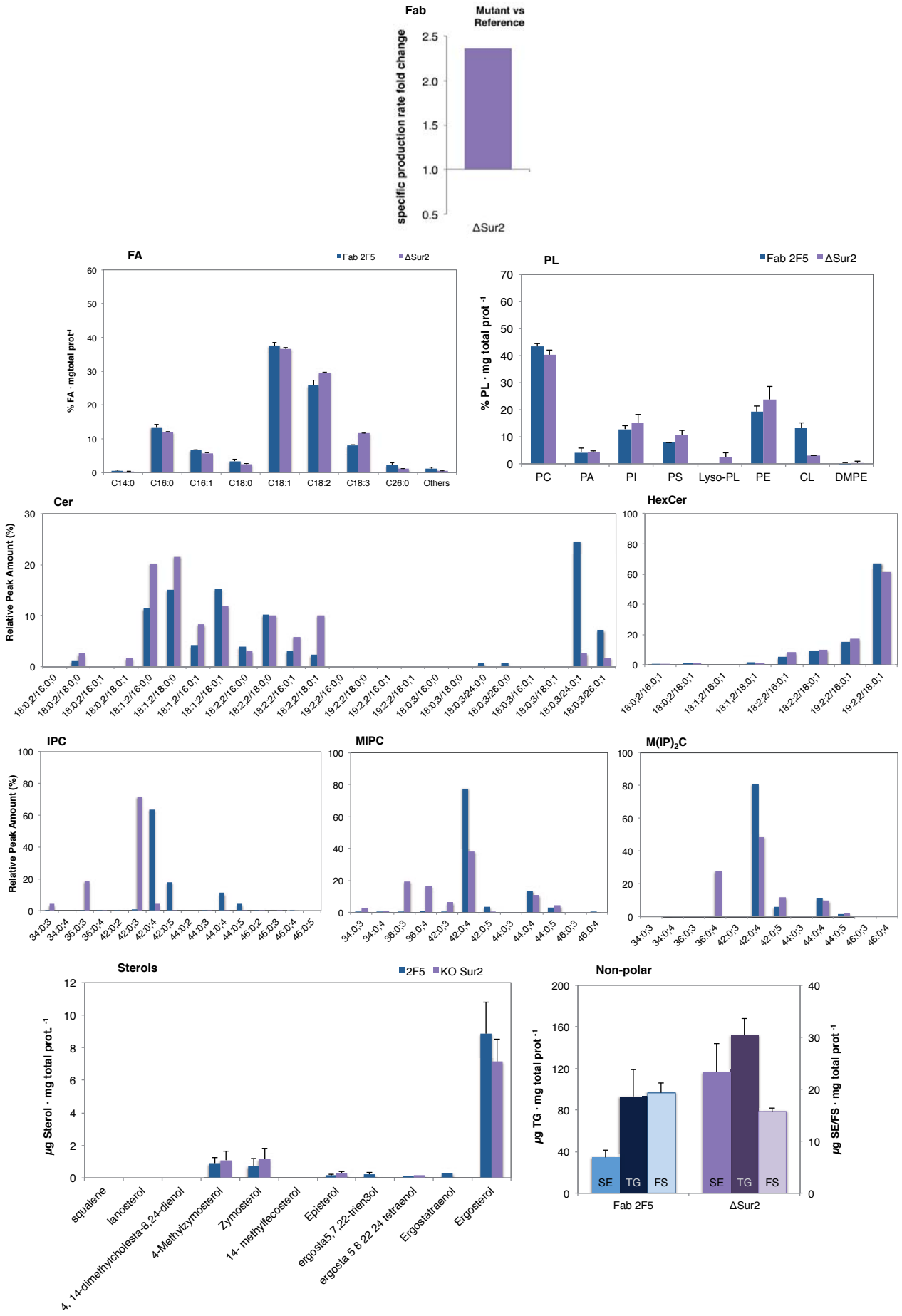

Figure 7.8: General overview of the recombinant protein production and lipid composition of the cells carrying a deletion of the gene *SUR2* (purple) and the values of the reference strain (blue) without the genetic modifications.

Whereas fatty acid and phospholipid (in contrast with the results from *S. cerevisae* [312]) did not contain significant changes, ΔSUR2 exhibited reduced levels of ergosterol in cell homogenates. Furthermore, levels of steryl esters and triacylglycerols turned out being significantly higher in the knockout strain. Similar increment in SE and TG was also observed for cells under hypoxic conditions (7.2).

Changes on lipid composition in the strain with *SUR2* deleted favoured the secretion of Fab by 2.4-fold compared to the reference strain (Figure 7.8 Fab panel). The amounts of increased productivity are close to the 2.9-fold increment observed as a result of cultivation under hypoxic conditions. Nonetheless, changes on lipid composition in the knockout strain and the reference strain in hypoxia are distinct. The characteristic phosphatidylinositol (PI) reduction on hypoxic conditions was not present in the ΔSUR2 cells, which slightly increased its PI relative amounts. Sphingolipid composition was totally different between both conditions (Figure 6.3), with the common lipid patterns observed in reduced levels of ergosterol (Table 6.8) and levels of non-polar lipids. Increased amounts of triacylglycerols and steryl esters were observed, while the increment of the SE in ΔSUR2 was much higher than in hypoxia. Furthermore, levels of free sterols were reduced in both cases when compared to the reference strain in normoxic conditions (Table 6.7).

Finally, when ΔSUR2 cells were cultured in hypoxia, most of the changes already described for the reference strain in terms of phospholipid, fatty acids and neutral-lipid composition were also observed. However, levels of ergosterol of the knockout strain in hypoxic conditions did not decrease as compared to the cells in normoxic conditions, but they rather slightly increase. A possible explanation for the absence of synergic effect on ergosterol levels due to both genetic modifications (i.e. gene deletion) and environmental conditions (i.e. hypoxia) could be that ergosterol is essential for cell growth and cell would maintain minimal ergosterol levels in order to survive. Presence of sphingolipids with shorter chain of the fatty acid moiety that was present in ΔSUR2 cells increased their relative amounts in the cells cultured in hypoxic conditions. All these modifications increased the levels of Fab secreted in hypoxia, but in this case the levels were lower than the 2.9-fold observed in the reference strain, possibly because cells had a limitation of Fab secretion.

7.5. Effect of strain engineering through ergosterol pathway

Fluconazole is an azole antifungal agent that blocks the ergosterol biosynthesis pathway by inhibiting the Erg11p activity, resulting in ergosterol depletion [223]. Fluconazole treated cells were used in order to reduce levels of ergosterol, as previously reported by Baumann *et al.* [192]. Furthermore, *ERG11* was overexpressed in the Fab producing strain in order to characterise the effect of altered ergosterol pathway on the levels of Fab secreted.

Bammert *et al.* [315] studied the transcriptional changes in *S. cerevisae* in response to treatment with antifungal agents. These changes included directly related genes of the ergosterol pathway but also other genes related to membrane structure and function, including the decrease of *SUR2* transcript levels.

As it can be observed in Figure 7.9, cell homogenates of fluconazole-treated cells presented lower relative amounts of monohydroxylated fatty acids (FA panel), which was compensated by a slight increment of linoleic acid (18:2) and cerotic acid (26:0). They also exhibit increased relative amounts of phosphatodylcholine, phosphatidic acid and phosphatidylserine (PL panel).

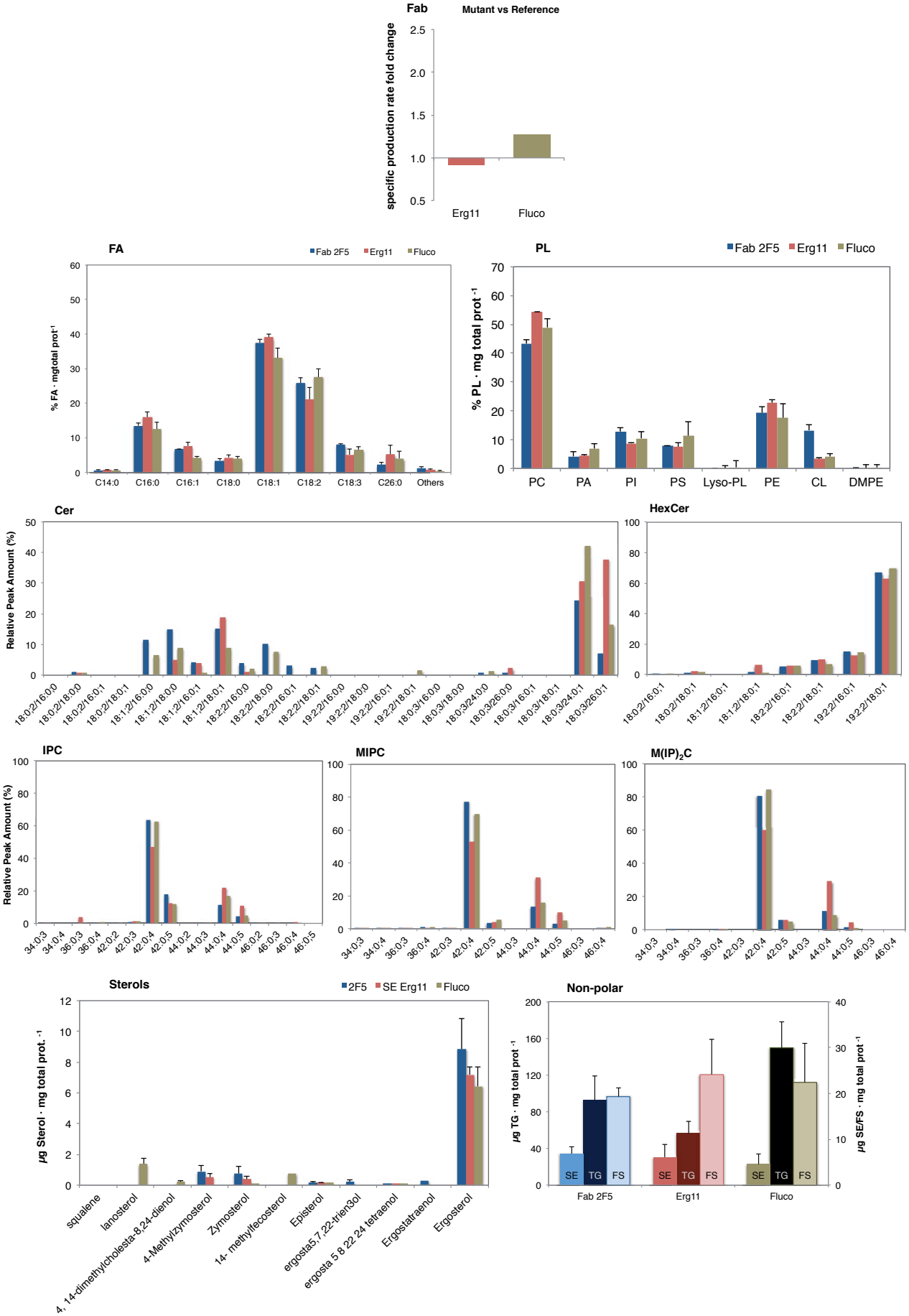

Figure 7.9: General overview of the recombinant protein production and lipid composition of the cells overexpressing the gene *ERG11* (maroon) or treated with fluconazole (khaki) and the values of the reference strain (blue) without the genetic modifications.

As expected, a reduction of ergosterol was present in the cells, and the sterol intermediate lanosterol, which is involved in the Erg11 reaction, was present in cell homogenates. Accumulation of lanosterol and other sterol precursors in cells treated with fluconazole has been previously reported for other yeasts [316, 317].
Regarding sphingolipid content, fluconazole treated cells presented reduced amounts of ceramides containing dihydrosphingosine and significant increment on relative levels of ceramides composed by phytosphingosine and C24-C26 fatty acyls. Hexosylceramides and inositol containing sphingolipids levels kept similar to the reference strain. Additionally, non-polar lipids increased significantly the triacylglycerol content on fluconazole-treated cells. Levels of steryl esters were slightly reduced, while free sterols increased compared to the reference strain. Esterification of sterols is a regulatory mechanism, which protects cell membranes against excess of lipid components and maintaining sterol homeostasis [318].

Steryl esters and free sterols are interconvertible. It has been reported that under sterol depletion, steryl esters are mobilised to free sterols as they are required for plasma membrane formation [319].
Azoles are known to induce expression of *ERG11* mRNA [320], which was also observed for cells cultured in hypoxia. However, reduction of ergosterol levels and induced expression of both fluconazole-treated and cells cultured in hypoxia did not totally coincide with the other lipid species, although these changes were more similar than the ones observed with *SUR2* deletion.
Changes in lipid composition due to fluconazole treatment increased Fab secretion by 1.24-fold. These observations could be explained either because adaptive response to low ergosterol content triggered by fluconazole treatment by changing lipid composition differs from the one caused in hypoxic conditions, or because hypoxic conditions lead to several changes in the cell, being low ergosterol content one of them, and provoking a deeper alteration of cell lipidome.
It was also observed that a synergic effect of fluconazole and hypoxic conditions did not exist.

Overexpressing *ERG11* cell homogenates also present changes on lipid composition. Strikingly, the amounts of ergosterol in this strain were lower than in the reference strain. Sterol-14α-demethylase (*ERG11*), together with squalene epoxidase (*ERG1*) are the major regulatory steps in the post-squalene part of the ergosterol pathway. Veen *et al.* [321] overexpressed *ERG11* in *S. cerevisiae*, obtaining decreased lanosterol content and the latter sterol intermediates increased, and the total sterol content rose up to 1.2-fold, mainly consisting in precursors and not ergosterol. This indicates additional regulation mechanisms in the cell in order to prevent quantitative conversion into ergosterol. Overexpression studies of *ERG11* in *S. cerevisiae* have shown that even the gene was highly expressed, only 50 % of the protein existed as active enzyme [322]. This is because sterol-14α-demethylase is dependent of NADPH and heme [323], and its association with heme is required to be active *in vivo*.
In our studies, levels of free sterols increased, triacylglycerols decreased and steryl esters remained similar. A 1.26-fold increment of free sterols was observed in the OE Erg11 strain, and it can be the result of *ERG11* overexpression, increasing the total sterol content but not ergosterol, as it has been previously discussed for *S. cerevisiae*.
Furthermore, *ERG11* overexpression led to higher relative amounts of palmitic acid (16:0) and cerotic acid, and reduction of linoleic (18:2) and α-linolenic (18:3) acid. Regarding phospholipids, levels of PC and PE increased in the overexpressing strain compared to the reference strain.
Sphingolipids had also altered pattern on the relative amounts of their species, being especially

remarkable the increment of ceramide composed by phytosphingosine as LCB and cerotic acid as fatty acyl. Furthermore, ceramides with nonhydroxylated fatty acids (e.g. 18:0;2/16:0;0, 18:1;2/18:0;0) were drastically reduced in OE Erg11 cells. Haxosylceramides did change neither relative amounts nor specie composition. IPC, MIPC and $M(IP)_2C$ increased their levels of 44:0;4 species and compensated by reduction on relative amounts of 42:0;4 species, which is in agreement with cermide results and meaning that an augment of sphingolipids with 26 carbons was occurring when *ERG11* was overexpressed. Whereas *S. cerevisiae* has a strong prevalence for C26:0 fatty acids [108], Grillitsch *et al* [96] reported almost equal amounts of C24:0 and C26:0 fatty acids for *P. pastoris*. In our studies, a strong preference for C24:0 fatty acids has been observed 6.3. *SUR4* is responsible for converting C24:0 fatty acids to C26:0. The obtained results suggest that *ERG11* overexpression could influence levels of *SUR4* in the cell, resulting on an increment of C26:0 species.

Changes on lipid composition of cells overexpressing *ERG11* were not beneficial for Fab secretion (Figure 7.9, Fab panel), as levels of Fab were lower than the obtained for the reference strain. However, 4.1-fold increment on Fab secretion was observed when OE Erg11 cells were cultured in hypoxia. Changes on lipid composition of these cells due t hypoxic effect were similar to the reference strain, but in this case, effect on Fab secretion was higher. On the other hand, no synergic effect of fluconazole treatment and hypoxia was observed, leading to 1.48-fold higher amounts of Fab secreted.

7.6. Effect of strain engineering through Hac1 transcription factor

The transcription factor Hac1 of *P. pastoris* has been coexpressed and the lipid composition has been determined. Hac1p can modulate the levels of chaperones, foldases, and proteins that are responsible for lipid and inositol metabolism. Coexpression of the activated, spliced variant of the *HAC1* gene has been used in several organisms as a target for strain engineering to improve protein secretion [41, 207, 324].
As Guerfal *et al*. had shown that constitutive expression of the Hac1 had little to no effect on heterologous protein production [191]. Our results confirm this statement, as no improvement on Fab secretion was observed (Figure 7.10 Fab panel).

Vogl *et al*. [325] studied effect of Hac1 coexpression in *P. pastoris* producing a membrane protein at transcriptomic level. They observed downregulation of ergosterol biosynthesis genes and upregulation of phosphatidylinositol (PI) and sphingolipid biosynthesis. These results are in agreement with ours, as ergosterol content of cells overexpressing Hac1 contained lower amounts of ergosterol. However, levels of free sterols were similar to the reference strain.
Relative levels of saturated fatty acids increased, accompanied by lower levels of mono- and polyunsaturated fatty acids, except for oleic acid (C18:1) that slightly increased in the Hac1 overexpressing strain. Levels of PI were similar to the reference strain, so that the reported upregulation of PI biosynthesis upon Hac1 expression did not lead to higher levels of PI in our studies. Regarding sphingolipids, ceramide species containing C16 fatty acids had a tendency to increase their relative levels at the expense of lower levels of C18 containing species. Haxosylceramides were exhibited a similar pattern, with higher content of species containing C16 fatty acids and lower content of the ones with C18. Inositol containing sphingolipids maintain similar levels in the OE Hac1 strain compared to the reference strain. Non-polar lipids presented

lower levels of TG and SE, while levels of free sterols were similar in both strains.

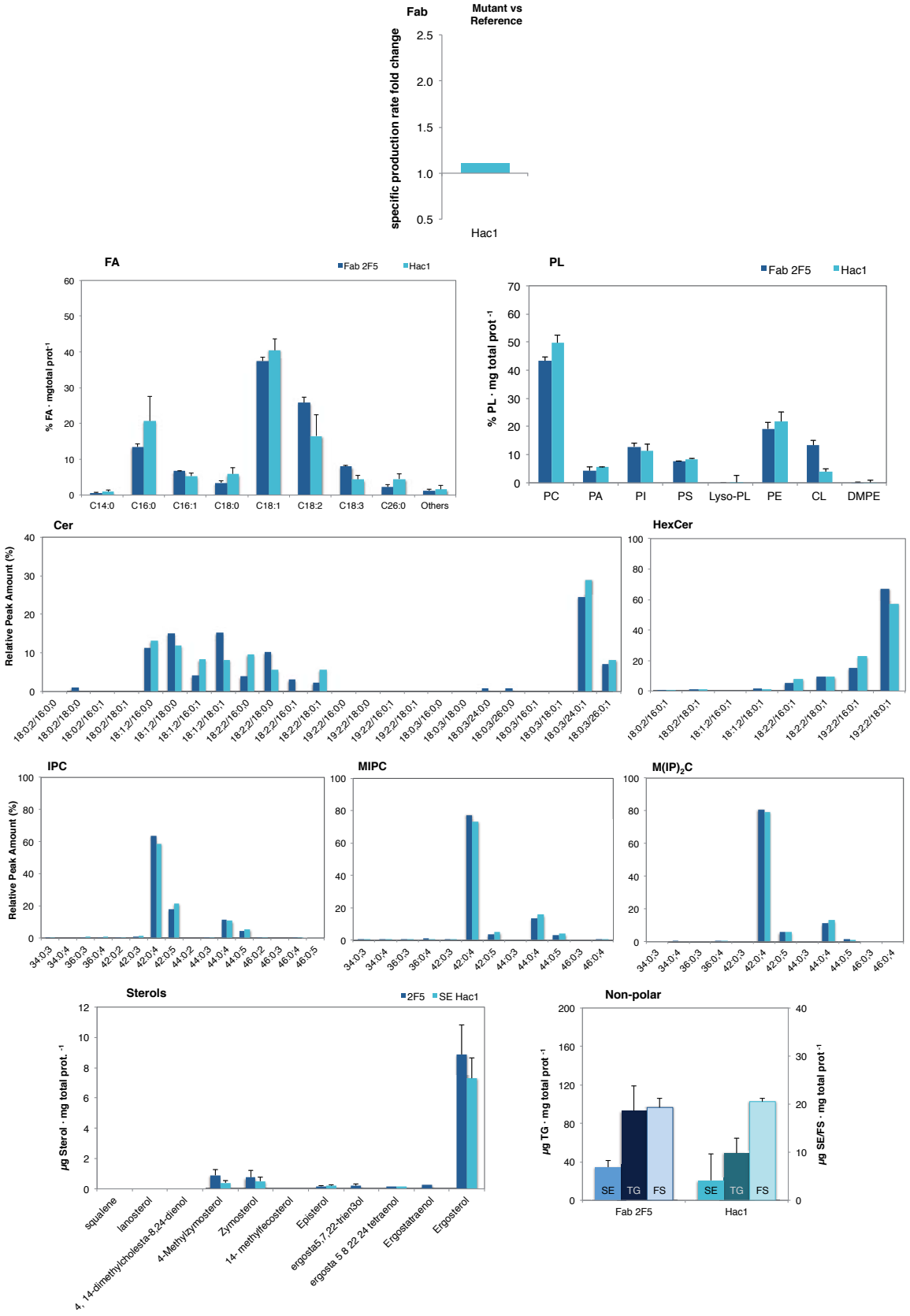

Figure 7.10: General overview of the recombinant protein production and lipid composition of the cells overexpressing the gene *HAC1* (turquoise) and the values of the reference strain (blue) without the genetic modifications.

7.7. Conclusions

- A beneficial effect due to culturing cells in hypoxic conditions have been determined for all the strains used in this study. Similar changes on lipid composition were observed as a result of hypoxia, which include reduction of polyunsaturated fatty acids, phosphatidylinositol, ergosterol and inositol containing sphingolipids with C24 fatty acids. These changes appeared with an increment of phosphatidylserine, triacylglycerols and inositol containing sphingolipids with C26 fatty acids.
- Significant changes on lipid composition were observed in the strains with engineered sphingolipid pathway. However, any of the modifications resulted in coincident lipid composition to the one corresponding to hypoxic conditions.
- Deletion of the gene encoding the C4-hydoxylase (*SUR2*) involved in sphingolipid pathway resulted in major changes on lipid composition, which resulted in changes on membrane composition that increased up to 2.4-fold the Fab secretion. However, these changes were different from the ones occurring in hypoxic conditions.
- A common pattern among the changes that result in higher levels of Fab secreted include a reduction of the free sterol content, the ergosterol content and an increment of triacylglycerols within the cell. This would mean that sterols are a key player on membrane composition and recombinant protein secretion.
- As it was expected, the effect of low oxygen culture conditions resulted in higher protein secretion than punctual changes on the lipid biosynthetic pathway.
- Changing cell lipid composition by means of genetic modifications could be a successful system to enhance recombinant protein production. It can be complemented with previous attempts on optimising recombinant protein secretion by coexpressing genes involved in protein folding and ER-stress.

General conclusions

Deep analysis of the transcriptomic data from cells cultured under low oxygen conditions was performed, focused on the genes involved in the lipid metabolism. Concretely, a cluster analysis let to identifying the most regulated genes in hypoxia. A set of genes involved in the ergosterol and sphingolipid pathways were selected as target genes for cell engineering: *DES1, SUR2,* and *ERG11*. Furthermore, the transcription factor Hac1 was also upregulated in hypoxia. Its involvement regulating genes of the lipid metabolism made it a good candidate to study the effect of lipid modifications on protein secretion and it was included in the set of selected genes.

The reference strain was used to construct a battery of strains where the selected genes were deleted (*DES1, SUR2*), or overexpressed (*DES1, ERG11, HAC1*). Two knockouts of *DES1* and one of *SUR2* were obtained using a split marker strategy, which was chosen to improve the efficiency by favouring homologous recombination instead of non-homologous end-joining. An efficiency around 1 % was obtained.
Despite the efforts of Ternes *et al*. to obtain a strain of *P. pastoris* with a deletion of *SUR2*, they were no successful, suggesting that α-hydroxylation of ceramides was required for the further steps to obtain inositol-containing sphingolipids. In this work, a deletion of *SUR2* in *P. pastoris* has been described for the first time.

All the strains were cultured in shake flask and were characterised in terms of cell growth and Fab production and a representative clone for each gene modification was selected for further studies. Remarkably, overexpression of *SUR2* resulted into non-viable clones.
The production of Fab was monitored in terms of protein secreted, and also intra/extracellular distribution was determined. Optimised disruption parameters were defined to maximise the recovered Fab in each fraction and allowed to observe a high percentage of Fab that was secreted.
Furthermore, in order to reduce the amounts of ergosterol, an essential element of cell membranes, fluconazole treatment was used for this purpose, and the quantity of fluconazole required to optimise protein secretion without impairing cell growth was determined. These results complement the previous data of fluconazole treatment, where only an initial concentration of fluconazole was defined and thus, high variability on the levels of Fab secreted were observed from culture to culture.

Chemostat cultures of each strain in normoxic and hypoxic conditions were performed in order to characterise them in terms of Fab production, intra/extracellular distribution, cell morphology and lipid content of cell homogenates. In all strains, an increase of Fab specific Fab productivity

was observed in hypoxia. This increase did not lead Fab accumulation in the intracellular fraction of the cells, and high percentages of the total Fab detected were present in the secreted fraction. Studies of the lipid composition indicated that changes due to hypoxia occur and include reduction of polyunsaturated fatty acids, phosphatidylinositol, ergosterol and inositol containing sphingolipids with C24 fatty acids. These changes were combined with an increment of phosphatidylserine, triacylglycerols and inositol containing sphingolipids with C26 fatty acids. Furthermore, genetic changes of lipid metabolism result in altered lipid pattern when compared to the reference strain. However, any of the modifications resulted in coincident lipid composition to the one corresponding to hypoxic conditions.

The most promising strain was the one harbouring the deletion of the gene encoding the C4-hydoxylase (*SUR2*) involved in sphingolipid pathway resulted in major changes on lipid composition, which resulted in changes on membrane composition that increased up to 2.4-fold the Fab secretion. However, these changes were different from the ones occurring in hypoxic conditions and the levels of Fab secreted due to hypoxic cultivation were not achieved.

A common pattern among the strains/conditions showing a beneficial effect on recombinant protein secretion were the reduction of the free sterol content, the ergosterol content, and the increment of triacylglycerols. These trends would suggest a key role of sterols defining membrane properties and its direct impact on protein secretion.

Finally, changes on lipid composition of cell membranes, specially focusing on the ergosterol content could be a promising target for future cell engineering strategies in order to increase protein secretion. These strategies could be complemented with other strategies focused on optimising the early steps of protein production.

References

[1] Cregg JM, Cereghino JL, Shi J, Higgins DR. Recombinant Protein Expression in Pichia pastoris. Mol Biotechnol. 2000;16(1):23–52.

[2] Potvin G, Ahmad A, Zhang Z. Bioprocess engineering aspects of heterologous protein production in Pichia pastoris: A review. Biochem Eng J. 2012;64:91–105.

[3] Corchero JL, Gasser B, Resina D, Smith W, Parrilli E, Vázquez F, et al. Unconventional microbial systems for the cost-efficient production of high-quality protein therapeutics. Biotechnol Adv. 2013;31(2):140–53.

[4] Bollok M, Resina D, Valero F, Ferrer P. Recent patents on the Pichia pastoris expression system: expanding the toolbox for recombinant protein production. Recent Pat Biotechnol. 2009 jan;3(3):192–201.

[5] Ahmad M, Hirz M, Pichler H, Schwab H. Protein expression in Pichia pastoris: recent achievements and perspectives for heterologous protein production. Appl Microbiol Biotechnol. 2014;98(12):5301–5317.

[6] Heyland J, Fu J, Blank LM, Schmid A. Quantitative physiology of Pichia pastoris during glucose-limited high-cell density fed-batch cultivation for recombinant protein production. Biotechnol Bioeng. 2010;107(2):357–368.

[7] Vogl T, Hartner FS, Glieder A. New opportunities by synthetic biology for biopharmaceutical production in Pichia pastoris. Curr Opin Biotechnol. 2013 dec;24(6):1094–1101.

[8] Gerngross TU. Advances in the production of human therapeutic proteins in yeasts and filamentous fungi. Nat Biotechnol. 2004;22(11):1409–14.

[9] Laukens B, Visscher CD, Callewaert N. Engineering yeast for producing human glycoproteins: where are we now? Future Microbiol. 2015;10(1):21–34.

[10] Gasser B, Prielhofer R, Marx H, Maurer M, Nocon J, Steiger MG, et al. Pichia pastoris: protein production host and model organism for biomedical research. Future Microbiol. 2013;8(2):191–208.

[11] Fickers P. Pichia pastoris: a workhorse for recombinant protein production. Curr Res Microbiol Biotechnol. 2014;2(3):354–363.

[12] Waterham HR, Digan ME, Koutz PJ, Lair SV, Cregg JM. Isolation of the Pichia pastoris glyceraldehyde-3-phosphate dehydrogenase gene and regulation and use of its promoter. Gene. 1997;186:37–44.

[13] Sunga AJ, Cregg JM. The Pichia pastoris formaldehyde dehydrogenase gene (FLD1) as a marker for selection of multicopy expression strains of P. pastoris. Gene. 2004;330:39–47.

[14] Zhang AL, Luo JX, Zhang TY, Pan YW, Tan YH, Fu CY, et al. Recent advances on the GAP promoter derived expression system of Pichia pastoris. Mol Biol Rep. 2009 jul;36(6):1611–9.

[15] Çalık P, Ata Ö, Güneş H, Massahi A, Boy E, Keskin A, et al. Recombinant protein production in Pichia pastoris under glyceraldehyde-3-phosphate dehydrogenase promoter: From carbon source metabolism to bioreactor operation parameters. Biochem Eng J. 2015;95:20–36.

[16] Romanos Ma, Scorer Ca, Clare JJ. Foreign gene expression in yeast: a review. Yeast. 1992 jun;8(6):423–88.

[17] Demain AL, Vaishnav P. Production of recombinant proteins by microbes and higher organisms. Biotechnol Adv. 2009;27(3):297–306.

[18] Choi BK, Bobrowicz P, Davidson RC, Hamilton SR, Kung DH, Li H, et al. Use of combinatorial genetic libraries to humanize N-linked glycosylation in the yeast Pichia pastoris. PNAS. 2003 apr;100(9):5022–5027.

[19] Jefferis R. Glycosylation as a strategy to improve antibody-based therapeutics. Nat Rev Drug Discov. 2009 mar;8(3):226–34.

[20] Jacobs PP, Geysens S, Vervecken W, Contreras R, Callewaert N. Engineering complex-type N-glycosylation in Pichia pastoris using GlycoSwitch technology. Nat Protoc. 2009 jan;4(1):58–70.

[21] Celik E, Calık P, Çelik E, Çalık P. Production of recombinant proteins by yeast cells. Biotechnol Adv. 2011 sep;30(5):1108–18.

[22] Xiong AS, Yao QH, Peng RH, Zhang Z, Xu F, Liu JG, et al. High level expression of a synthetic gene encoding Peniophora lycii phytase in methylotrophic yeast Pichia pastoris. Appl Microbiol Biotechnol. 2006;72(5):1039–1047.

[23] Hasslacher M, Schall M, Hayn M, Bona R, Rumbold K, Lückl J, et al. High-Level Intracellular Expression of Hydroxynitrile Lyase from the Tropical Rubber TreeHevea brasiliensisin Microbial Hosts. Protein Expr Purif. 1997 oct;11(1):61–71.

[24] Walsh G. Biopharmaceutical benchmarks 2010. Nat Biotechnol. 2010;28(9):1–10.

[25] Kim H, Yoo SJ, Kang HA. Yeast synthetic biology for the production of recombinant therapeutic proteins. FEMS Yeast Res. 2014;15:1–16.

[26] Walsh G. Biopharmaceutical benchmarks 2014. Nat Biotechnol. 2014;32(7):992–1000.

[27] De Schutter K, Lin YC, Tiels P, Van Hecke A, Glinka S, Weber-Lehmann J, et al. Genome sequence of the recombinant protein production host Pichia pastoris. Nat Biotechnol. 2009 jun;27(6):561–6.

[28] Mattanovich D, Callewaert N, Rouzé P, Lin YC, Graf A, Redl A, et al. Open access to sequence: browsing the Pichia pastoris genome. Microb Cell Fact. 2009 jan;8:53.

[29] Mattanovich D, Graf A, Stadlmann J, Dragosits M, Redl A, Maurer M, et al. Genome, secretome and glucose transport highlight unique features of the protein production host Pichia pastoris. Microb Cell Fact. 2009;13:1–13.

[30] Küberl A, Schneider J, Thallinger GG, Anderl I, Wibberg D, Hajek T, et al. High-quality genome sequence of Pichia pastoris CBS7435. J Biotechnol. 2011 jul;154(4):312–20.

[31] Hou J, Tyo KEJ, Liu Z, Petranovic D, Nielsen J. Metabolic engineering of recombinant protein secretion by Saccharomyces cerevisiae. FEMS Yeast Res. 2012;12(5):491–510.

[32] Delic M, Valli M, Graf AB, Pfeffer M, Mattanovich D, Gasser B. The secretory pathway: exploring yeast diversity. FEMS Microbiol Rev. 2013 mar;37(6):1–43.

[33] Gasser B, Saloheimo M, Rinas U, Dragosits M, Baumann K, Giuliani M, et al. Protein folding and conformational stress in microbial cells producing recombinant proteins: a host comparative overview. Microb Cell Fact. 2008;7:1–18.

[34] Puxbaum V, Mattanovich D, Gasser B. Quo vadis? The challenges of recombinant protein folding and secretion in Pichia pastoris. Appl Microbiol Biotechnol. 2015;99:2925–2938.

[35] Sha C, Yu XW, Li F, Xu Y. Impact of Gene Dosage on the Production of Lipase from Rhizopus chinensis CCTCC M201021 in Pichia pastoris. Appl Biochem Biotechnol. 2013;169(4):1160–1172.

[36] Damasceno LM, Huang CJ, Batt Ca. Protein secretion in Pichia pastoris and advances in protein production. Appl Microbiol Biotechnol. 2011 nov;93(1):31–9.

[37] Damasceno LM, Anderson Ka, Ritter G, Cregg JM, Old LJ, Batt Ca. Cooverexpression of chaperones for enhanced secretion of a single-chain antibody fragment in Pichia pastoris. Appl Microbiol Biotechnol. 2007 feb;74(2):381–9.

[38] Gasser B, Maurer M, Gach J, Kunert R, Mattanovich D. Engineering of Pichia pastoris for improved production of antibody fragments. Biotechnol Bioeng. 2006;94(2):353–361.

[39] Lin XQ, Liang SL, Han SY, Zheng SP, Ye YR, Lin Y. Quantitative iTRAQ LC-MS/MS proteomics reveals the cellular response to heterologous protein overexpression and the regulation of HAC1 in Pichia pastoris. J Proteomics. 2013 jul;91:58–72.

[40] Whyteside G, Alcocer MJC, Kumita JR, Dobson CM, Lazarou M, Pleass RJ, et al. Native-state stability determines the extent of degradation relative to secretion of protein variants from Pichia pastoris. PLoS One. 2011 jan;6(7):e22692.

[41] Gasser B, Sauer M, Maurer M, Stadlmayr G, Mattanovich D. Transcriptomics-based identification of novel factors enhancing heterologous protein secretion in yeasts. Appl Environ Microbiol. 2007 oct;73(20):6499–6507.

[42] Eiden-Plach A, Zagorc T, Heintel T, Breinig F, Schmitt MJ, Carius Y. Viral Preprotoxin Signal Sequence Allows Efficient Secretion of Green Fluorescent Protein by Candida glabrata , Pichia pastoris , Saccharomyces cerevisiae. Appl Environ Microbiol. 2004;70(2):961–966.

[43] Werten MWT, De Wolf Fa. Reduced proteolysis of secreted gelatin and Yps1-mediated ??-factor leader processing in a Pichia pastoris kex2 disruptant. Appl Environ Microbiol. 2005;71(5):2310–2317.

[44] Nocon J, Steiger MG, Pfeffer M, Sohn SB, Kim TY, Maurer M, et al. Model based engineering of Pichia pastoris central metabolism enhances recombinant protein production. Metab Eng. 2014;24:129–138.

[45] Hartner FS, Ruth C, Langenegger D, Johnson SN, Hyka P, Lin-Cereghino GP, et al. Promoter library designed for fine-tuned gene expression in Pichia pastoris. Nucleic Acids Res. 2008 jul;36(12):e76.

[46] Prielhofer R, Maurer M, Klein J, Wenger J, Kiziak C, Gasser B, et al. Induction without methanol: novel regulated promoters enable high-level expression in Pichia pastoris. Microb Cell Fact. 2013 jan;12(1):5.

[47] Camara E, Nils L, Sancho LR, Albiol J, Mattanovich D, Ferrer P. Investigating the physiological effect of increased heterologous gene dosage in Pichia pastoris using transcriptomics. N Biotechnol. 2014;31(Supplement):S59–S60.

[48] Wu M, Shen Q, Yang Y, Zhang S, Qu W, Chen J, et al. Disruption of YPS1 and PEP4 genes reduces proteolytic degradation of secreted HSA/PTH in Pichia pastoris GS115. J Ind Microbiol Biotechnol. 2013 jun;40(6):589–99.

[49] Jahic M, Gustavsson M, Jansen AK, Martinelle M, Enfors SO. Analysis and control of proteolysis of a fusion protein in Pichia pastoris fed-batch processes. J Biotechnol. 2003 apr;102(1):45–53.

[50] Ruth C, Buchetics M, Vidimce V, Kotz D, Naschberger S, Mattanovich D, et al. Pichia pastoris Aft1 - a novel transcription factor, enhancing recombinant protein secretion. Microb Cell Fact. 2014;13(1):1–15.

[51] Inan M, Aryasomayajula D, Sinha J, Meagher MM. Enhancement of protein secretion in Pichia pastoris by overexpression of protein disulfide isomerase. Biotechnol Bioeng. 2006 mar;93(4):771–8.

[52] Huangfu J, Qi F, Liu H, Zou H, Ahmed MS, Li C. Novel helper factors influencing recombinant protein production in Pichia pastoris based on proteomic analysis under simulated microgravity. Appl Microbiol Biotechnol. 2014;99(2):653–665.

[53] Sagt CMJ, Kleizen B, Verwaal R, De Jong MDM, Muller WH, Smits a, et al. Introduction of an N-glycosylation site increases secretion of heterologous proteins in yeasts. Appl Environ Microbiol. 2000;66(11):4940–4944.

[54] Hu H, Gao J, He J, Yu B, Zheng P, Huang Z, et al. Codon optimization significantly improves the expression level of a keratinase gene in Pichia pastoris. PLoS One. 2013 jan;8(3):e58393.

[55] Gu L, Zhang J, Liu B, Du G, Chen J. High-level extracellular production of glucose oxidase by recombinant Pichia pastoris using a combined strategy. Appl Biochem Biotechnol. 2015;175(3):1429–47.

[56] D'Anjou MC, Daugulis aJ. A rational approach to improving productivity in recombinant Pichia pastoris fermentation. Biotechnol Bioeng. 2001 jan;72(1):1–11.

[57] Vanz AL, Nimtz M, Rinas U. Decrease of UPR- and ERAD-related proteins in Pichia pastoris during methanol-induced secretory insulin precursor production in controlled fed-batch cultures. Microb Cell Fact. 2014;13(1):23.

[58] Spadiut O, Zalai D, Dietzsch C, Herwig C. Quantitative comparison of dynamic physiological feeding profiles for recombinant protein production with Pichia pastoris. Bioprocess Biosyst Eng. 2014;37(6):1163–1172.

[59] Kim S, D□Anjou M, Lanz KJ, Evans CE, Gibson ER, Olesberg JT, et al. Real-time monitoring of glycerol and methanol to enhance antibody production in industrial Pichia pastoris bioprocesses. Biochem Eng J. 2015;94:115–124.

[60] Maurer M, Gasser B, Kühleitner M, Mattanovich D. A rational approach to optimize feed profiles for the maximization of productivity of secreted proteins expressed in Pichia pastoris. Microb Cell Fact. 2006 jan;5:1–1.

[61] Rebnegger C, Graf AB, Valli M, Steiger MG, Gasser B, Maurer M, et al. In Pichia pastoris, growth rate regulates protein synthesis and secretion, mating and stress response. Biotechnol J. 2014;9(4):511–525.

[62] Garcia-Ortega X, Ferrer P, Montesinos JL, Valero F. Fed-batch operational strategies for recombinant Fab production with Pichia pastoris using the constitutive GAP promoter. Biochem Eng J. 2013 oct;79:172–181.

[63] Wang J, Nguyen V, Glen J, Henderson B, Saul A, Miller LH. Improved yield of recombinant merozoite Surface protein 3 (MSP3) fromPichia pastoris using chemically defined media. Biotechnol Bioeng. 2005;90(7):838–847.

[64] Mukaiyama H, Giga-Hama Y, Tohda H, Takegawa K. Dextran sodium sulfate enhances secretion of recombinant human transferrin in Schizosaccharomyces pombe. Appl Microbiol Biotechnol. 2009;85(1):155–64.

[65] Wanderley MSO, Oliveira C, Bruneska D, Domingues L, Lima Filho JL, Teixeira Ja, et al. Influence of trace elements supplementation on the production of recombinant frutalin by Pichia pastoris KM71H in fed-batch process. Chem Pap. 2013 mar;67(7):682–687.

[66] Woo JH, Liu YY, Stavrou S, David M, Jr N, Neville DM. Increasing Secretion of a Bivalent Anti-T-Cell Immunotoxin by Pichia pastoris. Appl Environ Microbiol. 2004;70(6):3370–3376.

[67] Dragosits M, Frascotti G, Bernard-Granger L, Vázquez F, Giuliani M, Baumann K, et al. Influence of growth temperature on the production of antibody Fab fragments in different microbes: a host comparative analysis. Biotechnol Prog. 2010 jan;27(1):38–46.

[68] Baumann K, Maurer M, Dragosits M, Cos O, Ferrer P, Mattanovich D. Hypoxic fed-batch cultivation of Pichia pastoris increases specific and volumetric productivity of recombinant proteins. Biotechnol Bioeng. 2008;100(1):177–83.

[69] Baumann K, Carnicer M, Dragosits M, Graf AB, Stadlmann J, Jouhten P, et al. A multi-level study of recombinant Pichia pastoris in different oxygen conditions. BMC Syst Biol. 2010 jan;4(1):141.

[70] Anasontzis GE, Salazar Penã M, Spadiut O, Brumer H, Olsson L. Effects of temperature and glycerol and methanol-feeding profiles on the production of recombinant galactose oxidase in Pichia pastoris. Biotechnol Prog. 2014;30(3):728–735.

[71] Çalık P, Bozkurt B, Zerze GH, İnankur B, Bayraktar E, Boy E, et al. Effect of co-substrate sorbitol different feeding strategies on human growth hormone production by recombinant Pichia pastoris. J Chem Technol Biotechnol. 2013 sep;88(9):1631–1640.

[72] Valero F. Bioprocess Engineering of Pichia pastoris, an Exciting Host Eukaryotic Cell Expression System. In: Ogawa T, editor. Protein Eng. - Technol. Appl. InTech; 2013. p. 3–32.

[73] Looser V, Bruhlmann B, Bumbak F, Stenger C, Costa M, Camattari A, et al. Cultivation strategies to enhance productivity of Pichia pastoris: A review. Biotechnol Adv. 2015;33(6):1177–1193.

[74] Arnau C, Casas C, Valero F. The effect of glycerol mixed substrate on the heterologous production of a Rhizopus oryzae lipase in Pichia pastoris system. Biochem Eng J. 2011 nov;57:30–37.

[75] Anastácio GS, Santos KO, Suarez PaZ, Torres FaG, De Marco JL, Parachin NS. Utilization of glycerin byproduct derived from soybean oil biodiesel as a carbon source for heterologous protein production in Pichia pastoris. Bioresour Technol. 2014;152:505–510.

[76] Prielhofer R, Cartwright SP, Graf AB, Valli M, Bill RM, Mattanovich D, et al. Pichia pastoris regulates its gene-specific response to different carbon sources at the transcriptional, rather than the translational, level. BMC Genomics. 2015;16(1):1–17.

[77] Dragosits M, Stadlmann J, Graf A, Gasser B, Maurer M, Sauer M, et al. The response to unfolded protein is involved in osmotolerance of Pichia pastoris. BMC Genomics. 2010 jan;11:207.

[78] Graf A, Gasser B, Dragosits M, Sauer M, Leparc GG, Tüchler T, et al. Novel insights into the unfolded protein response using Pichia pastoris specific DNA microarrays. BMC Genomics. 2008;9:390.

[79] Siso MIG, Becerra M, Maceiras ML, Vázquez ÁV, Cerdán ME. The yeast hypoxic responses, resources for new biotechnological opportunities. Biotechnol Lett. 2012;34(12):2161–2173.

[80] Becerra M, Becerra M, Lombard LJ, Lombard LJ, Hauser NC, Hauser NC, et al. The yeast transcriptome in aerobic and hypoxic conditions: effects of hap1, rox1, rox3 and srb10 deletions. Mol Microbiol. 2002;43(3):545–555.

[81] de Groot MJL, Daran-Lapujade P, van Breukelen B, Knijnenburg Ta, de Hulster EaF, Reinders MJT, et al. Quantitative proteomics and transcriptomics of anaerobic and aerobic yeast cultures reveals post-transcriptional regulation of key cellular processes. Microbiology. 2007 nov;153(Pt 11):3864–78.

[82] Carnicer M, Baumann K, Töplitz I, Sánchez-Ferrando F, Mattanovich D, Ferrer P, et al. Macromolecular and elemental composition analysis and extracellular metabolite balances of Pichia pastoris growing at different oxygen levels. Microb Cell Fact. 2009 jan;8:65.

[83] Alexeeva S, de Kort B, Sawers G, Hellingwerf KJ, de Mattos MJ. Effects of limited aeration and of the ArcAB system on intermediary pyruvate catabolism in Escherichia coli. J Bacteriol. 2000 sep;182(17):4934–40.

[84] Alexeeva S, Hellingwerf KJ, Mattos MJTD. Quantitative Assessment of Oxygen Availability : Perceived Aerobiosis and Its Effect on Flux Distribution in the Respiratory Chain of Escherichia coli. J Bacteriol. 2002;184(5):1402–1406.

[85] Liu L, Zhang Y, Liu Z, Petranovic D, Nielsen J. Improving heterologous protein secretion in anaerobic conditions by activationg hypoxia induced genes in Saccharomyces cerevisiae. FEMS Yeast Res. 2015;15(7):10.

[86] Baumann K, Dato L, Graf AB, Frascotti G, Dragosits M, Porro D, et al. The impact of oxygen on the transcriptome of recombinant S. cerevisiae and P. pastoris - a comparative analysis. BMC Genomics. 2011 jan;12(1):218.

[87] Carnicer M. Systematic metabolic analysis of recombinant Pichia pastoris under different oxygen conditions A Metabolome and Fluxome Based Study. UAB; 2012.

[88] Dennis Ea. Lipidomics joins the omics evolution. Proc Natl Acad Sci U S A. 2009 feb;106(7):2089–90.

[89] Ejsing CS, Sampaio JL, Surendranath V, Duchoslav E, Ekroos K, Klemm RW, et al. Global analysis of the yeast lipidome by quantitative shotgun mass spectrometry. Proc Natl Acad Sci U S A. 2009 feb;106(7):2136–41.

[90] Chumnanpuen P, Nookaew I, Nielsen J. Integrated analysis, transcriptome-lipidome, reveals the effects of INO-level (INO2 and INO4) on lipid metabolism in yeast. BMC Syst Biol. 2013;7(Suppl 3):S7.

[91] da Silveira dos Santos AX, Riezman I, Aguilera-Romero MA, David F, Piccolis M, Loewith R, et al. Systematic lipidomic analysis of yeast protein kinase and phosphatase mutants reveals novel insights into regulation of lipid homeostasis. Mol Biol Cell. 2014;25(20):3234–3246.

[92] Casanovas A, Sprenger RR, Tarasov K, Ruckerbauer DE, Hannibal-Bach HK, Zanghellini J, et al. Quantitative Analysis of Proteome and Lipidome Dynamics Reveals Functional Regulation of Global Lipid Metabolism. Chem Biol. 2015;22(3):412–425.

[93] Rußmayer H, Buchetics M, Gruber C, Valli M, Grillitsch K, Modarres G, et al. Systems-level organization of yeast methylotrophic lifestyle. BMC Biol. 2015;13(1):80.

[94] Boyle J. Lehninger principles of biochemistry. vol. 33. 4th ed. Nelson D, Cox M, editors. John Wiley & Sons Inc.; 2005.

[95] Klug L, Daum G. Yeast lipid metabolism at a glance. FEMS Yeast Res. 2014 may;14(3):369–388.

[96] Grillitsch K, Tarazona P, Klug L, Wriessnegger T, Zellnig G, Leitner E, et al. Isolation and characterization of the plasma membrane from the yeast Pichia pastoris. Biochim Biophys Acta - Biomembr. 2014 jul;1838(7):1889–97.

[97] Natter K, Kohlwein SD. Yeast and cancer cells - Common principles in lipid metabolism. Biochim Biophys Acta - Mol Cell Biol Lipids. 2013;1831(2):314–326.

[98] Dickison JR. The Metabolism and Molecular Physiology of Saccharomyces Cereuisiae. 2nd ed. Schweizer M, Dickinson JR, editors. Taylor & Francis; 2004.

[99] Yu AQ, Zhu JC, Zhang B, Xing LJ, Li MC. Knockout of fatty acid desaturase genes in Pichia pastoris GS115 and its effect on the fatty acid biosynthesis and physiological consequences. Arch Microbiol. 2012 dec;194(12):1023–32.

[100] Tehlivets O, Scheuringer K, Kohlwein SD. Fatty acid synthesis and elongation in yeast. Biochim Biophys Acta. 2007 mar;1771(3):255–70.

[101] Schneiter R, Kohlwein SD. Organelle structure, function, and inheritance in yeast: A role for fatty acid synthesis? Cell. 1997;88(4):431–434.

[102] Zanghellini J, Wodlei F, von Grünberg HH. Phospholipid demixing and the birth of a lipid droplet. J Theor Biol. 2010 jun;264(3):952–61.

[103] Henderson CM, Zeno WF, Lerno La, Longo ML, Block DE. Fermentation temperature modulates phosphatidylethanolamine and phosphatidylinositol levels in the cell membrane of Saccharomyces cerevisiae. Appl Environ Microbiol. 2013 sep;79(17):5345–56.

[104] Klose C, Surma Ma, Gerl MJ, Meyenhofer F, Shevchenko A, Simons K. Flexibility of a eukaryotic lipidome–insights from yeast lipidomics. PLoS One. 2012 jan;7(4):e35063.

[105] Galea AM, Brown AJ. Special relationship between sterols and oxygen: were sterols an adaptation to aerobic life? Free Radic Biol Med. 2009 sep;47(6):880–9.

[106] Exton JH. Phosphatidylcholine breackdown and signal transduction. Biochem Biophys Acta. 1994;1212:26–42.

[107] Carman GM, Han GS. Regulation of phospholipid synthesis in the yeast Saccharomyces cerevisiae. Annu Rev Biochem. 2011;18(9):1199–1216.

[108] Dickson RC. Thematic review series: sphingolipids. New insights into sphingolipid metabolism and function in budding yeast. J Lipid Res. 2008 may;49(5):909–21.

[109] Fairn GD, Hermansson M, Somerharju P, Grinstein S. Phosphatidylserine is polarized and required for proper Cdc42 localization and for development of cell polarity. Nat Cell Biol. 2011;13(12):1424–1430.

[110] Suetsugu S, Kurisu S, Takenawa T. Dynamic shaping of cellular membranes by phospholipids and membrane-deforming proteins. Physiol Rev. 2014;94(4):1219–48.

[111] Haviv H, Habeck M, Kanai R, Toyoshima C, Karlish SJD. Neutral Phospholipids Stimulate Na,K-ATPase Activity: A SPECIFIC LIPID-PROTEIN INTERACTION. J Biol Chem. 2013;288(14):10073–10081.

[112] Opekarová M, Robl I, Tanner W. Phosphatidyl ethanolamine is essential for targeting the arginine transporter Can1p to the plasma membrane of yeast. Biochim Biophys Acta - Biomembr. 2002 aug;1564(1):9–13.

[113] Joshi AS, Zhou J, Gohil VM, Chen S, Greenberg ML. Cellular functions of cardiolipin in yeast. Biochim Biophys Acta. 2009;1793(1):212–218.

[114] Hermesh O, Genz C, Yofe I, Sinzel M, Rapaport D, Schuldiner M, et al. Yeast phospholipid biosynthesis is linked to mRNA localization. J Cell Sci. 2014;127(15):3373–3381.

[115] De Kroon AIPM, Rijken PJ, De Smet CH. Checks and balances in membrane phospholipid class and acyl chain homeostasis, the yeast perspective. Prog Lipid Res. 2013;52(4):374–394.

[116] Henry Sa, Kohlwein SD, Carman GM. Metabolism and regulation of glycerolipids in the yeast Saccharomyces cerevisiae. Genetics. 2012;190(2):317–349.

[117] Siniossoglou S. Phospholipid metabolism and nuclear function: Roles of the lipin family of phosphatidic acid phosphatases. Biochim Biophys Acta - Mol Cell Biol Lipids. 2013;1831(3):575–581.

[118] Sturley SL. Conservation of eukaryotic sterol homeostasis: new insights from studies in budding yeast. Biochim Biophys Acta. 2000 dec;1529(1-3):155–63.

[119] Nes WD, Janssen GG, Crumley FG, Kalinowska M, Akihisa T. The structural requirements of sterols for membrane function in Saccharomyces cerevisiae. Arch Biochem Biophys. 1993;300(2):724–733.

[120] Sharma SC. Implications of sterol structure for membrane lipid composition, fluidity and phospholipid asymmetry in Saccharomyces cerevisiae. FEMS Yeast Res. 2006 nov;6(7):1047–51.

[121] Grutsch A, Grillitsch K, Tarazona P, Leitner E, Feussner I, Daum G. Characterization of Pichia pastoris Golgi and plasma membrane. N Biotechnol. 2014;31(Supplement):S152.

[122] Jin H, McCaffery JM, Grote E. Ergosterol promotes pheromone signaling and plasma membrane fusion in mating yeast. J Cell Biol. 2008;180(4):813–826.

[123] Jacquier N, Schneiter R. Mechanisms of sterol uptake and transport in yeast. J Steroid Biochem Mol Biol. 2012 mar;129(1-2):70–8.

[124] Munn aL, Heese-Peck A, Stevenson BJ, Pichler H, Riezman H. Specific sterols required for the internalization step of endocytosis in yeast. Mol Biol Cell. 1999 nov;10(11):3943–57.

[125] Heese-Peck A, Pichler H, Zanolari B, Watanabe R, Riezman H. Multiple Functions of Sterols in Yeast Endocytosis. Mol Biol Cell. 2002;13(August):2664 –2680.

[126] Baumann NA, Sullivan DP, Ohvo-rekila H, Simonot C, Pottekat A, Klaassen Z, et al. Transport of Newly Synthesized Sterol to the Sterol-Enriched Plasma Membrane Occurs via Nonvesicular Equilibration. Biochemistry. 2005;44:5816–5826.

[127] Smith SJ, Crowley JH, Parks LW. Transcriptional regulation by ergosterol in the yeast Saccharomyces cerevisiae. Mol Cell Biol. 1996 oct;16(10):5427–32.

[128] Daum G, Wagner A, Czabany T, Athenstaedt K. Dynamics of neutral lipid storage and mobilization in yeast. Biochimie. 2007 feb;89(2):243–8.

[129] Koch B, Schmidt C, Daum G. Storage lipids of yeasts: A survey of nonpolar lipid metabolism in Saccharomyces cerevisiae, Pichia pastoris, and Yarrowia lipolytica. FEMS Microbiol Rev. 2014;p. 1–24.

[130] Markgraf DF, Klemm RW, Junker M, Hannibal-Bach HK, Ejsing CS, Rapoport TA. An ER Protein Functionally Couples Neutral Lipid Metabolism on Lipid Droplets to Membrane Lipid Synthesis in the ER. Cell Rep. 2014;6(1):44–55.

[131] Ploier B, Korber M, Schmidt C, Koch B, Leitner E, Daum G. Regulatory link between steryl ester formation and hydrolysis in the yeast Saccharomyces cerevisiae. Biochim Biophys Acta - Mol Cell Biol Lipids. 2015;1851(7):977–986.

[132] Ivashov Va, Zellnig G, Grillitsch K, Daum G. Identification of triacylglycerol and steryl ester synthases of the methylotrophic yeast Pichia pastoris. Biochim Biophys Acta - Mol Cell Biol Lipids. 2013 jun;1831(6):1158–66.

[133] Ivashov Va, Grillitsch K, Koefeler H, Leitner E, Baeumlisberger D, Karas M, et al. Lipidome and proteome of lipid droplets from the methylotrophic yeast Pichia pastoris. Biochim Biophys Acta - Mol Cell Biol Lipids. 2012;1831(2):282–290.

[134] Zanghellini J, Natter K, Jungreuthmayer C, Thalhammer A, Kurat CF, Gogg-Fassolter G, et al. Quantitative modeling of triacylglycerol homeostasis in yeast–metabolic requirement for lipolysis to promote membrane lipid synthesis and cellular growth. FEBS J. 2008 nov;275(22):5552–63.

[135] Turkish A, Sturley SL. Regulation of triglyceride metabolism. I. Eukaryotic neutral lipid synthesis: "Many ways to skin ACAT or a DGAT". Am J Physiol Gastrointest Liver Physiol. 2007;292(4):G953–7.

[136] Kohlwein SD. Triacylglycerol Homeostasis: Insights from Yeast. J Biol Chem. 2010;285(21):15663–15667.

[137] Aguilera-Romero A, Gehin C, Riezman H. Sphingolipid homeostasis in the web of metabolic routes. Biochim Biophys Acta - Mol Cell Biol Lipids. 2014;1841(5):647–656.

[138] Ternes P, Wobbe T, Schwarz M, Albrecht S, Feussner K, Riezman I, et al. Two Pathways of Sphingolipid Biosynthesis Are Separated in the Yeast Pichia pastoris. J Biol Chem. 2011 feb;286(13):11401–11414.

[139] Warnecke D, Heinz E. Recently discovered functions of glucosylceramides in plants and fungi. Cell Mol Life Sci. 2003 may;60(5):919–41.

[140] van Meer G, Voelker DR, Feigenson GW. Membrane lipids: where they are and how they behave. Nat Rev Mol Cell Biol. 2008 feb;9(2):112–24.

[141] Dickson RC, Sumanasekera C, Lester RL. Functions and metabolism of sphingolipids in Saccharomyces cerevisiae. Prog Lipid Res. 2006;45:447–465.

[142] Dickson RC, Lester RL. Metabolism and selected functions of sphingolipids in the yeast Saccharomyces cerevisiae. Biochim Biophys Acta - Mol Cell Biol Lipids. 1999;1438(3):305–321.

[143] Chen PW, Fonseca LL, Hannun YA, Voit EO. Coordination of Rapid Sphingolipid Responses to Heat Stress in Yeast. PLoS Comput Biol. 2013 may;9(5):e1003078.

[144] Funato K, Vallée B, Riezman H. Biosynthesis and Trafficking of Sphingolipids in the Yeast Saccharomyces cerevisiae. Biochemistry. 2002;41(51):15105–15114.

[145] Huang X, Liu J, Dickson RC. Down-Regulating Sphingolipid Synthesis Increases Yeast Lifespan. PLoS Genet. 2012;8(2):e1002493.

[146] Dickson RC, Lester RL. Sphingolipid functions in Saccharomyces cerevisiae. Biochim Biophys Acta. 2002 jun;1583(1):13–25.

[147] Liu K, Zhang X, Sumanasekera C, Lester RL, Dickson RC. Signalling functions for sphingolipid long-chain bases in Saccharomyces cerevisiae. Biochem Soc Trans. 2005;33(Pt 5):1170–1173.

[148] Montefusco DJ, Matmati N, Hannun YA. The yeast sphingolipid signaling landscape. Chem Phys Lipids. 2014;177:26–40.

[149] Hannich JT, Umebayashi K, Riezman H. Distribution and functions of sterols and sphingolipids. Cold Spring Harb Lab Perspect Biol. 2011 may;3(5):47–62.

[150] Cowart LA, Obeid LM. Yeast sphingolipids: recent developments in understanding biosynthesis, regulation, and function. Biochim Biophys Acta. 2007 mar;1771(3):421–31.

[151] Hechtberger P, Zinser E, Saf R, Hummel K, Paltauf F, Daum G. Characterization, quantification and subcellular localization of inositol-containing sphingolipids of the yeast, Saccharomyces cerevisiae. Eur J Biochem. 1994 oct;225(2):641–649.

[152] Dickson R. Roles for Sphingolipids in Saccharomyces cerevisiae. In: Chalfant C, Poeta M, editors. Sphingolipids as Signal. Regul. Mol. SE - 15. vol. 688 of Advances in Experimental Medicine and Biology. Springer New York; 2010. p. 217–231.

[153] Breslow DK. Sphingolipid homeostasis in the endoplasmic reticulum and beyond. Cold Spring Harb Perspect Biol. 2013;5(4):1–16.

[154] Merrill AH. Sphingolipid and glycosphingolipid metabolic pathways in the era of sphingolipidomics. Chem Rev. 2011;111(10):6387–422.

[155] Gulati S, Liu Y, Munkacsi AB, Wilcox L, Sturley SL. Sterols and sphingolipids: Dynamic duo or partners in crime? Prog Lipid Res. 2010;49(4):353–365.

[156] Mollinedo F. Lipid raft involvement in yeast cell growth and death. Front Oncol. 2012 jan;2(October):140.

[157] Joosten V, Lokman C, Hondel CAVD, Punt PJ. The production of antibody fragments and antibody fragments by yeasts and filamentous fungi. Microb Cell Fact. 2003;2:1–15.

[158] de Marco A. Biotechnological applications of recombinant single-domain antibody fragments. Microb Cell Fact. 2011;10(1):44.

[159] Spadiut O, Capone S, Krainer F, Glieder A, Herwig C. Microbials for the production of monoclonal antibodies and antibody fragments. Trends Biotechnol. 2014;32(1):54–60.

[160] Buchetics M, Dragosits M, Maurer M, Rebnegger C, Porro D, Sauer M, et al. Reverse engineering of protein secretion by uncoupling of cell cycle phases from growth. Biotechnol Bioeng. 2011 may;108(10):2403–2412.

[161] Takahashi K, Toshifumi Y, Takai T, Ra C, Okumura K, Yokota T, et al. Production of humanized Fab fragment against human high affinity IgE receptor in Pichia pastoris. Biosci Biotechnol Biochem. 2000;64(10):2138–2144.

[162] Lange S, Schmitt J, Schmid RD. High-yield expression of the recombinant, atrazine-specific Fab fragment K411B by the methylotrophic yeast Pichia pastoris. J Immunol Methods. 2001;255:103–114.

[163] Ning D, Junjian X, Qing Z, Sheng X, Wenyin C, Guirong R, et al. Production of recombinant humanized anti-HBsAg Fab fragment from Pichia pastoris by fermentation. J Biochem Mol Biol. 2005;38:294–299.

[164] Stadlmayr G, Mecklenbräuker A, Rothmüller M, Maurer M, Sauer M, Mattanovich D, et al. Identification and characterisation of novel Pichia pastoris promoters for heterologous protein production. J Biotechnol. 2010 dec;150(4):519–29.

[165] Nishimura A, Morita M, Nishimura Y, Sugino Y. A rapid and highly efficient method for preparation of competent Escherichia coli cells. Nucleic Acids Res. 1990;18(20):6169.

[166] Woodman ME. Direct PCR of intact bacteria (colony PCR). In: Curr. Protoc. Microbiol. John Wiley & Sons, Inc.; 2008. p. 1–6.

[167] Lin-Cereghino J, Wong WW, Xiong S, Giang W, Luong LT, Vu J, et al. Condensed protocol for competent cell preparation and transformation of the methylotrophic yeast Pichia pastoris. Biotechniques. 2008;38(1):44–48.

[168] Resina D, Cos O, Ferrer P, Valero F. Developing high cell density fed-batch cultivation strategies for heterologous protein production in Pichia pastoris using the nitrogen source-regulated FLD1 Promoter. Biotechnol Bioeng. 2005 sep;91(6):760–767.

[169] Arnau C, Ramon R, Casas C, Valero F. Optimization of the heterologous production of a Rhizopus oryzae lipase in Pichia pastoris system using mixed substrates on controlled fed-batch bioprocess. Enzyme Microb Technol. 2010 may;46(6):494–500.

[170] Wechselberger P, Sagmeister P, Herwig C. Real-time estimation of biomass and specific growth rate in physiologically variable recombinant fed-batch processes. Bioprocess Biosyst Eng. 2013;36(9):1205–1218.

[171] Van Der Heijden RTJM, Heijnen JJ, Hellinga C, Romein B, Luyben KCaM. Linear constraint relations in biochemical reaction systems: I. Classification of the calculability and the balanceability of conversion rates. Biotechnol Bioeng. 1994;43(1):3–10.

[172] Wang NS, Stephanopoulos G. Application of macroscopic balances to the identification of gross measurement errors. Biotechnol Bioeng. 1983;25(9):2177–2208.

[173] Wechselberger P, Herwig C. Model-based analysis on the relationship of signal quality to real-time extraction of information in bioprocesses. Biotechnol Prog. 2012;28(1):265–275.

[174] Lünsdorf H, Gurramkonda C, Adnan A, Khanna N, Rinas U. Virus-like particle production with yeast: ultrastructural and immunocytochemical insights into Pichia pastoris producing high levels of the hepatitis B surface antigen. Microb Cell Fact. 2011 jan;10(1):48.

[175] Reynolds ES. The use of lead citrate at high pH as an electron-opaque stain in electron microscopy. J Cell Biol. 1963;17(1):208–212.

[176] Lowry OH, Rosebrough NJ, Farr AL, Randall RJ. Protein measurement with the folin phenol reagent. J Biol Chem. 1951;193(1):265–275.

[177] Folch J, Lees M, Slo. A simple method for the isolation and purification of total lipides from animal tissues. J Biol Chem. 1957;.

[178] Broekhuyse RM. Isolation, characterization and quantitative analysis by two-dimensional thin-layer chromatography of diacyl and vinyl-ether phospholipids. Biochem Biophys Acta. 1967;152(1968):307–315.

[179] Quail Ma, Kelly SL. The extraction and analysis of sterols from yeast. In: Evans, editor. Yeast Protoc.. vol. 53. To: Humana Press; 1996. p. 123–31.

[180] Markham JE, Li J, Cahoon EB, Jaworski JG. Separation and Identification of Major Plant Sphingolipid Classes from Leaves. J Biol Chem. 2006;281(32):22684–22694.

[181] Ejsing CS, Moehring T, Bahr U, Duchoslav E, Karas M, Simons K, et al. Collision-induced dissociation pathways of yeast sphingolipids and their molecular profiling in total lipid extracts: a study by quadrupole TOF and linear ion trap-orbitrap mass spectrometry. J Mass Spectrom. 2006;41(3):372–89.

[182] Jackson P, Attalla MI. N-Nitrosopiperazines form at high pH in post-combustion capture solutions containing piperazine: a low-energy collisional behaviour study. Rapid Commun Mass Spectrom. 2010;24(24):3567–3577.

[183] Meltzer PS. Large-scale genome analysis. In: Baxevanis AD, Ouellette BFF, editors. Bioinforma. A Pract. Guid. to Anal. Genes Proteins. second edi ed. New York: John Wiley and Sons, Inc.; 2001. p. 393–412.

[184] Dale JW, von Schantz M. Analysis of Gene Expression. In: Dale JW, von Schantz M, editors. From Genes to Genomes Concepts Appl. DNA Technol.. vol. 7. West Sussex, England: John Wiley & Sons, Ltd; 2002. p. 227–257.

[185] Duggan DJ, Bittner M, Chen Y, Meltzer P, Trent JM. Expression profiling using cDNA microarrays. Nat Genet. 1999;21(1 Suppl):10–14.

[186] D'haeseleer P, Liang S, Somogyi R. Genetic network inference: from co-expression clustering to reverse engineering. Bioinformatics. 2000;16(8):707–726.

[187] MacQueen J. Some methods for classification and analysis of multivariate observations. In: Proc. fifth Berkeley Symp. Math. Stat. Probab.. vol. 1. Oakland, CA, USA.; 1967. p. 281–297.

[188] Carnicer M, Canelas aB, ten Pierick A, Zeng Z, van Dam J, Albiol J, et al. Development of quantitative metabolomics for Pichia pastoris. Metabolomics. 2012;8(2):284–298.

[189] Petranovic D, Tyo K, Vemuri GN, Nielsen J. Prospects of yeast systems biology for human health: integrating lipid, protein and energy metabolism. FEMS Yeast Res. 2010 dec;10(8):1046–59.

[190] Cox JS, Chapman RE, Walter P. The unfolded protein response coordinates the production of endoplasmic reticulum protein and endoplasmic reticulum membrane. Mol Biol Cell. 1997 sep;8(9):1805–14.

[191] Guerfal M, Ryckaert S, Jacobs PP, Ameloot P, Craenenbroeck KV, Derycke R, et al. The HAC1 gene from Pichia pastoris: characterization and effect of its overexpression on the production of secreted, surface displayed and membrane proteins. Microb Cell Fact. 2010;9(49):1–12.

[192] Baumann K, Adelantado N, Lang C, Mattanovich D, Ferrer P. Protein trafficking, ergosterol biosynthesis and membrane physics impact recombinant protein secretion in Pichia pastoris. Microb Cell Fact. 2011 nov;10(1):93.

[193] Ternes P, Franke S, Zähringer U, Sperling P, Heinz E. Identification and characterization of a sphingolipid Δ4-desaturase family. J Biol Chem. 2002;277(28):25512–25518.

[194] Ternes P, Sperling P, Albrecht S, Franke S, Cregg JM, Warnecke D, et al. Identification of fungal sphingolipid C9-methyltransferases by phylogenetic profiling. J Biol Chem. 2006 mar;281(9):5582–92.

[195] Michaelson LV, Zäuner S, Markham JE, Haslam RP, Desikan R, Mugford S, et al. Functional characterization of a higher plant sphingolipid Delta4-desaturase: defining the role of sphingosine and sphingosine-1-phosphate in Arabidopsis. Plant Physiol. 2009 jan;149(1):487–98.

[196] Obeid LM, Okamoto Y, Mao C. Yeast sphingolipids: metabolism and biology. Biochim Biophys Acta. 2002 dec;1585(2-3):163–71.

[197] Haak D, Gable K, Beeler T, Dunn T. Hydroxylation of Saccharomyces cerevisiae ceramides requires Sur2p and Scs7p. J Biol Chem. 1997 nov;272(47):29704–10.

[198] Grilley MM, Stock SD, Dickson RC, Lester RL, Takemoto JY. Syringomycin action gene SYR2 is essential for sphingolipid 4-hydroxylation in Saccharomyces cerevisiae. J Biol Chem. 1998 may;273(18):11062–8.

[199] Veen M, Stahl U, Lang C. Combined overexpression of genes of the ergosterol biosynthetic pathway leads to accumulation of sterols in. FEMS Yeast Res. 2003 oct;4(1):87–95.

[200] Lees ND, Bard M. 6 Sterol biochemistry and regulation in the yeast Saccharomyces cerevisiae. In: Daum G, editor. Lipid Metab. Membr. Biog. SE - 7. vol. 6 of Topics in Current Genetics. Springer Berlin Heidelberg; 2004. p. 213–240. Available from: http://dx.doi.org/10.1007/978-3-540-40999-1{_}7.

[201] Turi TG, Loper JC. Multiple regulatory elements control expression of the gene Encoding the Saccharomyces cerevisiae Cytochrome P450, lanosterol 14a-demethylase (ERG11). J Biol Chem. 1992;267(January 25):2046–2056.

[202] Stansfield I, Cliffe KR, Kelly SL. Chemostat studies of microsomal enzyme induction in Saccharomyces cerevisiae. Yeast. 1991;7(2):147–156.

[203] Chang HJ. Role of the Unfolded Protein Response Pathway in Secretory Stress and Regulation of INO1 Expression in Saccharomyces cerevisiae. Genetics. 2004;168(4):1899–1913.

[204] Idiris A, Tohda H, Kumagai H, Takegawa K. Engineering of protein secretion in yeast: strategies and impact on protein production. Appl Microbiol Biotechnol. 2010 feb;86(2):403–417.

[205] Ashe MP, Bill RM. Mapping the yeast host cell response to recombinant membrane protein production: relieving the biological bottlenecks. Biotechnol J. 2011 jun;6(6):707–14.

[206] Whyteside G, Nor RM, Alcocer MJC, Archer DB. Activation of the unfolded protein response in Pichia pastoris requires splicing of a HAC1 mRNA intron and retention of the C-terminal tail of Hac1p. FEBS Lett. 2011 apr;585(7):1037–41.

[207] Valkonen M, Penttilä M, Saloheimo M, Penttila M. Effects of Inactivation and Constitutive Expression of the Unfolded- Protein Response Pathway on Protein Production in the Yeast Saccharomyces cerevisiae. Mol Microbiol. 2003 feb;69(4):2065–2072.

[208] Klinner U, Schäfer B. Genetic aspects of targeted insertion mutagenesis in yeasts. FEMS Microbiol Rev. 2004;28(2):201–223.

[209] Schorsch C, Köhler T, Boles E. Knockout of the DNA ligase IV homolog gene in the sphingoid base producing yeast Pichia ciferrii significantly increases gene targeting efficiency. Curr Genet. 2009 aug;55(4):381–9.

[210] Chen Z, Sun H, Li P, He N, Zhu T, Li Y. Enhancement of the Gene Targeting Efficiency of Non-Conventional Yeasts by Increasing Genetic Redundancy. PLoS One. 2013 mar;8(3):e57952.

[211] Güldener U, Heck S, Fiedler T, Beinhauer J, Hegemann JH. A new efficient gene disruption cassette for repeated use in budding yeast. Nucleic Acids Res. 1996;24(13):2519–2524.

[212] Higgins DR, Cregg JM. Pichia Protocols. Humana Press Inc; 1998.

[213] Li P, Anumanthan A, Gao XG, Ilangovan K, Suzara VV, Düzgüneş N, et al. Expression of recombinant proteins in Pichia pastoris. Appl Biochem Biotechnol. 2007;142(2):105–124.

[214] Näätsaari L, Mistlberger B, Ruth C, Hajek T, Hartner FS, Glieder A. Deletion of the Pichia pastoris KU70 homologue facilitates platform strain generation for gene expression and synthetic biology. PLoS One. 2012 jan;7(6):e39720.

[215] Nett JH, Hodel N, Rausch S, Wildt S. Cloning and disruption of the Pichia pastoris ARG1, ARG2, ARG3, HIS1, HIS2, HIS5, HIS6 genes and their use as auxotrophic markers. Yeast. 2005 mar;22(4):295–304.

[216] Cosano IC, Martín H, Flández M, Nombela C, Molina M. Pim1, a MAP kinase involved in cell wall integrity in Pichia pastoris. Mol Genet Genomics. 2001 jun;265(4):604–614.

[217] Saraya R, Krikken AM, Kiel JAKW, Baerends RJS, Veenhuis M, van der Klei IJ. Novel genetic tools for Hansenula polymorpha. FEMS Yeast Res. 2011 nov;p. 1–8.

[218] Chung KR, Lee MH. Split-Marker-Mediated Transformation and Targeted Gene Disruption in Filamentous Fungi. In: van den Berg MA, Maruthachalam K, editors. Genet. Transform. Syst. Fungi. vol. 2. Springer International; 2015. p. 175–180.

[219] Choquer M, Dekkers KL, Chen HQ, Cao L, Ueng PP, Daub ME, et al. The CTB1 gene encoding a fungal polyketide synthase is required for cercosporin biosynthesis and fungal virulence of Cercospora nicotianae. Mol Plant Microbe Interact. 2005;18(5):468–476.

[220] You BJ, Lee MH, Chung KR. Gene-specific disruption in the filamentous fungus Cercospora nicotianae using a split-marker approach. Arch Microbiol. 2009;191(7):615–622.

[221] Heiss S, Maurer M, Hahn R, Mattanovich D, Gasser B. Identification and deletion of the major secreted protein of Pichia pastoris. Appl Microb Cell Physiol. 2012 jul;97(3):1241–1249.

[222] Odds F. Antifungal agents: mechanisms of action. Trends Microbiol. 2003 jun;11(6):272–279.

[223] Sorgo AG, Heilmann CJ, Dekker HL, Bekker M, Brul S, de Koster CG, et al. Effects of fluconazole on the secretome, the wall proteome, and wall integrity of the clinical fungus Candida albicans. Eukaryot Cell. 2011 aug;10(8):1071–81.

[224] Beney L, Gervais P. Influence of the fluidity of the membrane on the response of microorganisms to environmental stresses. Appl Microbiol Biotechnol. 2001 oct;57:34–42.

[225] Learmonth RP. Membrane Fluidity in Yeast Adaptation: Insights from Fluorescence Spectroscopy and Microscopy. In: Geddes CD, editor. Rev. Fluoresc.. 1st ed. New York: Springer; 2010. p. 388.

[226] Lentz BR. Use of fluorescent probes to monitor molecular order and motions within liposome bilayers. Chem Phys Lipids. 1993;64(1-3):99–116.

[227] Lackowicz JR. Fluorescence Anisotropy. In: Princ. Fluoresc. Spectrosc.; 2006. p. 353–382.

[228] Liu D, Zeng XA, Sun DW, Han Z. Disruption and protein release by ultrasonication of yeast cells. Innov Food Sci Emerg Technol. 2013;18:132–137.

[229] Lin DQ, Dong JN, Yao SJ. Target control of cell disruption to minimize the biomass electrostatic adhesion during anion-exchange expanded bed adsorption. Biotechnol Prog. 2007;23:162–167.

[230] Pfeffer M, Maurer M, Stadlmann J, Grass J, Delic M, Altmann F, et al. Intracellular interactome of secreted antibody Fab fragment in Pichia pastoris reveals its routes of secretion and degradation. Appl Microbiol Biotechnol. 2012 mar;93(6):2503–12.

[231] Wang TJ, Naglak HY. Protein release from the yeast Pichia pastoris by chemical permeabilisation: comparison to mechanical disruption and enzymatic lysis. In: Pyle DL, editor. Sep. Biotechnol. 2. vol. 8. London and New York: SCI; 1990. p. 472–480.

[232] Boettner M, Prinz B, Holz C, Stahl U, Lang C. High-throughput screening for expression of heterologous proteins in the yeast Pichia pastoris. J Biotechnol. 2002 oct;99(1):51–62.

[233] Shepard SR, Stone C, Cook S, Bouvier A, Boyd G, Weatherly G, et al. Recovery of intracellular recombinant proteins from the yeast Pichia pastoris by cell permeabilization. J Biotechnol. 2002;99:149–160.

[234] Lenassi Zupan A, Trobec S, Gaberc-Porekar V, Menart V. High expression of green fluorescent protein in Pichia pastoris leads to formation of fluorescent particles. J Biotechnol. 2004;109(1-2):115–122.

[235] Johnson SK, Zhang W, Smith LA, Hywood-Potter KJ, Todd Swanson S, Schlegel VL, et al. Scale-up of the fermentation and purification of the recombinant heavy chain fragment C of botulinum neurotoxin serotype F, expressed in Pichia pastoris. Protein Expr Purif. 2003;32(1):1–9.

[236] Tam Y, Allaudin Z, Lila MA, Bahaman A, Tan J, Rezaei M. Enhanced cell disruption strategy in the release of recombinant hepatitis B surface antigen from Pichia pastoris using response surface methodology. BMC Biotechnol. 2012;12(1):70.

[237] Gurramkonda C, Zahid M, Nemani SK, Adnan A, Gudi SK, Khanna N, et al. Purification of hepatitis B surface antigen virus-like particles from recombinant Pichia pastoris and in vivo analysis of their immunogenic properties. J Chromatogr B Analyt Technol Biomed Life Sci. 2013 dec;940:104–11.

[238] Middelberg APJ. Process-Scale Disruption of Microorganisms. Biotechnol Adv. 1995;13(3):491–551.

[239] Canales M, Buxadó Ja, Heynngnezz L, Enríquez A. Mechanical disruption of Pichia pastoris yeast to recover the recombinant glycoprotein Bm86. Enzyme Microb Technol. 1998;23(1-2):58–63.

[240] Garcia-Ortega X, Reyes C, Montesinos JL, Valero F. Overall Key Performance Indicator to Optimizing Operation of High-Pressure Homogenizers for a Reliable Quantification of Intracellular Components in Pichia pastoris. Front Bioeng Biotechnol. 2015;3(August):1–9.

[241] Hohenblum H, Gasser B, Maurer M, Borth N, Mattanovich D. Effects of gene dosage, promoters, and substrates on unfolded protein stress of recombinant Pichia pastoris. Biotechnol Bioeng. 2004;85(4):367–375.

[242] Spiden EM, Scales PJ, Kentish SE, Martin GJO. Critical analysis of quantitative indicators of cell disruption applied to Saccharomyces cerevisiae processed with an industrial high pressure homogenizer. Biochem Eng J. 2013 jan;70:120–126.

[243] Pfeffer M, Maurer M, Köllensperger G, Hann S, Graf AB, Mattanovich D. Modeling and measuring intracellular fluxes of secreted recombinant protein in Pichia pastoris with a novel 34S labeling procedure. Microb Cell Fact. 2011 jan;10(1):47.

[244] Zeder-Lutz G, Cherouati N, Reinhart C, Pattus F, Wagner R. Dot-blot immunodetection as a versatile and high-throughput assay to evaluate recombinant GPCRs produced in the yeast Pichia pastoris. Protein Expr Purif. 2006 nov;50(1):118–27.

[245] Lórenz-Fonfría V, Perálvarez-Marín A, Padrós E, Lazarova T. Solubilization, Purification, and Characterization of Integral Membrane Proteins. In: Robinson AS, editor. Prod. Membr. Proteins Strateg. Expr. Isol.. 1st ed. Wiley-VCH Verlag GmbH & Co.; 2011. p. 317–360.

[246] Sarramegna V, Muller I, Mousseau G, Froment C, Monsarrat B, Milon A, et al. Solubilization, purification, and mass spectrometry analysis of the human mu-opioid receptor expressed in Pichia pastoris. Protein Expr Purif. 2005;43(2):85–93.

[247] Chi WK, Ku CH, Chang CC, Tsai JN. Two-step cell disruption for the extraction of membrane-associated recombinant protein from Saccharomyces cerevisiae. Ann N Y Acad Sci. 1994 may;721:365–73.

[248] Kim SK. Effect of Expression of Genes in the Sphingolipid Synthesis Pathway on the Biosynthesis of Ceramide in Saccharomyces cerevisiae. J Microbiol Biotechnol. 2010;20(October 2009):356–362.

[249] Li Z, Xiong F, Lin Q, D'Anjou M, Daugulis AJ, Yang DSC, et al. Low-Temperature Increases the Yield of Biologically Active Herring Antifreeze Protein in Pichia pastoris. Protein Expr Purif. 2001 apr;21(3):438–445.

[250] Piper MDW, Daran-Lapujade P, Bro C, Regenberg B, Knudsen S, Nielsen J, et al. Reproducibility of Oligonucleotide Microarray Transcriptome Analyses. J Biol Chem. 2002;277(40):37001–37008.

[251] Hoskisson PA. Continuous culture - making a comeback? Microbiology. 2005;151(10):3153–3159.

[252] Kohlwein SD. The beauty of the yeast: live cell microscopy at the limits of optical resolution. Microsc Res Tech. 2000 dec;51(6):511–29.

[253] Wright R. Transmission electron microscopy of yeast. Microsc Res Tech. 2000 dec;51(6):496–510.

[254] Spurr AR. A low-viscosity epoxy resin embedding medium for electron microscopy. J Ultrastruct Res. 1969;26(1-2):31–43.

[255] Santos AXSS, Riezman H. Yeast as a model system for studying lipid homeostasis and function. FEBS Lett. 2012 aug;586(18):2858–67.

[256] Rajakumari S, Rajasekharan R, Daum G. Triacylglycerol lipolysis is linked to sphingolipid and phospholipid metabolism of the yeast Saccharomyces cerevisiae. Biochim Biophys Acta - Mol Cell Biol Lipids. 2010 aug;.

[257] Guan XL, Souza CM, Pichler H, Schaad O, Kajiwara K, Wakabayashi H, et al. Functional interactions between sphingolipids and sterols in biological membranes regulating cell physiology. Mol Biol Cell. 2009;20(April):2083–2095.

[258] Los Da, Murata N. Membrane fluidity and its roles in the perception of environmental signals. Biochim Biophys Acta - Biomembr. 2004;1666(1-2):142–157.

[259] Daum G, Lees ND, Bard M, Dickson R. Biochemistry, cell biology and molecular biology of lipids of Saccharomyces cerevisiae. Yeast. 1998;14(16):1471–1510.

[260] Yu AQ, Shi TL, Zhang B, Xing LJ, Li MC. Transcriptional regulation of desaturase genes in Pichia pastoris GS115. Lipids. 2012 nov;47(11):1099–108.

[261] Lindberg L, Santos AXS, Riezman H, Olsson L, Bettiga M. Lipidomic Profiling of Saccharomyces cerevisiae and Zygosaccharomyces bailii Reveals Critical Changes in Lipid Composition in Response to Acetic Acid Stress. PLoS One. 2013;8(9):1–12.

[262] Jenkins GM, Richards A, Wahl T, Mao C, Obeid L, Hannun Y. Involvement of yeast sphingolipids in the heat stress response of Saccharomyces cerevisiae. J Biol Chem. 1997 dec;272(51):32566–72.

[263] de Ghellinck A, Fragneto G, Laux V, Haertlein M, Jouhet J, Sferrazza M, et al. Lipid polyunsaturation determines the extent of membrane structural changes induced by Amphotericin B in Pichia pastoris yeast. Biochim Biophys Acta - Biomembr. 2015;.

[264] Wriessnegger T, Gübitz G, Leitner E, Ingolic E, Cregg J, de la Cruz BJ, et al. Lipid composition of peroxisomes from the yeast Pichia pastoris grown on different carbon sources. Biochim Biophys Acta. 2007 apr;1771(4):455–61.

[265] Wriessnegger T, Leitner E, Belegratis MR, Ingolic E, Daum G. Lipid analysis of mitochondrial membranes from the yeast Pichia pastoris. Biochim Biophys Acta. 2009 mar;1791(3):166–72.

[266] Klug L, Tarazona P, Gruber C, Grillitsch K, Gasser B, Trötzmüller M, et al. The lipidome and proteome of microsomes from the methylotrophic yeast Pichia pastoris. Biochim Biophys Acta. 2013 nov;.

[267] Bligh EG, Dyer WJ. A rapid method of total lipid extraction and purification. Can J Biochem Physiol. 1959;37:911–917.

[268] Jacob Z. Yeast Lipids: Extraction, Quality Analysis, and Acceptability. Crit Rev Biotechnol. 1992 jan;12(5-6):463–491.

[269] Schneiter R, Daum G. Analysis of yeast lipids. In: Xiao W, editor. Methods Mol. Biol.. vol. 313. 2nd ed. Totowa, NJ: Humana Press Inc.; 2006. p. 75–84.

[270] Fuchs B, Süß R, Teuber K, Eibisch M, Schiller J. Lipid analysis by thin-layer chromatography-A review of the current state. J Chromatogr A. 2011;1218(19):2754–2774.

[271] Christie WW. Gas Chromatography and Lipids. 3rd ed. Christie WW, editor. Bridgwater: Oily Press Ltd.; 1989.

[272] Heupel RC. Isolation and Primary Characterization of Sterols. In: Parish WDNJBTAoS, Steroids OBS, editors. Anal. Sterols Other Biol. Signif. Steroids. Academic Press; 1989. p. 1–31.

[273] Rosenfeld E, Beauvoit B. Role of the non-respiratory pathways in the utilization of molecular oxygen by Saccharomyces cerevisiae. Yeast. 2003;20(13):1115–1144.

[274] De Ghellinck A, Schaller H, Laux V, Haertlein M, Sferrazza M, Maréchal E, et al. Production and analysis of perdeuterated lipids from Pichia pastoris cells. PLoS One. 2014;9(4):1–9.

[275] Carman GM, Henry Sa. Phospholipid biosynthesis in yeast. Annu Rev Biochem. 1989;58:635–669.

[276] Bagnat M, Keränen S, Shevchenko A, Simons K. Lipid rafts function in biosynthetic delivery of proteins to the cell surface in yeast. Proc Natl Acad Sci U S A. 2000 mar;97(7):3254–9.

[277] Proszynski TJ, Klemm RW, Gravert M, Hsu PP, Gloor Y, Wagner J, et al. A genome-wide visual screen reveals a role for sphingolipids and ergosterol in cell surface delivery in yeast. Proc Natl Acad Sci U S A. 2005 dec;102(50):17981–6.

[278] Zhang L, Díaz-Díaz N, Zarringhalam K, Hermansson M, Somerharju P, Chuang J. Dynamics of the ethanolamine glycerophospholipid remodeling network. PLoS One. 2012;7(12):e50858.

[279] Carman GM, Henry Sa. Phospholipid biosynthesis in the yeast Saccharomyces cerevisiae and interrelationship with other metabolic processes. Prog Lipid Res. 1999;38(5-6):361–399.

[280] Nohturfft A, Zhang SC. Coordination of Lipid Metabolism in Membrane Biogenesis. Annu Rev Cell Dev Biol. 2009;25(1):539–566.

[281] Gaspar ML, Hofbauer HF, Kohlwein SD, Henry SA. Coordination of Storage Lipid Synthesis and Membrane Biogenesis: Evidence for cross-talk between triacylglycerol metabolism and phospholipidylinositol synthesis. J Biol Chem. 2011;286(3):1696–1708.

[282] Alvarez-Vasquez F, Sims KJ, Voit EO, Hannun Ya. Coordination of the dynamics of yeast sphingolipid metabolism during the diauxic shift. Theor Biol Med Model. 2007;4:42.

[283] Zaman S, Lippman SI, Zhao X, Broach JR. How Saccharomyces responds to nutrients. Annu Rev Genet. 2008;42:27–81.

[284] Young BP, Shin JJH, Orij R, Chao JT, Li SC, Guan XL, et al. Phosphatidic Acid Is a pH Biosensor that links membrane biogenesis to metabolism. Science (80-). 2010;329(August):1085–1088.

[285] Tuller G, Nemec T, Hrastnik C, Daum G. Lipid composition of subcellular membranes of an FY1679-derived haploid yeast wild-type strain grown on different carbon sources. Yeast. 1999;15(14):1555–1564.

[286] Gaspar ML, Aregullin MA, Jesch SA, Henry SA. Inositol Induces a Profound Alteration in the Pattern and Rate of Synthesis and Turnover of Membrane Lipids in Saccharomyces cerevisiae. J Biol Chem. 2006;281(32):22773–22785.

[287] De Smet CH, Vittone E, Scherer M, Houweling M, Liebisch G, Brouwers JF, et al. The yeast acyltransferase Sct1p regulates fatty acid desaturation by competing with the desaturase Ole1p. Mol Biol Cell. 2012;23(7):1146–1156.

[288] Gonzalez CI, Martin CE. Fatty Acid-responsive Control of mRNA Stability UNSATURATED FATTY ACID-INDUCED DEGRADATION OF THE SACCHAROMYCES OLE1 TRANSCRIPT. J Biol Chem. 1996;271(42):25801–25809.

[289] Kato H, Sakaki K, Mihara K. Ubiquitin-proteasome-dependent degradation of mammalian ER stearoyl-CoA desaturase. J Cell Sci. 2006;119(11):2342–2353.

[290] Braun S, Matuschewski K, Rape M, Thoms S, Jentsch S. Role of the ubiquitin?selective CDC48UFD1/NPL4 chaperone (segregase) in ERAD of OLE1 and other substrates. EMBO J. 2002;21(4):615–621.

[291] Bigay J, Antonny B. Curvature, Lipid Packing, and Electrostatics of Membrane Organelles: Defining Cellular Territories in Determining Specificity. Dev Cell. 2012;23(5):886–895.

[292] Grinstein S. Imaging signal transduction during phagocytosis: phospholipids, surface charge, and electrostatic interactions. Am J Physiol Cell Physiol. 2010;299(5):C876–81.

[293] Holthuis JCM, Menon AK. Lipid landscapes and pipelines in membrane homeostasis. Nature. 2014;510(7503):48–57.

[294] Di Paolo G, De Camilli P. Phosphoinositides in cell regulation and membrane dynamics. Nature. 2006;443(7112):651–657.

[295] Loewen CJR, Gaspar ML, Jesch Sa, Delon C, Ktistakis NT, Henry Sa, et al. Phospholipid metabolism regulated by a transcription factor sensing phosphatidic acid. Science. 2004;304(5677):1644–1647.

[296] Jesch SA, Liu P, Zhao X, Wells MT, Henry SA. Multiple Endoplasmic Reticulum-to-Nucleus Signaling Pathways Coordinate Phospholipid Metabolism with Gene Expression by Distinct Mechanisms. J Biol Chem. 2006;281(33):24070–24083.

[297] Jesch SA, Zhao X, Wells MT, Henry SA. Genome-wide analysis reveals inositol, not choline, as the major effector of Ino2p-Ino4p and unfolded protein response target gene expression in yeast. J Biol Chem. 2005;280(10):9106–9118.

[298] Nikawa J, Hosaka K, Yamashita S. Differential regulation of two myo□inositol transporter genes of Saccharomyces cerevisiae. Mol Microbiol. 1993;10(5):955–961.

[299] Kimata Y, Ishiwata-Kimata Y, Yamada S, Kohno K. Yeast unfolded protein response pathway regulates expression of genes for anti-oxidative stress and for cell surface proteins. Genes to Cells. 2006;11(1):59–69.

[300] Tavassoli S, Chao JT, Young BP, Cox RC, Prinz Wa, de Kroon AIPM, et al. Plasma membrane–endoplasmic reticulum contact sites regulate phosphatidylcholine synthesis. EMBO Rep. 2013;14(5):434–440.

[301] Garcia-Ortega X, Valero F, Montesinos JL. A versatile approach to implement oxygen-limiting conditions for improving recombinant protein production in Pichia pastoris. Appl Microbiol Biotechnol. 2015;.

[302] Surma MA, Klose C, Peng D, Shales M, Mrejen C, Stefanko A, et al. A Lipid E-MAP Identifies Ubx2 as a Critical Regulator of Lipid Saturation and Lipid Bilayer Stress. Mol Cell. 2013;51(4):519–530.

[303] Ron D, Walter P. Signal integration in the endoplasmic reticulum unfolded protein response. Nat Rev Mol Cell Biol. 2007 jul;8(7):519–29.

[304] Pineau L, Colas J, Dupont S, Beney L, Fleurat-Lessard P, Berjeaud JM, et al. Lipid-induced ER stress: synergistic effects of sterols and saturated fatty acids. Traffic. 2009 jun;10(6):673–90.

[305] Volmer R, van der Ploeg K, Ron D. Membrane lipid saturation activates endoplasmic reticulum unfolded protein response transducers through their transmembrane domains. Proc Natl Acad Sci U S A. 2013;110(12):4628–4633.

[306] Bien CM, Espenshade PJ. Sterol regulatory element binding proteins in fungi: Hypoxic transcription factors linked to pathogenesis. Eukaryot Cell. 2010;9(3):352–359.

[307] Hughes AL, Todd BL, Espenshade PJ. SREBP Pathway Responds to Sterols and Functions as an Oxygen Sensor in Fission Yeast. Cell. 2005;120(6):831–842.

[308] Zanghellini J, Natter K, Jungreuthmayer C, Thalhammer A, Kurat CF, Gogg□Fassolter G, et al. Quantitative modeling of triacylglycerol homeostasis in yeast–metabolic requirement for lipolysis to promote membrane lipid synthesis and cellular growth. FEBS J. 2008;275(22):5552–5563.

[309] Kurat CF, Wolinski H, Petschnigg J, Kaluarachchi S, Andrews B, Natter K, et al. Cdk1/Cdc28-dependent activation of the major triacylglycerol lipase Tgl4 in yeast links lipolysis to cell-cycle progression. Mol Cell. 2009;33(1):53–63.

[310] Rosenberger S, Daum G. Lipids of yeast mitochondria. In: Res. Signpost; 2005. p. 51–83.

[311] Kim S, Fyrst H, Saba J. Accumulation of phosphorylated sphingoid long chain bases results in cell growth inhibition in Saccharomyces cerevisiae. Genetics. 2000;156(4):1519–1529.

[312] Desfarges L, Durrens P, Juguelin H, Cassagne C, Bonneu M, Aigle M. Yeast mutants affected in viability upon starvation have a modified phospholipid composition. Yeast. 1993;9(3):267–77.

[313] Klose C, Ejsing CS, García-Sáez AJ, Kaiser HJ, Sampaio JL, Surma Ma, et al. Yeast lipids can phase separate into micrometer-scale membrane domains. J Biol Chem. 2010 jul;285(39):30224–32.

[314] Gaigg B, Toulmay A, Schneiter R. Very long-chain fatty acid-containing lipids rather than sphingolipids per se are required for raft association and stable surface transport of newly synthesized plasma membrane ATPase in yeast. J Biol Chem. 2006 nov;281(45):34135–45.

[315] Bammert GF, Fostel JM. Genome-wide expression patterns in Saccharomyces cerevisiae: comparison of drug treatments and genetic alterations affecting biosynthesis of ergosterol. Antimicrob Agents Chemother. 2000 may;44(5):1255–65.

[316] Ghannoum Ma, Rice LB. Antifungal agents: mode of action, mechanisms of resistance, and correlation of these mechanisms with bacterial resistance. Clin Microbiol Rev. 1999 oct;12(4):501–17.

[317] Hull CM, Parker JE, Bader O, Weig M, Gross U, Warrilow AGS, et al. Facultative sterol uptake in an ergosterol-deficient clinical isolate of candida glabrata harboring a missense mutation in ERG11 and exhibiting cross-resistance to azoles and amphotericin B. Antimicrob Agents Chemother. 2012;56(8):4223–4232.

[318] Veen M, Lang C. Production of lipid compounds in the yeast Saccharomyces cerevisiae. Appl Microbiol Biotechnol. 2004;63:635–646.

[319] Leber R, Zinser E, Hrastnik C, Paltauf F, Daum G. Export of steryl esters from lipid particles and release of free sterols in the yeast, Saccharomyces cerevisiae. Biochim Biophys Acta - Biomembr. 1995;1234(1):119–126.

[320] Song JL, Harry JB, Eastman RT, Brian G, White TC, Oliver BG. The Candida albicans Lanosterol 14- α -Demethylase (ERG11) Gene Promoter Is Maximally Induced after Prolonged Growth with Antifungal Drugs The Candida albicans Lanosterol 14- □ -Demethylase (ERG11) Gene Promoter Is Maximally Induced after Prolonged Gr. Antimicrob Agents Chemother. 2004;48(4):1136–1144.

[321] Veen M, Stahl U, Lang C. Combined overexpression of genes of the ergosterol biosynthetic pathway leads to accumulation of sterols in. FEMS Yeast Res. 2003;4(1):87–95.

[322] Weber JM, Ponti CG, Kappeli O, Reiser J. Factors affecting homologous overexpression of the Saccharomyces cerevisiae lanosterol 14 alpha-demethylase gene. Yeast. 1992;8(7):519–533.

[323] Bard M, Lees ND, Turi T, Craft D, Cofrin L, Barbuch R, et al. Sterol synthesis and viability of erg11 (cytochrome P450 lanosterol demethylase) mutations in Saccharomyces cerevisiae and Candida albicans. Lipids. 1993;28(11):963–967.

[324] Valkonen M, Ward M, Wang H, Penttilä M, Saloheimo M. Improvement of Foreign-Protein Production in Aspergillus niger var. awamori by Constitutive Induction of the Unfolded-Protein Response. Appl Environ Microbiol. 2003 dec;69(12):6979–6986.

[325] Vogl T, Thallinger GG, Zellnig G, Drew D, Cregg JM, Glieder A, et al. Towards improved membrane protein production in Pichia pastoris: General and specific transcriptional response to membrane protein overexpression. N Biotechnol. 2014 mar;00(00):1–14.

Appendix

7.8. Gene sequences

7.8.1. *DES1* sequence

P. pastoris DES1 gene (PAS_chr3_0939): 938 bp

ATGATAACTCACAGATCCAATAACGTTCAGTATGAAGTAACACCGCCTTCTGTGGAAGAAGATTTAGGCCCACAGTTTG
AGTTCTACTGGACCCGTCAAAAAGATCCACACAGTATCCGAAGGAAGCTAATTTTAGCCAAGCATCCGGAAGTAGCCA
AGTTATGTGGACCCGAGTGGAGGACGAAATATATTGCTTCCGCTGTCGTTCTTCTACAGCTCTCCATTGCATATGCTCTA
AAGAATACACCAGTACTGTCTTTCAAATTTTTGGCACTTGCATACGTCGTTGGTGCTACTGCAAACCAAAACTGTTTCCTC
TGTATTCACGAGCTGAGCCATAACCTGGCATTCAGAAAACCACTTCACAACAAACTATTCGCAATTTGGGTCAATCTAC
CCATTGGAGTCCCATATAGCGCTTCATTCCAACCATATCACCAACTCCATCACAAATTTTTAGGCGATGAAGTGCTGGAC
ACTGATCTTCCAACGCCTCTAGAAGCGACTGTTTTGTCCTCATTGCTGGGTAAAGCCTTCTTCGCCACTTTCCAAATATTC
TTTTACGCGTTGAGGCCCATGATGGTTACGTCTATTGACATGACTTTTATTCATTTGTTGAACGTGCTGGTTTGCTTGGTTA
GCGATTTTATCCTGATCAAGTTCGGCTCAGCTAACAGTTTATGGTACCTGATATTGAGTTCCTTCTTTGCGGGTTCGTTGC
ATCCTACGGCAGGGCACTTCATAGCTGAGCACTATTTATTGGATCCTCCAAAGCATTATACCCAATTCCAGGATGTTCCC
CCGTTAGAGACTTACTCCTACTACGGAATGCTGAATTTGTTCACTTGGAATGTAGGATATCACAACGAGCATCACGACTT
TCCATTCATTGCTTGGTCTAAGCTGCCTCTTCTGAGAACCATAGCACATGACTTTTAA

7.8.2. *SUR2* sequence

P. pastoris SUR2 gene (PAS_chr3_0425): 1058 bp

ATGGACAAGTTCAGTCAGTATATCCCCAAAAACACGACCGGATTTCTCAACCAGCCATACCCTCCAACTTCGGTTGTGA
TCAGGCGGCCTGACTTGATTCAAGGCGTTCCTGACGGCATCTTAAGTCTCTGTGTTCCGATCGTATTGTACTGGAGCTA
TTCAACTTTCTTTCATATTGTGGACACTTACGAGTTGGCAGAGAAATACCGAATTCATCCGTCTGAAGAAGTTCTTCAAC
GTAACAAAGTCACGCTAAGGGTGGTAATCCAAGACGTCATTGTACAACACATTATTCAAACGTTAGTCGGTTTAGTTTTT
TACAAGTTGGACCCTGTCCCCACTACGGGATACGAACAAAGAGAAATGTGGTACTTGAAACAGAGACTGCCGCCTTTT
TTCAAATGGAATGACACGATAGCAAACCTTTTTGTATATTATGGTTATTGGTATGGTTTATCTGCTACAAAAATTATCATTG
CTTTCGTTATCATCGATACATGGCAATTTTTTTTGCATCGTTTAATGCATGTGAATAAAACTTTATACCGAAAGTTTCATTCT
CGTCATCACAAGCTGTATGTCCCGTACGCTTTTGGAGCCCTTTTCAATGACCCATTTGAAGGATTTCTCTTGGACACTGT
TGGGGCAGGCCTAGCTGCCATATTCACAGGACTAACTCCCAGGGAGTCCATGGTTCTATATGGTTTTTCTACTCTTAAAA
CTGTGGATGACCACTGTGGATACTCTTTGCCTTTTGACATTTTCCAAATCATATTCCCTAATGACTCCATTTATCACGATAT
CCATCACCAACATTTTGGAATCAAATCTAATTTTTCTCAACCATTTTTCACCTTTTGGGACAAGTTTTTTGGTACAACATTC
CATGGGGTCGACCAATATAAGCAGTCTCAACAGAAGATCACTCTGGAAAGGTACAAAGAGTTCTTGGCCTCTAGACAG
AAATCACGCATTCAAAAACAACAACAGCAACACTCCAAGGTTGAACGCTACAGCGACAGTGAAGATGAACCGGATCA
CCAAAAGAAAGAACAGTAA

7.8.3. *ERG11* sequence

P. pastoris GS115 PAS_chr3_0957: 1548 bp

ATGAGTCTGGTCCAGGAGTTGATTCAAAAGATAAGCTCTTTGGAGCTCACCTTGGTGGAAAAGCTTTCCATCCTGTTCGT
AGCTCCCTTCTTGTTGAACGCGCTATGGCAGTTTATCTACAGTTTCAGAAAGGACAGAGTTCCTTTGGTATTCCACTGGG
TTCCATGGGTAGGCTCAGCAGTCACATATGGAATGCAACCATATGAATTTTTTGCAGACTGTCAAAGAAAATACGGAGA
CGTGTTTGCCTTTGTTTTGTTGGGTAAAGTTATGACAGTGTACCTCGGACCAAAAGGCCATGAGTTTATTTTAAATGCTAA
ACTAAACGACGTTTGTGCTGAAGATGCCTACAAGCACCTGACCACTCCTGTATTTGGTGAAGGTGTTATTTACGATTGTC

CCAACTGGAAGTTGATGGACCAGAAGAAGTTTGTTAAAGGATCTTTAACCAAGGAGTCCTTCAGATCTTATGTCCCTAA
GATTAGAGATGAAGTCCTGGATTACATCAATAATGACCCTAACTTCATGGGAGGTGATTCTAAAAAGAAAACTGGAAAG
ACCAATGTCCTGAACTCTCAGTCCGAGCTTACGATCTTGACCGCTTCCAGATCTCTACTGGGAGATGATATGAGAAAAC
TACTGACTAAGAAATGGGCTAAACTGTTTAGTGACCTAGACAAAGGATTTACTCCTTTAAACTTCATTTTCTCTCATCTTC
CTCTACCAAGTTACTGGACTCGTGATCATGCTCAAAAGACCATTTCTGAGACTTATTTATCTTTGATTAACAAGAGAAGA
GCTACAAACGACATTGGTGACAGAGATTTGATCGATTCATTAATGAAATCTTCTACATACAAAGATGGTAGCAAGATGA
CCGACGAGGAGATTTCCCACTTGTTAATCGGAGTTCTTATGGGTGGCCAGCACACTTCTGCCTCCACTTCATCGTGGTT
TTTGTTGCATCTCGGAGAGAAACCAGAGCTGCAGGAGGAATTATTTGAAGAACAGGAAAGGGTACTTCAAGGGCGTGA
GTTGACTTATGACGATCTTGCTAATATGCCTTTACACAATCAAGTCATCAAGGAAACTTTGCGCATGCACATGCCTCTAC
ACTCAATCTTTAGAAAGGTCACTCGTCCTCTTCCCGTTCCTAACTCAAAGTATGTGGTTCCTAAGGGTCATTATGTATTGG
TTTCACCTGGATTTGCCATGACCAACGATGCGTACTTCCCAAACGCTAGTGACTTCCAGCCACACAGATGGGATGAAAC
TGTTGAACCAGTCTCAGCTGACGCAAAGGAAACTGTTGACTACGGATTTGGTAAAGTCTCCAAAGGTGTTTCTTCTCCTT
ACTTACCATTTGGAGGAGGAAGACATAGATGTATTGGCGAACATTTTGCGTACTGTCAGTTAGGAACCATCTTGAACAC
ATTCGTTAGAACCTTCAAGTGGAAGGCCGTAGTCCCTCAGCCGGACTATACCTCAATGGTTACTCTTCCTGAACCTAATT
TGTCTACTATTACATGGGAAAGACGCGATAATTAG

7.8.4. HAC1 sequence

P.pastoris HAC1spliced: 915 bp

ATGCCCGTAGATTCTTCTCATAAGACAGCTAGCCCACTTCCACCTCGTAAAAGAGCAAAGACGGAAGAAGAAAAGGAG
CAGCGTCGAGTGGAACGTATCCTACGTAATAGGAGAGCGGCCCATGCTTCCAGAGAGAAGAAACGAAGACACGTTGA
ATTTCTGGAAAACCACGTCGTCGACCTGGAATCTGCACTTCAAGAATCAGCCAAAGCCACTAACAAGTTGAAAGAAATA
CAAGATATCATTGTTTCAAGGTTGGAAGCCTTAGGTGGTACCGTCTCAGATTTGGATTTAACAGTTCCGGAAGTCGATTT
TCCCAAATCTTCTGATTTGGAACCCATGTCTGATCTCTCAACTTCTTCGAAATCGGAGAAAGCATCTACATCCACTCGCA
GATCTTTGACTGAGGATCTGGACGAAGATGACGTCGCTGAATATGACGACGAAGAAGAGGACGAAGAGTTACCCAGG
AAAATGAAAGTCTTAAACGACAAAAACAAGAGCACATCTATCAAGCAGGAGAAGTTGAATGAACTTCCATCTCCTTTGT
CATCCGATTTTTCAGACGTAGATGAAGAAAAGTCAACTCTCACACATTTAAAGTTGCAACAGCAACAACAACAACCAGT
AGACAATTATGTTTCTACTCCTTTGAGTCTTCCGGAGGATTCAGTTGATTTTATTAACCCAGGTAACTTAAAAATAGAGTC
CGATGAGAACTTCTTGTTGAGTTCAAATACTTTACAAATAAAACACGAAAATGACACCGACTACATTACTACAGCTCCAT
CAGGTTCCATCAATGATTTTTTTAATTCTTATGACATTAGCGAGTCGAATCGGTTGCATCATCCAGCAGCACCATTTACCG
CTAATGCATTTGATTTAAATGACTTTGTATTCTTCCAGGAATAG